

**ASYMMETRIC INDUCTION USING METHYL (S)-LACTATE
AND APPLICATION TO THE SYNTHESIS OF BAO GONG TENG A**

BY

VINH C. PHAM

A thesis

**submitted to the Faculty of Graduate Studies in partial fulfillment
of the requirements for the Degree of**

DOCTOR OF PHILOSOPHY

**Department of Chemistry
University of Manitoba
Winnipeg, Manitoba, Canada**

June 1997



**National Library
of Canada**

**Acquisitions and
Bibliographic Services**

395 Wellington Street
Ottawa ON K1A 0N4
Canada

**Bibliothèque nationale
du Canada**

**Acquisitions et
services bibliographiques**

395, rue Wellington
Ottawa ON K1A 0N4
Canada

Your file Votre référence

Our file Notre référence

The author has granted a non-exclusive licence allowing the National Library of Canada to reproduce, loan, distribute or sell copies of this thesis in microform, paper or electronic formats.

The author retains ownership of the copyright in this thesis. Neither the thesis nor substantial extracts from it may be printed or otherwise reproduced without the author's permission.

L'auteur a accordé une licence non exclusive permettant à la Bibliothèque nationale du Canada de reproduire, prêter, distribuer ou vendre des copies de cette thèse sous la forme de microfiche/film, de reproduction sur papier ou sur format électronique.

L'auteur conserve la propriété du droit d'auteur qui protège cette thèse. Ni la thèse ni des extraits substantiels de celle-ci ne doivent être imprimés ou autrement reproduits sans son autorisation.

0-612-23652-8

**THE UNIVERSITY OF MANITOBA
FACULTY OF GRADUATE STUDIES
COPYRIGHT PERMISSION**

**ASYMMETRIC INDUCTION USING METHYL (S)-LACTATE
AND APPLICATION TO THE SYNTHESIS OF BAO GONG TENG A**

BY

VINH C. PHAM

**A Thesis submitted to the Faculty of Graduate Studies of the University of Manitoba
in partial fulfillment of the requirements of the degree of**

DOCTOR OF PHILOSOPHY

Vinh C. Pham © 1997

**Permission has been granted to the LIBRARY OF THE UNIVERSITY OF MANITOBA
to lend or sell copies of this thesis, to the NATIONAL LIBRARY OF CANADA to microfilm this
thesis and to lend or sell copies of the film, and to UNIVERSITY MICROFILMS to publish an
abstract of this thesis.**

**This reproduction or copy of this thesis has been made available by authority of the copyright
owner solely for the purpose of private study and research, and may only be reproduced and
copied as permitted by copyright laws or with express written authorization from the copyright
owner.**

Acknowledgments

I would like to extend my sincerest appreciation to my supervisor, Dr. J. L. Charlton, for his guidance, instruction, discussion and all his help during the course of my research project and thesis write up.

I would like to thank my committee, Dr. A. Queen, Dr. A. McIntosh and Dr. N. Hunter, for their helpful discussions about my project.

I am deeply indebted to my family for their love, support and encouragement.

I am grateful to my wife, Linda Han, for her love, encouragement and friendship.

I would also like to thank Dr. P. Hultin for many interesting discussions about some problems of my research project.

Finally, I would like to thank T. Foniok for acquiring all my 300 MHz ^1H -nmr spectra, W. Buchanon for running all my mass spectra and Dr. K. Marat for helpful discussions dealing with nmr problems.

Financial support from both University of Manitoba and Dr. J. L. Charlton is gratefully acknowledged.

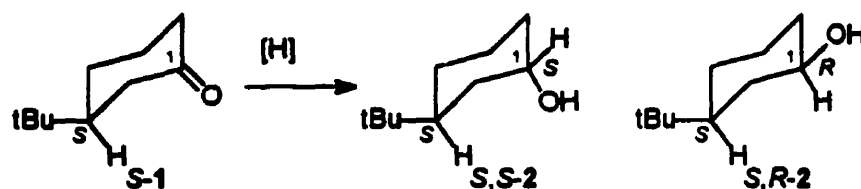
Results and Discussion	54
Chapter 4	54
Asymmetric photodeconjugation of a chiral α,β -unsaturated ester	54
Chapter 5	66
Section 5.2 : Preparation of chiral vinylsulfonate esters	66
Section 5.2 : Diels-Alder reactions of chiral vinylsulfonyl esters	70
Section 5.2.1 : Structure elucidation of the cycloadducts	70
Section 5.2.2 : The selectivity of chiral sulfonyl esters in Diels-Alder reactions	98
Section 5.3 : Conclusion	103
Chapter 6	104
Section 6.1 : 1,3-Dipolar cycloadditions of chiral vinylsulfonate	105
Section 6.2 : 1,3-Dipolar cycloadditions of acrylate of methyl (<i>S</i>)-lactate	116
Section 6.3 : Bao Gong Teng synthesis	124
Section 6.4 : Other possible applications	143
Overall Conclusion	148
Experimental	151
Chapter 7	151
References	170

Preamble

Developing strategies toward the synthesis of enantiomerically pure compounds is one of the goals of modern organic chemistry. This goal becomes more and more important as the need for enantiomerically pure drugs grows.¹ A well known strategy for achieving this goal is the utilization of stereoselective synthesis.

Stereoselective synthesis is the generation of new stereogenic (chiral) centers in a molecule in such a way that one absolute configuration for these centers is favored. An example of an stereoselective reaction is illustrated by the reduction of optically pure (3*S*)-3-*tert*-butylcyclohexanone, (*S*)-1 as shown in Scheme 1. The reduction generates a new chiral center at C1, forming (3*S*,1*R*)-2 and (3*S*,1*S*)-2 in unequal amount, therefore, this reaction is an stereoselective reaction. A common strategy for performing an stereoselective synthesis is to place a control element, usually of one absolute configuration, in the reactant so that asymmetric induction can be achieved in a subsequent reaction. This control element is referred to as a chiral auxiliary.

Scheme 1:



The known efficiency of methyl (*S*)-lactate as a chiral auxiliary in some Diels-Alder reactions² encouraged further study of the use of this chiral auxiliary in other reactions. In these studies, the asymmetric induction imposed by the chiral auxiliary was examined. A

final goal was to use reactions with high asymmetric induction for natural product synthesis.

Photodeconjugation was one of the reactions chosen for a study of the effectiveness of the methyl (*S*)-lactate chiral auxiliary. In this study, the methyl (*S*)-lactate was incorporated into an α,β -unsaturated ester, which was then subjected to irradiation in order to asymmetrically form the corresponding β,γ -unsaturated ester with a new chiral center at the α position. Obtaining a high asymmetric induction, such that the reaction might be synthetically useful, and rationalizing the mechanism of the induction were the two main objectives of this study. Thus, the photodeconjugation reaction was performed under various conditions in order to search for the optimum induction, and also to examine trends in induction. It was hoped that the changes in induction observed on changing reaction conditions might provide information about the mechanism of the asymmetric control.

The diels-Alder reaction was the next reaction chosen for study of the asymmetric induction imposed by the lactate chiral auxiliary. The aim of this study was to incorporate methyl (*S*)-lactate or methyl (*R*)-mandelate, a similar chiral auxiliary, into a new type of dienophile, a vinylsulfonate. The effectiveness of these new chiral dienophiles was examined in Diels-Alder reactions. These chiral vinylsulfonates should provide more choice for introducing specific functionality in chiral Diels-Alder cycloadducts. The chiral vinylsulfonates should also be highly reactive dienophiles due to the strong electron withdrawing ability of the sulfonate groups, and they should be useful for reactions with less reactive dienes such as furan and its derivatives.

A 1,3-dipolar cycloaddition reaction was the last type of reaction chosen for the study of asymmetry induced by the methyl (*S*)-lactate chiral auxiliary. A study of *N*-benzyl 3-oxidopyridinium betaine undergoing a 1,3-dipolar cycloaddition with either a vinylsulfonate, or an acrylate, bearing the methyl (*S*)-lactate chiral auxiliary was undertaken. These reactions should form the azabicyclo[3.2.1]octane ring skeleton, a building block for a number of natural products, including the tropane alkaloids. The object of this study was to obtain high diastereoselectivities in the cycloadditions so that they could be used for the synthesis of Bao Gong Teng A, a tropane alkaloid.

Introduction

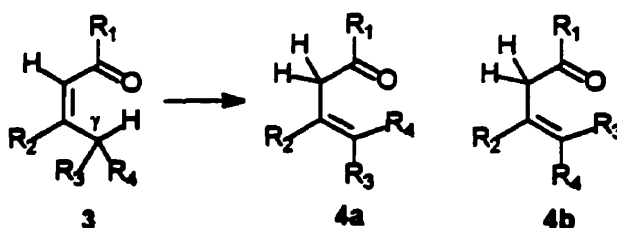
As mentioned in the preamble, this thesis consists of the study of three different types of reactions. Hence the introduction is divided into three chapters. The first part of the thesis focuses on the use of methyl (*S*)-lactate as a chiral auxiliary in photodeconjugation reactions. Thus, the introduction for this part, Chapter 1, includes a discussion of the generally accepted mechanism of photodeconjugation. Also a brief review of the asymmetric photodeconjugation reaction will be provided. The next part of the thesis concerns a study of chiral vinylsulfonates as dienophiles in the Diels-Alder reactions. The introduction for this part, Chapter 2, will include a brief review of the Diels-Alder reaction of alkyl vinylsulfonates. Finally, in the last part of the thesis, reactions using chiral dipolarophiles in 1,3-dipolar cycloadditions will be described. Also in this part, the asymmetric 1,3-dipolar cycloaddition reaction was applied to the synthesis of Bao Gong Teng A, a tropane alkaloid having antiglaucoma properties. The introduction of this part of the thesis, Chapter 3, will include a brief review of the 1,3-dipolar cycloaddition reactions of N-substituted 3-oxidopyridinium betaines, and a discussion of the total synthesis of racemic Bao Gong Teng A via a 1,3-dipolar cycloaddition reaction.

Chapter 1

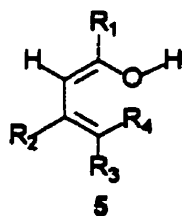
Section 1.1: Mechanism of Photodeconjugation

The first formal reports of photodeconjugation reactions appeared in the literature in the mid-sixties. Jorgenson³ and Rando *et al.*⁴ had observed that α,β -unsaturated esters or ketones bearing hydrogen at the γ position, as in **3**, underwent photochemical reactions to form the corresponding β,γ -unsaturated compounds **4a** and **4b** (Scheme 2).

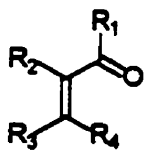
Scheme 2:



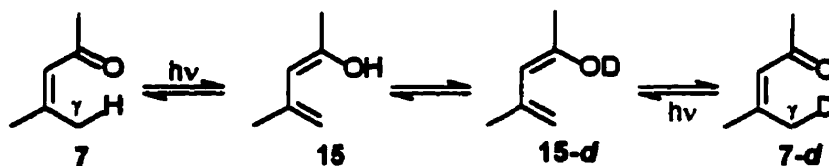
The currently accepted mechanism for the photodeconjugation reaction is constructed around a proposal by Yang and Jorgenson.^{3a} They proposed that the γ -hydrogen atom migrates to the carbonyl oxygen intramolecularly, forming the corresponding dienol **5**. The dienol **5** can then tautomerize to form the corresponding deconjugated products, **4a** and **4b**.



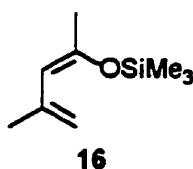
Their hypothesis requires the availability of the *cis*-isomer of the α,β -unsaturated ketone or ester as illustrated in structure *cis*-**6**. This requirement can be achieved

Scheme 3:

Compound	R_1	R_2	R_3	R_4
7	Me	H	Me	Me
8	Me	Me	Me	H
9	Me	H	Me	H
10	Me	Me	Me	Me
11	nPr	H	Me	Me
12	Ph	H	Ph	Me
13	Me	OMe	Me	Me
14	Me	H	iPr	Me

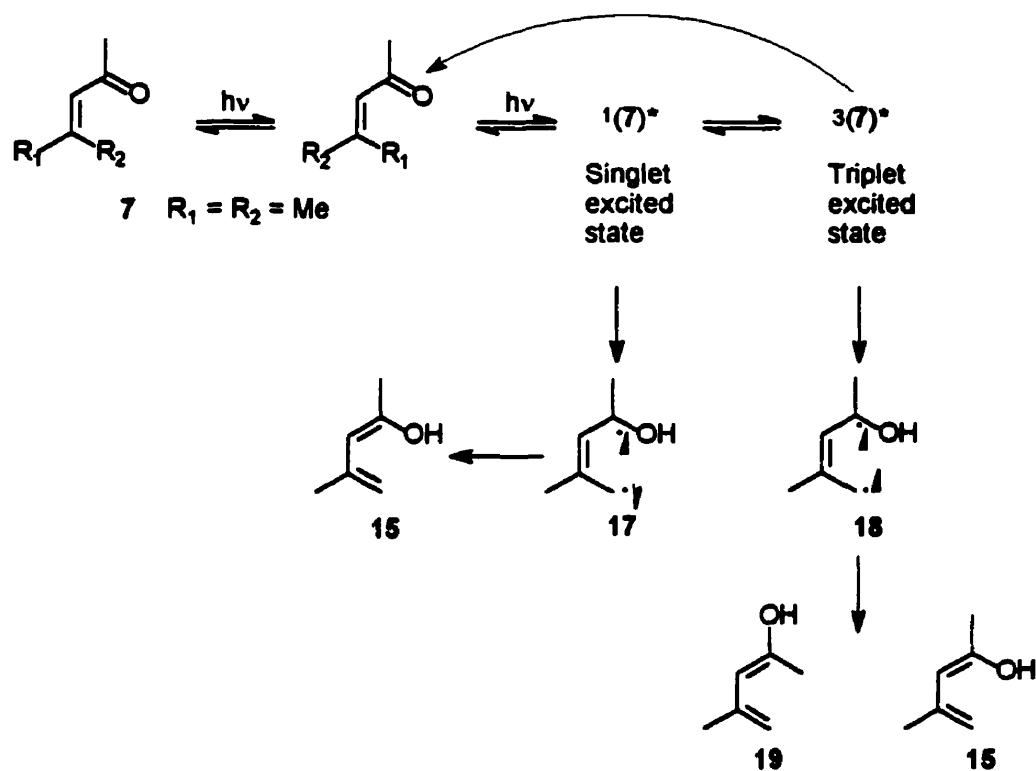
Scheme 4:

Further evidence of dienol formation by a photochemical process was demonstrated by a dienol trap experiment.⁶ In this experiment, the α,β -unsaturated ketone **7** was irradiated in dimethylformamide containing chlorotrimethylsilane and imidazole. The major product of the photochemical reaction was the silyloxy (Z)-diene **16**.



This experiment also led to the conclusion that the γ -hydrogen abstraction in ketones occurs from the singlet excited state. This conclusion was based on the fact that only the *Z*-silyl ether **16** was formed. The triplet excited state was expected to give rise to both the *Z* and *E* isomers as shown in Scheme 5.

Scheme 5:



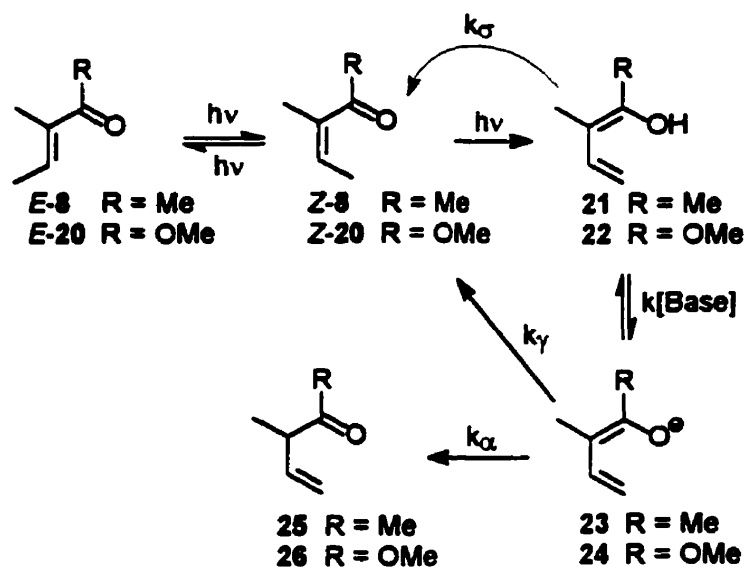
Ketone **7**, on irradiation, first forms the singlet excited state. This singlet excited state can decay to starting ketone by *E-Z* isomerization, can undergo γ -hydrogen abstraction, or can intersystem cross to the triplet excited state. The γ -hydrogen abstraction by the singlet excited state of **7** leads to the singlet biradical **17** which rapidly

forms dienol **15** only. The triplet excited state could possibly also undergo γ -hydrogen abstraction to give the triplet biradical **18** in competition with decay back to ground state **7**. If formed, the triplet biradical **18** could undergo bond rotation, during the time it takes for spin inversion to occur, forming both *Z* and *E*-dienols **15** and **19**. The dienol trapping experiment, mentioned above, yielded only *Z*-dienol **16** as the major reaction product. This indicated that the γ -hydrogen abstraction occurred only in the singlet excited state. More evidence for the photoenolization occurring in the singlet excited state was obtained from the irradiation of **7** in the presence of base (imidazole) and a triplet sensitizer (3-methoxyacetophenone). The only observable reaction in this experiment was *E-Z* isomerization of the ketone indicating that there was no photodeconjugation from the triplet state.⁶

An overall view of the photodeconjugation mechanism for ketones and esters is shown in Scheme 6. The first part of the mechanism is the formation of dienol, **21** or **22**, as mentioned above. The next part of the mechanism involves the conversion of the dienol to the corresponding deconjugated products, **25** or **26**, or the conjugated starting material, **8** or **20**. There are, *a priori*, three ways that this might happen. Reconversion of the dienols **21** or **22** to the conjugated carbonyl compounds, **8** or **20**, might occur via a thermal suprafacial 1,5-sigmatropic hydrogen shift (designated by rate constant k_s in Scheme 6).^{6,7} The dienol intermediate, **21** or **22**, could also lose a proton to form the dienolate anion, **23** or **24**. These intermediates could be subsequently protonated at the γ position (rate constant k_γ), leading to conjugated starting materials, or protonated at the α position (rate constant k_α), leading to the deconjugated products. Lastly, there is the

possibility that protonation of dienols **21** or **22** could occur prior to deprotonation of the enol hydroxyl group.

Scheme 6:



It was mentioned previously that the irradiation of the β -alkyl α,β -unsaturated ketones **7** to **14** in the absence of base resulted in E-Z isomerization and that the dienols that formed only underwent a thermal suprafacial 1,5-sigmatropic hydrogen shift, reverting back to the starting materials.^{6,7,8,9} The irradiation did not form any deconjugated product. However, the β -alkyl α,β -unsaturated ketones underwent photodeconjugation in the presence of a base. The base appears to deprotonate the dienols to form the corresponding anions as shown in Scheme 6. These anions are then reprotonated at the α position leading to deconjugated products. No evidence in the literature has been advanced for a mechanism involving protonation of the dienol prior to deprotonation.

Photochemistry of α,β -unsaturated esters appears to be quite different from that of α,β -unsaturated ketones. The irradiation of β -alkyl α,β -unsaturated esters, such as **20**,

resulted in the formation of the photodeconjugated product even in the absence of base.^{3,4,7} The different reactivity of β -alkyl α,β -unsaturated ketones and esters is related to the higher pKa of ketone-derived dienols compared to that of the ester-derived dienols.⁷ It has been proposed that the ester-derived dienol **22** forms the anion **24** more easily than the corresponding ketone-derived dienol **21** since **22** is more acidic (see Scheme 6).⁷

The quantum yields of *E-Z* photoisomerization for the ketone **8** and the ester **20** were found to be 0.82 and 0.41, respectively.⁷ The value of the quantum yield indicates that 82% of the excited state of ketone **8** produced by direct irradiation decays via *E-Z* isomerization while only 41% of the excited ester **20** decays via this route. In the ester **20**, photoenolization only accounts for 8% of the excited states and processes other than those already listed (51%), account for the rest of the excited states.⁷

A deuterium exchange experiment was performed to calculate the k_{α}/k_{γ} ratio for the ester **20**. The result indicated that the anion **24** was predominantly protonated at the α -position to give deconjugated product **26** as a major product and the ratio of k_{α}/k_{γ} was 4.4 ± 1.4 .⁷

There are two explanations that have been given for the lower *E-Z* isomerization efficiency of esters compared to ketones. In one explanation, it was proposed that closer proximity of the $n\pi^*$ and $\pi\pi^*$ states in the esters could enhance the rate of internal conversion to the ground state without *E-Z* isomerization. The absorption spectra of the ketone **8** and the ester **20** support this idea.⁷ For the ester **20**, the $n\pi^*$ band is submerged beneath the $\pi\pi^*$ band whereas for ketone **8** they are well separated. The other possible explanation is that intersystem crossing to the triplet is faster in the enone than in the ester.^{6,7,10} This would result in a shorter singlet lifetime for the ketone and more efficient

triplet formation that would then undergo *E-Z* isomerization. The triplet energy of both the ester **20** and the ketone **8** are found to be 72.0 ± 0.5 kcal mol⁻¹.¹⁰ The singlet energy for **20** and **8** are 130 and 97 kcal mol⁻¹, respectively. Thus, the energy difference between the singlet and triplet excited states for ester **20** and ketone **8** are 58 and 25 kcal mol⁻¹, respectively.¹⁰ The larger singlet-triplet splitting of ester **20** might slow its intersystem crossing compared to the ketone **8**.

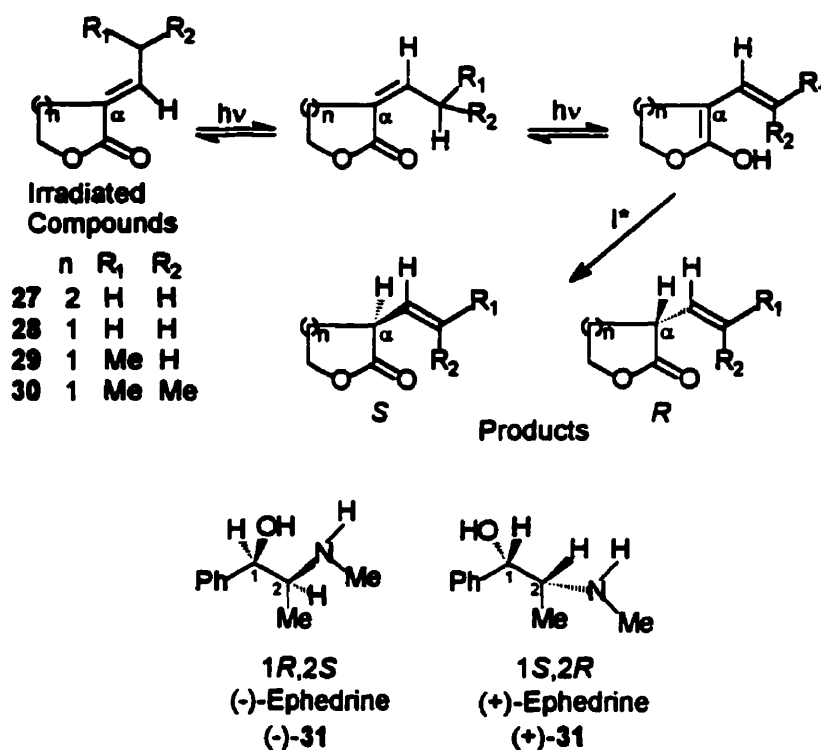
Section 1.2: Asymmetric photodeconjugation

Photodeconjugation of α -substituted- α,β -unsaturated esters or ketones to the corresponding β,γ -unsaturated esters or ketones can produce a new chiral center at the α -carbon as shown in Scheme 7. There are two main strategies for controlling the asymmetric induction of the new chiral center. The first is to use a catalytic amount of a chiral protonating agent, also known as chiral inductor, I^* , to asymmetrically protonate the dienol intermediate at the α -carbon. The second strategy is to place a chiral auxiliary on the α,β -unsaturated ester substrate. The dienol intermediate from such esters may assume a conformation in which protonation will occur more readily on one face of the α -center than on the other. Thus, one configuration will be produced in excess at the new chiral center. In this part of the introduction, studies of chiral inductors will first be summarized. The use of chiral auxiliaries in asymmetric photodeconjugation will be described next. Lastly, the simultaneous use of both chiral inductors and chiral auxiliaries will be discussed.

Scheme 7 illustrates the asymmetric induction which can occur during the photodeconjugation reactions of α -alkylidene butyro and valero lactones, compounds

which have restricted conformational mobility.¹¹ Compounds **27** to **30** were irradiated in aprotic solvents in the presence of a catalytic amount of the chiral inductor (I^*) (-)-ephedrine, **31**. The optical activities of the deconjugated products (each an unequal mixture of *R* and *S* enantiomers), were used to determine enantiomeric excesses.

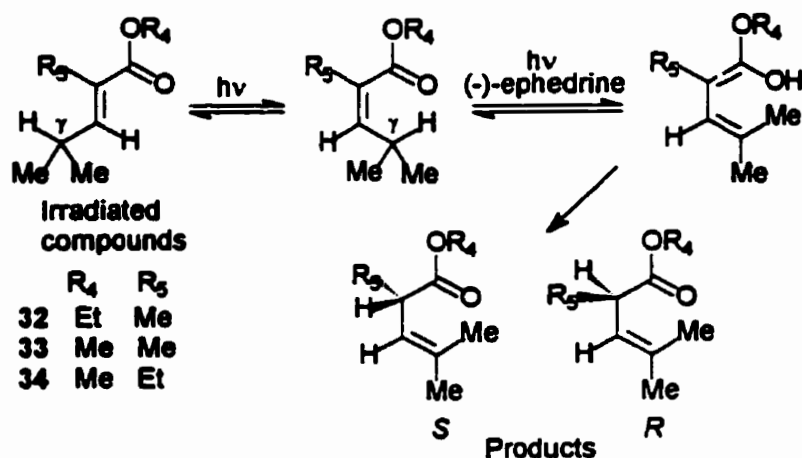
Scheme 7:



The results indicated that (-)-ephedrine asymmetrically induced the formation of the *R* configuration at the α -carbon in the deconjugated products. The diastereotopic discrimination increased when the temperature was decreased. The enantiomeric excess achieved from (-)-ephedrine catalysed photodeconjugation of **27** and **30**, a reaction that produced the *R* configuration at the α center, increased from 2.2% and 5%, respectively, at room temperature to 27% and 25% at -78°C.

The success of using (-)-ephedrine, as a chiral catalyst in the above photodeconjugation reactions, led to similar studies on the aliphatic α,β -unsaturated esters, 32 to 34, as shown in Scheme 8.¹² (-)-Ephedrine also induced an excess of the *R* configuration at the new chiral centers of the deconjugated products (enantiomeric excess for the irradiation of 32, 33 and 34 were 16, 18 and 12%, respectively).

Scheme 8:



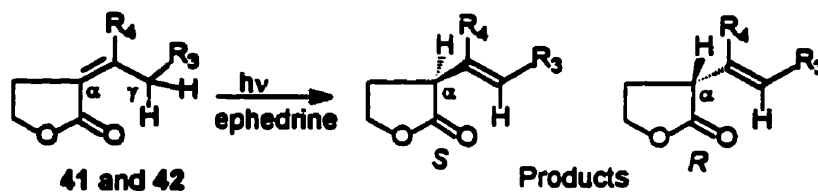
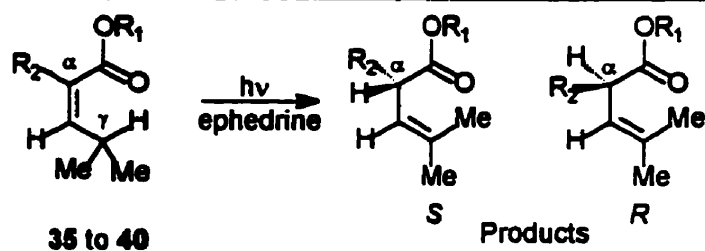
A knowledge of the transition state structure and the interactions responsible for the chiral discrimination is important for future design of more efficient and more selective reactions. In an effort to obtain additional information, variation of the kind and position of substituents in the starting conjugated esters or lactone (compounds 35 to 42 in Table 1) was examined in order to determine the effect on the asymmetric induction.¹³

The results in Table 1 showed that the absolute configuration of the new asymmetric center, α -C, in the photodeconjugated products did not depend on the nature of the ester group of the starting esters.¹³ The absolute configuration induced was also still the same when the α -methyl group was replaced by an α -ethyl group. The

configuration at α -C of the photodeconjugated products was always *R* when the chiral inductor was (-)-ephedrine and was always *S* when the chiral inductor was (+)-ephedrine.

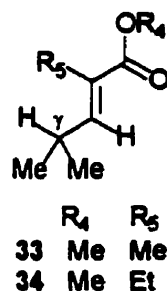
Table 1: The efficiency of ephedrine as a chiral inductor in photodeconjugation reactions of α,β -unsaturated esters.

Irradiated Cmpds	ephedrine	R ₁ (35 - 40) R ₃ (41, 42)	R ₂ (35 - 40) R ₄ (41, 42)	Config. at α -C	ee (%)
35	(+)	(CH ₃) ₂ CH	Me	<i>S</i>	20
36	(+)	C ₆ H ₅ -(CH ₂) ₂	Me	<i>S</i>	29
37	(+)	C ₆ H ₅ -(CH ₂) ₃	Me	<i>S</i>	22
38	(+)	C ₆ H ₁₁ -CH ₂	Me	<i>S</i>	17
39	(+)	(CH ₃) ₂ C=CHCH ₂	Me	<i>S</i>	20
40	(-)	C ₆ H ₅ -CH ₂	Me	<i>R</i>	28
40	(+)	C ₆ H ₅ -CH ₂	Me	<i>S</i>	31
41	(-)	-(CH ₂) ₄ -	-	-	0
42	(-)	H	Me	<i>R</i>	0.5



When the ester group was changed from methyl (**33** in Scheme 8), to ethyl (**32** in Scheme 8), to isopropyl (**35**) or even cyclohexylmethyl (**38**) very little change in enantioselectivity was observed. This indicated that only small steric interactions were present between ephedrine and the ester group of the photoenol intermediate. Interestingly, the enantiomeric excess increased more when the ester group was changed to a phenyl (**39**) or benzyl (**40**) group. This may indicate that there are secondary interactions between the phenyl group and the ephedrine. However, the real nature of these interactions is still unknown.

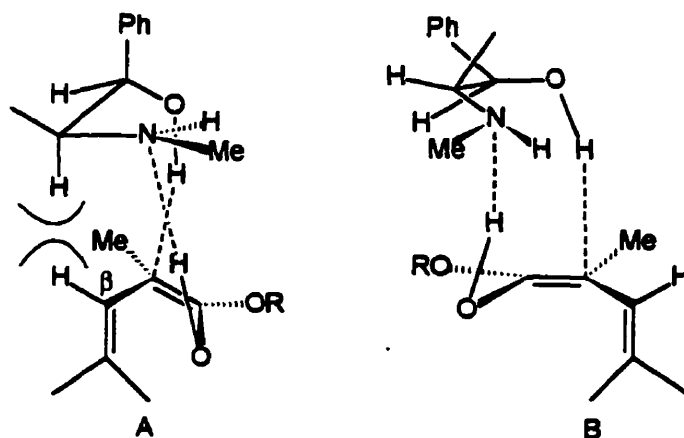
A more important effect on enantiomeric excess was found on altering the substituents on the conjugated part of the esters, i.e. at the α , β and γ positions. A significant decrease in enantiomeric excess for the photodeconjugation reaction was observed when the α -methyl of the starting material **33** was replaced with the α -ethyl substituent as in **34** (18% to 12%, respectively). Furthermore, β -substitution, as in **41** and **42**, decreased the induction to near zero.



Two models for the transition state for the (-)-ephedrine catalyzed tautomerism of the intermediate photodienol were proposed by Pete *et al.* and are shown in Figure 1.¹³ In A, a transition state that would lead to the *S* product, a major steric interaction exists between the substituents on the β -carbon atom of the dienol and the carbon atom that

bears the amino group in ephedrine. In B, the transition state that leads to the observed *R* product, no such interaction occurs.

Figure 1: Proposed transition states for (-)-ephedrine catalysed tautomerization of the photodienol

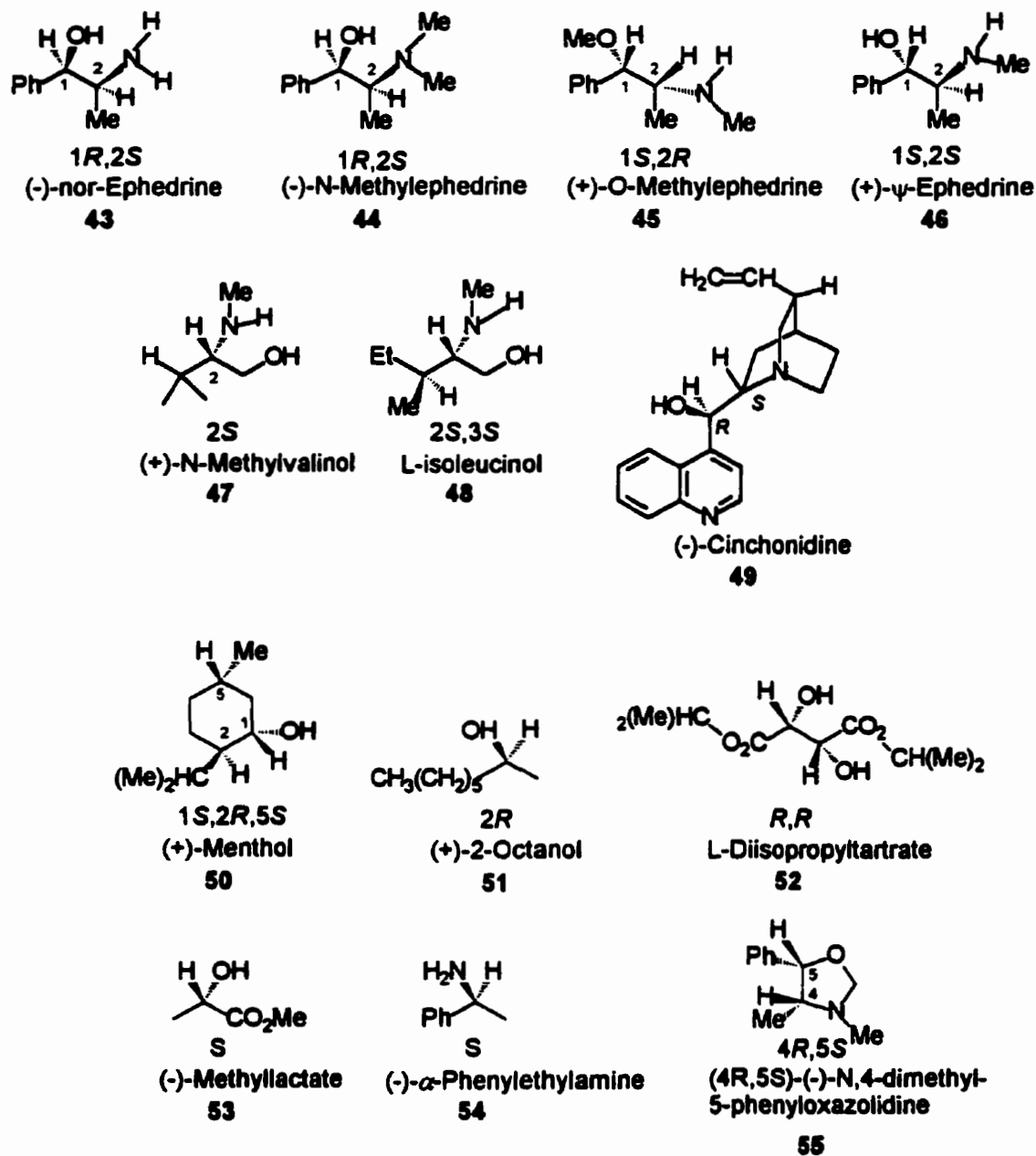


It was suggested that complex B, formed between (-)-ephedrine and the prochiral dienol, is stabilized by four factors. Firstly, there is a strong interaction between the hydroxyl of the dienol and the nitrogen of the ephedrine. Secondly, the hydroxyl proton of the inductor interacts strongly with the π orbital of the dienol. Thirdly, the large substituents on the inductor, phenyl and methyl, are as far as possible from the dienol. Lastly, the least hindered conformation of ephedrine is retained.

The proposed model B in Figure 1 incorporates two hydrogen bonds between the inductor and the dienol intermediate. It was suggested that the configuration of the carbon atom next to the amine group dictated the selectivity of the photodeconjugation reaction.¹³ To examine this suggestion and the importance of the hydrogen bonds mentioned, the stereochemistry induced by various chiral inductors in the

photodeconjugation of benzyl-2,4-dimethyl-2-pentenoate, **40**, was studied.^{14,15} The results are reported in Table 2.

Figure 2: Chiral inductors used in photodeconjugation reactions.



When ephedrine was replaced by a catalytic amount of a chiral alcohol (run 3 to 4) clean deconjugation took place but almost no asymmetric induction was observed. This

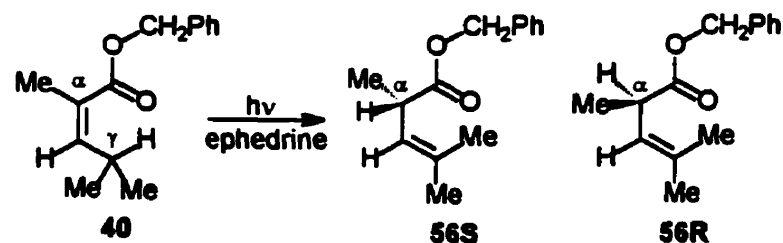
result suggested that a hydrogen bond between the amine group of an inductor and the hydroxyl group of the dienol was important to the enantioselectivity of the reaction.

Table 2 shows that (-)- α -phenylethylamine (run 7) gave very low selectivity. Also, O-methylated (+)-ephedrine (run 8) lowered the enantiomeric excess by a factor of 4. This showed the importance of the hydrogen bond between the inductor and the π -orbital of the dienol. The chiral amines bearing no hydroxyl group in the molecule led to a considerably lower enantioselectivity than ephedrine.

The strong interaction developed between the acidic enolic proton^{14,16} and the nitrogen atom of a chiral amine appears to influence the enantioselectivity of the reaction.^{14,17} The strength of this interaction can be altered by changing the substituents on the nitrogen. The importance of the substitution on the nitrogen atom can be seen in runs 1, 11 and 12. The replacement of the secondary amino group of (-)-ephedrine by a primary amine in (-)-nor-ephedrine or a tertiary amine in (-)-N-methyl-ephedrine lowered the enantioselectivity of the photodeconjugation of 40. One exception to this was seen in run 9, where cinchonidine, a tertiary amine, increased the enantioselectivity when it was used as chiral inductor.

Chiral inductors possessing both an amino and a hydroxyl group increased the enantiomeric excess. This can be seen in the results of runs 12,14 and 15, obtained with (-)-nor-ephedrine, (+)-N-methylvalinol and L-isoleucinol.

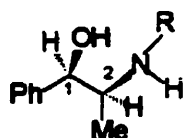
Table 2: The efficacy of various chiral inductors in photodeconjugation reactions of α,β -unsaturated esters **40**. (see Figure 2 for the structures of inductors)



Run	Inductors (I*)			Major config. at α -C	ee (%)
1	(-)-ephedrine	<i>R</i>	<i>S</i>	<i>R</i>	28
2	(+)-ephedrine	<i>S</i>	<i>R</i>	<i>S</i>	31
3	(+)-menthol	<i>R</i>	-	-	-
4	(+)-octanol	<i>R</i>	-	-	-
5	L-diisopropyltartrate	<i>R,R</i>	-	-	<1
6	(-)-Methylactate	<i>S</i>	-	<i>R</i>	1.5
7	(-) α -phenyl-ethylamine	-	<i>S</i>	<i>R</i>	4
8	(+) O-methyl-ephedrine	<i>S</i>	<i>R</i>	<i>S</i>	7
9	Cinchonidine	<i>R</i>	<i>S</i>	<i>R</i>	37
10	(-)-Oxazolidine	<i>S</i>	<i>R</i>	<i>S</i>	<2
11	(-)-N-Methyl-ephedrine	<i>R</i>	<i>S</i>	<i>R</i>	6
12	(-)-nor-ephedrine	<i>R</i>	<i>S</i>	<i>R</i>	14
13	(+)- ψ -ephedrine	<i>S</i>	<i>S</i>	<i>R</i>	4
14	(+)-N-methylvalinol	-	<i>S</i>	<i>R</i>	14
15	L-isoleucinol	-	<i>S</i>	<i>R</i>	14

The results in Table 2 also indicated that the configuration of the major enantiomer of the photodeconjugated product seemed to depend only on the configuration of the carbon atom linked to the nitrogen atom. The *R* configuration of the deconjugated product (**56R**) was always a major enantiomer when the configuration of the carbon linked to nitrogen of the inductor has the *S* configuration. The presence of a hydroxyl group was essential for the increase in the enantiomer excess, however, results in Table 2 indicated that the configuration of the carbon linked to the hydroxyl group did not seem to affect the selectivity of the photodeconjugation reaction.

For the reactions described above the highest enantiomeric excess achieved was 37%, a selectivity that is too low for practical synthetic applications. Thus, more efficient chiral inductors needed to be designed. Several newly designed chiral inductors were built around the structure of the amino-alcohol ephedrine by altering the substituent on the nitrogen.¹⁸



1*R*,2*S*

- 57** R = Ph-CH₂
- 58** R = p-CH₃OC₆H₄-CH₂
- 59** R = (CH₃)₂CH-CH₂
- 60** R = (CH₃)₂CH
- 61** R = 3-pentyl
- 62** R = cyclopentyl
- 63** R = cyclohexyl

Irradiation of **40** in the presence of the N-isopropyl substituted inductor, **60**, gave the highest enantiomeric excess, 70% for the *R* enantiomer. When the N-substituent was

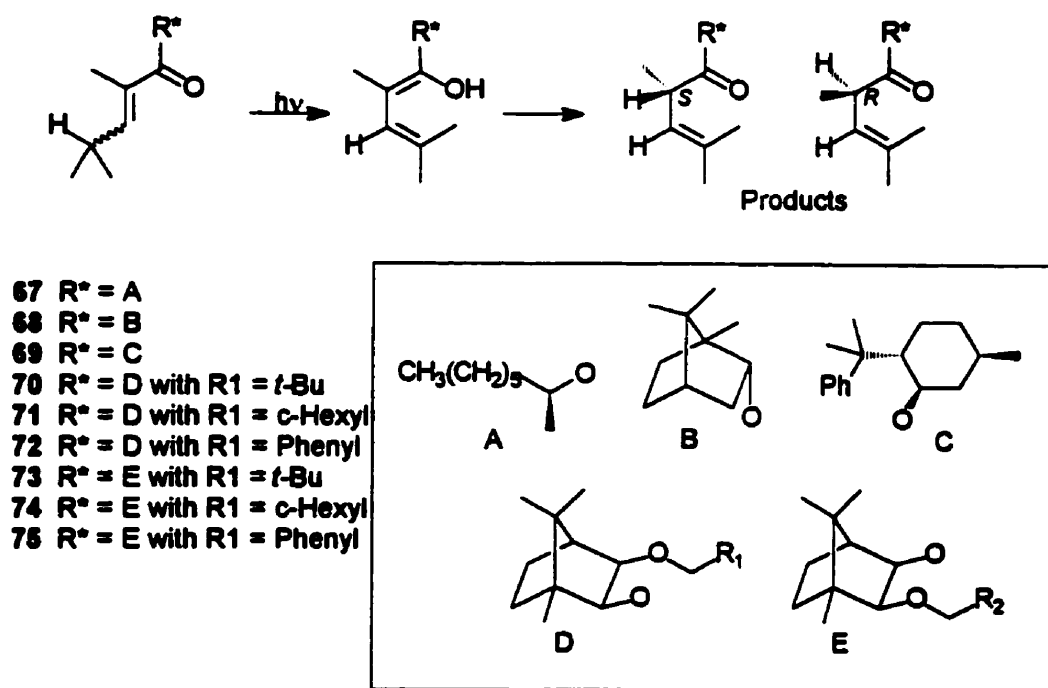
By contrast, irradiation of **40** in the presence of the *exo,exo* isomers **66a** to **66e** resulted in high enantioselectivity of the deconjugated product (see below), especially if the nitrogen atom carried an isopropyl (**66c**), or a benzyl (**66e**), group. As already observed with acyclic aminoalcohols, the substitution of the nitrogen atom considerably influenced the enantioselectivity.

Unexpectedly, the configuration of the new chiral center of the photodeconjugated product was reversed on enlarging the substituent on the nitrogen of **66a**. **56S** was a major product with enantiomeric excess of 54% when **40** was irradiated in the presence of chiral inductor **66a**. When the N-substituent was made larger, as in **66b**, the enantiomeric excess (ee) for **56S** decreased to 5%. Larger N-substituents, such as isopropyl in **66c** (ee of 89%), cyclohexyl in **66d** (ee of 80%) or benzyl in **66e** (ee of 91%), inverted the stereoselectivity to give deconjugated product to **56R**.

Since high selectivity was obtained (ee up to 91% at -55 °C), photodeconjugation of other unsaturated esters and alkylidene lactones was performed in the presence of **66c**. Irradiating various α -substituted α,β -unsaturated esters in the presence of **66c** consistently yielded better enantiomeric excess than previous inductors.¹⁹

Another way of controlling the asymmetric induction during a photodeconjugation reaction is to place a chiral auxiliary in the ester group of the α,β -unsaturated ester in order that the chiral esters may exert intramolecular asymmetric induction during the protonation step of the photodienol. To study the selectivity induced by different chiral auxiliaries, the photodeconjugation of chiral esters of 2,4-dimethyl-2-pentenoic acid was investigated (Scheme 9).^{20,21}

Scheme 9:

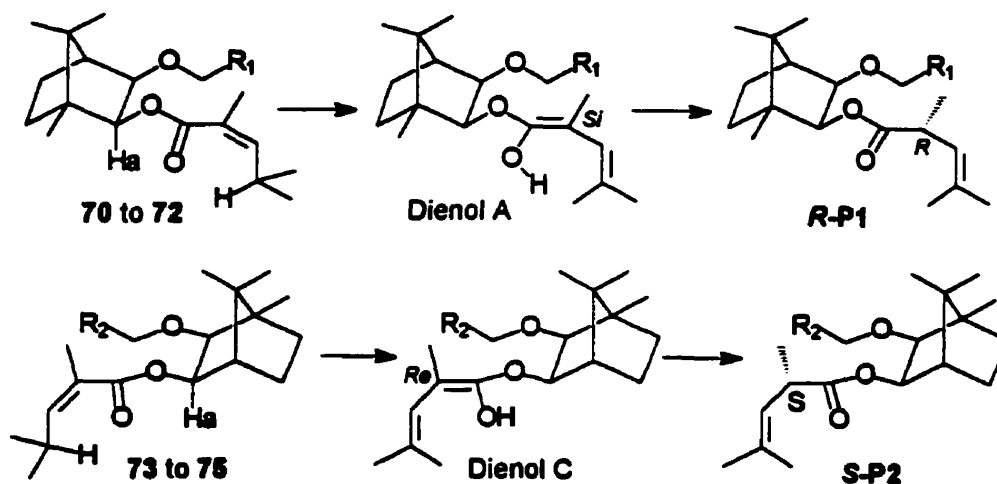


When ester **67** was photodeconjugated at $-78\text{ }^{\circ}\text{C}$ in hexane containing anhydrous methanol, a low diastereoisomeric excess (19%) of the *S* deconjugated products was observed, while there was no selectivity at all from irradiating ester **68**. These results indicated that the chiral auxiliaries in the ester group were able to exert only a minor effect on the facial selectivity of the protonation at the α center of the dienol from **67** or **68**.

Esters containing larger and more rigid chiral auxiliary groups gave much better diastereoselectivities. A diastereoisomeric excess (de) of 55% was obtained for the phenyl menthyl ester **69**. For the more hindered esters, **70** to **75**, diastereoselectivity increased significantly, especially in the presence of diisopropylamine where a de of up to 88% was obtained. The deconjugated products for the irradiation of compound **70** to **72** produced mainly the *R* configuration at the new α chiral center, while compound **73** to **75** produced the *S* configuration products. This selectivity was rationalized as illustrated in Scheme

10.²¹ Selective protonation of the dienol from the outside face of the dienol led to the observed product.

Scheme 10:

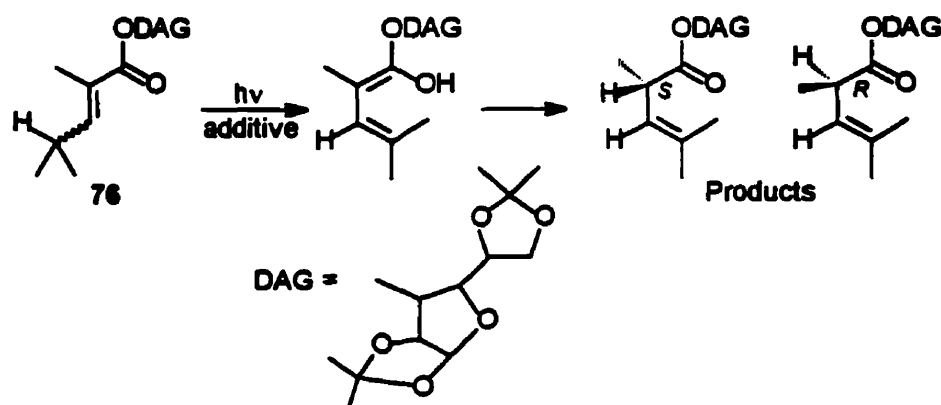


Camphor derivatives such as compounds 70 to 75 required multistep synthesis, and a more readily available chiral auxiliary that could yield high selectivity in the photodeconjugation reaction was sought. A commercially available reagent, 1,2,5,6-isopropylidene- α -D-glucofuranose (commonly known as diacetone D-glucose, DAGOH), has been used successfully to obtain high asymmetric induction in various types of reactions. This reagent was therefore chosen for study as a chiral auxiliary in the photodeconjugation reaction, as shown in Scheme 11.²²

Generally, irradiation of 76 in dichloromethane produced the *S* configuration at the α -carbon of the deconjugated product, when alcohol was used as an additive. The selectivity was reversed when amine was used as an additive. This indicated that one face of the photodienol was selectively protonated in the presence of alcohols and other face in the presence of amines. When both an alcohol and an amine were present, the protonation occurred preferentially on the same face as with the amines alone. The preferential control

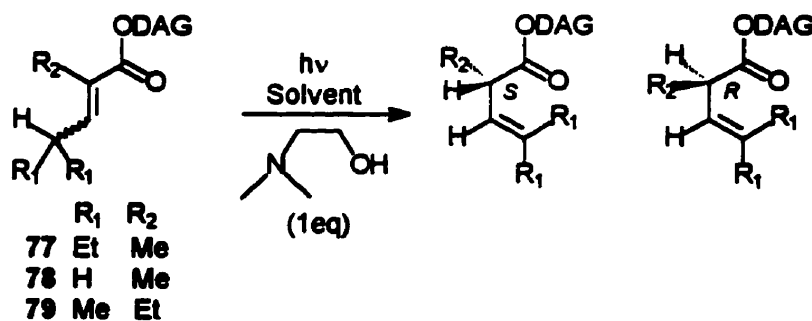
of the reaction by amine might be due to the stronger interaction of the amine with the photodienolic proton of the intermediate. Currently, there has not been a proposal for the mechanistic role of the alcohol and amine additives. High selectivity (up to 88% de) was obtained in the presence of a catalytic amount of an achiral agent bearing both a hydroxyl group and an amino function such as *N,N*-dimethylaminoethanol.²²

Scheme 11:



Irradiation of **76** at a lower temperature increased the diastereoselectivity considerably. In the presence of the *N,N*-dimethylaminoethanol as an additive and the nonpolar solvent octane, the de of the *R* product was increased to 98%. Finally, the photodeconjugation reaction was generalized to other α,β -unsaturated esters as shown in Scheme 12 and the corresponding β,γ -isomers, **77** to **79**, which have also been obtained with very high diastereomeric excess (up to 98%).

Scheme 12:

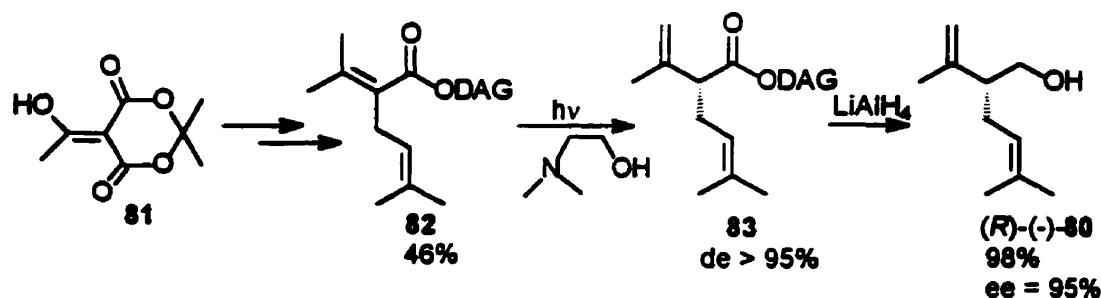


The simultaneous use of a chiral auxiliary and a chiral inductor did not enhance the absolute stereoselectivity at the α -carbon.^{20,21} When esters **67** and **68** were irradiated in the presence of ephedrine, the observed diastereomeric excess (up to 33%) was very close to the enantiomeric excess obtained by irradiation of an achiral ester, such as isopropyl 2,4-dimethyl-2-pentenoate, **35**. When bulky esters **69** to **75** were irradiated in the presence of ephedrine, the diastereoselectivity decreased and sometimes inverted. No increase in diastereoselectivity was observed although a synergistic effect was expected from the proposed model in Figure 1. Where mismatched interactions were expected, the observed diastereoselectivities were considerably lowered or were inverted.

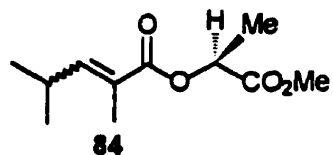
An asymmetric photodeconjugation reaction was utilized to synthesize (*R*)-(-)-lavandulol **80**.²³ (*R*)-(-)-lavandulol, a component of lavender oil that is an important additive in the perfume industry, has been isolated and identified as a defensive pheromone of the red-line carrion beetle. (*R*)-(-)-lavandulol had been prepared in racemic and optically active form²³ but photodeconjugation was able to provide a shorter method for its synthesis (see Scheme 13). Compound **82** was prepared from acetyl Meldrum's acid, **81**, in four steps with an overall yield of 46%. Compound **82** was then irradiated in CH₂Cl₂ with an equivalent of N,N-dimethylethanolamine. (*R*)-(-)-lavandulol **80** was

obtained in 98% yield from **82**, by reducing the deconjugated ester **83** with lithium aluminum hydride.

Scheme 13:



During the progress of the work described above, a decision was made to study the use of methyl (*S*)-lactate as a chiral auxiliary in esters undergoing asymmetric photodeconjugations. There were two reasons for choosing the methyl (*S*)-lactate as the chiral auxiliary: a) methyl (*S*)-lactate had been used successfully to obtain high asymmetric induction in certain Diels-Alder reactions,² and b) it is possible that the carbonyl in the carboxymethyl group of the chiral auxiliary might hydrogen bond to a protonating agent and help deliver the proton to one face of the α -carbon of the dienophile selectively. In this thesis work, methyl (*S*)-lactate was placed in the ester group of the α,β -unsaturated ester, **84**, and the photodeconjugation reaction of the ester was studied under various conditions.



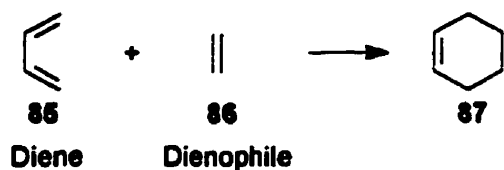
Chapter 2

Section 2.1: Diels-Alder reactions

In 1928 two German chemists, Otto Diels and Kurt Alder, discovered that the addition of 1,3-dienes to substituted alkenes was a general phenomenon.²⁴ Since then, this type of reaction, which now bears their names, has become one of the most intensively researched reactions in organic chemistry. In 1950, Diels and Alder were awarded the Nobel prize for the discovery of this important and versatile reaction.

The Diels-Alder reaction is a reaction of a conjugated diene with an olefin (often referred to as the dienophile) that generates a six membered ring. The simplest example of the Diels-Alder reaction consists of the cycloaddition of butadiene **85** with ethylene **86** to form cyclohexene **87** as shown in Scheme 14.

Scheme 14:

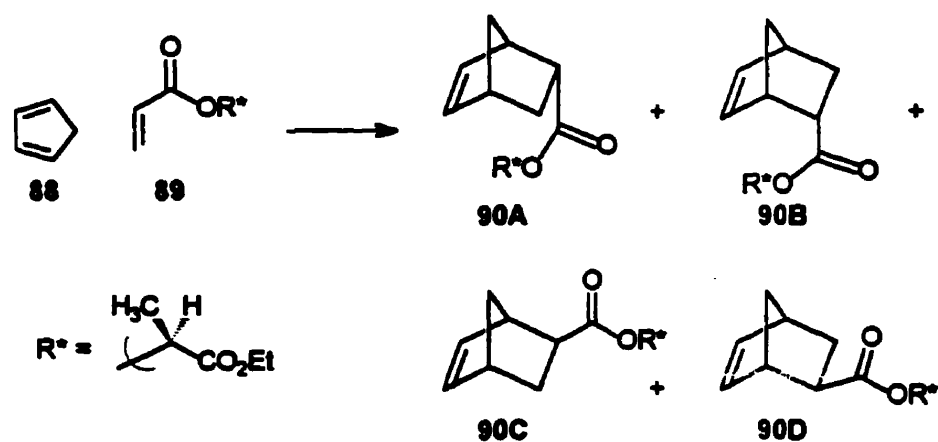


The Diels-Alder reaction is believed to occur by a concerted mechanism. A concerted mechanism requires a single transition state, and therefore no intermediate lies on the reaction path between reactants and adduct. Basic rules of the Diels-Alder reaction can be found in most organic chemistry books.²⁵ The reaction proceeds for the unsubstituted case as shown in Scheme 14, however, it occurs more readily when electron withdrawing groups (EWGs) are located on the dienophile and electron donating substituents (EDGs) are located on the diene.

Section 2.2: Asymmetric Diels-Alder reactions of sulfur base dienophiles

A common strategy for an asymmetric Diels-Alder reaction is to react a chiral dienophile with an achiral diene (Scheme 15). A chiral dienophile usually assumes a conformation such that one face is more sterically hindered than the other. Hence a diene approaches the chiral dienophile from the least sterically hindered face, and, as a result, one absolute configuration of the product is produced in preference to the other.

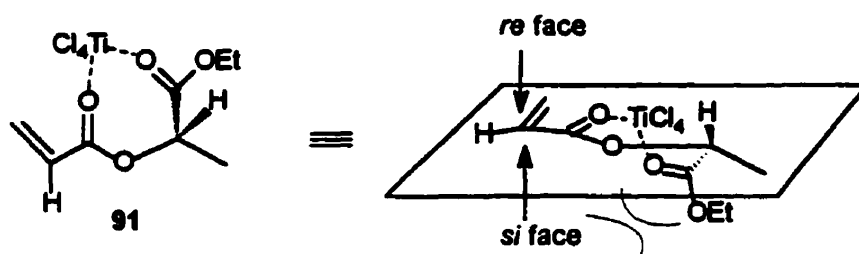
Scheme 15:



Lactate esters have been successfully used as chiral auxiliaries in certain asymmetric Diels-Alder reactions.^{2,26} A simple example is shown in Scheme 15, the acrylate of ethyl (*S*)-lactate 89 reacts with cyclopentadiene 88 to form four different diastereomers 90 (A to D).²⁶ Firstly in the absence of any added Lewis acid, high diastereoselectivity for 90 was observed in hexane with ratios of A:B and C:D of 20:80 and 15:85, respectively. The stereoselectivity between the *endo* (A and B) and *exo* (C and D) was 1.68 to 1. However, higher diastereoselectivities were obtained in the presence of a Lewis acid. In the presence of 0.75 equivalents of $TiCl_4$, the Diels-Alder reaction shown in Scheme 15, yielded an *endo:exo* ratio of 39 to 1, with the ratio of *endo* isomers A:B

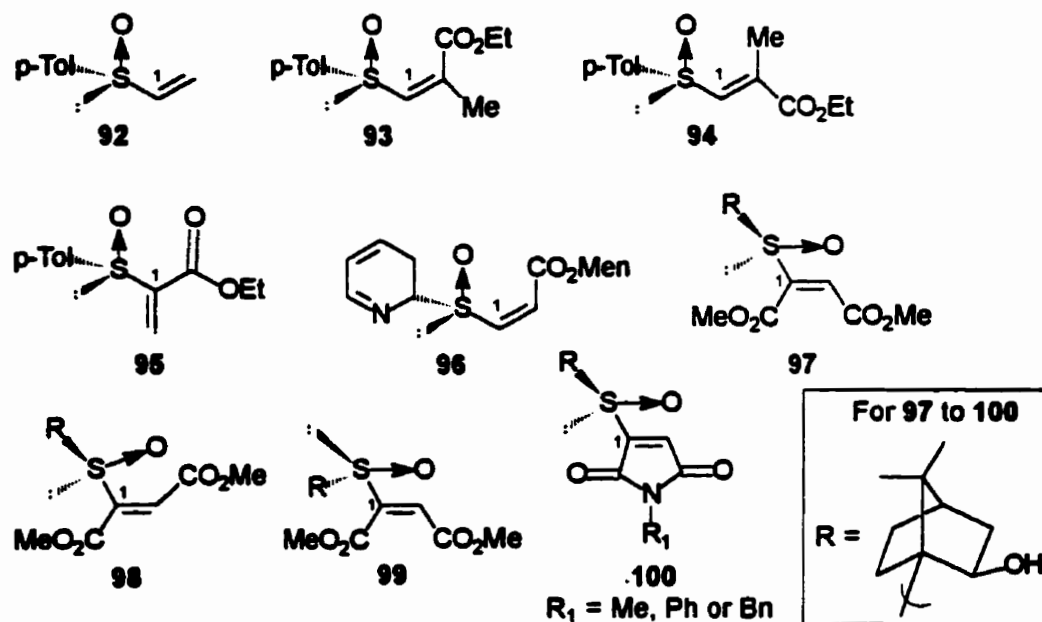
being 7 to 93. The high diastereoselectivity of this latter case was explained by the formation of a complex between the two carbonyl oxygens and the Lewis acid as shown in Figure 4.²⁷ The complex holds the large CO₂Et group firmly over the lower (*si*) face of the double bond, causing this face to be more sterically hindered. Cyclopentadiene thus prefers to approach from the less hindered (*re*) face to form **90B** as the major adduct.

Figure 4: Coordination of the two carbonyls of the dienophile to the metal (Ti).

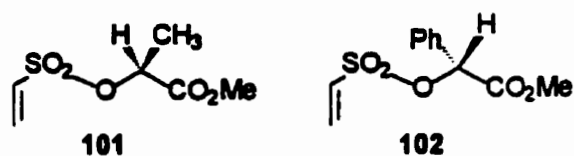


Chiral sulfoxides (Figure 5) are an excellent choice of chiral auxiliary for the Diels-Alder reaction^{28,29} although unsubstituted vinyl sulfoxides such as **92** are not very reactive. Under forcing conditions (90°C, 19 hours) cycloaddition with dienes takes place but there is very poor diastereoselectivity. Higher diastereoselectivity can be obtained when there is an additional carbonyl group conjugated to the vinyl group, as in compounds **93** to **100**. Adding an extra carbonyl group to the chiral vinyl sulfoxide also serves to enhance the reactivity of the dienophile. The presence of an extra carbonyl group at the C2 position serves to control the conformation by restricting the rotation of the C1-S bond. Diastereoselectivities increase even more when Lewis acids are present.

Figure 5: Some examples of chiral sulfoxides.



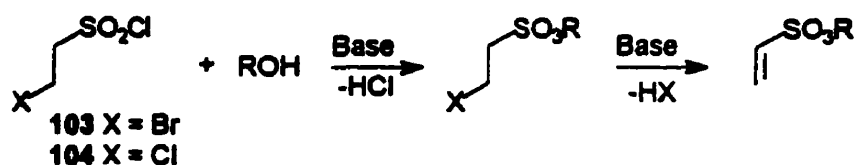
Vinylsulfonates are reactive dienophiles that readily participate in Diels-Alder reactions, and the sulfonate activating group can easily be removed after the reaction. Although there are reports of both intermolecular and intramolecular Diels-Alder reactions of vinylsulfonates, there do not appear to be any reports of asymmetric intermolecular cycloadditions of chiral vinylsulfonates. In this thesis, the chiral sulfonate dienophiles (methyl (*S*)-lactyl) vinylsulfonate **101** and (methyl (*R*)-mandelyl) vinylsulfonate **102**, were prepared and their asymmetric cycloaddition reactions examined. In this part of the introduction, methods of preparing vinylsulfonate esters will be discussed. Previous examples of both inter- and intramolecular Diels-Alder reactions of vinylsulfonate esters will also be briefly reviewed.



Section 2.3: Preparation of alkyl vinylsulfonates

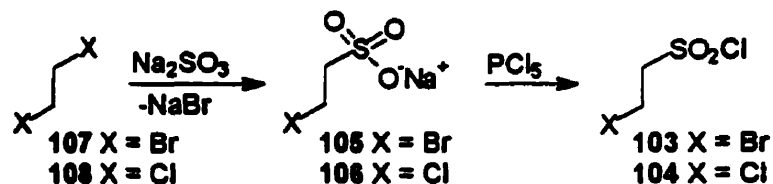
A general method for preparing alkyl vinylsulfonates has been described in the literature (Scheme 16).^{30,31,32} This method makes use of the reaction of a β -haloethanesulfonyl chloride with an alcohol in the presence of two equivalents of base. In this reaction, the base plays two roles. Firstly, it induces the addition of alcohol to the sulfonyl chloride, forming the sulfonate, and secondly, it causes the elimination of the β -halogen to form the corresponding alkene. Pyridine in an organic solvent, or KOH in water, has been generally used as the base in these reactions. The latter base has been used for preparing stable alkyl vinylsulfonates and aryl vinylsulfonates. However, the more reactive alkyl vinylsulfonates were best prepared in an organic solvent, using pyridine as the base.

Scheme 16:



The vinylsulfonate precursor, 2-bromoethanesulfonyl chloride 103 can be prepared as illustrated in scheme 17.^{33,34,35,36} Sodium sulfite is used to displace one of the bromines on ethylene bromide and the resulting salt can be recrystallized from ethanol.

Scheme 17:



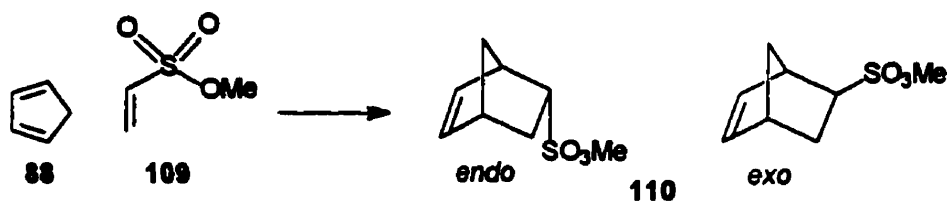
Heating **105** with an excess of phosphorus pentachloride produced the acid chloride **103**.^{34,35}

Whitmore and Landau provided a detailed method for the preparation of alkyl vinylsulfonates from β -haloethanesulfonyl halides.³⁰ They mixed the alcohol with one equivalent of the β -haloethanesulfonyl chloride in CH_2Cl_2 at 0°C followed by slow addition of pyridine, with stirring, to induce the coupling of sulfonyl chloride to the alcohol. A second equivalent of pyridine was then added to eliminate the β -halogen to yield the corresponding alkyl vinylsulfonate. After washing with dilute HCl, the reaction was worked up to give the crude product which was purified by distillation or recrystallization.

Section 2.4: Intermolecular Diels-Alder reactions of alkyl vinylsulfonates

The use of methyl vinylsulfonate **109** as a dienophile in a Diels-Alder reaction was first demonstrated by Lambert and Rose (Scheme 18).³⁷ They reacted **109** with cyclopentadiene at 150°C in a sealed tube to yield 75% of the *endo* cycloadduct *endo*-**110** after isolation.

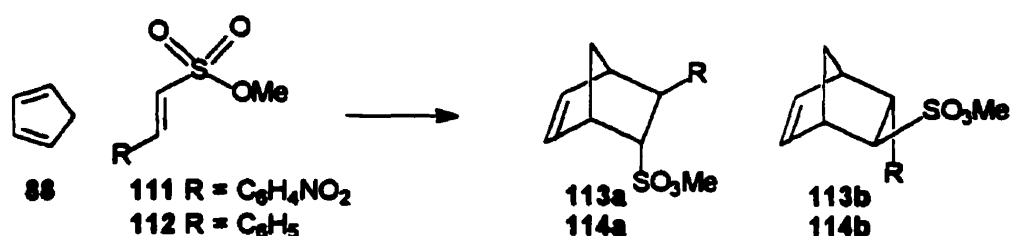
Scheme 18:



Methyl 2-(*p*-nitrophenyl)ethylene-1-sulfonate **111** and methyl 2-phenylethylene-1-sulfonate **112** were also investigated (Scheme 18).³⁸ Refluxing **111** with cyclopentadiene

for one hour in bromobenzene gave a 68% yield of a mixture of adducts. Variations in time or temperature reduced the yield, either increasing tar formation or returning more starting material. The adduct consisted of 113a and 113b in a ratio of 65:35. The phenyl substituted compound 112 yielded only 9% adduct.

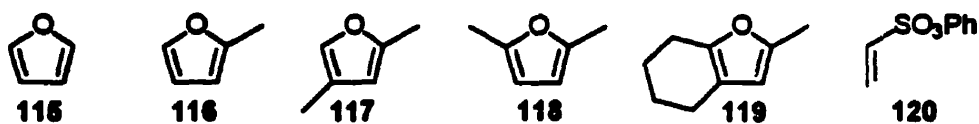
Scheme 19:



Intermolecular Diels-Alder cycloadditions of furan dienes (115 to 119 as shown in Table 3) require an extremely reactive dienophile. Diels-Alder reactions of furan derivatives usually require a doubly activated dienophile,³⁹ the presence of Lewis acids,⁴⁰ or high pressure conditions.⁴¹ Even in these cases, yields of products have not been consistently high, most particularly in the case of 2,5-disubstituted furan dienes. In contrast to most other dienophiles, phenyl vinyl sulfonate 120 (Table 3) gives consistently high yields when reacted with furan derivatives.⁴²

Table 3: Diels-Alder reaction of phenyl vinyl sulfonate 120 with furan derivatives.

Reactants



Products

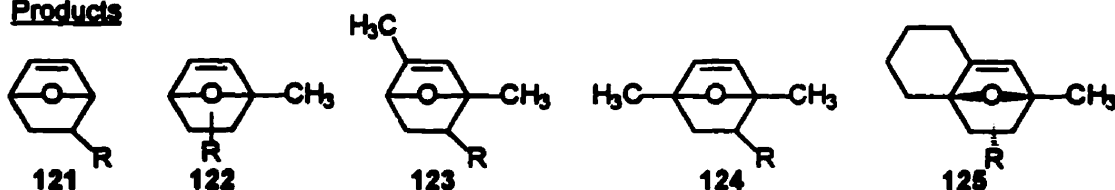


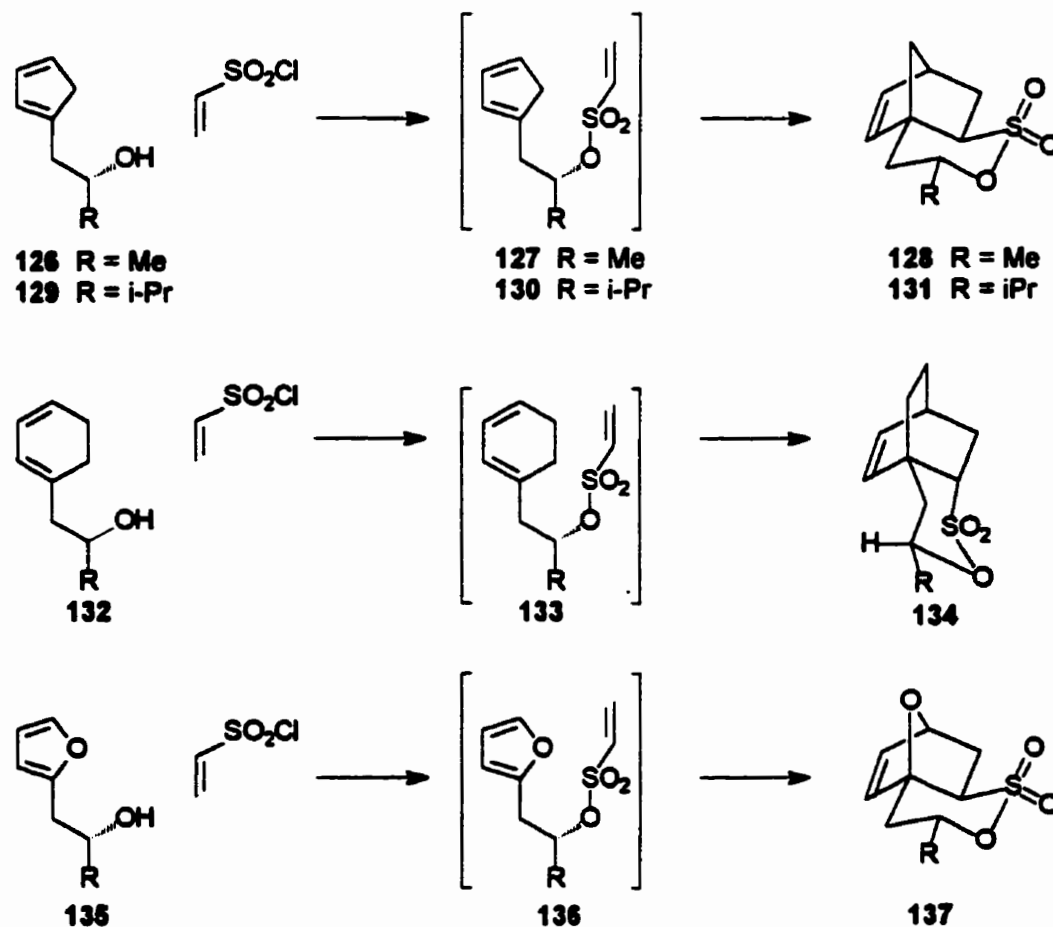
Table 3: continue

Run	Diene	Product	Yield (%)	<i>exo/endo</i>
1	115	121	84	1:2.6
2	115	121	48	5:1
3	116	122	85	2:5
4	117	123	88	1:2.6
5	118	124	87	1:5.4
6	118	124	48	1:2
7	119	125	90	<i>endo</i> only
8	119	125	88	1:1

Section 2.5: Asymmetric Intramolecular Diels-Alder reactions

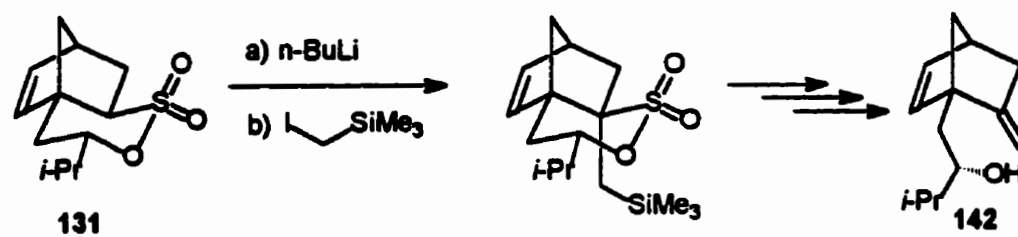
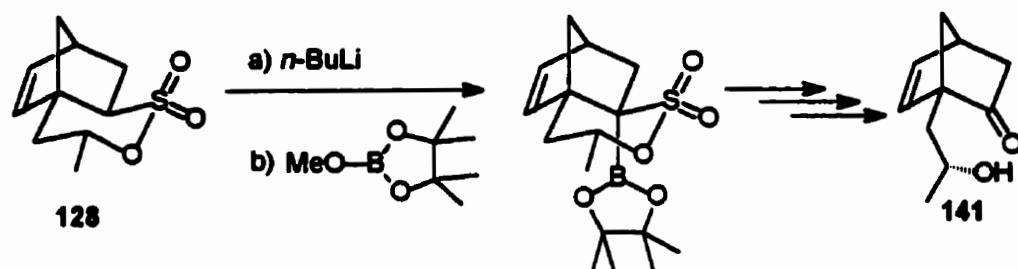
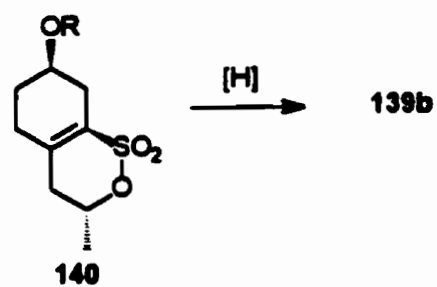
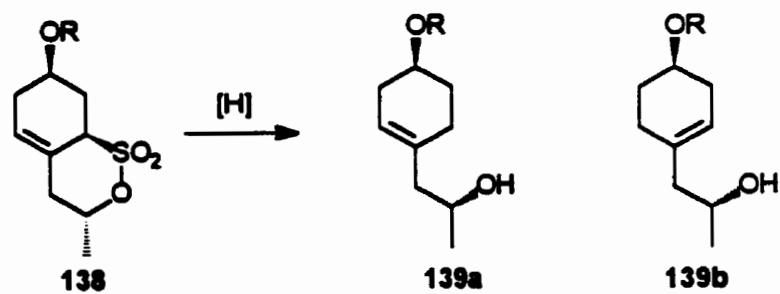
Asymmetric Diels-Alder reactions of vinylsulfonate esters have been carried out intramolecularly with high diastereoselectivity (Scheme 20).^{43,44} Esterification of alcohols **126** and **129** with sulfonyl chloride led directly to *exo* sultones **128** and **131**, respectively (d.e. >92% for both substrates). Cyclohexadiene **133** derived from alcohol **132** required reflux in toluene for complete conversion to **134**. In this case the *endo* sultone **134** was obtained predominantly with a diastereomeric excess greater than 87%. Intramolecular Diels-Alder reaction of the furan derivative **135** (Scheme 20) also proceeded readily with high diastereoselectivity (d.e. >90).

Scheme 20:



A sulfonate group is not only an excellent activating group, but it also can be easily removed or transformed into other functional groups (Scheme 21). When sodium in liquid ammonia was used to reductively cleave the allylic C-S bond of sulfone **138**, two isomeric products **139a** and **139b** were formed in approximately equimolar amounts.⁴⁵ A smooth desulfurization without migration of the double bond was achieved for vinylic sulfone **140** using lithium in liquid ammonia.⁴⁵ The sulfonate functional group can also be desulfurized and converted to a carbonyl or alkene functional group (Scheme 21).⁴⁶

Scheme 21:

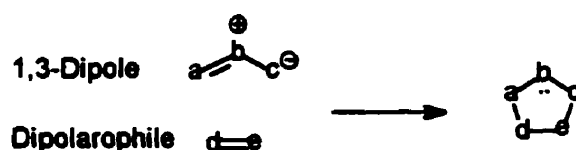


Chapter 3

Section 3.1: Dipoles.

The name 1,3-dipolar cycloaddition was first introduced in 1960 to describe the reaction of certain neutral, three atom, π systems, with a π bond to form five-membered rings (Scheme 22).^{47,48,49} This reaction occurs by a concerted mechanism.

Scheme 22:



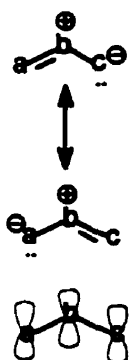
A feature shared by all 1,3-dipoles is a three atom π -electron system with four π -electrons delocalized over the three atoms. The name 1,3-dipole is derived from the fact that it is impossible to write electron-paired resonance structures for these species without incorporating charges. However, this does not imply that the compounds are particularly polar since the charges are not localized. Another feature shared by all 1,3-dipoles is that their central atom, atom *b* in Scheme 22, is a heteroatom.

There are two classes of 1,3-dipoles, the allyl and the propargyl-allenyl. 1,3-Dipoles of the allyl class are bent in the ground state, while the propargyl-allenyl ones are linear due to an extra π bond as shown in Scheme 23. The center atom *b* of 1,3-dipoles in the allyl class can be a group V element (N, P, etc.) or a group VI element (O, S). The choice is smaller for *b* in 1,3-dipoles of the propargyl-allenyl class where only tetravalent, group V elements bearing a positive charge are possible. By restricting the atoms *a* and *c*

to second row elements (C, N, and O), six 1,3-dipoles of propargyl-allenyl class and twelve 1,3-dipoles of allyl class can be envisioned (Table 4).

Scheme 23:

Allyl type



Propargyl-Allenyl type

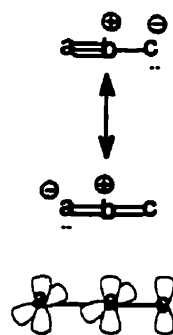


Table 4: Classification of 1,3-dipoles consisting of carbon, nitrogen and oxygen.

Allyl class			
	\longleftrightarrow		Azomethine Ylides
	\longleftrightarrow		Azomethines Imines
	\longleftrightarrow		Nitrones
	\longleftrightarrow		Azimines
	\longleftrightarrow		Azoxy compounds
	\longleftrightarrow		Nitro Compounds

Table 4: continued

Allyl class			
	↔		Carbonyl Ylides
	↔		Carbonyl Imines
	↔		Carbonyl Oxides
	↔		Nitrosimines
	↔		Nitrosoxides
	↔		Ozones
Propargyl-Allenyl class			
	↔		Nitrile Ylides
	↔		Nitrile Imines
	↔		Nitrile Oxides
	↔		Diazoalkanes
	↔		Azides
	↔		Nitrous Oxides

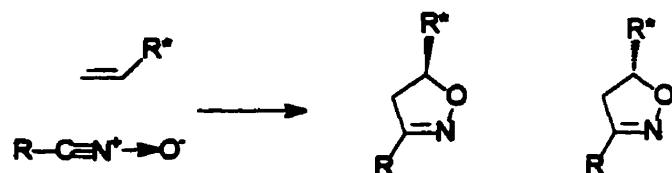
Section 3.2: Dipolarophiles

The other reactant in a 1,3-dipolar cycloaddition, usually an alkene or an alkyne, is referred to as the dipolarophile. Similar to the asymmetric Diels-Alder reaction, a

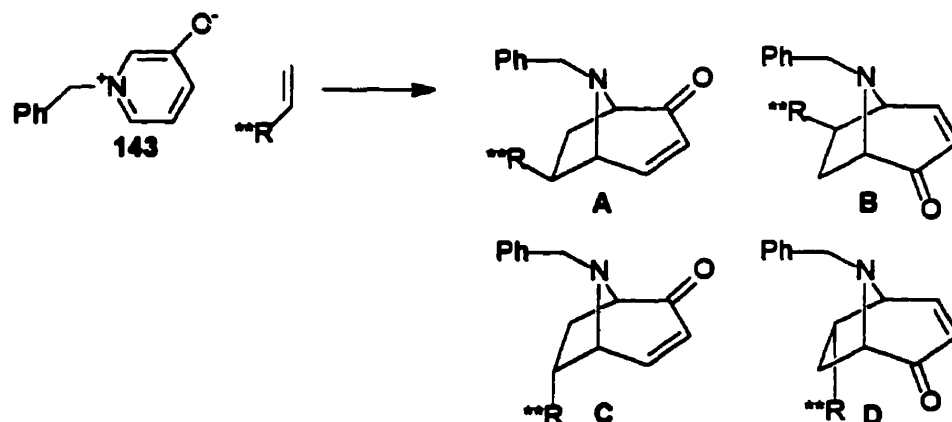
common strategy for an asymmetric 1,3-dipolar cycloaddition is to react a chiral dipolarophile with an achiral 1,3-dipole (Scheme 24).⁵⁰ In this thesis, asymmetric 1,3-dipolar cycloadditions of N-benzyl-3-oxidopyridinium betaine, a 1,3-dipolar species, were studied (Scheme 24). The following discussion leading to Chapter 4 consists of four parts. In the first part, preparation of N-substituted betaines will be briefly discussed. In the second part, different kinds of cycloadditions that betaines are capable of, will be reviewed. The third part will include a discussion of regio and relative stereoselectivities (*endo/exo*) of 1,3-dipolar cycloaddition reactions of betaines. In the last part of this introduction, asymmetric 1,3-dipolar cycloadditions of pyridinium betaines and their applications will be reviewed.

Scheme 24:

Asymmetric 1,3-dipolar cycloaddition of nitrile oxides



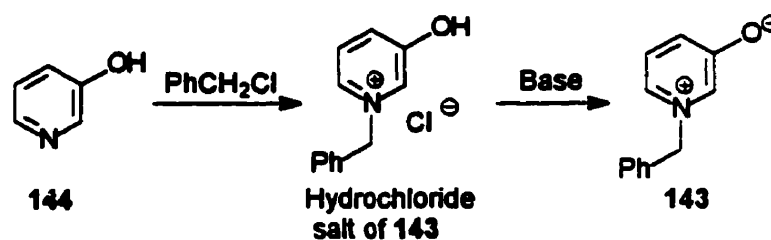
Asymmetric 1,3-dipolar cycloaddition of N-benzyl-3-oxidopyridinium betaine



Section 3.3: Preparation of N-substituted 3-oxidopyridinium betaines

Known N-substituted 3-oxidopyridinium betaines have been reviewed by Katritzky and Dennis.⁵¹ A simple procedure for preparing the salts of N-substituted pyridinium betaines involves the alkylation of 3-hydroxypyridine **144** by an appropriate alkyl halide. Thus the hydrohalide salt of **143** is obtained from the reaction of benzyl chloride or benzyl bromide with 3-hydroxypyridine as shown in Scheme 25.^{51,52} The hydrohalide salt can be converted to the corresponding 3-oxidopyridinium betaine **143** by reacting with bases such as NaOH, Amberlite IRA-401 (OH⁻) resin, or triethylamine.

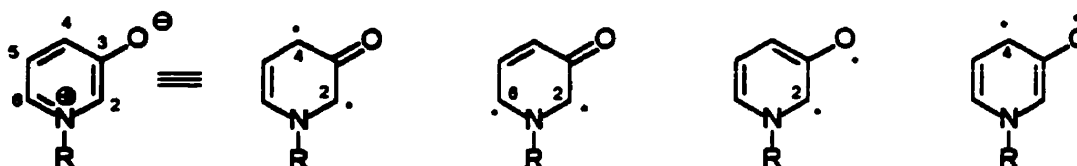
Scheme 25:



Section 3.4: Reactions of 3-oxidopyridinium betaines

The 3-oxidopyridinium betaines are versatile cycloaddition components capable of undergoing four different kinds of cycloaddition. Referring to the numbering in Figure 6, cycloaddition reactions have been observed across positions C2 and C4, C2 and C6, O and C2, and O and C4.

Figure 6: Reactive positions of betaines



Betaines with N-aryl substituents such as **146** to **150** in Table 5, readily undergo photochemically induced dimerization to the corresponding photodimers as shown in Entry 1 of Scheme 26. In these reactions, both betaines behave as 2π electron systems. Less reactive betaines, **143** (R = Benzyl) and **145** (R = Methyl) do not dimerize when irradiated alone or in the presence of benzophenone as a sensitiser.^{53,54}

Entry 2 illustrates that betaines with heteroaryl N-substituents (**147**, **148**, **150**, **151** and **152**) can also thermally dimerize, acting as either 2π or 4π electron systems.^{55,56,57} An experimental study showed that the rate of thermal dimerization increased for **148** < **147** < **152**. Furthermore, N-methyl **145** and N-phenyl **146** had no tendency to dimerize. Thus far, experimental results indicate that betaines with R = Me or benzyl are not likely to behave as a 2π electron system (such as in entries 1 and 2 of Scheme 26).

There are two ways that betaines can act as an 8π electron system. They can cycloadd to a 2π electron system either across the oxygen and C-4, or across the oxygen and C-2 (Entry 3 of Scheme 26).^{58,59} However, these types of reactions require a very reactive 2π electron addend.

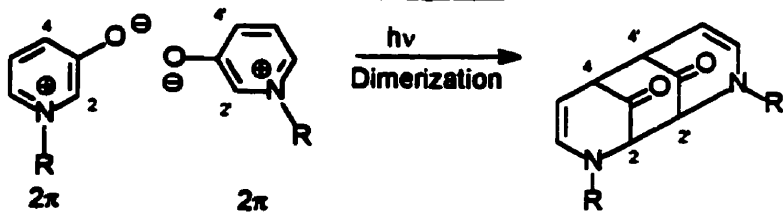
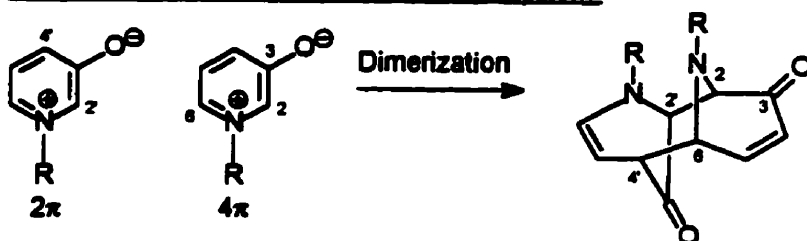
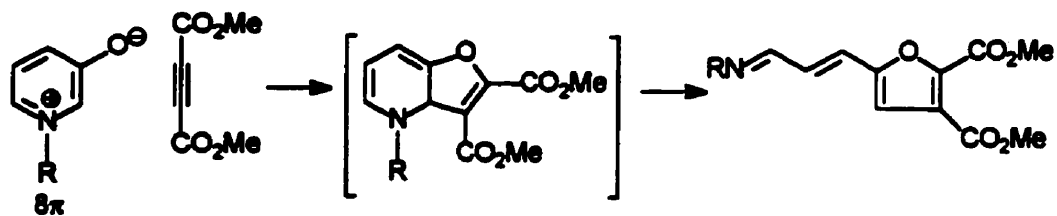
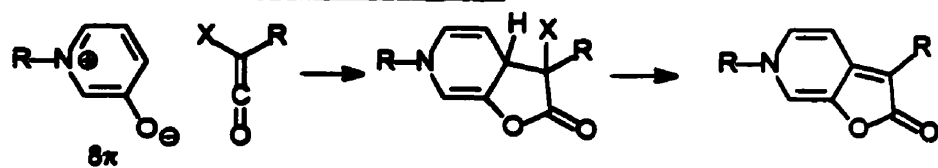
Scheme 26:**Entry 1: Betaine behaving as 2 π system****Entry 2: Betaine behaving as 2 π and 4 π system****Entry 3: Betaine behaving as 8 π system**

Table 5: N-substituted 3-oxidopyridinium betaines of Scheme 26.

Betaine	R
143	Benzyl
145	Methyl
146	Phenyl
147	2-Pyridyl
148	4-Pyridyl
149	Styryl
150	4,6-Dimethylpyrimidin-2-yl
151	4-Nitro-2pyridyl
152	Pyrimidin-2-yl

Section 3.5: 1,3-Dipolar cycloaddition of N-substituted-3-oxidopyridinium betaines

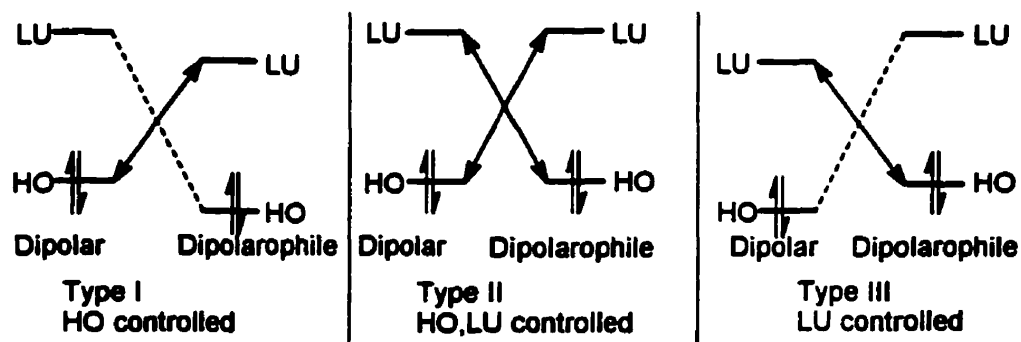
One of the most important features of N-substituted-3-oxidopyridinium betaines is their ability to behave as 1,3-dipoles, adding to a dipolarophile across positions C2 and C6. These betaines are categorized as azomethine ylides of the allyl class of 1,3-dipoles. Most of the known betaines can undergo 1,3-dipolar cycloadditions to common dipolarophiles such as acrylonitrile, and acrylate, maleate or fumarate esters, etc.^{51,56,57,60-65}

Frontier molecular orbital (FMO) theory has been successfully applied to explain both the reactivity and the regiochemistry of 1,3-dipolar cycloadditions.^{49,66} 1,3-Dipolar cycloadditions can be classified into three types, depending on the relative energy gap between the 1,3-dipole and dipolarophile frontier orbitals (Figure 7). These three types (I,

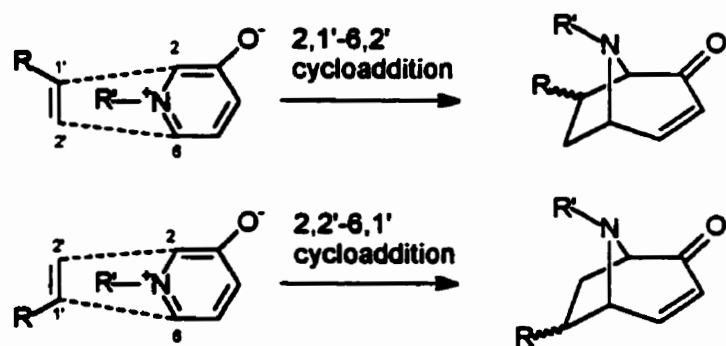
II, and III) are called HOMO-controlled, HOMO/LUMO-controlled and LUMO-controlled, respectively (HOMO = highest occupied molecular orbital, LUMO = lowest unoccupied molecular orbital). The HOMO-controlled types consist of cycloadditions with the greatest interaction between the dipole_{HOMO} and the dipolarophile_{LUMO}. The HOMO/LUMO-controlled types consist of those cycloadditions with bidirectional HOMO-LUMO interactions between dipole and dipolarophile. The third type, LUMO-controlled, consists of cycloadditions with the greatest interaction between the dipole_{LUMO} with the dipolarophile_{HOMO}.

In general, substituents that raise the dipole HOMO energy, or lower the dipolarophile LUMO energy, will accelerate HOMO-controlled reactions and decelerate LUMO-controlled reactions. Conversely, substituents that lower the dipole LUMO energy or raise the dipolarophile HOMO energy will accelerate LUMO-controlled reactions and decelerate HOMO-controlled reactions. HOMO/LUMO-controlled reactions are accelerated by an increase of either frontier orbital interaction. Calculations of the energies of various orbitals involved in different types of cycloadditions on this basis revealed that the ylides (including azomethine ylides) are all electron-rich species characterized by relatively high-energy HOMOs and LUMOs.⁴⁹ Such species react preferentially with electron-deficient alkenes because such a pair of reactants has a narrow dipole HOMO-dipolarophile LUMO gap, i.e. a HOMO-controlled type of reaction.

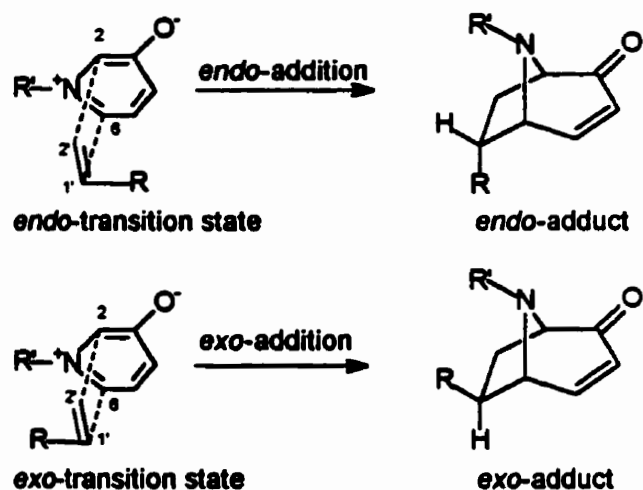
Figure 7: Three types of 1,3-dipolar cycloadditions.



1,3-Dipolar cycloadditions of pyridinium betaines to mono substituted ethylenes can result in two possible regioisomers as shown in Scheme 27. In most cases, cycloadducts formed by 2,2'-6,1' cycloaddition are favored over the 2,1'-6,2' cycloaddition.^{51,56,57,60-65} This regioselectivity was rationalized using Frontier Molecular Orbital Theory. Frontier orbital energy levels and coefficients for the orbitals of N-methyl-3-oxidopyridinium 145, methyl vinyl ether, acrylonitrile and methyl acrylate were calculated.⁵⁶ Calculations of the dipole_{HOMO}-dipolarophile_{LUMO} and dipolarophile_{HOMO}-dipole_{LUMO} energy gaps indicated that the 1,3-dipolar cycloadditions between betaine and mono substituted ethylene listed above were dominated by reactions that are HOMO-controlled.^{56,57} The orbital energies and coefficients have also been used to calculate the interaction energies for adduct formation arising from the two possible orientations for the reaction shown in Scheme 27. The results from these calculations indicated that the dominant cycloadducts should be the regioisomers of the 2,2'-6,1' type.⁵⁶

Scheme 27:

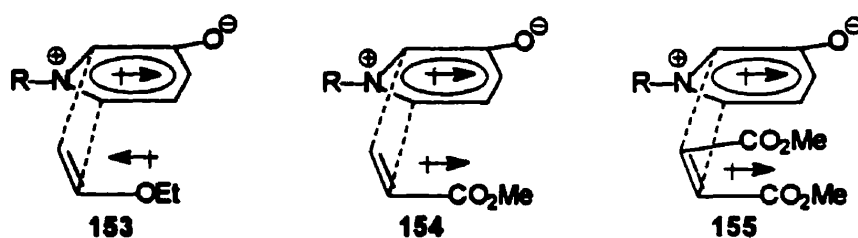
1,3-Dipolar cycloaddition of N-substituted pyridinium betaines to a mono substituted ethylene can give rise to two possible transition states (Scheme 28). When the substituent on the dipolarophile is located over the betaine ring the transition state is referred to as *endo*. However, when the substituent on the dipolarophile is extended away from the betaine ring the transition state is referred to as *exo*.

Scheme 28:

While secondary orbital overlap interaction favors the formation of *endo* isomer, there is a more important interaction influencing the stereoselectivity of 1,3-dipolar cycloadditions, the dipole-dipole interaction (Scheme 29). Permanent dipoles that are

opposite in orientation, such as **153** in Scheme 29, will attract, and favor *endo* addition. When dipoles are parallel, such as **154** or **155** in Scheme 29, they will repel and overcome the weaker secondary orbital overlap to favor *exo* addition. One factor affecting stereoselectivity is the solvent polarity. Increase in the solvent polarity progressively stabilizes the *endo* transition state. Another factor that can effect the stereoselectivity of 1,3-dipolar cycloaddition is the substituents on the nitrogen atom of the betaine. FMO calculations indicated that when the N-substituent is a hydrogen atom or a methyl group (**145**), the *exo*-adduct should be favored. However, when the N-substituent is an aryl group, *endo*-adduct should be favored. Experimental data show some support for these calculations: hydrogen and the methyl group (**145**) substituents on nitrogen lead to about equal amounts of *endo* and *exo* isomers, whereas some of the aryl substituted betaines, such as **146** (N-phenyl) and **148** (N-4-pyridyl) give a predominance of *endo* isomers.⁵⁷

Scheme 29:



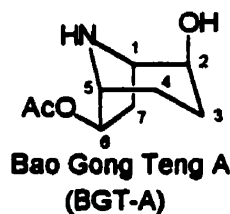
Section 3.6: 1,3-Dipolar cycloaddition of pyridinium betaine in Bao Gong Teng synthesis

Cycloaddition of a pyridinium betaine to a substituted alkene is a convenient method for constructing an azabicyclo[3.2.1]octane system. This bicyclic system is also referred to as a nortropane. Tropane alkaloids, long known to have anticholinergic,

antiemetic, anesthetic and many other actions, have been featured in an extremely wide number of pharmacological reports.⁶⁷

Bao Gong Teng A (BGT-A), an optically active alkaloid, was first isolated from the Chinese herb, *Erycibe obtusifolia* (Convolvulaceae), in 1978.^{68,69} Its absolute configuration was determined as shown in Figure 8, and it has the full chemical name of (1*R*, 2*S*, 5*R*, 6*S*)-6-(acetyloxy)-8-azabicyclo[3.2.1]octane-2-ol.^{69,70} BGT-A has been used to treat fever in humans, however, these treatments also caused strong side effects.^{69,71} Later, it was found that BGT-A was possibly useful for the treatment of glaucoma when used in eyedrops.⁶⁹

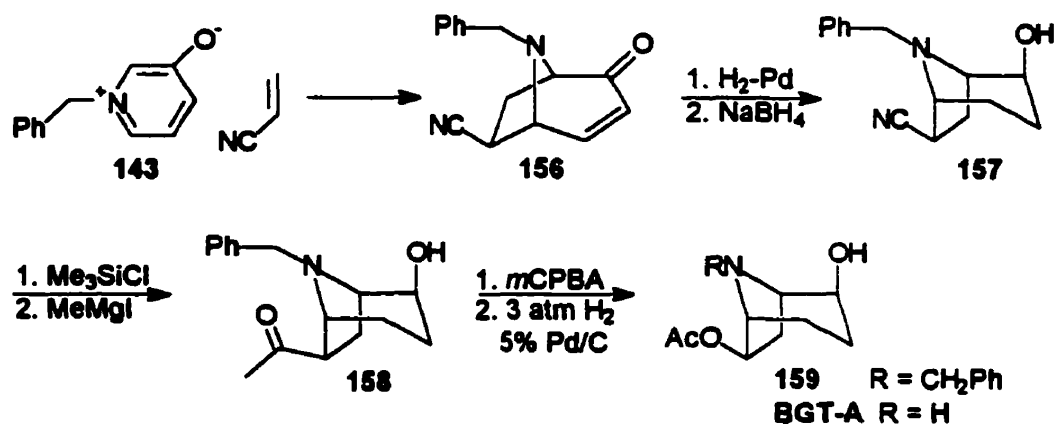
Figure 8: Absolute structure of Bao Gong Teng A.



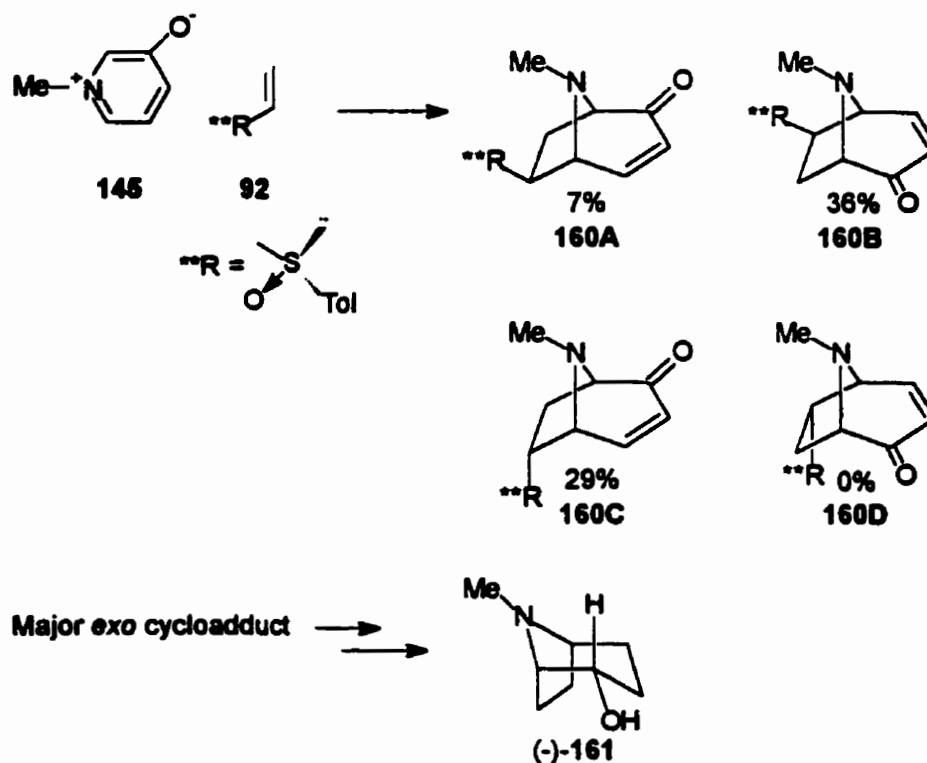
Jung *et al.* prepared the basic tropane carbon skeleton with appropriate functional groups and correct relative stereochemistry, via a 1,3-dipolar cycloaddition of acrylonitrile to the benzyl pyridinium betaine 143 (Scheme 30).⁶⁹ The cycloadduct 156 was converted to a racemic mixture of BGT-A by a series of functional group transformations. Intermediate 156 was hydrogenated, then reduced to the corresponding alcohol 157. Protection of the alcohol was followed by addition of methyl Grignard to obtain the ketone 158. The synthesis of BGT-A was completed by first converting the ketone functional group in 158 to an acetyl group using a Baeyer-Villiger oxidation. The N-

benzyl group of **159** was then cleaved by hydrogenolysis to produce a racemic mixture of BGT-A in an overall yield of 8 %.

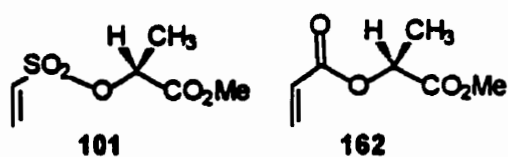
Scheme 30:



On the basis of the above synthesis, an asymmetric synthesis of an optically pure BGT-A might be possible if the 1,3-dipolar cycloaddition could be performed asymmetrically. The feasibility of asymmetric 1,3-dipolar cycloaddition to betaines was demonstrated by Koizumi *et al.* (Scheme 31).⁷² N-methyl-3-oxidopyridinium betaine **145** was reacted with a chiral dipolarophile, (*R*)-(+)-*p*-tolyl vinyl sulfoxide **92**, to give cycloaddition with marginal selectivity. The absolute configuration of the major *exo* cycloadduct was determined by converting it to the corresponding 2- α -tropanol and measuring its optical rotation. The optical rotation was compared to the literature value for (1*S*)-(-)-2- α -tropanol, (-)-**161**. In this way the major *exo* cycloadduct was identified as **160B**.

Scheme 31:

A better chiral dipolarophile is needed if a practical asymmetric synthesis of BGT-A is to be developed. In this thesis, the cycloadditions of the chiral dipolarophiles (methyl (*S*)-lactyl) vinylsulfonate 101, and the acrylate of methyl (*S*)-lactate 162 to betaine 158 were studied. The asymmetric 1,3-dipolar cycloaddition of the chiral acrylate was later utilized for the synthesis of optically pure BGT-A.



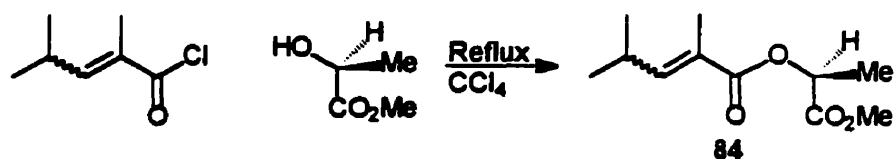
Results and Discussions

Chapter 4

Asymmetric photodeconjugation of a chiral α,β -unsaturated ester

Photodeconjugation of α -substituted α,β -unsaturated esters to the corresponding β,γ -unsaturated esters produces a new chiral center at the α -carbon. Placing a chiral auxiliary on the α,β -unsaturated ester substrate has proven to be an effective strategy for controlling the asymmetric induction of the new chiral center. Prior to this work, highly diastereoselective photodeconjugations of α,β -unsaturated esters had been reported by *Pete et al.*,^{20,21} when camphor derivatives were used as chiral auxiliaries. Unfortunately the camphor based chiral auxiliaries were not readily available and required multistep synthesis. In an effort to improve asymmetric induction in photodeconjugation reactions of chiral esters, and to make the reaction more attractive as a synthetic method, more readily available and effective chiral auxiliaries were required. In this work, methyl (*S*)-lactate, a readily available chiral auxiliary, was chosen for a study of its ability to afford high diastereoselectivity in photodeconjugation reactions.

The chiral α,β -unsaturated ester **84** had been previously prepared by Charlton,⁷³ and the ability of the lactate chiral auxiliary to induce diastereoselectivity in the photodeconjugation reaction of the ester had been examined. He prepared ester **84** (Scheme 32) and irradiated it in an oxygen free methanol solution to give a quantitative conversion to a mixture of diastereomers **163S** and **163R** (Scheme 33).

Scheme 32:

The ¹H-nmr spectrum of each diastereomer had been completely assigned at 300 MHz.⁷³ The absolute configuration at the α center of each diastereomer had also been determined by converting the lactyl esters 163S and 163R to the corresponding methyl esters and identifying them by means of their ¹H-nmr spectra in the presence of a chiral shift reagent.⁷³

In this work, solvent effects on the photodeconjugation of 84 to the diastereomers 163S and 163R were studied. The ratio of the two deconjugated diastereomers was analyzed by GC-MS. Results are given in Table 6.

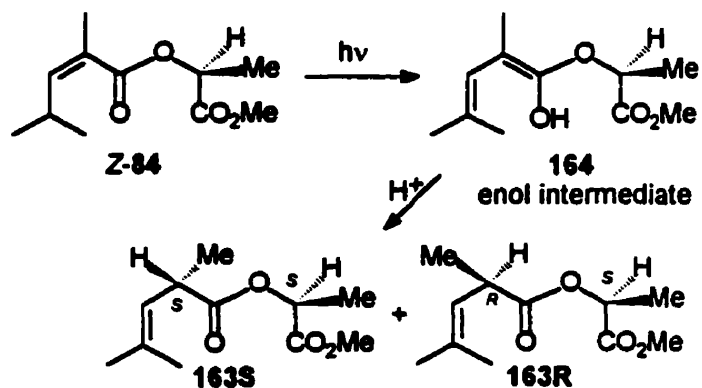
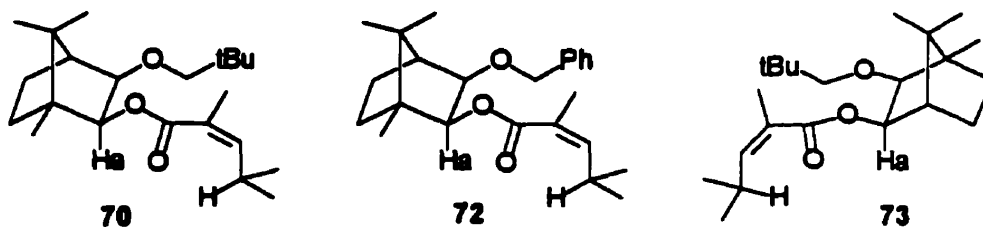
Scheme 33:

Table 6: The diastereoselectivity for deconjugation of α,β -unsaturated ester **84** in different solvents at 0°C.

Solvents	163S	163R	de (%)
Methanol	24	76	-52
Ethanol	65	35	30
2-Propanol	79	21	58
<i>tert</i> -Butyl alcohol	84	16	68
Hexane	73	27	46

The highest diastereoisomeric excess (68 %) of **163S** was obtained when ester **84** was irradiated in *tert*-butyl alcohol. The diastereoisomeric excesses for the photodeconjugation reactions of **84** were comparable to those obtained for the photodeconjugation of the ester bearing a bulky camphor chiral auxiliaries; compounds **70** (73 %, *R*), **72** (68 %, *R*) and **73** (68 %, *S*).^{20,21}

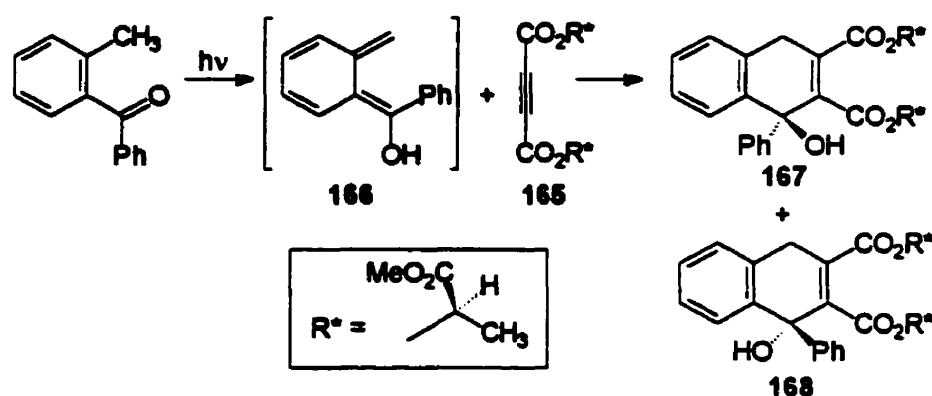


The diastereomer with an *S* configuration at the α center, **163S**, was the major product when ethanol, 2-propanol, *tert*-butyl alcohol or hexane was used as solvent (Table 6), while, surprisingly, the *R* configuration, **163R**, was the major product when the solvent was methanol, a more polar solvent.

Inversion of asymmetric induction on changing solvent polarity has seldom been reported. Interestingly, this kind of inversion of diastereoselectivity was also observed by

Chee in a Diels-Alder reaction of di(methyl (*S*-lactyl) acetylenedicarboxylate, **165**,⁷⁴ a dienophile bearing the same chiral auxiliary as used in the photodeconjugation reaction described above. Chee reacted **165** with α -hydroxy- α -phenyl-*o*-quinodimethane (**166**) generated by irradiation of 2-methylbenzophenone, yielding a mixture of two diastereomers **167** and **168** in a ratio of 1 to 2.1 when the reaction was carried out in benzene (Scheme 34). When more polar solvents such as ethyl acetate, acetone, acetonitrile, or methanol were used, the ratio of the two diastereomers was reversed.

Scheme 34:



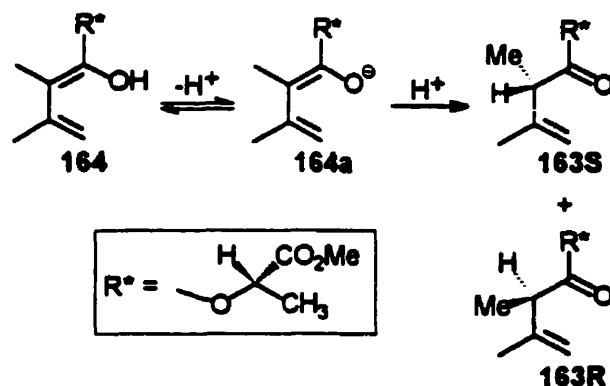
The results obtained from irradiating **84** in a mixture of H_2O and 2-propanol (Table 7) parallels the solvent effects given in Table 6. The more polar the solvent, the more there was a tendency for the reaction to produce the *R* configuration at the new chiral center. There was a decrease in the ratio of deconjugated product **163S** to **163R** as water was added to 2-propanol. When the percentage of H_2O in 2-propanol exceeded 60%, the diastereoselectivity was inverted to favor the **163R** diastereomer as the major isomer.

Table 7: The diastereoselectivity for deconjugation of α,β -unsaturated ester **84** in mixture of 2-propanol and water.

Solvent	Additive (H ₂ O)	163S	163R	de (%)
2-propanol	H ₂ O (0% of H ₂ O in 2-propanol)	79	21	58
2-propanol	H ₂ O (20% of H ₂ O in 2-propanol)	53	47	6
2-propanol	H ₂ O (40% of H ₂ O in 2-propanol)	48	52	4
2-propanol	H ₂ O (60% of H ₂ O in 2-propanol)	44	56	-12
2-propanol	H ₂ O (80% of H ₂ O in 2-propanol)	35	65	-30

The photodeconjugation reaction (see introduction, Scheme 6) occurs in two steps. In the first step of the reaction, irradiation converts the α,β -unsaturated ester to the dienol. In the second step, it is believed that the enol first loses a proton to form an enolate anion which is subsequently protonated at the α carbon (Scheme 35). The facial selectivity of the protonation step determines the diastereoselectivity of the reaction.

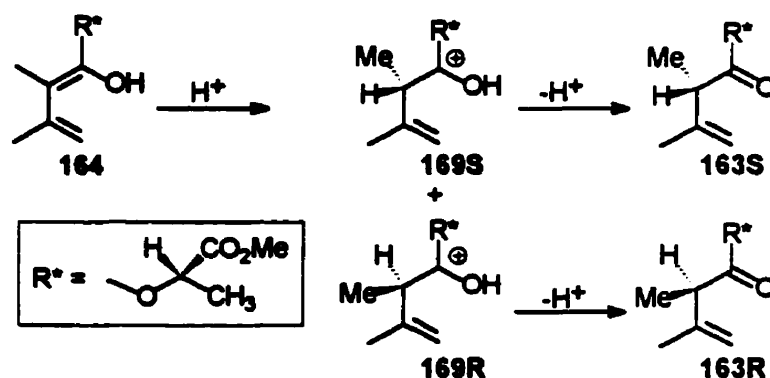
Scheme 35:



In order for there to be a reversal of asymmetric induction either the protonation step must be very solvent dependent, or the mechanism of the reaction must change in

some other way on changing solvent. As for other mechanisms, it is possible that the protonation of the α -carbon occurs simultaneously with the deprotonation of the enol, or that the enol is actually protonated prior to the deprotonation at oxygen. The idea of simultaneous transfer of protons is the basis of Pete's mechanism of asymmetrically catalyzed photodeconjugation (see introduction, Figure 1, page 17), although Pete provided no experimental evidence for the exact sequence of the proton transfers.¹³ In a more polar solvent, such as methanol, the anion **164a** may be formed more easily than in the less polar solvents, since methanol will be better at solvating the polar anion. In less polar solvents, or in more acidic medium, a mechanism involving simultaneous proton transfer, or protonation in the first step, may take over. The mechanism in which protonation occurs in the first step is shown in Scheme 36. In an attempt to determine the sequence of proton transfer steps in the reaction, the effect of added acids and bases on diastereoselectivity was studied.

Scheme 36:



The results of irradiating ester **84** in methanol in the presence of acids and bases are listed in Table 8. The presence of ammonium chloride, sulfuric acid and acetic acid enhanced the diastereoselectivity of the *S* isomer, **163S**. Charlton had previously observed

that the presence of 0.04M Et₄N⁺Cl⁻ in methanol had little or no effect on the diastereoselectivity of the reaction.^{73b} This would be consistent with the idea that the effect of NH₄⁺Cl⁻ is not simply a salt effect, but is related to its acidity. The weak base, KOAc, did not cause any change in the ratio of products, with the *R* isomer still favored. A strong base such as potassium hydroxide was unsuitable for the experiment since it caused hydrolysis and transesterification of the starting material and products.

Table 8: The effect of various additives on the photodeconjugation of ester **84** in methanol.

Solvent	Additive (M)	163S	163R	de (%)
Methanol	none	24	76	-52
Methanol	KOAc (0.0950)	24	76	-52
Methanol	HOAc (0.0100)	25	75	-50
Methanol	HOAc (0.1000)	30	70	-40
Methanol	H ₂ SO ₄ (0.1000)	64	36	28
Methanol	H ₂ SO ₄ (0.0005)	40	60	-20
Methanol	NH ₄ Cl (0.1000)	69	31	38
Methanol	NH ₄ Cl (0.0010)	35	65	-30

The effect of acid on the photodeconjugation reaction in methanol is consistent with the mechanism discussed above. The enolate mechanism, which favors the *R* configuration at the α -carbon, is suppressed when acids are added and the *S* configuration is produced by one of the alternate mechanisms (see above).

The effects of the presence of bases and acids on the diastereoselectivity of the photodeconjugation of ester **84** in 2-propanol were examined next (Table 9). Irradiation in 2-propanol with dissolved KOAc increased the selectivity for formation of the *R* configuration at the α center, moving the selectivity towards that observed in methanol. Despite the limited solubility of ammonium chloride in 2-propanol, it seemed to consistently enhance the selectivity of the *S* isomer, **163S**. This result is also similar to that observed in methanol. Unexpectedly, the effect of sulfuric acid in 2-propanol was totally opposite from that observed in methanol. In 2-propanol, the presence of sulfuric acid resulted in the formation of the *R* isomer, **163R**, as a major photodeconjugated product, while in methanol, added sulfuric acid favored the *S* isomer, **163S**!

Table 9: The effect of acids and bases on the photodeconjugation of ester **84** in 2-propanol.

Solvent	Additive (M)	163S	163R	de (%)
2-propanol	none	79	21	58
2-propanol	KOAc (0.022)	53	47	6
2-propanol	H ₂ SO ₄ (0.1000)	29	71	-42
2-propanol	H ₂ SO ₄ (0.001)	37	63	-26
2-propanol	NH ₄ Cl (0.0038)	85	15	70

Irradiation of **84** in the presence of acids and bases in mixtures of water and 2-propanol (Table 10), confirmed the unexpected effects of sulfuric acid in pure 2-propanol and pure methanol. As expected, ammonium chloride enhanced the formation of **163S** in all mixtures of H₂O and 2-propanol. The weak base KOAc slightly increased the

diastereoselectivity for **163R**, consistent with the result from the experiment in 2-propanol. Acetic acid, hydrochloric acid and sulfuric acid all enhanced the induction of the *R* isomer, **163R** in 2-propanol containing up to 60% water. For mixtures with more than 60% water, acid caused an increase in the *S* configuration at the α carbon.

Table 10: The effects of bases and acids in mixtures of water and 2-propanol.

Solvent + Salts	Additive (M)	178S	178R	de (%)
80% 2-propanol in H ₂ O	none	53	47	6
80% 2-propanol in H ₂ O	KOAc (0.10)	48	52	-4
80% 2-propanol in H ₂ O	HOAc (0.10)	44	56	-12
80% 2-propanol in H ₂ O	HCl (0.10)	40	60	-20
80% 2-propanol in H ₂ O	H ₂ SO ₄ (0.10)	35	65	-30
80% 2-propanol in H ₂ O	H ₂ SO ₄ (0.01)	45	55	-10
80% 2-propanol in H ₂ O	NH ₄ Cl (0.10)	83	17	66
60% 2-propanol in H ₂ O	none	48	52	-4
60% 2-propanol in H ₂ O	KOAc (0.10)	48	52	-4
60% 2-propanol in H ₂ O	HOAc (0.10)	44	56	-12
60% 2-propanol in H ₂ O	HCl (0.10)	41	59	-18
60% 2-propanol in H ₂ O	H ₂ SO ₄ (0.10)	37	63	-26
60% 2-propanol in H ₂ O	H ₂ SO ₄ (0.01)	45	55	-10
60% 2-propanol in H ₂ O	NH ₄ Cl (0.10)	80	20	40
40% 2-propanol in H ₂ O	none	44	56	-12
40% 2-propanol in H ₂ O	KOAc (0.10)	45	55	-10

Table 10: continued

Solvent + Salts	Additive (M)	178S	178R	de (%)
40% 2-propanol in H ₂ O	HOAc (0.10)	44	56	-12
40% 2-propanol in H ₂ O	HCl (0.10)	41	59	-18
40% 2-propanol in H ₂ O	H ₂ SO ₄ (0.10)	37	63	-26
40% 2-propanol in H ₂ O	H ₂ SO ₄ (0.01)	43	57	-14
40% 2-propanol in H ₂ O	NH ₄ Cl (0.10)	75	25	50
20% 2-propanol in H ₂ O	none	35	65	-30
20% 2-propanol in H ₂ O	KOAc (0.10)	37	63	-26
20% 2-propanol in H ₂ O	HOAc (0.10)	44	56	-12
20% 2-propanol in H ₂ O	HCl (0.10)	47	53	-6
20% 2-propanol in H ₂ O	H ₂ SO ₄ (0.10)	42	58	-16
20% 2-propanol in H ₂ O	H ₂ SO ₄ (0.01)	43	57	-14
20% 2-propanol in H ₂ O	NH ₄ Cl (0.10)	60	40	20

In summary, the presence of ammonium chloride salts enhanced the induction of the *S* diastereoisomer, **163S**, while the weak base KOAc increased the formation of the *R* isomer, **163R**, in methanol, 2-propanol, and in mixtures of H₂O and 2-propanol. Interestingly, acids inverted the diastereoselectivity in both a highly polar solvent, methanol (*R* to *S*), and a less polar solvent, 2-propanol (*S* to *R*).

The proposal that acid might protonate the dienol **164** at the α position prior to the elimination of the hydroxy proton as shown in Scheme 35 leading primarily to the *S* configuration at the α center does not seem to be consistent with the effects of acid in 2-

propanol. There must be some other explanation for both the solvent effects and the effect of acid.

A possible explanation for the above results may be related to the conformation of the methyl (*S*)-lactyl group in different solvents. If the conformation of the lactyl chiral auxiliary is different in different solvents then one might expect the asymmetric induction to change with solvent polarity as it was observed. In other words, the photodeconjugation reaction may have the same mechanism in both methanol and in 2-propanol, but the chiral auxiliary may control the facial selectivity of the protonation differently in different solvents. This explanation seems most plausible as it would also explain the solvent polarity induced inversion in diastereoselectivity observed by Chee when using the same chiral auxiliary in a Diels-Alder reaction.⁷⁴

If the conformations of the chiral auxiliary were solvent dependent, one might be able to detect the change in conformation by a change in the optical activity. The optical rotation of **84** was measured in both methanol and in 2-propanol and the rotations were found to be the same within experimental error. Thus, no support for a change in the conformation of the chiral auxiliary with a change in solvent could be found. Nevertheless it remains an attractive hypothesis.

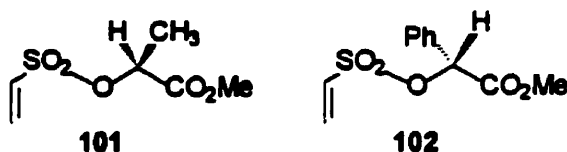
Even if one accepts the notion of solvent dependent conformations for the chiral auxiliary, that factor alone would not explain the unusual effect of acid on the stereoselectivity. In order to explain the effect of acid one would have to combine both the idea of a solvent dependent conformational change *and* an acid dependent mechanism change. In neutral solvent, the enol **164** could lose the hydroxyl proton to form the anion **164a** as shown in Scheme 34. In neutral methanol, the conformation of **164a** would be

oriented in such a way that protonation to form **163R** would be preferred. In a less polar solvent, such as 2-propanol, a different conformation of **164a** would exist so that protonation to form **163S** would be favored. Irradiation of **84** in the presence of strong acid would suppress the enolate mechanism and favor a mechanism with simultaneous proton transfers, or one like that shown in Scheme 35. The results in methanol could now be explained if the predominant conformation of the chiral auxiliary in methanol induces the *S* configuration at the α carbon *when protonation occurs by the acid catalyzed mechanism*. Similarly the major conformation of the chiral auxiliary in 2-propanol would have to induce the *R* configuration when the reaction proceeds by the acid catalyzed mechanism. No other explanation seems to be able to account for all of the results.

Up to this point, the best diastereoisomeric excess observed for the photodeconjugation reaction using the methyl (*S*)-lactate group as a chiral auxiliary was 70%. Although this was quite high it was not good enough for synthetic applications. In addition, during the time that this work was in progress, Pete *et al.* published several examples of photodeconjugation reactions of chiral esters with more impressive diastereoselectivities (de of 98%) (see Introduction, Chapter 1, page 26). In view of this fact, investigation of the use of the methyl lactyl chiral auxiliary in asymmetric photodeconjugation reactions was terminated.

Chapter 5

Vinylsulfonate esters have been demonstrated to be efficient dienophiles in Diels-Alder reactions with furan derivatives. This efficiency and the fact that the sulfonate activating group can be readily removed after the reaction attracted our attention. The reaction would be particularly useful in synthesis if it could be carried out asymmetrically. Although *intramolecular* Diels-Alder reactions of vinylsulfonates have been carried out asymmetrically, there are no examples of asymmetric *intermolecular* cycloadditions in the literature. It would be interesting to study the diastereoselectivity in Diels-Alder reactions of dienophiles (such as **101** and **102**) having the activating vinylsulfonate group combined with the effective chiral auxiliaries, methyl (*S*)-lactate and methyl (*R*)-mandelate. To this end, syntheses of both of the sulfonate esters **101** and **102** were undertaken, and their Diels-Alder reactions with cyclopentadiene were studied.



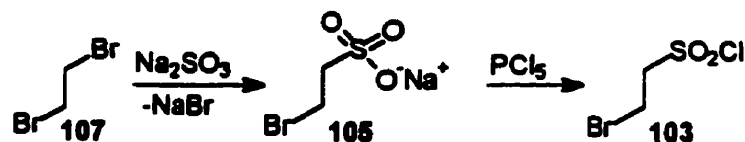
Section 5.1: Preparation of chiral vinylsulfonate esters.

The preparation of chiral vinylsulfonate esters was accomplished via the general procedure shown in Schemes 37 and 38. The vinylsulfonate precursor, 2-bromoethanesulfonyl chloride was prepared following the literature procedure, as illustrated in Scheme 36.^{33,34,35,36} Sodium sulfite was reacted with an excess of ethylene

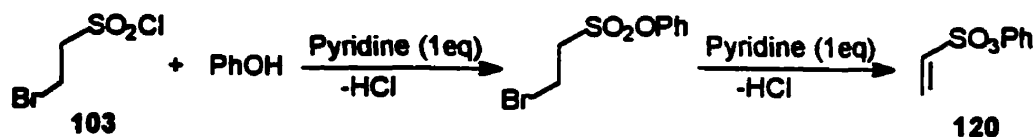
bromide to replace only one bromine by a sulfite group and produce sodium 2-bromoethanesulfonate **105**.

The final step in the preparation of 2-bromoethanesulfonyl chloride involved the heating of **105** with an excess of phosphorus pentachloride. Workup gave a brown oil that was distilled under high vacuum with collection of several fractions. The fraction distilling at 64-66°C (2.5 mm Hg) had both the boiling point^{34,75} and ¹H-nmr spectrum consistent with compound **103**.

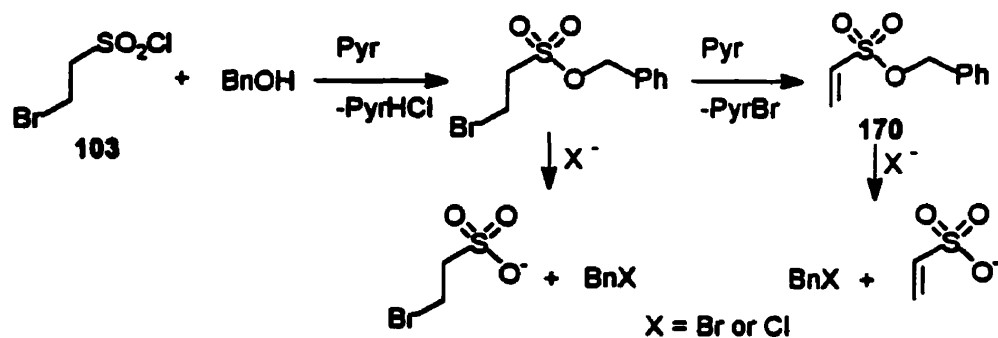
Scheme 37:



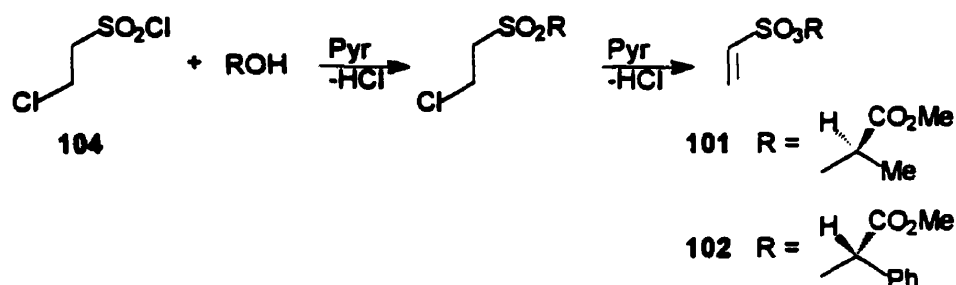
Following the Whitmore and Landau method,³⁰ phenyl vinylsulfonate **120**, was prepared from phenol and 2-bromoethanesulfonyl chloride **103** (Scheme 38). Pyridine was slowly added to a stirred mixture of phenol and one equivalent of β -bromoethanesulfonyl chloride at 0°C to induce coupling of the sulfonyl chloride to phenol. A second equivalent of pyridine was then added to eliminate the β -bromine to yield **120**. After washing with dilute HCl (3%), the reaction was worked up to give crude **120** which was purified by chromatography on silica gel. The ¹H-nmr spectrum of the product was typical of all of the vinylsulfonates that were prepared. It exhibited three vinylic signals in the 6-7 ppm region, the most downfield signal appearing as a double doublet and the other two as doublets (ABX pattern).

Scheme 38:

An attempt to use the same procedure to prepare the less stable benzyl (170 Scheme 39) and (methyl (*R*)-mandelyl) vinylsulfonates (102 Scheme 40), was unsuccessful. In the case of benzyl vinylsulfonate 170 (Scheme 39), the ^1H -nmr spectrum of the crude product did not exhibit any of the expected peaks in the 6-7 ppm region. Analysis of the product by GC-MS showed the presence of both benzyl chloride and benzyl bromide in a ratio of 1:2. The presence of these products suggested that the halide ions, released from the coupling of the alcohol to the sulfonyl chloride, and from the elimination of the bromide, had attacked the benzyl sulfonate as shown in Scheme 39. A similar situation occurred in the preparation of the (methyl (*R*)-mandelyl) vinylsulfonate, 102 (Scheme 40), with none of the expected product produced. The only products which could be tentatively identified by MS were methyl α -chloro and methyl α -bromo phenyl acetates. Therefore, the procedure was modified to reduce the side reactions.

Scheme 39:

The preparation of the benzyl vinylsulfonate 170 had been undertaken only as a model study and due to the problem in its synthesis, it was dropped from the study. Since the (methyl (*R*)-mandelyl) vinylsulfonate 102 was an important part of the later asymmetric Diels-Alder study, changes were made to optimize its synthesis (Scheme 40). Firstly, 2-chloroethanesulfonyl chloride was used instead of 2-bromoethanesulfonyl chloride. This modification reduced the side reaction by eliminating the presence of bromide ion in the reaction mixture. Bromide ion is a softer nucleophile than chloride ion and is expected to react more rapidly with the nucleophilic site of the (methyl (*R*)-mandelyl) sulfonyl ester which has a soft electrophile character. Secondly, an excess of 2-chloroethanesulfonyl chloride was used to force the reaction to completion. Thirdly, the chloride ion was removed continuously by filtering off the pyridinium chloride as it was formed, hopefully decreasing the presence of the free chloride ion and reducing the side reaction. Fourthly, the reaction was worked up at near 0°C by quickly washing the cold mixture with saturated aqueous CuSO₄ to remove pyridine and chloride ion. In the original procedure, the reaction was carried out at 0°C then warmed to room temperature in the presence of halide ions and base which increased the probability of side reaction. The crude product from the extraction was dried, evaporated and promptly chromatographed on a silica gel column, giving a colorless solid which was stable at refrigerator temperature (5°C) indefinitely. The ¹H-nmr spectrum of the solid was consistent with that expected for (methyl (*R*)-mandelyl) vinylsulfonate, 102 (Scheme 40).

Scheme 40:

The (methyl (*S*)-lactyl) vinylsulfonate, **101**, (Scheme 40) was successfully prepared by a similar method. It was isolated as a light yellow oil that was stable at refrigerator temperature (5°C).

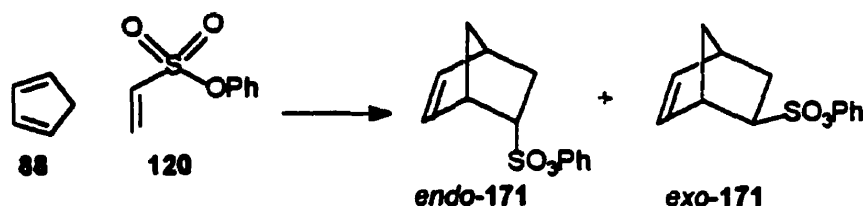
Section 5.2: Diels-Alder reactions of the chiral vinylsulfonyl esters.**Section 5.2.1: Structure elucidation of the cycloadducts.**

The Diels-Alder reaction of cyclopentadiene with alkyl vinylsulfonates should produce 2-alkyl sulfonate norbornene derivatives as shown in Scheme 41. Unfortunately, there were no spectroscopic data available in the literature for these types of sulfonate derivatives. Such data would have provided an easy means to assign structures to the cycloadducts prepared in this study. A model study of a Diels-Alder reaction of a simple alkyl vinylsulfonate with cyclopentadiene was necessary to obtain the full spectroscopic data for the 2-alkyl sulfonate norbornene derivatives.

Phenyl vinylsulfonate, **120**, was a good candidate for the model study as it could be easily prepared. Also, the ¹H-nmr spectra of expected cycloadducts *endo*-**171** and *exo*-**171**, from the Diels-Alder reaction of **120** with cyclopentadiene, should have easily

interpretable ^1H NMR spectra, since the aromatic protons should not overlap with the bicyclic ring signals.

Scheme 41:

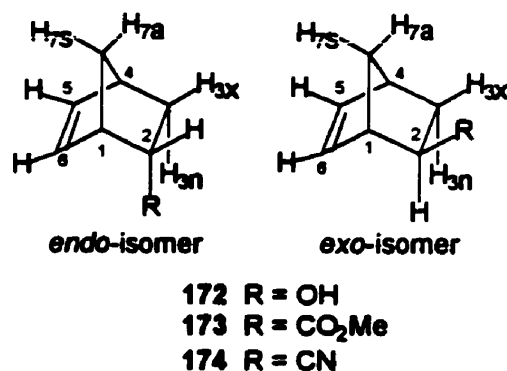


The Diels-Alder reaction was carried out by adding an excess of cyclopentadiene to a solution of 120 in benzene. The resulting mixture was stirred for 10 h, and then the benzene was evaporated to leave a clear oil. This oil was placed on a short column of silica gel and the nonpolar compounds, such as cyclopentadiene and dicyclopentadiene, were eluted with hexane. The remaining product was then eluted as a single fraction with 30% EtOAc in hexane in 80% yield. The ^1H -nmr spectrum of this mixture had two sets of peaks with different intensities suggesting that the Diels-Alder reaction had produced two compounds in different amounts. The mixture was rechromatographed on a silica gel column using 15% EtOAc in hexane in order to separate the two components, which were expected to be *exo*-171 and *endo*-171.

The bicyclo[2.2.1]heptane ring system of 171 is rigid and has a known geometry (Figure 9). Fraser, Musher, and Paasivirta have pointed out that the *exo*-protons in norbornane and norbornene derivatives are deshielded relative to the *endo*-protons at the same carbon atom.⁷⁶ Additionally, in 2-substituted norbornanes, the 2-*exo*-protons of the *endo* isomer are generally deshielded relative to the 2-*endo*-protons of the *exo* isomer. Literature values of chemical shifts for 2-substituted norbornenes which illustrate this

point are shown in Table 11.⁷⁶⁻⁷⁸ Thus, the *endo*-171 and the *exo*-171 cycloadducts should be distinguishable based on the chemical shift of their H2 protons.

Figure 9: Bicyclo [2.2.1] heptane ring systems



Based on the above information, a reasonable strategy for complete analysis of the ¹H-nmr spectrum of the cycloadducts from the Diels-Alder reaction of 120 can be devised. The assignment of the H2 signal is the first step. This assignment should allow the cycloadducts to be classified as *endo* or *exo*. The remaining ¹H-nmr signals can be assigned completely using ¹H-¹H COSY spectra. Finally, these assignments and the precise chemical shifts and coupling constants can be confirmed by computer simulation of the spectra.

Table 11: ¹H-nmr data for the Bicyclo [2.2.1] heptane ring systems.

Cmpd	Solvents	H1	H2	H3x	H3n	H4	H5	H6	H7a	H7s
<i>exo-172</i> ⁷⁸	CDCl ₃	2.75	1.61	1.09	1.23	2.81	6.06	6.09	1.31	1.28
<i>endo-172</i> ⁷⁸	CDCl ₃	2.93	2.29	1.80	0.49	2.79	6.12	5.95	1.73	1.25
<i>exo-172</i> ⁷⁷	CCl ₄	2.72	3.78	1.72	1.25	2.72	5.92	6.08	1.55	1.37
<i>endo-172</i> ⁷⁷	CCl ₄	2.90	4.35	1.97	0.80	2.73	5.98	6.27	1.22	1.42
<i>exo-173</i> ⁷⁷	CCl ₄	2.88	2.13	1.87	1.28	2.98	6.10	6.10	1.50	1.37
<i>endo-173</i> ⁷⁷	CCl ₄	3.13	2.90	1.97	0.80	2.73	5.98	6.27	1.22	1.42
<i>exo-174</i> ⁷⁷	CCl ₄	3.17	2.18	1.92	1.50	3.02	6.03	6.13	1.55	1.43
<i>endo-174</i> ⁷⁷	CCl ₄	3.17	2.85	2.10	1.20	2.97	6.15	6.30	1.20	1.40

To assign the H2 signals of the cycloadducts, an assumption was made that these protons should be in the region of 3-4 ppm. This assumption was based on the fact that the chemical shifts of protons at the α position of sulfonate groups, such as H2, are usually in this range.⁴² In the ¹H-nmr spectra of the cycloadducts, there were three signals located in the 3-4 ppm region: 3.43 (m), 3.10 (ddd) and 3.07 (m) ppm for the first eluted cycloadduct and 3.87 (ddd), 3.43 (m), and 3.05 (m) for the second eluted cycloadduct (For the present time, the first and the second eluted cycloadducts will be referred to as 171a and 171b, respectively). One of the three signals for each cycloadduct should be the H2 proton and the other signals should be the H1 and H4 tertiary-allylic protons. The data in Table 11 indicated that the chemical shifts of H1 and H4 in 2-*endo*-substituted norbornene derivatives were very similar to the corresponding protons in the 2-*exo*-substituted norbornene derivatives. The data in this table also suggested that the chemical

shifts of the 2-*exo*-protons of the *endo* isomers were usually downfield, more than 0.5 ppm, relative to the 2-*endo*-protons of the *exo* isomers. A comparison of the peaks in the 3–4 ppm region of the cycloadducts showed that the two multiplets peaks, 3.43(m) and 3.05 (m) ppm, in 171a were very similar to those in 171b, 3.43 (m) and 3.07 (m) ppm. Moreover, the chemical shifts of the ddd peaks of these two cycloadducts differed by more than 0.5 ppm. Based on the data in Table 11, the multiplet peaks were assigned to the H1 and H4 protons and the ddd signal to the H2 proton. The H1 protons are located closer to the electron withdrawing sulfonate group than the H4 protons, and therefore H1 should have a higher chemical shift than H4. This assumption led to the conclusion that the 3.43 (m) ppm peaks in both cycloadducts, 171a and 171b, were due to the H1 protons. The 3.05 (m) and 3.07 (m) ppm peaks in 171a and 171b, respectively, were assigned as the H4 protons. The remaining signal in the 3–4 ppm region, 3.10 (ddd) ppm for 171a and 3.87 (ddd) ppm for 171b were assigned to H2. From this assignment, the cycloadduct eluted first had H2 of lower chemical shift than the corresponding proton in the second eluted cycloadduct. Hence the first eluted cycloadduct (171a) was assigned as *exo*-171 and the other (171b) was assigned as *endo*-171.

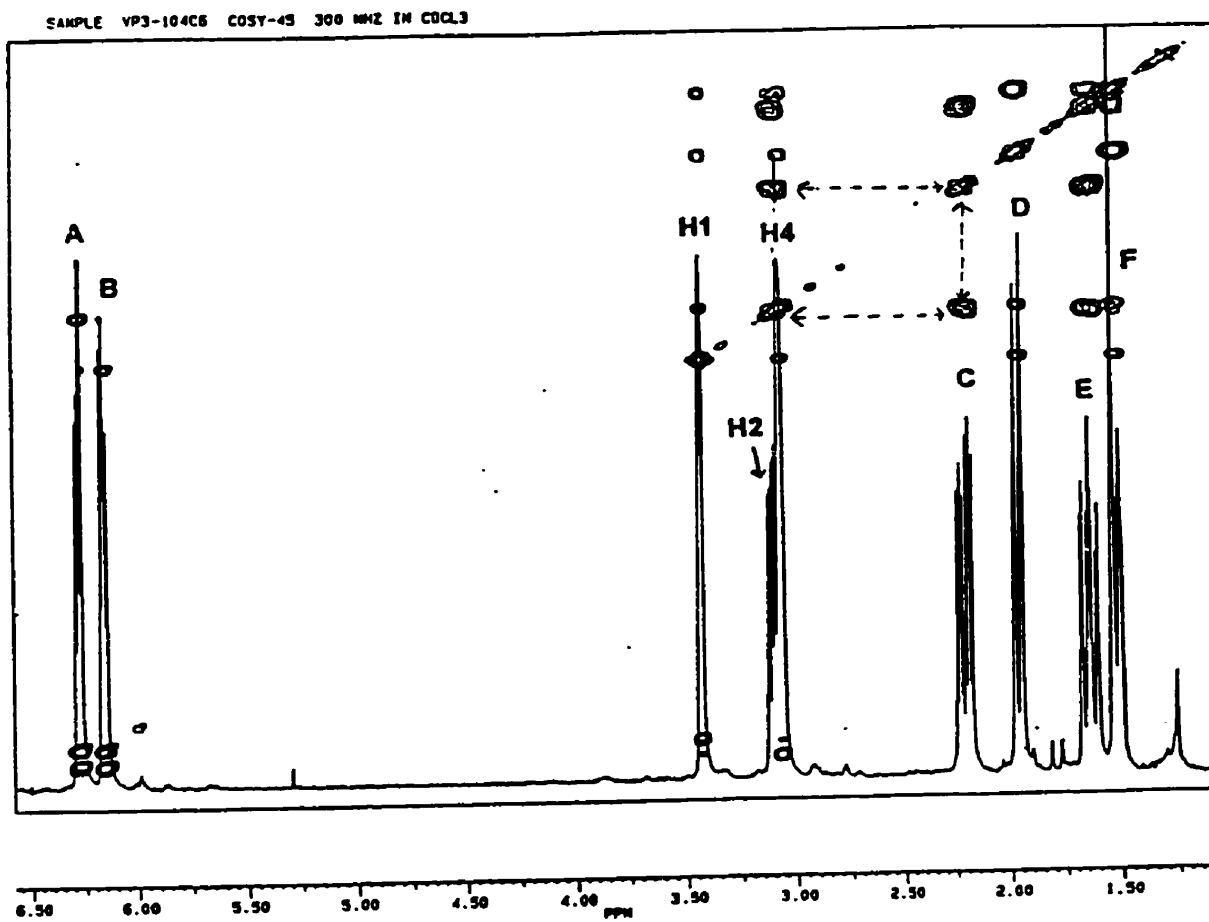
Once the positions of the H1, H2 and H4 proton signals had been established, ^1H - ^1H COSY spectra were used to assign all other ring protons of the *endo*-171 and the *exo*-171 isomers. The results are given in Table 13 (page 89) and more discussion of these assignments follows.

^1H - ^1H COSY is an important 2D nmr technique, that generates spectra that display ^1H chemical shifts in both dimensions. ^1H - ^1H COSY spectra are usually plotted in the contour form and are symmetrical with respect to the diagonal. There are two different

types of signals that appear in ^1H - ^1H COSY spectra. Those on the diagonal (diagonal peaks) represent the original spectrum, as observed in a 1D nmr experiment. The off-diagonal signals are so called cross-peaks, which indicate the existence of scalar (through bond) coupling between nuclei. The signals from the coupled nuclei can be found by horizontally and vertically extrapolating from the cross-peak to the diagonal spectrum. Owing to the symmetry of the spectrum, this procedure can be performed in either the upper left or the lower right triangle (see Figure 10).

To simplify the task of describing the assignment of the ^1H - ^1H COSY spectrum of *exo-171* (Figure 10) in deuterated chloroform, signals on the spectrum are labeled for easy identification. Signals in the 3-4 ppm region were already assigned to H1, H2, and H4. The remaining six signals were labeled in alphabetical order from left to right (A to F).

Figure 10: ^1H - ^1H COSY spectrum of *exo*-171 in deuterated chloroform.



The assignment of the six unassigned protons began by drawing a horizontal line across the ^1H - ^1H COSY spectrum, through the diagonal peak of the H4 proton. Neglecting the H2 signal, there were seven other peaks in the spectrum that had off-diagonal signals on this horizontal line. This indicated that these seven protons were coupled to the H4 proton. In the case of H1, a medium intense cross-signal on the H4 horizontal indicated a strong W coupling between these two protons. The appearance of the two cross-signals between the H4 proton to the A and B signals was a clue to their assignment. Based on their chemical shift, these two peaks, in the 5-7 ppm region, were most likely due to the vinylic protons, H5 and H6. Protons H5 and H6 should couple differently to H4. The three bond coupling of H5 to H4 ($^3J_{\text{H5,H4}}$) should be strong and the four bond coupling of H6 to H4 ($^4J_{\text{H6,H4}}$) should be very weak. The off-diagonal signal of peak A was very intense and that of B was very faint, suggesting that peak A was the H5 proton and peak B was the H6 proton. Further evidence for the H5 and H6 assignment was obtained from their coupling to H1. A very weak cross-signal connecting peak A to the H1 proton indicated that peak A should be the H5 proton, since its four bond coupling to H1, $^4J_{\text{H5,H1}}$, should be weak. On the contrary, an intense cross-signal connecting peak B to H1 suggested that B should be proton H6 since the three bond coupling of H6 to H1, $^3J_{\text{H6,H1}}$, should be strong. The latter assignment left four unassigned peaks, two H7 and two H3 protons.

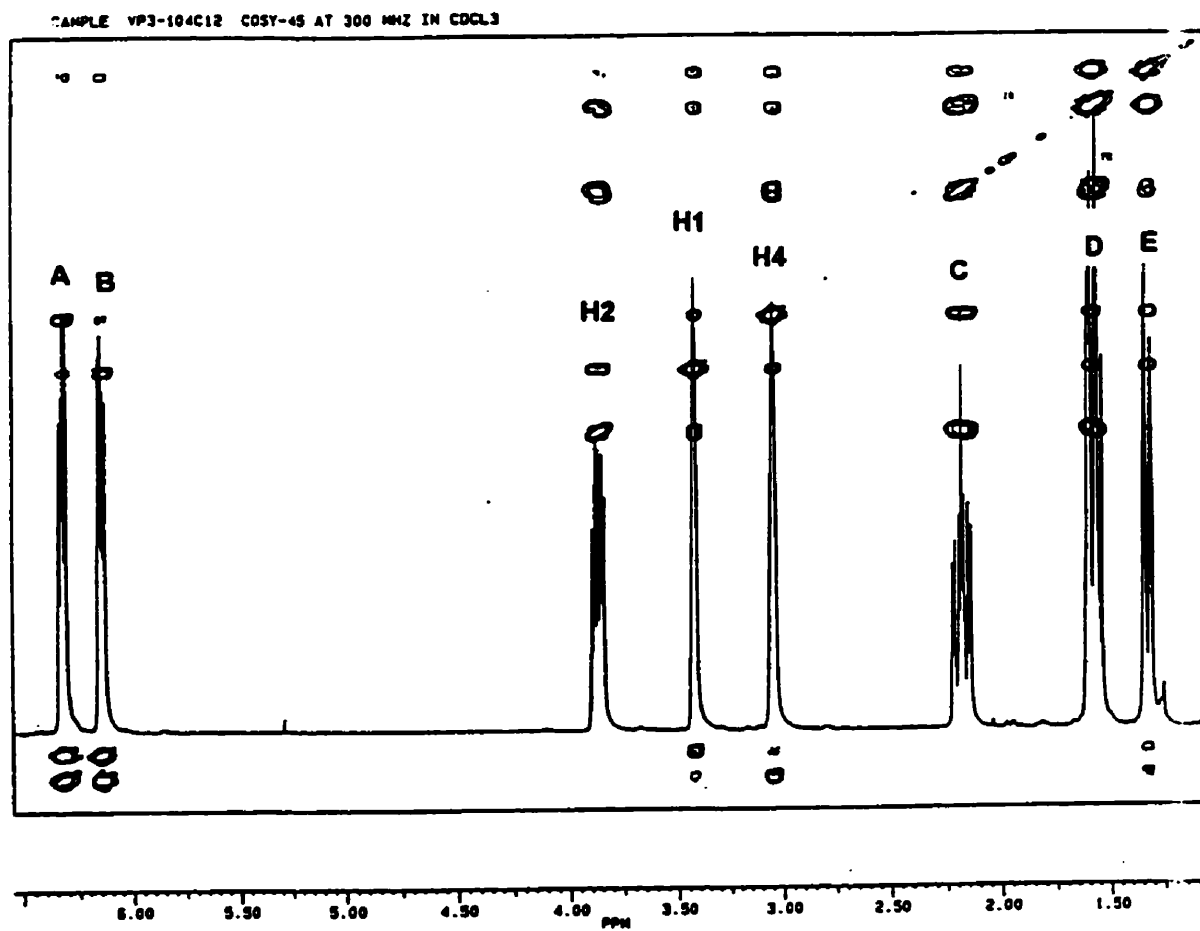
A feature that distinguishes the H7 protons from the H3 protons is their difference in coupling to the H1 proton. The three bond coupling of H7s (H7 *syn*) and H7a (H7 *anti*) to H1 should be strong and their cross-signals, on the horizontal line through the diagonal peak of H1, should be clearly observable. By comparison, the four bond

coupling of H3n (H3 *endo*) and H3x (H3 *exo*) to H1 should be very weak and their cross-signals are less likely to appear on the horizontal line through the diagonal peak of H1. A horizontal line crossing the H1 diagonal peak was drawn. The two off-diagonal signals from peak D and F on this line suggested that these two peaks were the two H7 protons, and by elimination, peaks C and D must be the two H3 protons.

To finish the exact assignment of H3n, H3x, H7a, and H7s, an assumption was made that the four bond W coupling of H7s to H3n and H7s to H2 should be significantly stronger than the four bond coupling of H7a to H3n and H7a to H2. Previous studies by Fisher *et al.* on 2-*exo*-norbornenol have shown that the coupling of H7s to H3n is much stronger than the four bond coupling of H7a to H3n, consistent with the above assumption. Thus a horizontal line drawn through the diagonal peak of H7s should pass through the cross-peaks of H3n and H2. In figure 10, a horizontal line through diagonal signal F passed through the cross-peaks of H2 and peak E. This suggested that peak F was H7s and peak E was H3n. By elimination, peaks C and D were H3x and H7a, respectively.

There was no cross-signal of H2 with H1 indicating that there was no coupling between these two protons. The zero coupling constant for the three bond coupling might be due to the relative arrangement of the two protons. That is, if the dihedral angle of the two protons were close to 90°, the coupling constant would be close to zero.

Figure 11: ^1H - ^1H COSY spectrum of *endo*-171 deuterated chloroform.



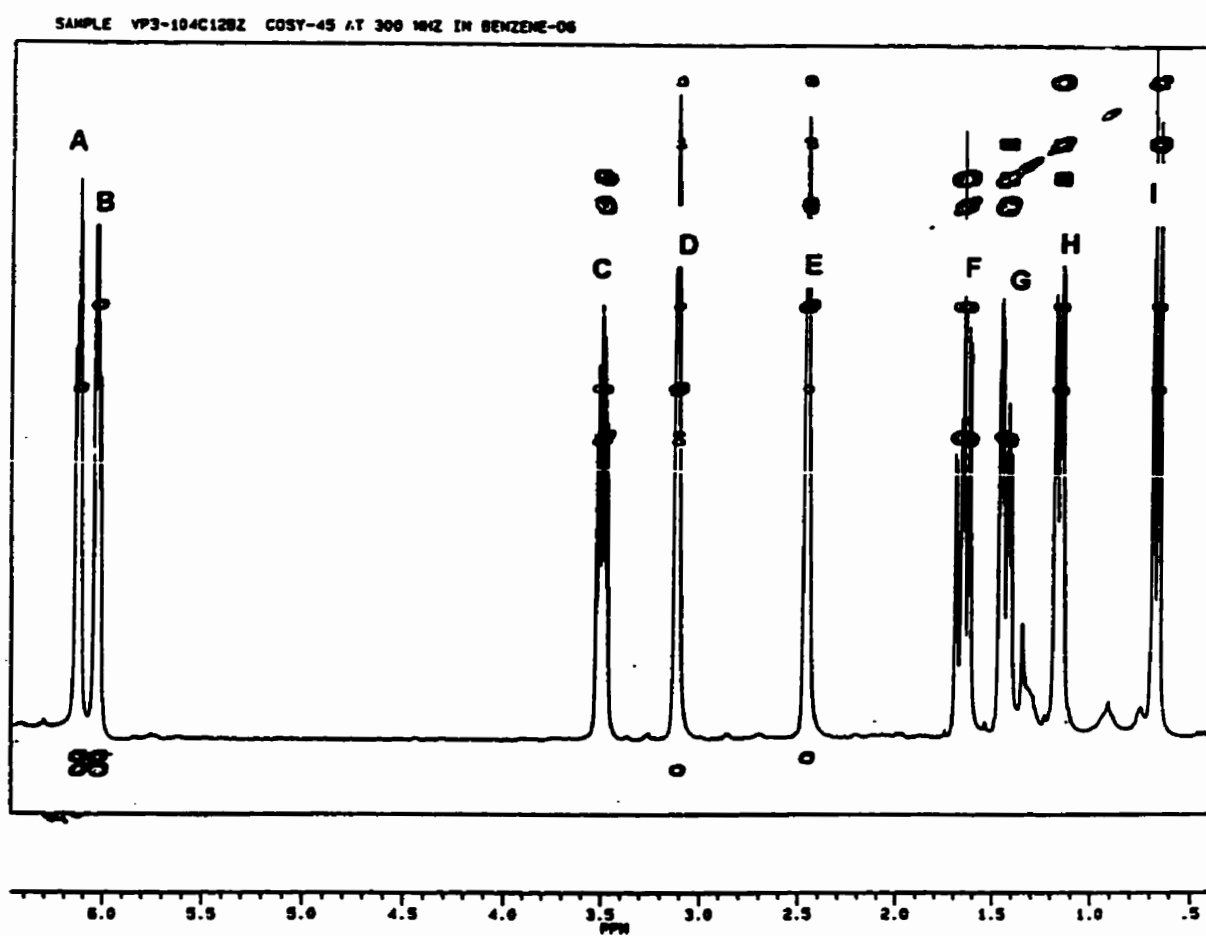
The spectrum of compound *endo*-171 in deuterated chloroform was next assigned using ^1H - ^1H COSY (Figure 11). The ^1H - ^1H COSY spectrum consisted of eight peaks for the nine ring protons. The H1, H2, and H4 protons, in the 3-4 ppm region, had already been assigned (see discussion above). The remaining five signals were labeled in alphabetical order from left to right (A to E). Integration of the area of each signal indicated that signal D arose from two overlapping single proton signals. This overlap complicated the assignment of the COSY spectrum, since it was hard to retrieve information from the overlapped signal. Therefore, a different solvent was chosen for the ^1H -nmr analysis.

The analysis was focused on the ^1H -nmr spectrum of *endo*-171 in deuterated benzene, a solvent in which no overlap of signals occurred. Once the assignment of the ^1H -nmr spectrum of *endo*-171 in deuterated benzene was completed, a comparison of the splitting pattern of the signals in the deuterated benzene spectrum was used for assigning the signals of *endo*-171 in deuterated chloroform.

The ^1H -nmr spectrum of *endo*-171 in deuterated benzene (Figure 12) consisted of nine signals for nine ring protons, i.e. no overlap occurred. To simplify the task of describing the assignment of this ^1H - ^1H COSY spectrum, signals on the spectrum are labeled in alphabetical order (A to I).

In figure 12, the value of three couplings measured and calculated from signal C is very similar to that of the H2 of *endo*-171 in deuterated chloroform (Figure 11), previously assigned. Therefore, the assignment of the ^1H - ^1H COSY spectrum of *endo*-171 in deuterated benzene started with the assignment of signal C to the H2 proton.

Figure 12: ^1H - ^1H COSY spectrum of *endo*-171 in deuterated benzene.



The next step in the analysis was to assign the H1 and H4 protons. For this assignment, an assumption was made that the three bond couplings between H2 and H1, and between H2 and the two H3 protons, $^3J_{H1,H2}$, $^3J_{H2,H3n}$ and $^3J_{H2,H3x}$, should be strong. Moreover, the four bond coupling between the H2 proton and the H4 proton, $^4J_{H2,H4}$, should be weak. In figure 12, signals D, F, and G have off-diagonal signals that indicate coupling to H2. Therefore D, F, and G should correspond to the H1 and the two H3 protons. The tertiary allylic H1 proton should be located at a lower field than the two secondary H3 protons. This assumption led to the assignment of signals F and G to the two H3 protons and signal D to the H1 proton.

Signals A and B, in the 5-7 ppm region, should be the two vinylic protons, H5 and H6. A feature distinguishing these two protons is their coupling to H1. The H6 proton should couple strongly to the H1 proton, while there should be no coupling between the H1 and the H5 protons. A cross peak between the H1 proton and A indicated a scalar coupling between the two protons. Signal A was thus assigned to H6, and signal B to H5. Following these assignments, the off-diagonal signal linking the H5 proton to signal E was used to assign signal E to the H4 proton.

The two remaining signals, H and I, should be the two H7 protons. Among the combination of four bond couplings between the two H7 protons and the two H3 protons, only the four bond W coupling of H7s to H3n should be strong and observable in the COSY spectrum. There was an off-diagonal signal linking G to H, suggesting that signals G and H were the H3n and the H7s protons, respectively. By elimination, signals F and I must be the H3x and the H7a protons.

Figure 13: The irradiation of signal H in a ^1H -nmr NOE experiment of *endo*-171 in deuterated benzene.

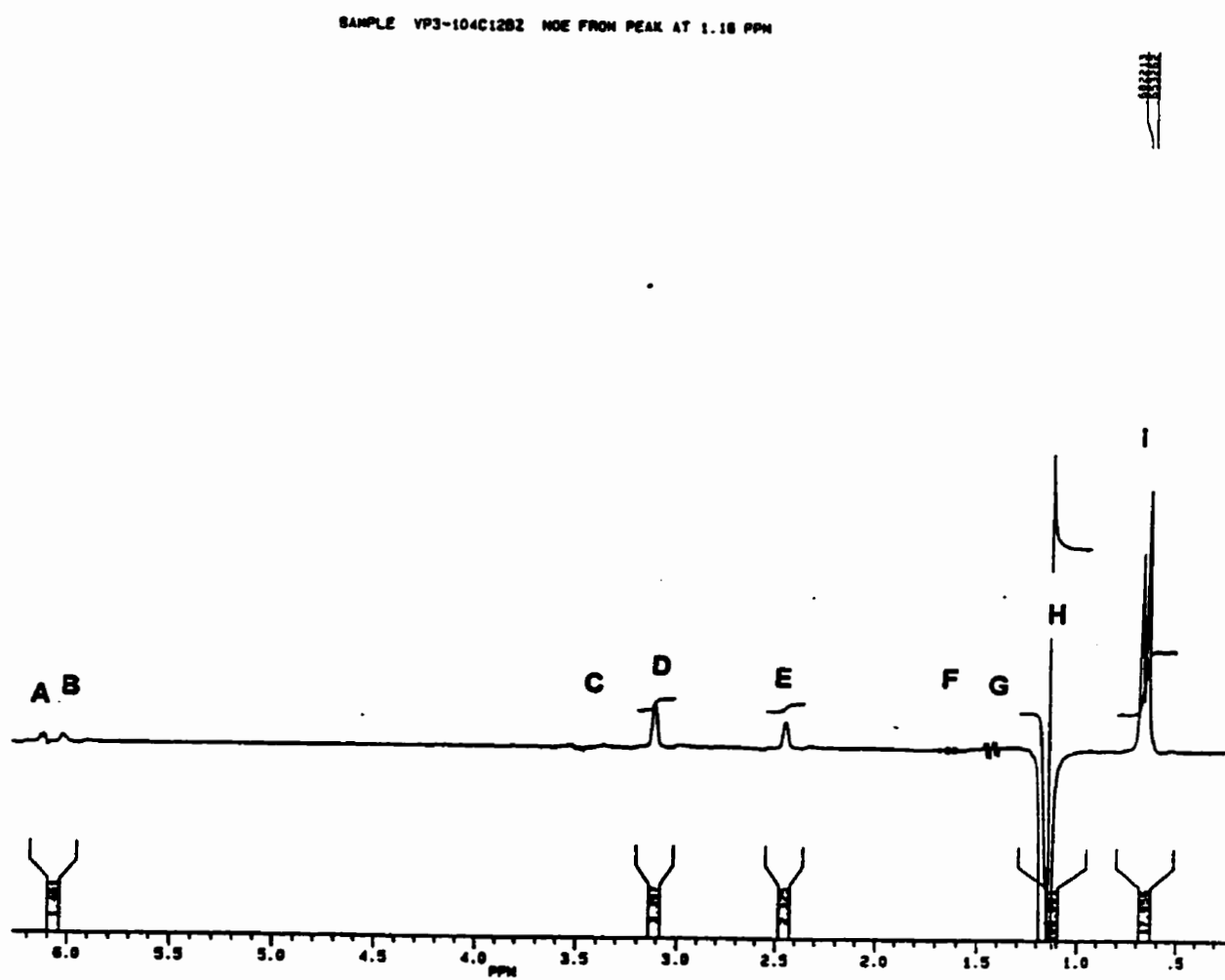
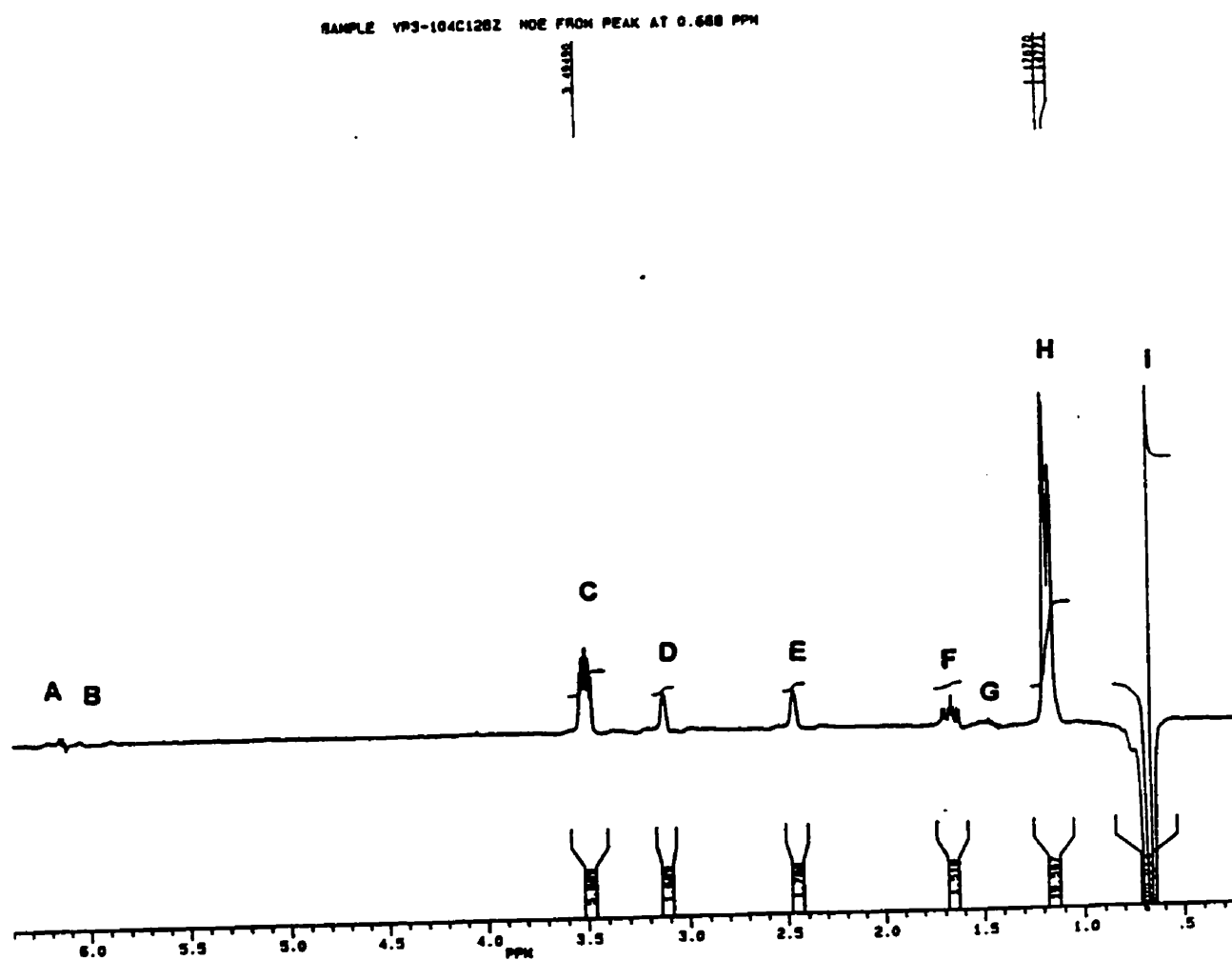
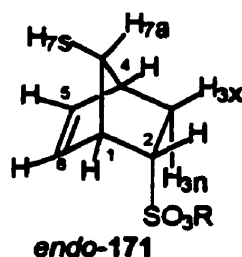


Figure 14: The irradiation of signal I in ^1H -nmr NOE experiment of *endo*-171 in deuterated benzene.



To confirm the assignment of the ^1H - ^1H COSY spectrum of *endo*-171 in deuterated benzene, nuclear Overhauser effects (NOE) were measured.

In an NOE experiment one observes an enhanced NMR signal for a nucleus when its neighboring nuclei are irradiated. NOE effects depend on direct magnetic coupling between nuclei (dipolar coupling), and do not depend on scalar coupling. The NOE experiment provides an indirect way to extract information about this dipolar coupling, which in turn can be related to internuclear distances.



In compound *endo*-171, the assignment of the two H7 protons can be obtained by irradiating either the signal of the H7a proton or the signal of the H7s proton. The irradiation of the H7a signal should cause an enhancement in intensities of the nearby nuclei, H1, H4, H7s, H2 and H3x. Moreover, there should be no enhancement in intensities for far away nuclei such as H5, H6 and H3n. In addition, the irradiation of H7s should cause an enhancement in intensities for signals from H5, H6, H7a, H1, and H4. Also, there should be no enhancement in intensities for H2, H3n, H3x.

To check the validity of the COSY assignment, two NOE spectra of *endo*-171 in deuterated benzene were obtained. Signal H, assigned as H7s, was irradiated in one spectrum (Figure 13) and signal I, assigned as H7a, was irradiated in another (Figure 14). The irradiation of signal H showed an enhancement in the signals from H5, H6, H1, H4 and the signal labeled I, indicating that signal H must be the H7s proton. Moreover, the

irradiation of signal I showed an enhancement in H2, H1, H4, H7s and H3x signals. This confirmed that signal I was the H7a proton. The assignments using COSY and NOE methods agree with one another, confirming the COSY assignment.

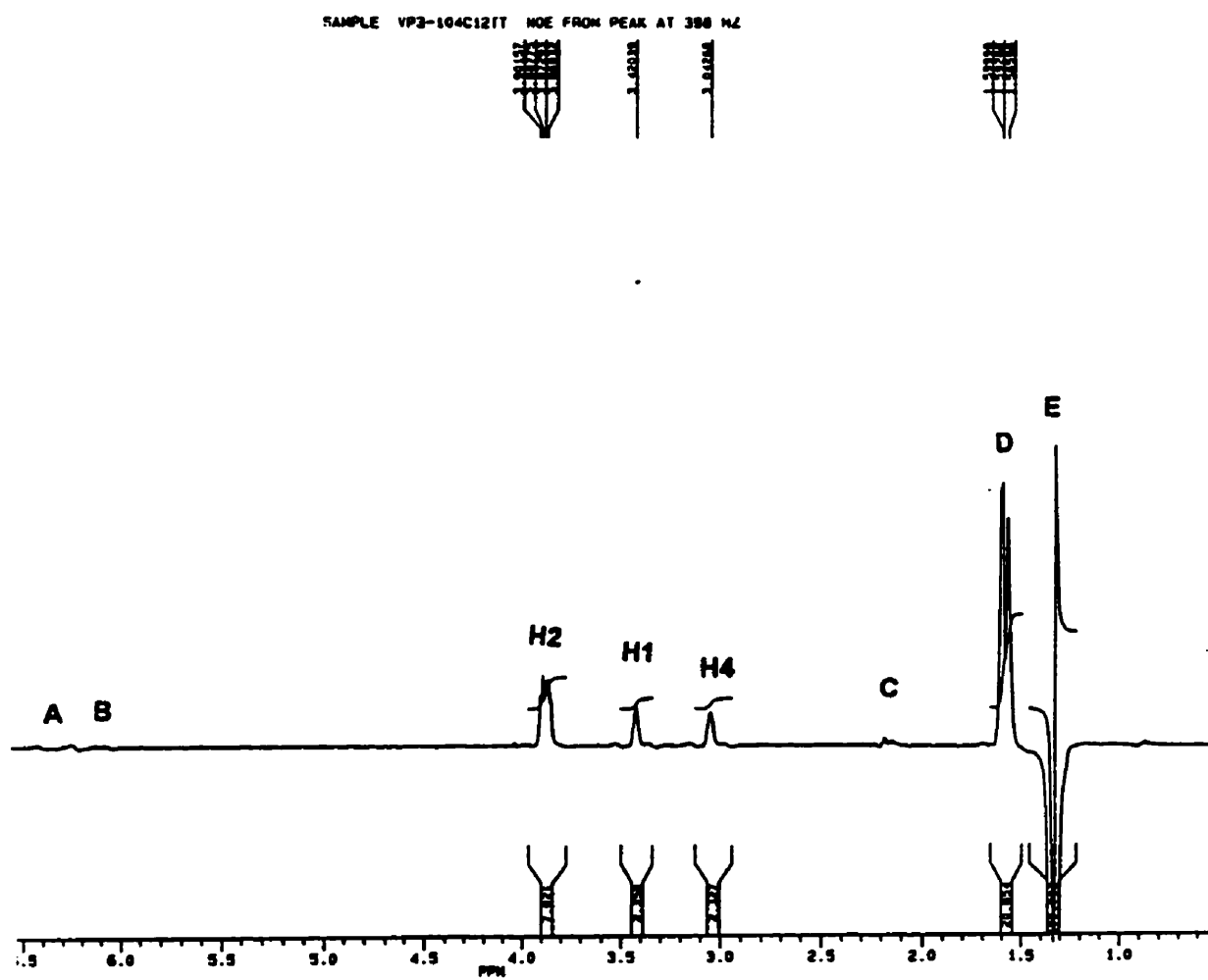
A complete assignment of the ^1H -nmr spectrum of *endo*-171 in deuterated benzene facilitated the analysis of the ^1H -nmr spectrum of *endo*-171 in deuterated chloroform (Figure 11).

The assignment of peaks A and B in the ^1H - ^1H COSY spectrum of *endo*-171 (Figure 11) in deuterated chloroform, started with an examination of their couplings to the H4 proton. The ^1H - ^1H COSY spectrum indicated that signal A was strongly coupled with the H4 proton, whereas signal B was weakly coupled to the same proton. Using the same argument as in the analysis of the *exo*-171 in deuterated chloroform and of the *endo*-171 in deuterated benzene, signals A and B were assigned to H5 and H6, respectively.

The differentiation of the two H3 protons from the two H7 protons was based on their coupling to the H1 proton. The two H7 protons should be strongly coupled to H1, while the two H3 protons should not be coupled to this proton. Both peaks D and E showed off-diagonal signals indicating coupling to H1, suggesting that peak E and one proton of peak D were the two H7 protons. By elimination, peak F and one remaining proton in peak D must be the two H3 protons.

The exact assignment of the four protons, H3n, H3x, H7a and H7s, could not be made based on the ^1H - ^1H COSY spectrum since the coupling partners of the two protons in signal D could not be confidently determined. Instead, the NOE method was used to assign these protons.

Figure 15: The irradiation of signal H in ^1H -nmr NOE experiment of *endo*-171 in deuterated chloroform.



A NOE experiment on compound *endo-171* in deuterated chloroform was carried out by irradiating signal E (Figure 15). This experiment showed that nucleus E was close to the H1, H2, H4, and D signals, therefore signal E was assigned to the H7a proton. By elimination, one proton in signal D must be the H7s proton.

The irradiation of the H7a signal (signal E) did not show enhancement of signals other than those noted above, even though enhancement of H3x was expected. Since the distance between the two H3 protons is shorter than that between the H7a and the H3x protons, the dipolar relaxation of the H3x nuclei was probably dominated by the H3n nuclei, causing a leakage in the relaxation. Thus, there was no enhancement of the H3x signal. Consequently, the H3 protons could not be assigned using the evidence from the NOE experiment.

To assign the two H3 protons, an assumption was made that the values of the three bond couplings do not change significantly on changing solvent. The three coupling constants that can be calculated from the splitting of signal C in deuteriochloroform (3.7, 9.3, and 12.8 Hz) were very similar to the couplings derived from the signal assigned to H3x in deuterated benzene (3.7, 9.2, and 12.7 Hz). Thus signal C must be the H3x proton, and by elimination one proton in signal D should be the H3n proton.

The complete assignment of the signals in the spectrum of compound *endo-171* in deuterated chloroform followed from the measurement of all of the internuclear coupling constants (Table 12). Although the signals of H1, H4, H7s, H7a and H3x were not resolved, coupling constants could be obtained from measurements made on the remaining signals (H2, H5, H6 and H3x). These values are very similar to those obtained from the

¹H-nmr spectrum of *endo*-171 in deuterated benzene, suggesting that the assignments were correct.

Table 12: The measured couplings (Hz) of *endo*-171.

	<i>endo</i> -171 in CDCl ₃	<i>endo</i> -171 in benzene-d ₆
³ J _{H1,H2}	3.3	3.3
³ J _{H2,H3n}	4.7	4.8
³ J _{H2,H3x}	9.2	9.2
³ J _{H3n,H3n}	12.8	12.5
³ J _{H3n,H7s}	not resolved	2.8
³ J _{H3x,H4}	3.7	3.7
³ J _{H4,H5}	3.1	3.1
³ J _{H4,H6}	2.8	2.8
³ J _{H5,H6}	5.6	5.6

Table 13: Measured ¹H-nmr chemical shift data for *exo*- and *endo*-171 in CDCl₃.

Cmpd	H-1	H-2	H-3x	H-3n	H-4	H-5	H-6	H-7a	H-7s
<i>endo</i> -171	3.43	3.87	2.18	1.58	3.05	6.32	6.14	1.33	1.59
<i>exo</i> -171	3.43	3.10	2.21	1.64	3.07	6.27	6.15	3.93	1.51

^a a mixture of 2 diastereomers

Final confirmation of the ¹H-nmr assignments for *exo*- and *endo*-171 were made using computer simulation of the spectra. These calculations also permitted a more exact determination of all coupling constants for both the *exo*-171 and the *endo*-171 isomers. The program used for the simulation required a processed spectrum, and an estimate of

the chemical shifts and coupling constants. The estimated chemical shifts and coupling constants were used to calculate an experimental spectrum. The chemical shifts and coupling constants were then adjusted manually until the simulated spectrum was similar to the observed spectrum. Finally, transitions in the observed spectrum were assigned to those in the calculated spectrum and the program used to iteratively adjust the chemical shifts and coupling constants in order to achieve the best fit.

The simulation started with the spectrum of *exo-171* in CDCl₃. Estimations of chemical shifts, and coupling constants greater than one Hz, were easily obtainable from the processed spectrum. The splitting pattern of the H4 signal was complicated and the frequencies and intensities of the H4 proton could not assigned to the corresponding transitions of the calculated spectrum, hence this proton was not taken into account for the calculation. The simulation involved the assignment of 1119 transitions for the eight ring proton signals, and converged with an overall RMS deviation of 0.011 Hz between calculated and assigned transitions. The calculated chemical shifts and coupling constants for *exo-171* from the simulation are listed in Table 14 and 15.

Once all the large couplings were obtained from the above simulation, smaller long range couplings were obtained from a simulation of a more highly resolved spectrum. The high resolution ¹H-nmr spectrum of *exo-171* was acquired in acetone-d₆ since acquiring ¹H-nmr spectrum in this solvent gives a much better line width than in CDCl₃. The chemical shifts of all the protons signals were different when compared to the corresponding spectrum in CDCl₃, however, the relative positions and splitting patterns of the corresponding proton signals were unchanged (Table 14). Even though the higher resolution ¹H-nmr spectrum allowed most of the coupling constants to be measured and

calculated, the H4 signals were still not resolved and were too complicated to analyze. Thus, the H4 signal was not taken into the calculation. There were 1360 transitions assigned for the eight ring protons and the simulation converged with an overall RMS deviation in transitions 0.014 Hz.

Table 14: Calculated ^1H chemical shifts (Hz) for *exo*-171.

	<i>exo</i> -171 in CDCl_3	<i>exo</i> -171 in acetone- d_6
H-5	1882.256 (0.002)	1891.002 (0.004)
H-6	1847.167 (0.002)	1866.357 (0.004)
H-1	1030.338 (0.002)	1009.277 (0.002)
H-2	930.632 (0.002)	956.560 (0.002)
H-4	921.100	920.900
H-3x	662.878 (0.002)	631.206 (0.002)
H-7a	588.942 (0.010)	565.824 (0.002)
H-3n	491.782 (0.002)	503.574 (0.002)
H-7s	454.784 (0.003)	432.509 (0.003)
RMS error	0.011	0.014

Table 15: Calculated coupling constants for *exo*-171.

$J_{x,y}$	<i>exo</i> -171 (CDCl ₃)	<i>exo</i> -171 (acetone-d ₆)
$J_{1,3x}$		0.537 (0.002)
$J_{1,4}$	1.456 (0.004)	1.565 (0.004)
$J_{1,6}$	3.236 (0.002)	3.180 (0.004)
$J_{1,7a}$	1.446 (0.002)	1.569 (0.002)
$J_{1,7b}$	1.457 (0.004)	1.558 (0.004)
$J_{2,3a}$	8.664 (0.002)	8.670 (0.002)
$J_{2,3x}$	4.873 (0.002)	4.861 (0.002)
$J_{2,4}$		0.396 (0.004)
$J_{2,6}$		0.413 (0.004)
$J_{2,7a}$	1.406 (0.002)	1.434 (0.004)
$J_{3a,3x}$	-12.529 (0.002)	-12.517 (0.002)
$J_{3a,5}$		0.726 (0.004)
$J_{3a,7a}$		0.259 (0.002)
$J_{3a,7b}$	2.656 (0.002)	2.666 (0.004)
$J_{3x,4}$	3.408 (0.002)	3.484 (0.004)
$J_{3x,5}$		0.147 (0.004)
$J_{4,5}$	2.978 (0.002)	2.926 (0.008)
$J_{4,6}$		0.611 (0.006)
$J_{4,7a}$	1.545 (0.018)	1.574 (0.004)
$J_{4,7b}$	1.545 (0.004)	1.821 (0.006)

Table 15: continue

$J_{x,y}$	<i>exo</i> -171 (CDCl ₃)	<i>exo</i> -171 (acetone-d ₆)
$J_{5,6}$	5.596 (0.002)	5.559 (0.006)
$J_{5,7a}$		0.646 (0.004)
$J_{5,7b}$		0.306 (0.004)
$J_{6,7a}$		0.646 (0.004)
$J_{6,7b}$		0.318 (0.004)
$J_{7a,7b}$	-9.053 (0.004)	-8.926 (0.004)

The H3n and H7 signals of *endo*-171 were overlapped in CDCl₃, thus it was rather difficult to estimate the chemical shifts and coupling constant for these two protons. A feasible way to simulate the spectrum of this compound was to obtain the spectrum in different solvents in which all the peaks were separated. Acetone-d₆ was the first choice since it would be a convenient solvent in which to acquire a high resolution ¹H-nmr spectrum. However, there were three overlapping proton signals in this solvent, making the ¹H-nmr spectrum even harder to simulate. The ¹H-nmr spectrum of *endo*-171 in deuterated benzene had no overlapping proton signals and was reasonably well resolved allowing estimation of all of the large coupling constants (>1 Hz). The H4 signal was again too complicated to analyze. The ⁴ $J_{2,7}$ of *endo*-171 was expected to be close to zero Hz, and a reasonable way to confirm this coupling constant was to include this and most of the other small couplings in the simulation with initial estimates near zero. The estimation of small coupling constants, those long range couplings that should be similar in

endo and *exo* isomers, were based on the coupling constants from the simulation of the *exo*-171 in acetone- d_6 . The simulation involved assigning 1220 transitions for eight proton signals and converged to give an overall RMS error of 0.0121 Hz. The coupling constants are listed in Table 16, and the most significant coupling was the very small coupling of $J_{2,7s}$ (about zero Hz), indicating that this was an *endo* isomer.

It was important to simulate the ^1H nmr spectra of *endo*-171 in the same solvent as *exo*-171 in order to achieve a consistent comparison of the two. Thus, the spectrum of *endo*-171 in CDCl_3 was simulated using the coupling constants obtained from the simulated spectrum obtained using the benzene- d_6 solvent data as a starting point (Table 16 and 17). The simulation converged with a RMS error of 0.012 Hz and the number of transitions assigned was 1071. This simulation, similar to the benzene- d_6 simulation, showed that the coupling constant between H-2 and H-7s was close to zero. These simulations and the above analysis of the chemical shifts confirmed that this isomer was an *endo* isomer.

Table 16: Calculated coupling constants for 2-*endo*-norboernene derivatives.

J_{xy}	<i>endo</i> -171 (CDCl ₃)	39 in C ₆ D ₆
$J_{1,2}$	3.141 (0.004)	3.279 (0.002)
$J_{1,3n}$	-0.032 (0.004)	-0.003 (0.002)
$J_{1,3x}$	-0.008 (0.002)	-0.002 (0.003)
$J_{1,4}$	1.524 (0.004)	1.386 (0.004)
$J_{1,5}$	0.592 (0.004)	0.521 (0.003)
$J_{1,6}$	2.900 (0.002)	2.788 (0.003)
$J_{1,7a}$	1.478 (0.002)	1.377 (0.003)
$J_{1,7b}$	1.609 (0.004)	1.900 (0.003)
$J_{2,3n}$	4.832 (0.004)	4.778 (0.003)
$J_{2,3x}$	9.209 (0.002)	9.291 (0.003)
$J_{2,4}$	-0.001 (0.004)	-0.001 (0.003)
$J_{2,6}$	-0.000 (0.002)	-0.001 (0.002)
$J_{2,7a}$	-0.069 (0.004)	-0.002 (0.002)
$J_{3n,x}$	-12.430 (0.004)	-12.169 (0.003)
$J_{3n,4}$		-0.048 (0.004)
$J_{3n,5}$	0.591 (0.004)	0.607 (0.003)
$J_{3n,a}$	0.002 (0.002)	0.000 (0.002)
$J_{3n,s}$	2.267 (0.004)	2.881 (0.003)
$J_{3x,4}$	3.607 (0.004)	3.591 (0.004)
$J_{3x,5}$	-0.002 (0.004)	-0.188 (0.003)

Table 16: continue

$J_{x,y}$	<i>endo</i> -171 (CDCl ₃)	39 in C ₆ D ₆
$J_{3x,a}$	0.002 (0.002)	0.000 (0.002)
$J_{3x,b}$	-0.070 (0.004)	-0.034 (0.003)
$J_{4,5}$	3.071 (0.004)	2.794 (0.004)
$J_{4,6}$	0.713 (0.004)	0.693 (0.003)
$J_{4,7a}$	1.372 (0.004)	1.376 (0.003)
$J_{4,7b}$	1.6000 (0.004)	1.849 (0.004)
$J_{5,6}$	5.715 (0.004)	5.638 (0.003)
$J_{5,7a}$	0.608 (0.004)	0.689 (0.003)
$J_{5,7b}$	-0.019 (0.004)	0.000 (0.003)
$J_{6,7a}$	0.688 (0.002)	0.684 (0.002)
$J_{6,7b}$	-0.002 (0.002)	-0.001 (0.003)
$J_{7a,7b}$	-8.612 (0.004)	-8.742 (0.003)

Table 17: Calculated ^1H chemical shifts (Hz) for 2-*endo*-norbornene derivatives.

	<i>endo</i> -171 in CDCl_3	<i>endo</i> -171 in C_6D_6
H-5	1896.801 (0.003)	1802.873 (0.002)
H-6	1844.028 (0.002)	1800.101 (0.002)
H-2	1161.240 (0.002)	1037.961 (0.002)
H-1	1027.657 (0.003)	930.031 (0.002)
H-4	914.500	728.202
H-3x	654.451 (0.002)	484.558 (0.002)
H-7s	475.528 (0.003)	341.815 (0.002)
H-3n	475.411 (0.003)	431.361 (0.002)
H-7a	398.849 (0.002)	186.727 (0.002)
RMS error	0.012	0.009

Section 5.2.2: The selectivity of the chiral sulfonyl esters in Diels-Alder reactions.

It has been demonstrated that the Diels-Alder reaction of phenyl vinylsulfonate, **120**, with cyclopentadiene produced two compounds, *exo*-**171** and *endo*-**171**. The ratio of these two isomers was deduced from the integration of the ¹H-nmr spectrum of the crude mixture. The integration of the H5 signals were used to calculate the *endo* and *exo* ratio as the two signals were reasonably well separated (see Table 19). The diastereomeric (*exo* vs *endo*) selectivity of this reaction was not very high. Nevertheless an investigation of the overall stereoselectivity for the addition of the chiral sulfonyl esters to cyclopentadiene was pursued.

The Diels-Alder reaction of chiral vinylsulfonyl esters with cyclopentadiene should result in the four bicyclic structures of **A**, **B**, **C**, **D** as shown in Scheme 42. The procedure for reacting (methyl (*S*)-lactyl) vinylsulfonate **101** to cyclopentadiene was similar to that of the Diels-Alder reaction with phenyl vinylsulfonate, Scheme 42. A comparison of ¹H and ¹³C-nmr of the mixture of products to *endo*-**171** and *exo*-**171** hinted that there were at least four cycloadducts. Two compounds had ¹H- and ¹³C-nmr patterns similar to those in *exo*-**171**. Thus they should be *exo*-**175C** and **D**. The other two compounds had ¹H- and ¹³C-nmr patterns similar to those in *endo*-**171**. Hence, they should be the *endo*-**175A** and **B**. In this case, the *endo* and *exo* ratio was determined by integrating the H-6 protons of the crude ¹H-nmr spectrum (see Table 19). The results showed that the *endo* isomers were the major products from reactions run at both 80 °C and at room temperature. The isomeric selectivity (*exo* vs *endo*) was better than that of the corresponding phenyl derivative. The *endo* and the *exo* cycloadducts were separated on silica gel using 30% EtOAc in hexane. *Exo*-**175** was eluted first followed by *endo*-**175**. The proton and

carbon spectra of *exo*-175 showed that there were two sets of proton and carbon peaks with equal intensities. This indicated that the two *endo* cycloadducts, *endo*-175A and *endo*-175B, were produced in equal amounts. Similarly, the two *exo* cycloadducts, *exo*-175C and *exo*-175D, were formed in equal amounts. These results indicated that there was no diastereofacial selectivity in the Diels-Alder reaction of chiral dienophile methyl (*S*)-lactate vinylsulfonate, 101.

Scheme 42:

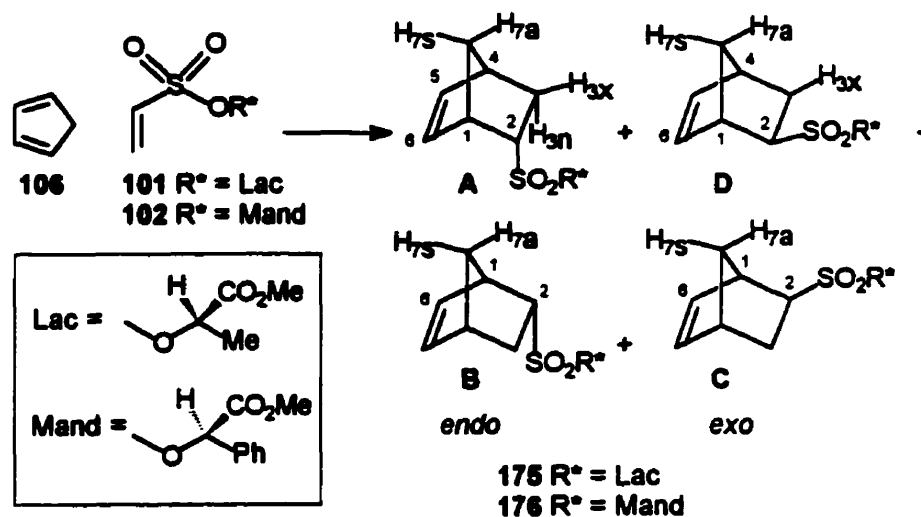


Table 18: Measured ¹H-nmr chemical shift data for cycloadducts 175 and 176 in CDCl₃.

Cmpd	H1	H2	H3x	H3n	H4	H5	H6	H7a	H7s
<i>endo-171</i>	3.43	3.87	2.18	1.58	3.05	6.32	6.14	1.33	1.59
<i>endo-175*</i>	3.42	3.87	2.17	1.50	3.03	6.29	6.10	1.33	1.56
	3.39	3.87	2.21	1.54	3.03	6.29	6.09	1.33	1.56
<i>endo-176*</i>	3.36	3.81	2.09	1.48	2.99	6.26	6.09	1.27	1.53
	3.36	3.81	2.09	1.48	2.99	6.24	6.06	1.27	1.53
<i>exo-171</i>	3.43	3.10	2.21	1.64	3.07	6.27	6.15	3.93	1.51
<i>exo-175*</i>	3.38	3.09	2.13	1.62	3.03	6.26	6.17	1.90	1.47
	3.38	3.08	2.12	1.62	3.03	6.26	6.17	1.90	1.47
<i>exo-176*</i>	3.35	2.99	2.12	1.57	3.00	6.22	6.12	1.88	1.44
	3.33	2.95	2.10	1.51	3.00	6.20	6.01	1.88	1.44

Table 19: Stereoselectivity of the Diels-Alder reactions of vinylsulfonates in benzene (see Scheme 42 and 43).

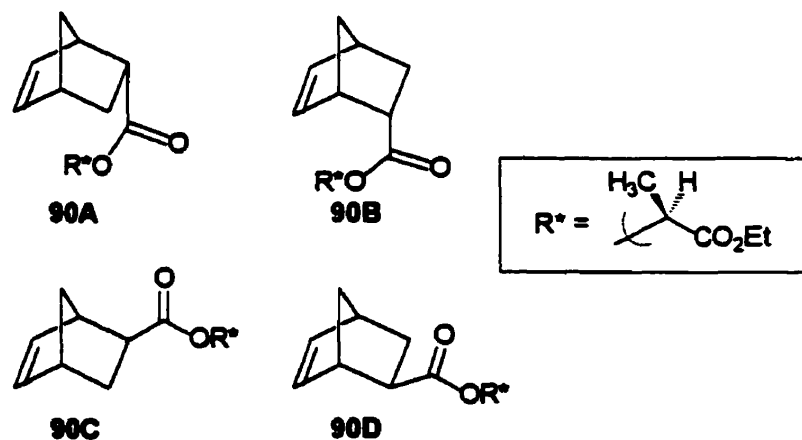
Compound	Chiral auxiliary	Catalysts	Temperature	A+B:C+D	A:B	C:D
				<i>(endo:exo)</i>		
171	Phenyl	-	rt	2.42	-	-
171	Phenyl	-	reflux	2.10	-	-
175	methyl (<i>S</i>)-lactyl	-	rt	3.58	1:1	1:1
175	methyl (<i>S</i>)-lactyl	-	reflux	4.04	1:1	1:1
175	methyl (<i>S</i>)-lactyl [*]	MeAlCl ₂	0°C	3.60	1:1	1:1
176	methyl (<i>R</i>)-mandelyl	-	rt	4.38	1:1	1:1
176	methyl (<i>R</i>)-mandelyl	-	reflux	3.18	1:1	1:1
90 ^{***}	ethyl (<i>S</i>)-lactyl ^{**}	-	rt	1.94	73:27	20:80
90 ^{***}	ethyl (<i>S</i>)-lactyl [*]	-	rt	3.22	58:42	32:68
90 ^{***}	ethyl (<i>S</i>)-lactyl [*]	TiCl ₄	-63.5°C	16	85:15	-

^{*} CH₂Cl₂ as a solvent

^{**} Toluene as a solvent

^{***} see Scheme 43 and section 2.2, page 30 (reference 26).

Scheme 43:



The effect of MeAlCl_2 , a Lewis acid, on the Diels-Alder reaction of **101** to cyclopentadiene was also studied. The presence of Lewis acids during the Diels-Alder reaction of the acrylate of ethyl (*S*)-lactate to cyclopentadiene increased both the diastereo and facial selectivity of the reaction (see Section 2.2, page 30). Thus, by adding MeAlCl_2 to the Diels-Alder reaction of **101** with cyclopentadiene, the diastereo and facial selectivity might be improved. A solution of MeAlCl_2 in CH_2Cl_2 was added to a mixture of **101** and cyclopentadiene in CH_2Cl_2 at 0°C and the resulting mixture was stirred for 5 h. Workup and chromatography as in the procedure described for the Diels-Alder reaction of **120** provided the results listed in Table 19. Unfortunately neither the diastereofacial or *endo/exo* selectivity was improved.

The reaction of (methyl (*R*)-mandelyl) vinylsulfonate **102** with cyclopentadiene produced a mixture of four cycloadducts, **176**. A comparison of their ^1H - and ^{13}C -nmr patterns to that of *endo*- and *exo*-**171** suggested that two of the cycloadducts were *endo*-**176A** and **B** and the other two were *exo*-**176C** and **D**. The cycloaddition of (methyl (*R*)-mandelyl) vinylsulfonate, **102**, to cyclopentadiene produced a very similar result to the

reaction of **101** (Table 19) with cyclopentadiene in that no diastereofacial selectivity was observed.

Section 5.3: Conclusion

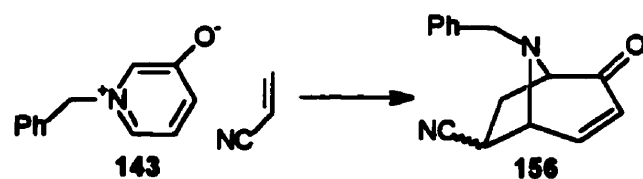
In this work, chiral vinylsulfonates, **101** and **102**, were successfully prepared. The Diels-Alder reaction of the achiral vinylsulfonate, **120**, was studied first and the two expected products, *exo*-**171** and *endo*-**171**, were identified and the ^1H and ^{13}C -nmr spectra were completely assigned. Their identification was further confirmed by computer simulation of the ^1H -nmr spectra. These assignments were used as a basis to identify the more complicated cycloadducts produced from the Diels-Alder reaction of the chiral vinylsulfonates.

The diastereofacial selectivity of the Diels-Alder reaction of chiral vinylsulfonates, **101** and **102**, to cyclopentadiene were rather disappointing. In both the reaction of **101** and **102** with the cyclopentadiene, there was no diastereofacial selectivity observed. Moreover, lowering the reaction temperature to 0°C and adding of MeAlCl_2 to the Diels-Alder reaction of **101** did not improve the diastereofacial selectivity. Perhaps the chiral auxiliary groups in the vinylsulfonate have a low rotational barrier that allows them to adopt many different conformations at the reaction temperature. As a consequence there may be very little difference in the steric hindrance for approach to the *re* and *si* faces of the vinyl group. It was obvious from the results that these chiral vinylsulfonates would not be useful for asymmetric Diels-Alder reactions.

Chapter 6

1,3-Dipolar cycloaddition of a N-substituted 3-oxidopyridinium betaine to a substituted alkene provides a convenient method for constructing the azabicyclo[3.2.1]octane ring system, a building block for a vast number of natural products, the tropane alkaloids (Scheme 44).

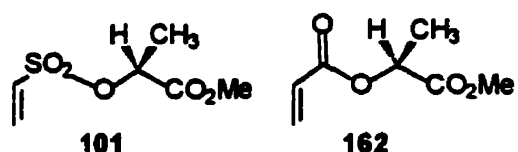
Scheme 44:



Although cycloadditions of N-substituted 3-oxidopyridinium betaines to dipolarophiles have been studied extensively,⁵¹ only one study of asymmetric addition, with marginal diastereoselectivity, was found in the literature.⁷² Improving the diastereoselectivity of the 1,3-dipolar cycloadditions of 3-oxidopyridinium betaines, by searching for a better chiral dipolarophile so that it will be more useful in the synthesis of natural products, is the main goal of the study described in this thesis.

The two chiral dipolarophiles chosen for the study of asymmetric 1,3-dipolar cycloadditions were (methyl (*S*)-lactyl) vinylsulfonate 101 and (methyl (*S*)-lactate) acrylate 162. Although vinylsulfonate esters have been shown to be very reactive as dienophiles in Diels-Alder reactions, there were no examples of 1,3-dipolar cycloadditions to the vinylsulfonate esters. Thus, in this study, the ability of vinylsulfonate esters to behave as dipolarophiles in 1,3-dipolar cycloaddition reactions with 3-oxidopyridinium betaines was first examined. If simple vinylsulfonate esters react efficiently as dipolarophiles, then

further studies on the diastereoselectivity of the cycloaddition of chiral vinylsulfonates, such as **101**, to betaines would be examined. Although, there was no asymmetric induction found in Diels-Alder reactions of **101** (see previous chapter), it was still considered possible that dipolar cycloaddition might show better diastereoselectivity.



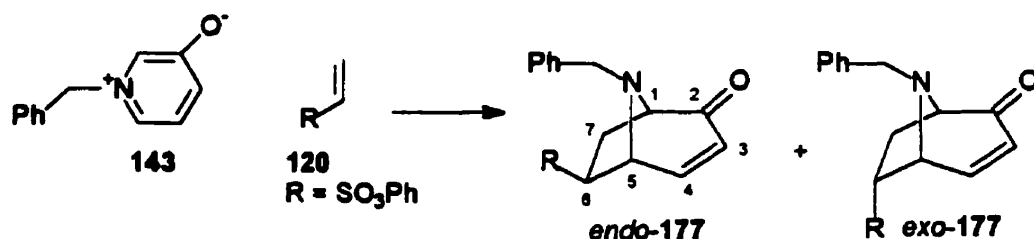
The other candidate as chiral dipolarophile, **162**, has already been extensively studied in asymmetric Diels-Alder reactions, and these cycloadditions have been shown to occur preferentially at the *re* face of the dienophile with high stereoselectivity. In this study, the diastereoselectivity of the 1,3-dipolar cycloaddition of **162** to a 3-oxidopyridinium betaine was examined, and this reaction was ultimately used for the synthesis of Bao Gong Teng A.

Section 6.1: 1,3-Dipolar cycloadditions of chiral vinylsulfonates:

1,3-Dipolar cycloadditions of 3-oxidopyridinium betaines have been typically carried out in neat dipolarophile at reflux temperature.^{51,63,64,69} Although this method has been generally successful for readily available dipolarophiles, it would not be a practical method for asymmetric cycloadditions to chiral dipolarophiles since these dipolarophiles are usually not available in large quantities. For this reason, trial cycloadditions of phenyl vinylsulfonate (**120**) to N-benzyl-3-oxidopyridinium betaine (**143**) were carried out using a 1:1 molar ratio of dipolarophile and betaine (Scheme 45).

The hydrochloride salt of betaine **143** (1.3 equivalents) was stirred in an excess of base (Et_3N) in ethyl acetate for two hours to obtain the betaine **143**. The betaine was added to one equivalent of phenyl vinylsulfonate (**120** Scheme 45) and the mixture was refluxed under nitrogen atmosphere for twelve hours. Another equivalent of betaine was then added and refluxing continued for another twelve hours. The solvent was evaporated and the crude product was purified by chromatography on a column of silica gel with a mixture of CH_2Cl_2 :EtOAc:hexane (17:22:56). The product was obtained as a yellow oil in 75 % yield (assuming a 1:1 cycloadduct structure). The ^1H -nmr spectrum of the product had two sets of peaks with different intensities, suggesting that the 1,3-dipolar cycloaddition reaction of **120** to betaine **143** had produced two isomeric adducts in different amounts. Based on previous cycloaddition reactions of **143**, the cycloadducts *endo*-**177** and *exo*-**177** (Scheme 45) were expected. The isomeric products were not separable by column chromatography.

Scheme 45:



^1H -nmr analyses of [3.2.1] bicyclic ring systems, similar in structure to **177**, have been reported by Katritzky (Table 20 and 21).⁶¹ The H3 and H4 proton signals are easily identified on the basis of their chemical shift and splitting pattern. For compounds listed in Table 20 and 21, the H4 proton signals have a chemical shift higher than all of the remaining aliphatic protons. H4 appears as a doublet of doublets with $J_{3,4}$ and $J_{4,5}$ of

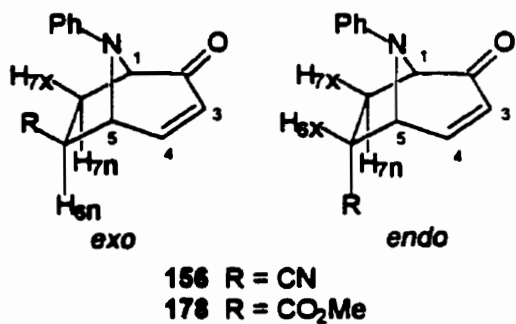
approximately 10.0 and 5.0 Hz, respectively. The next highest chemical shift signal belongs to the H3 proton, usually more than half of a ppm lower field than the H4 signals when CDCl_3 is used as solvent. The H3 signal also appears as a doublet of doublets with $J_{3,4}$ and $J_{1,3}$ of about 10.0 and 1.4 Hz, respectively.

The splitting patterns of the bridge head proton H5 characterize the stereochemistry of the cycloadducts, since the coupling between the H5 proton and the H6 proton ($J_{5,6}$) in *exo*-isomers is negligible whereas $J_{5,6}$ in *endo*-isomer is relatively large (6 to 8 Hz). The H5 signal of *exo*-isomers appears as a doublet with $J_{4,5}$ of about 5.0 Hz, while the H5 signal of *endo*-isomers appears as a doublet of doublets with $J_{4,5}$ and $J_{5,6}$ of about 5.0 and 6.0 Hz, respectively.

The splitting pattern of the H6 signal can provide even more help in identifying the *endo* and the *exo*-isomers. For *exo*-isomers, the H6 signal appears as a doublet of doublets with $J_{6,7x}$ and $J_{6,7n}$ of about 3.4 and 9.4 Hz, respectively. For *endo*-isomers, the H6 signal appears as a triplet of doublets, due to the additional large coupling between the H5 proton and the H6 protons ($J_{6,7x}$ and $J_{6,7n}$ and $J_{6,5}$ of about 10.0, 6.0 and 6.0 Hz, respectively).

In all four isomers listed in Table 20 and 21, the H7x signals are doublet of doublet of doublets, the H7n signals are doublet of doublets and the H1 signals are doublets.

Table 20: Chemical shifts of the [3.2.1] bicyclic ring protons of some cycloadduct compounds.⁶¹



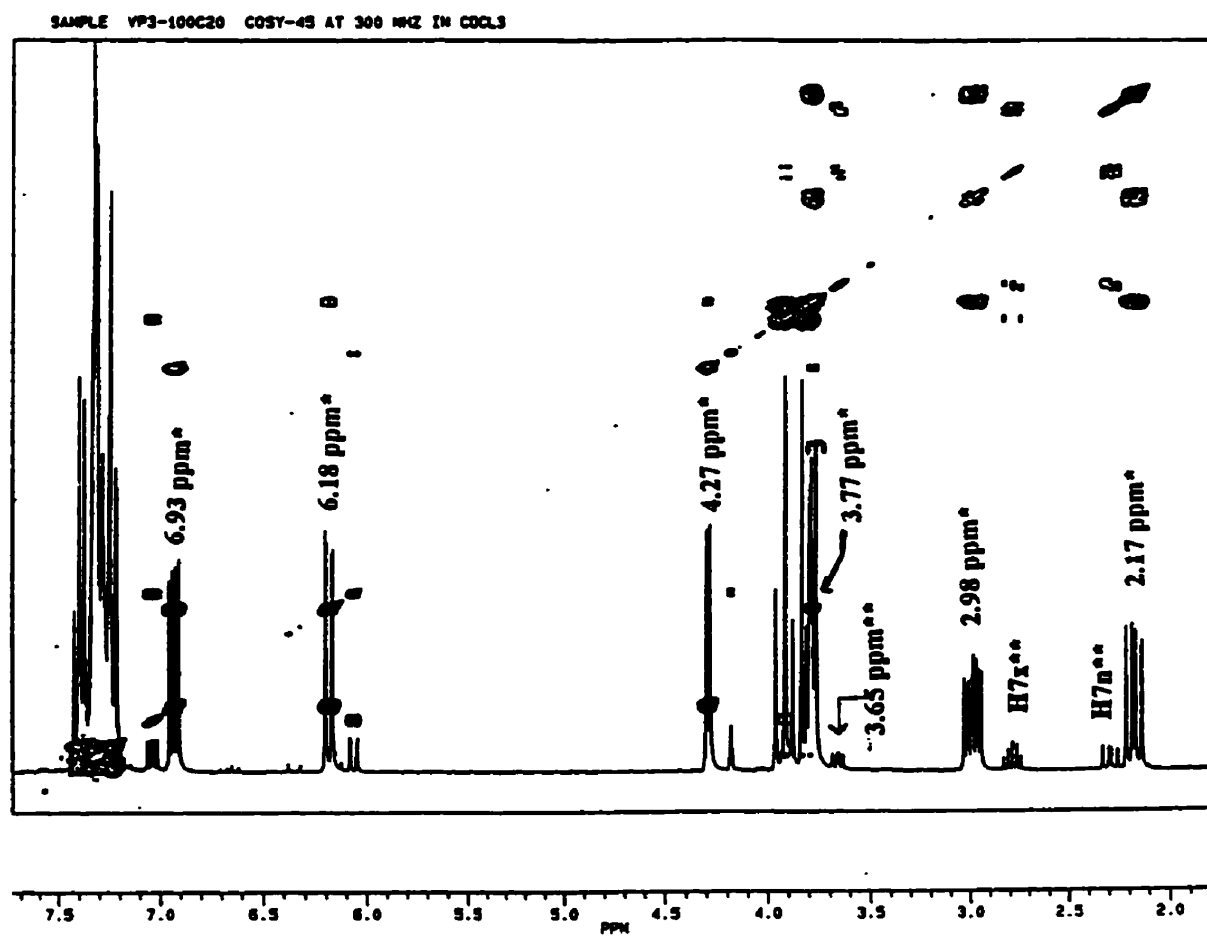
Cmpd	Solvents	H1	H3	H4	H5	H6	H7n	H7x
<i>exo</i> -156	CDCl ₃	4.55	5.98	7.28	4.92	3.12	3.22	2.87
<i>endo</i> -156	CDCl ₃	4.46	6.14	7.18	4.88	3.50	2.06	2.95
<i>exo</i> -178	CDCl ₃	4.48	5.93	7.13	5.09	3.07	2.11	3.02
<i>endo</i> -178	CDCl ₃	4.42	5.92	7.03	4.92	3.69	2.22	2.76
<i>exo</i> -178	C ₆ D ₆	4.30	5.59	6.19	4.76	2.41	1.66	2.75
<i>endo</i> -178	C ₆ D ₆	4.24	5.71	6.50	4.45	3.12	2.04	2.28

Table 21: Coupling constants of the [3.2.1] bicyclic ring of some cycloadduct compounds.⁶¹

Coupling constants	<i>exo</i> -172 in CDCl ₃	<i>endo</i> -172 in CDCl ₃	<i>exo</i> -178 in CDCl ₃	<i>endo</i> -178 in CDCl ₃	<i>exo</i> -178 in C ₆ D ₆	<i>endo</i> -178 in C ₆ D ₆
$J_{1,3}$	1.5	1.5	1.5	1.5	1.5	1.5
$J_{1,7n}$	1.0	1.0	1.0	1.5	0.8	1.5
$J_{1,7x}$	8.0	8.0	8.0	8.0	7.6	7.5
$J_{3,4}$	10.0	10.0	10.0	10.0	10.1	9.8
$J_{4,5}$	5.0	5.0	5.0	4.8	4.8	5.0
$J_{5,6}$	0.8	6.0	0.8	6.0	0.4	6.0
$J_{6,7n}$	9.4	6.0	9.4	6.1	9.8	6.5
$J_{6,7x}$	3.4	10.4	3.4	10.0	3.2	9.8
$J_{7n,7x}$	13.8	13.8	13.8	13.8	13.4	13.8

The ¹H-nmr spectrum of the mixture of cycloadducts 177 in Scheme 45 was analyzed by first identifying the H3 and H4 proton signals. The ¹H-¹H COSY spectrum was then used for the assignment of the other ring proton signals (Figure 16). Once all the signals were assigned, the splitting patterns of H5 and H6 signals were used to determine the stereochemistry of each isomer. As mentioned previously, there were two unequal sets of proton signals in the ¹H-nmr of the cycloadduct mixture. The description of the analysis of the spectrum of the major isomer will be given first followed by the analysis of the minor spectrum.

Figure 16: ^1H - ^1H COSY spectrum of the cycloadducts mixture, *endo* and *exo*-177 in CDCl_3 .



* = Major isomer

** = minor isomer

The H4 and H3 proton signals in Figure 16 were easily identified as the two doublet of doublets at 6.93 and 6.18 ppm, respectively. A horizontal line through the diagonal signal of H4 passed through the cross-peaks of the H3 proton and a doublet signal at 4.27 ppm, suggesting that this doublet was the H5 proton. A signal with multiplet splitting at 3.77 ppm, with integration for three protons, had off-diagonal signals that indicated coupling to H3, suggesting that one part of this signal corresponded to the H1 proton.

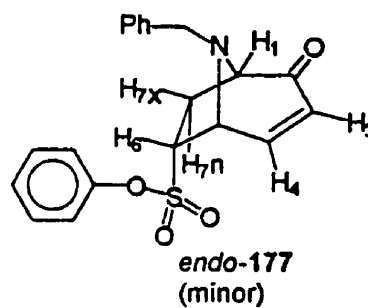
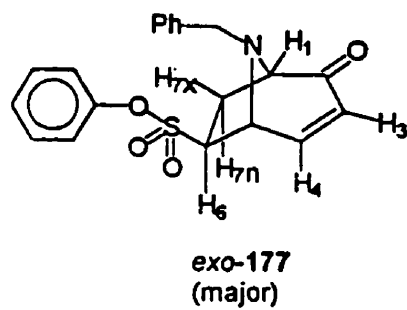
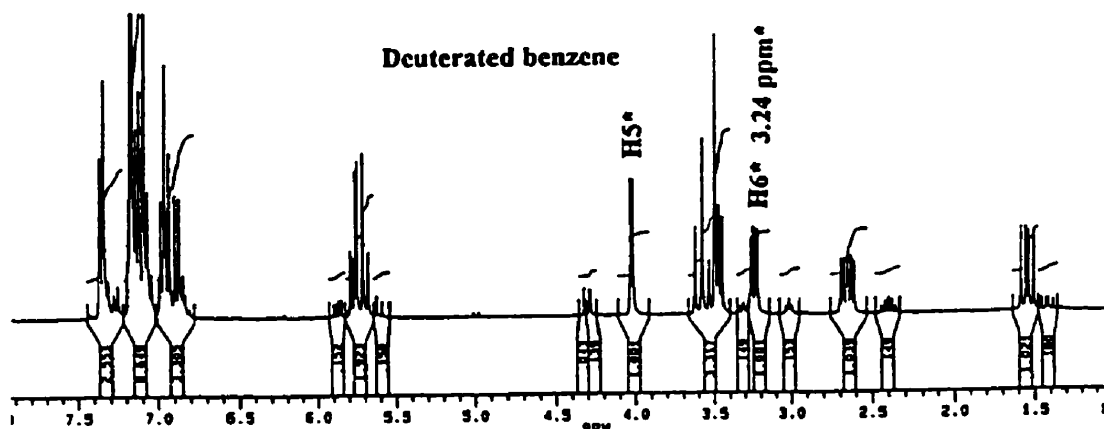
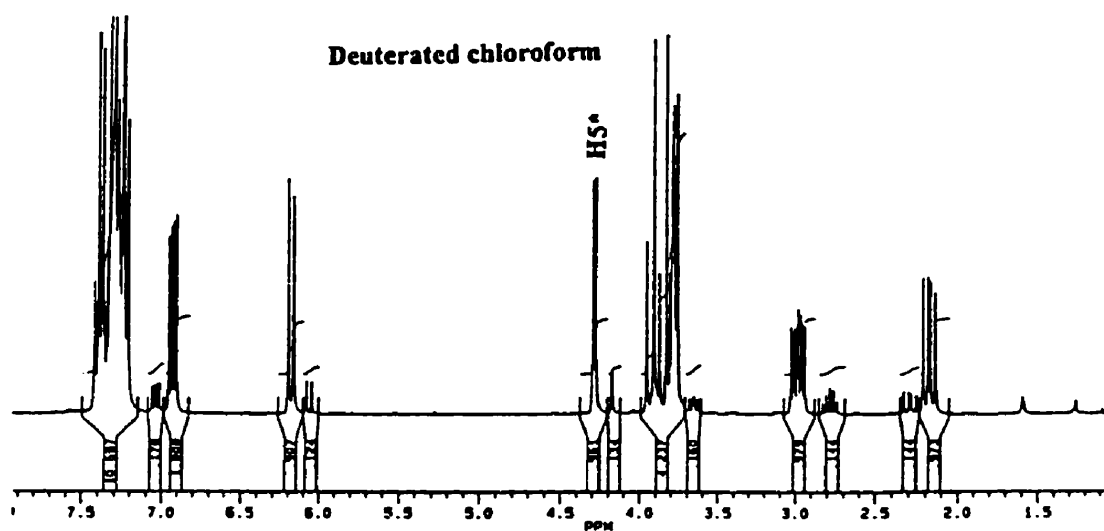
A doublet of doublets at 2.17 ppm and a doublet of doublet of doublets at 2.98 ppm were assigned to the H7n and H7x ($n = \textit{endo}$, $x = \textit{exo}$) protons signals, respectively. A multiplet at 3.77 ppm had an off-diagonal signal that indicated coupling to the H7x and H7n protons, suggesting that a part of this multiplet belongs to the H6 proton. Thus, the signals of H6 and H1 were overlapping at 3.77 ppm.

The splitting of the H5 signal (doublet), identified the major isomer as the *exo*-isomer (*exo*-177). To observe the splitting pattern of H6, deuterated benzene was used as a solvent in an effort to eliminate the overlap of this proton's signal with that of H1. In deuterated benzene (Figure 17), the H6 signal was located at 3.24 ppm, not overlapping with any other signal. Its splitting pattern, a doublet of doublets ($J = 4.4$ and 9.2 Hz), was consistent with H6 of the *exo*-isomer, hence the major isomer was *exo*-177.

The H6 signal of the minor isomer was determined by its coupling to the two H7 protons (see off-diagonal peaks in Figure 16). The H6 signal, located at 3.65 ppm, had a doublet of doublets of doublets splitting pattern, consistent with the *endo* structure of *endo*-177.

Figure 17: ^1H -nmr spectrum of the cycloadducts mixture, *endo* and *exo*-177 in CDCl_3 and C_6D_6 .

• = Major isomer

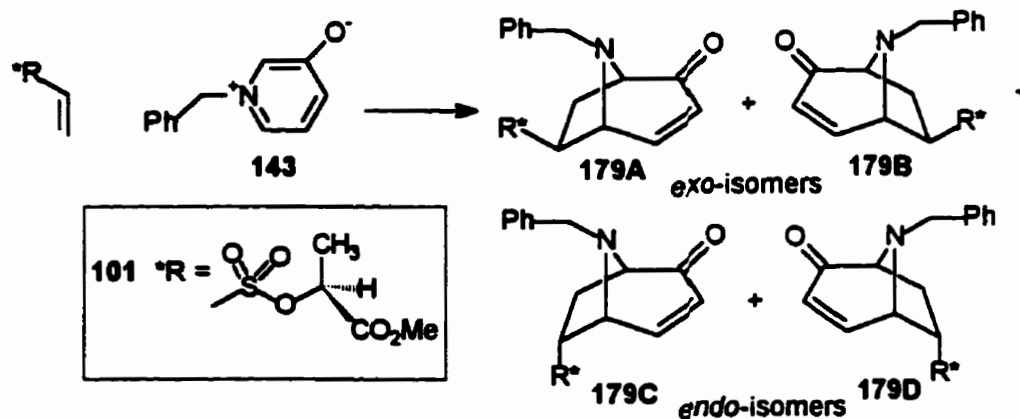


The ratio of the *endo*-177 and the *exo*-177, deduced from the integration of the H3 signals, was 1.0:7.3. The high yield and high diastereoselectivity of this reaction suggested that cycloaddition reactions of alkyl vinylsulfonate dipolarophiles with pyridinium betaines might be synthetically useful. An attempt to carry out an asymmetric version of this reaction was made using (methyl (*S*)-lactyl) vinylsulfonate 101.

The (methyl (*S*)-lactyl) vinylsulfonate ester 101 was shown to be very susceptible to nucleophilic attack by chloride ion (see section 4.1). Since the preparation of betaine 143 leaves some chloride ion in solution it was anticipated that the reaction with the lactyl vinylsulfonate might be complicated by this unwanted side reaction. In order to avoid this side reaction, the cycloaddition of 101 to 143 was performed at a lower temperature (room temperature).

A mixture of dipolarophile 101, hydrochloride salt of betaine 143 and an excess of triethylamine in ethyl acetate was stirred for one week at room temperature (Scheme 46). The reaction was worked up, then chromatographed on silica gel using 30% ethyl acetate in hexane to obtain a light yellow oil (46%). The ¹H-nmr spectrum of this oil indicated that there were two isomers produced in nearly equal amounts (Figure 18).

Scheme 46:

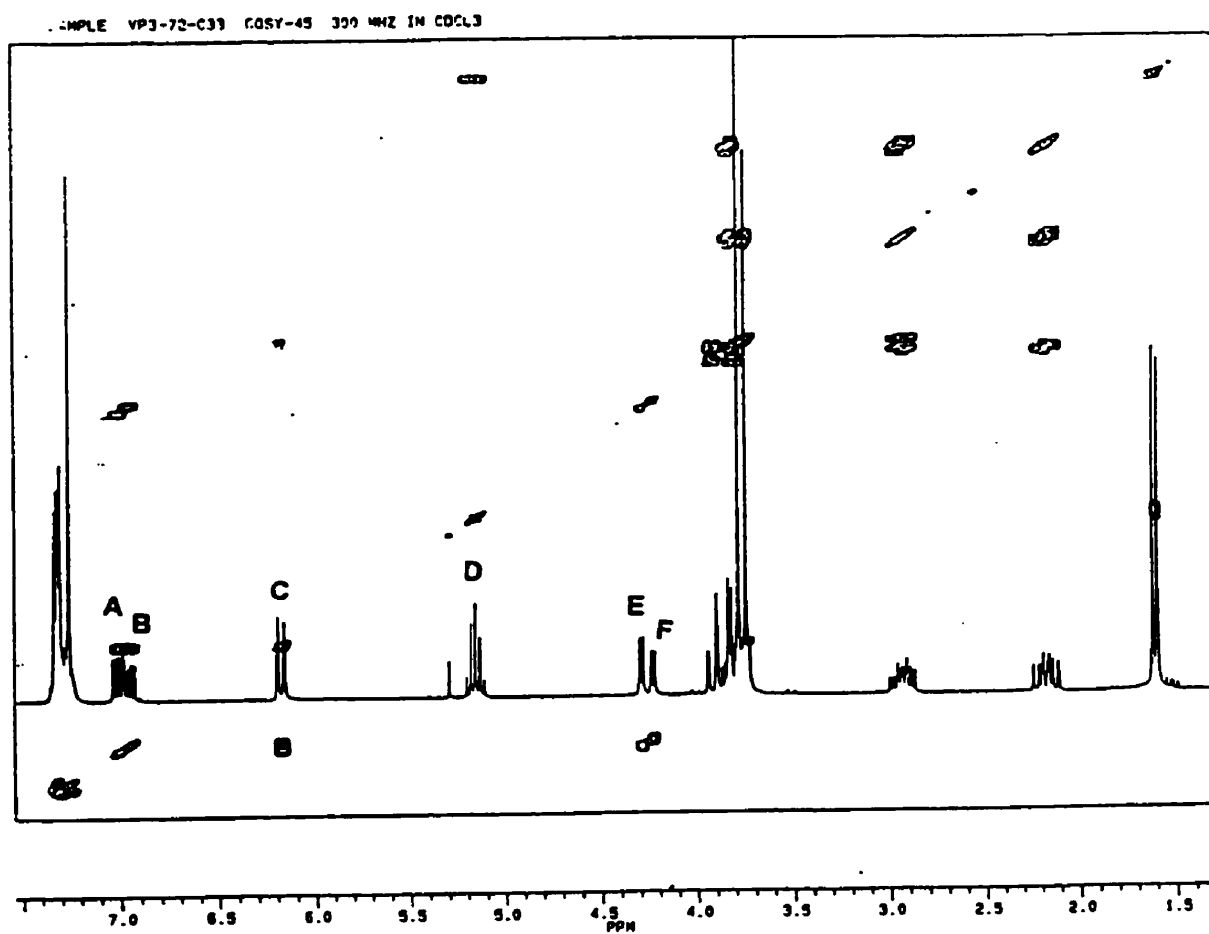


The signals in the Figure 18 have been labeled alphabetically in order to simplify the task of describing the assignment of this ^1H - ^1H COSY spectrum.

The H4 proton signals of the two cycloadducts were easily identified as signal A and B by comparison to the spectra of *endo*- and *exo*-177. A horizontal line through diagonal signal A passed through the cross-peaks of signal C and E. Thus, one proton in signal C corresponded to H3, and signal E corresponded to H5, for the cycloadduct having signal A as H4. This H5 (signal E) appeared as a doublet, hinting that this cycloadduct was the *exo*-isomer. For the cycloadduct with signal B as H4, there were off-diagonal signals linking C and F, suggesting that one proton in signal C was H3, and that signal F was H5. This H5 also had a doublet splitting pattern, indicating that it was also an *exo*-isomer.

The H6 proton signals of the two cycloadduct isomers were overlapped with six other proton signals, H1 (1H), OMe (3H) and benzyl (2H). Thus, it was impossible to use the splitting pattern of the H6 protons to determine the stereochemistry of the isomer. Moreover, changing the solvent to deuterated benzene did not resolve these overlapping signals.

Figure 18: ^1H - ^1H COSY spectrum of the cycloadduct mixture, from the reaction of **101** with betaine **143**, in CDCl_3 .



From the ^1H -nmr analysis, it appears that the 1,3-dipolar cycloaddition of (methyl (*S*)-lactyl) vinylsulfonate **101** to betaine **143** in ethyl acetate produced only the two *exo*-isomers, **179A** and **179B**, in a 1:1 ratio. Carrying out the reaction in benzene, dichloromethane or chloroform did not change the selectivity of the reaction. The poor selectivity of **101** as dipolarophile can be rationalized as it was in the corresponding Diels-Alder study of this compound (see Section 5.2). "The chiral groups in the vinyl sulfonate have a low rotational barrier that allows them to adopt many different conformations at the reaction temperature. As a consequence there may be very little difference in the steric hindrance for approach to the *re* and *si* faces". Thus, it appeared that (methyl (*S*)-lactyl) vinylsulfonate **101** would not be useful for the asymmetric synthesis of chiral [3.2.1]bicyclic structures.

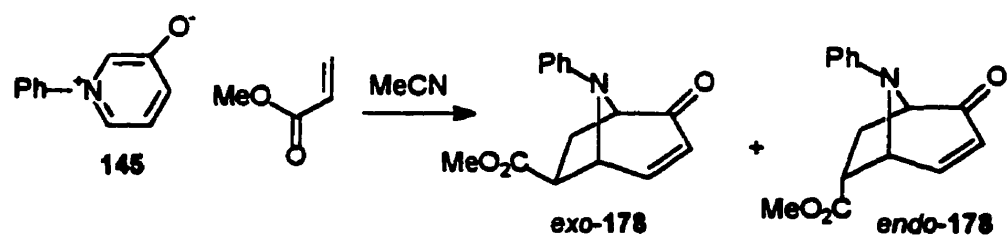
Section 6.2: 1,3-Dipolar cycloaddition of acrylate of methyl (*S*)-lactate:

In a further study of the effectiveness of the lactyl chiral auxiliary on cycloaddition reactions, a study was made of the dipolar cycloaddition of the acrylate of methyl (*S*)-lactate (**162**) to benzyl-3-oxidopyridinium betaine (**143**). The prospects for successful asymmetric cycloaddition in this reaction seemed much better than for the cycloaddition to (methyl (*S*)-lactyl) vinylsulfonate **101**. In the first place the acrylate of methyl (*S*)-lactate **162** has already been extensively studied in asymmetric Diels-Alder reactions and these cycloadditions have been shown to occur preferentially at the *re* face of the dienophile with high stereoselectivity. Secondly, achiral acrylate esters such as methyl acrylate, are known to react efficiently with betaines such as **145** (Entry 1 of Scheme 47).⁶³ Refluxing

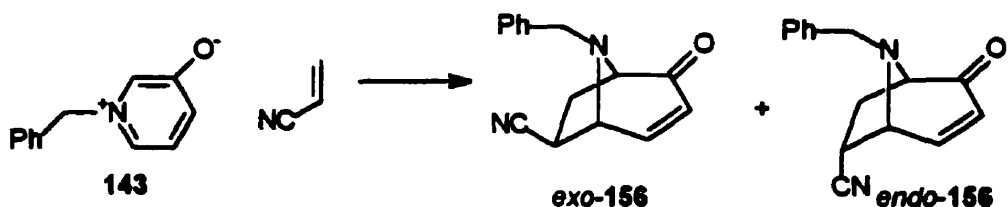
methyl acrylate with betaine **145** yielded an *endo:exo* ratio of 1.7 to 1. Thus it appeared very likely that **162** would behave as a good chiral dipolarophile in the 1,3-dipolar cycloaddition reaction with betaine **143**.

Scheme 47:

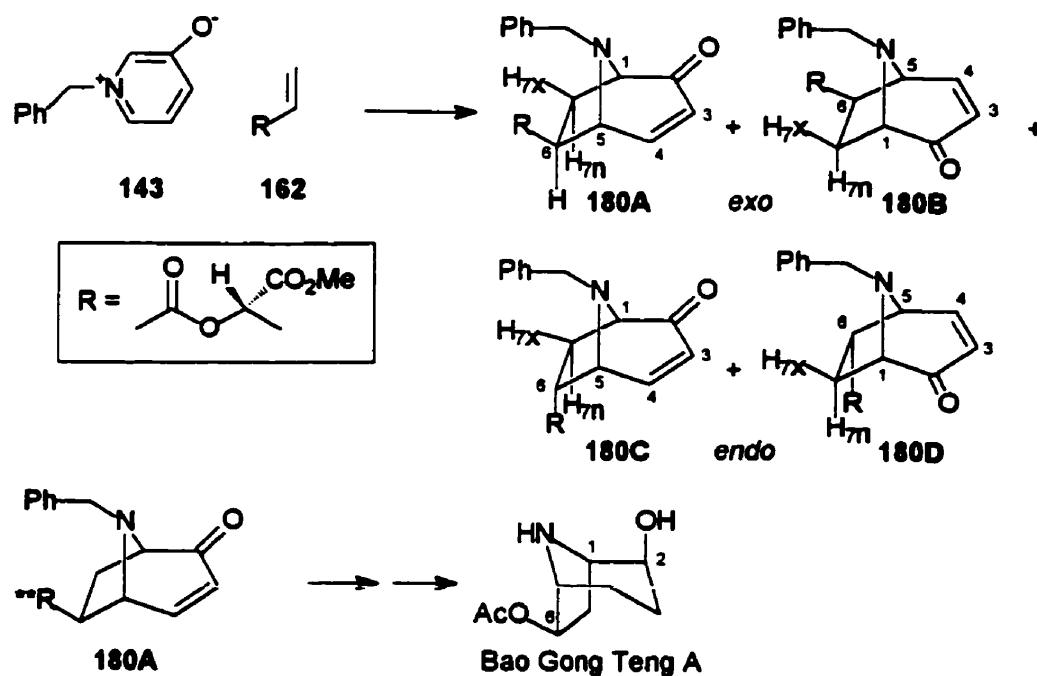
Entry 1:



Entry 2:



Contrary to results from cycloadditions to N-aryl-3-oxopyridinium betaines, 1,3-dipolar cycloaddition of N-alkyl-3-oxopyridinium betaines are known to give 6-*exo* cycloadducts as shown in Entry 2 of Scheme 47. Thus, cycloaddition of **162** to betaine **143** should yield the 6-*exo*-isomers **180A** and **180B** as major adducts (Scheme 48). Combining this with the *re* face selectivity of **162**, the latter cycloaddition should lead to a cycloadduct with the relative and absolute stereochemistry shown in structure **180A**. As pointed out in the introduction (Section 3.6) this adduct would have the appropriate absolute configuration for the preparation of the natural product Bao Gong Teng A (Scheme 48).

Scheme 48:

Initial attempts to add dipolarophile **162** to the betaine **143** as shown in Scheme 48 were carried out using 1.5 equivalents of **162** in refluxing acetone solution. This resulted in a very low conversion to adducts, and the ¹H-nmr spectrum of the crude cycloadduct mixture exhibited four sets of doublet of doublets at δ 6.90 - 7.20 ppm. From previous experience with this type of bicyclic ring (see above), these doublets of doublets should belong to the H4 protons. The intensities of these four sets of double doublets were very similar, indicating that four cycloadducts had been formed in nearly equal amounts (see Table 22 below).

When the cycloaddition was performed in refluxing benzene, the conversion to product was still low but selectivity was slightly better, producing one major isomer in about 55% yield. Lowering the temperature appeared to improve the selectivity of the cycloaddition. When the hydrochloride salt of betaine **143**, triethylamine (2 equivalents),

1.5 equivalents of **162** and a small amount of hydroquinone were stirred in benzene at room temperature for four months, 87% conversion was reached. ¹H-nmr analysis indicated that the major isomer made up at least 50 to 60% of the mixture of adducts. The solid precipitate (Et₃N·HCl) was filtered off and the filtrate washed with aqueous sodium bicarbonate (5 %), followed by extraction of the cycloadducts into 3% HCl. The acid phase was made basic by adding sodium bicarbonate, and then extracting with dichloromethane. The dichloromethane extract was dried (MgSO₄), and evaporated to give a mixture of cycloadducts. It was not possible to separate the isomeric cycloadducts by column chromatography although a small amount of the major isomer was eventually isolated by HPLC.

Table 22: Total yields and selectivity for the major isomer in the asymmetric 1,3-dipolar cycloaddition of **162** to betaine **143**.

Solvent	Temperature	Time	Selectivity (% of the major isomer) ^a	Yields (%)
acetone	reflux	5 h	36	19
benzene	reflux	1 day	55	15
benzene	room	11 days	63	11
benzene	room	4 months	63	87
EtOAc	room	10 days	65	>90

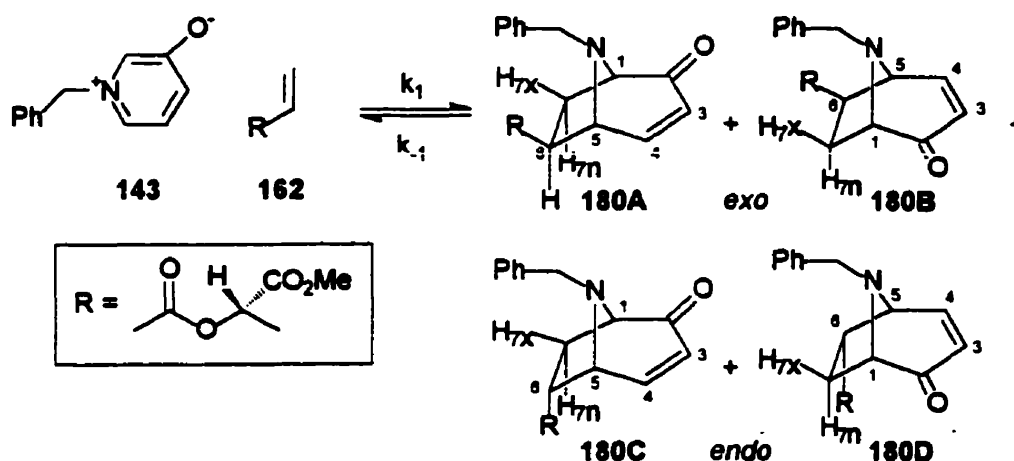
^a estimated from ¹H-nmr spectra.

Cycloadditions of **162** to betaine **143** were performed in various solvents at room temperature in a search for a solvent that would provide a faster rate of reaction without compromising selectivity. When the cycloaddition was performed in ethyl acetate, the reaction time was shortened to ten days (from four months in benzene) with no loss in

yield or selectivity (Table 22). However, when the reaction time of this latter reaction was extended to two weeks, the yield decreased considerably.

It was observed that the ^1H -nmr spectrum of the pure major cycloadduct began to show signals of the starting materials after standing 22 hours in CDCl_3 . This suggested that the cycloadducts were not thermally stable and slowly reverted to starting material over time.

Scheme 48a :



From the experimental results, high temperature seemed to disfavor the forward reaction, resulting in low yield for the cycloaddition. Higher temperatures also gave lower selectivity. It appeared that at high temperature the products were in equilibrium with each other and with the starting materials, and that the equilibrium favored the starting materials. The temperature dependence of the equilibrium constant can be explained on the basis of the expected relative values of enthalpy and entropy of reaction. The equilibrium constant for a reaction is related to the Gibbs free energy of reaction by the equation based on the Van't Hoff principle.

$$K = e^{-\Delta G/RT} \quad \text{where } \Delta G = \Delta H - T\Delta S$$

Given that the reaction involves the combination of two substrates to form a single product of restrained geometry, one expects the entropy of reaction to be fairly large and negative. Thus at higher temperature ΔG must be dominated by the $T\Delta S$ term making ΔG positive ($K < 1$). At lower temperatures the products appear to be favored ($K > 1$), therefore ΔG is negative and must be dominated by a negative ΔH .

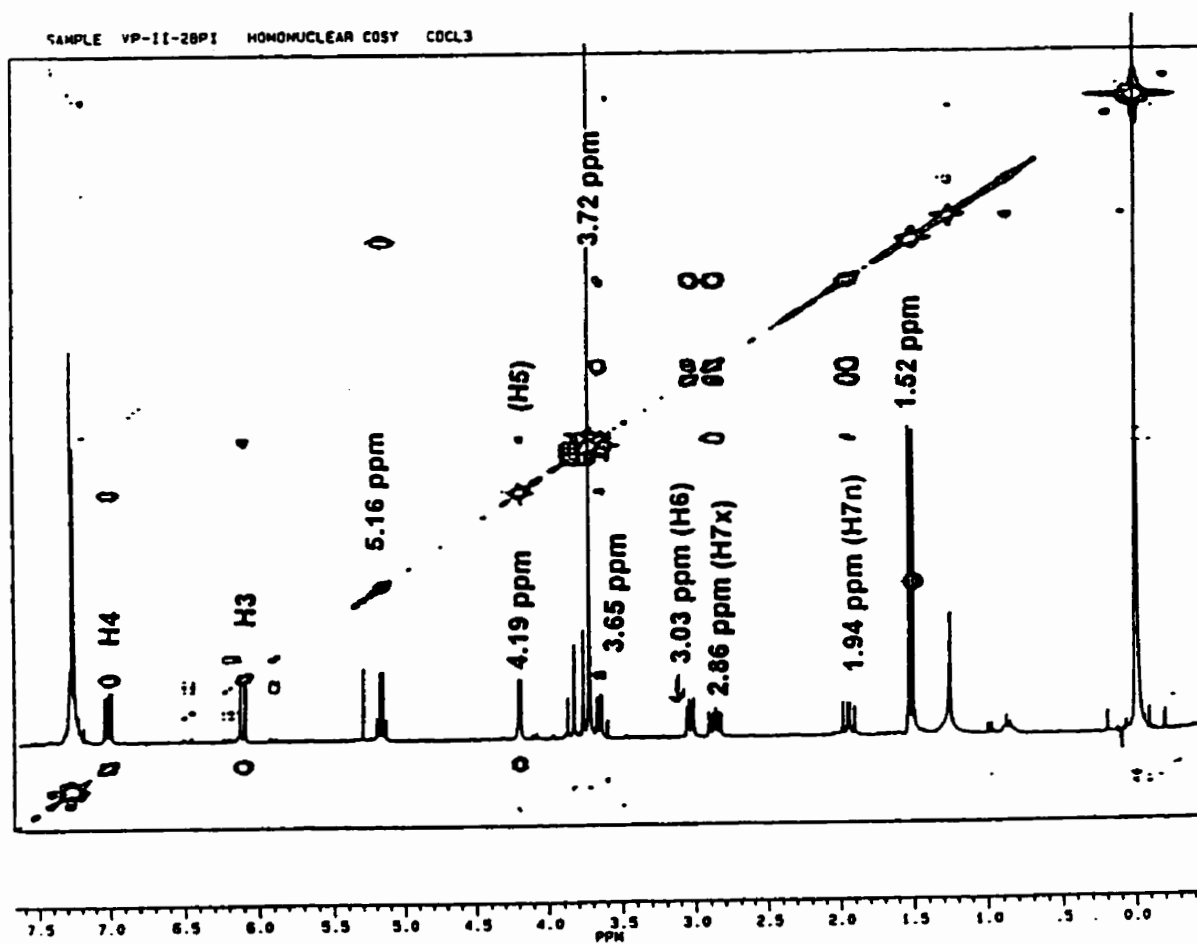
The lower selectivity at the higher temperature is a reflection of the equilibration among the products and the starting materials. The reaction would be under thermodynamic control with the most stable species dominating. The fact that the cycloadducts are formed in nearly equal amounts suggests that they have similar thermodynamic stability. At lower temperatures where ΔG is negative and favors the products, the reaction may be under kinetic control with the fastest forming product dominating. There is no obvious explanation for the increased rate of reaction in ethyl acetate relative to other polar solvents.

Proton signals from the lactate part of the major cycloadduct were easily identified from the proton spectrum (Figure 19). The methyl group appeared as a doublet (1.52 ppm), the methoxy group as a singlet (3.72 ppm), and the methine hydrogen as a quartet (5.16 ppm). The next most obvious signals were the doublet of doublets at both 7.02 and 6.10 ppm, belonging to the H4 and H3 protons respectively. In the COSY spectrum there was an off-diagonal signal linking H4 to the doublet at 4.19 ppm, indicating that this doublet was due to the H5 proton. The off-diagonal signal linking the H3 proton to the doublet at 3.65 ppm was used to assign this doublet to the H1 proton. A horizontal line crossing the diagonal signal of H1 passed through the cross-peaks of the two H7 protons. The H7x ($x = \text{exo}$) signal appeared as a doublet of doublet of doublets (2.86 ppm) and the

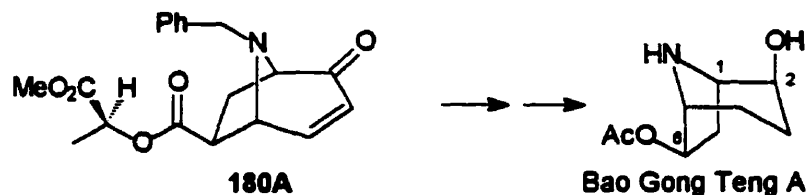
H7n (n = *endo*) signal appeared as a doublet of doublets (1.94 ppm). The remaining signal at 3.03 ppm was assigned to the H6 proton. The splitting pattern of H5 and H6 indicated that the major cycloadduct was an *exo*-isomer, either **180A** or **180B** (see Scheme 48 above), however, the absolute configuration of the major cycloadduct could not be determined experimentally at this stage. It was nevertheless assumed that the major cycloadduct was **180A** based on the expectation that the chiral acrylate had reacted at its *re* face (based on previous experience with this dienophile in Diels-Alder reactions).

The two doublets at 3.84 ($J = 13.5$ Hz) and 3.74 ppm ($J = 13.5$ Hz) did not exhibit any coupling to rings protons and were assigned to the two benzylic protons.

Figure 19: ^1H - ^1H COSY spectrum of the major cycloadduct from the reaction of **162** with betaine **143** in CDCl_3 .

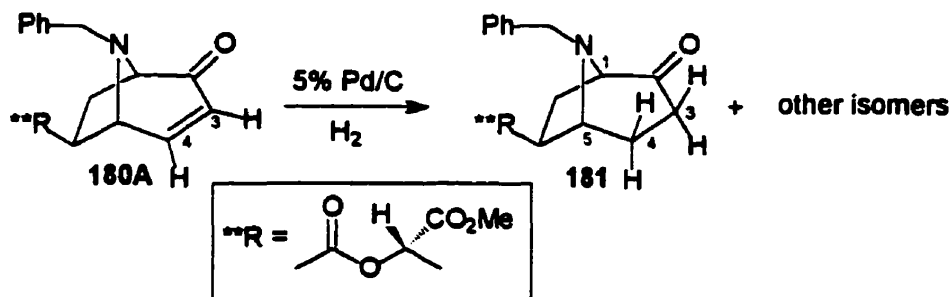


Section 6.3: A Synthesis Bao Gong Teng A



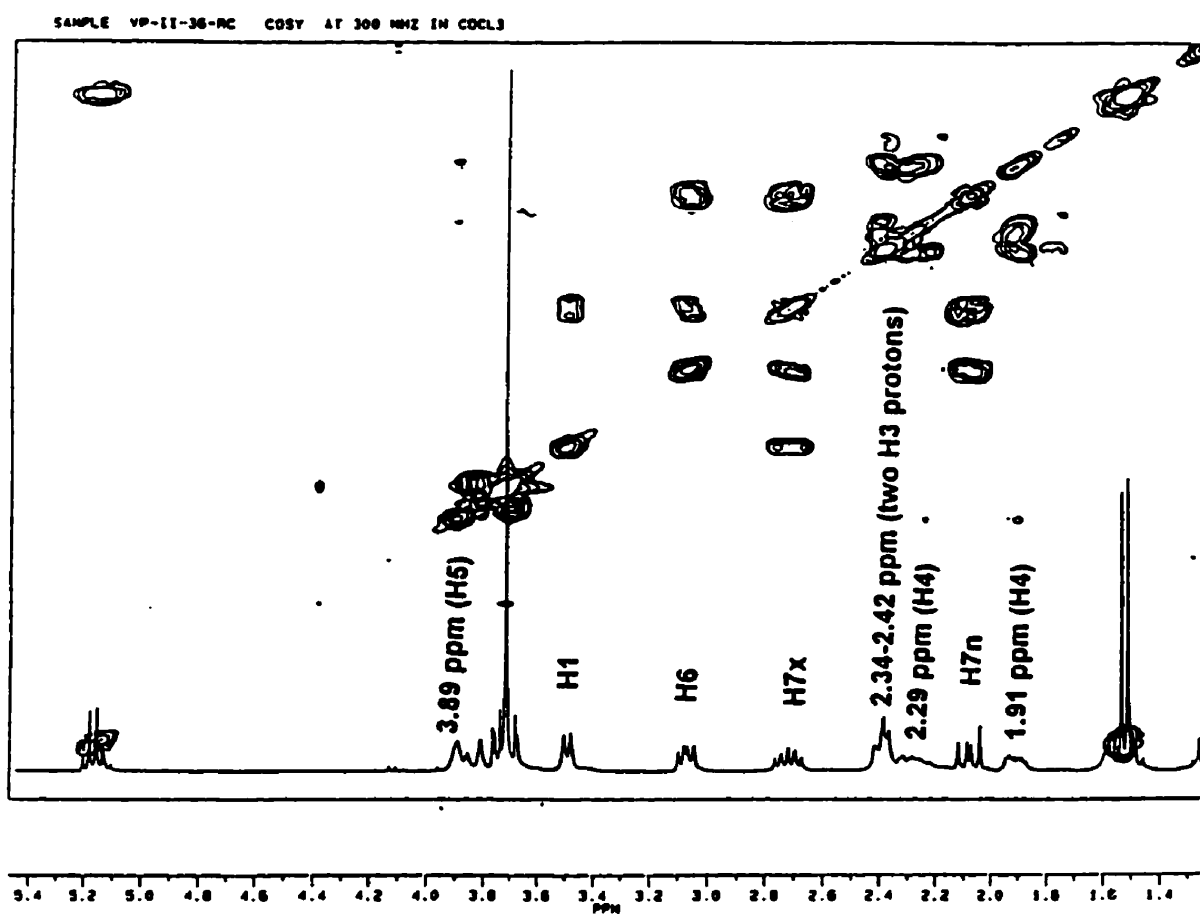
One way to determine the absolute configuration of the major cycloadduct from above would be to convert it to a known compound, whose optical rotation is known. The conversion of the cycloadduct to a known natural product would also demonstrate the synthetic usefulness of the cycloaddition reaction. Bao Gong Teng A (see introduction Section 3.6) was chosen as the synthetic target due to its structural similarity to cycloadducts **180**. If the major cycloadduct were indeed **180A** as expected (see above) then it should be possible to prepare Bao Gong Teng A in its natural absolute configuration.

Due to the thermal instability of the cycloadduct (**180** and isomers), the crude product mixture was hydrogenated using 5% Pd/C in ethyl acetate at room temperature to give a mixture of saturated isomers (Scheme 49). The major ketone was isolated by chromatography on silica gel and crystallized from 20% ethyl acetate in hexane to give a single product with a melting point of 87-88.5°C. The overall yield of the major ketone (presumed to be **181**) from the cycloaddition and reduction steps was 61 %.

Scheme 49:

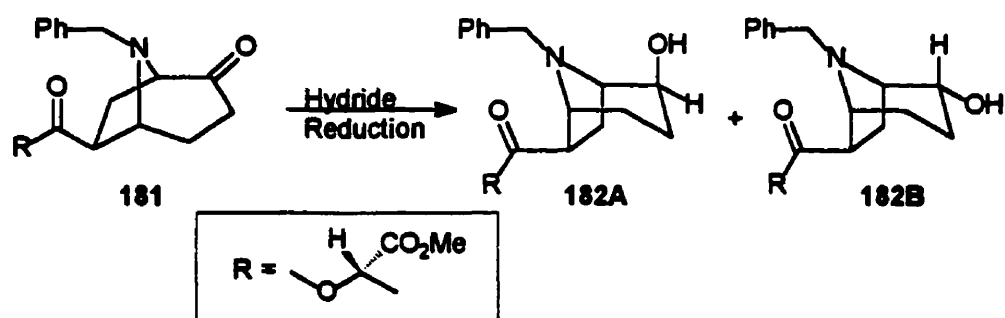
The ^1H -nmr spectrum of this product showed that the H5 signal had shifted upfield to 3.89 ppm (from 4.19 ppm in 180A), since it was no longer an allylic proton. Its splitting pattern changed to a broad singlet due to additional coupling to an additional H4 proton. The ^1H -nmr spectrum also showed the absence of the two vinylic protons signals, H3 and H4. There were three new multiplets with integration of four protons. From the ^1H - ^1H COSY spectrum (Figure 20), the two multiplets at 2.29 and 1.91 ppm, with integration for one proton each, have off-diagonal signals that indicate coupling to the H5 proton. These two multiplets were assigned to the two H4 protons. The remaining multiplet at 2.34-2.42 ppm with integration for two protons was assigned to the two H3 protons. The ^1H -nmr spectral assignment of this compound is consistent with the expected product 181 (or its diastereomer produced from 180B).

Figure 20: ^1H - ^1H COSY spectrum of the major product from the hydrogenation of the 180 mixture.



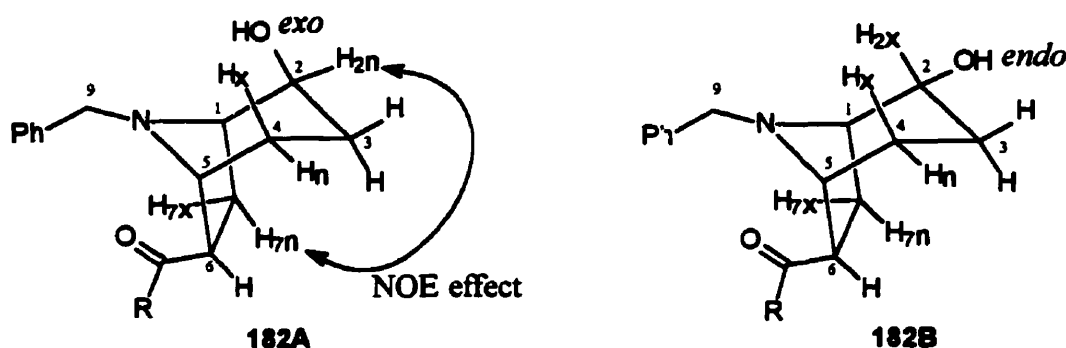
In the next step of the synthesis, an attempt was made to reduce ketone **181** to the 2-*exo* alcohol **182A** having the appropriate stereochemistry for Bao Gong Teng A (Scheme 50). The reduction of ketone **181** using sodium borohydride in methanol, following Jung's procedure for a similar ketone, produced a complicated mixture that could neither be separated nor analyzed as a whole. Using 2-propanol or ethyl alcohol as solvent produced similar results. Using dry THF as a solvent at 0°C gave two products that could be separated by chromatography on a silica gel column with 30% ethyl acetate in hexane. To simplify the description for the analysis of infrared and ¹H-nmr spectra, the first eluted product, the minor product, will be referred to as **182C1** and the second eluted product (the major fraction) as **182C2**.

Scheme 50:



The alcohols **182A** and **182B** should be easily differentiated by infrared spectroscopy due to the expected strong intramolecular hydrogen bonding between the hydroxyl group and the amine nitrogen in the 2-*exo*-alcohol **182A**.⁶⁹ The infrared spectrum of **182C1** showed a broad hydroxyl function signal while **182C2** showed a sharp hydroxyl function signal, suggesting that **182C1** was the 2-*exo*-hydroxy compound **182A**, and that **182C2** was the 2-*endo*-hydroxy compound **182B**.

The alcohols **182A** and **182B** should also be differentiable by NOE experiments. Irradiation of the H_{2n} signal in **182A** should cause an enhancement in intensity of the H_{7n} signal, while no similar effect should be found in **182B**. However, before these experiments could proceed, the proton signals in both ¹H-nmr spectra had to be assigned.



A ¹H-¹H COSY spectrum of compound **182C1** is presented in Figure 21. Signals belonging to the lactate part of the compound were easily identified from the proton spectrum. The methyl appeared as a doublet (1.51 ppm), the methoxy as a singlet (3.68 ppm) and the methine hydrogen as a quartet (5.14 ppm). The two doublets at 3.66 ppm ($J = 13.4$ Hz) and 3.42 ppm ($J = 13.4$ Hz) were assigned to signals from the two benzylic (H₉) protons. The remaining signals should be signals from the ring protons. They are labeled alphabetically from A to H.

Signal F, a doublet of doublets ($J = 14.1$ and 9.5 Hz) at 1.8 ppm, was assigned to the H_{7n} proton, and signal E, a doublet of doublet of doublets ($J = 14.1, 7.2, 5.9$ Hz) at 2.6 ppm, was assigned to the H_{7x} proton signal. Signal D, a double doublet ($J = 9.5$ and 5.9 Hz) at 2.95 ppm, had off-diagonal signals linking it to the two H₇ protons. This doublet of doublets was therefore assigned to the H₆ proton.

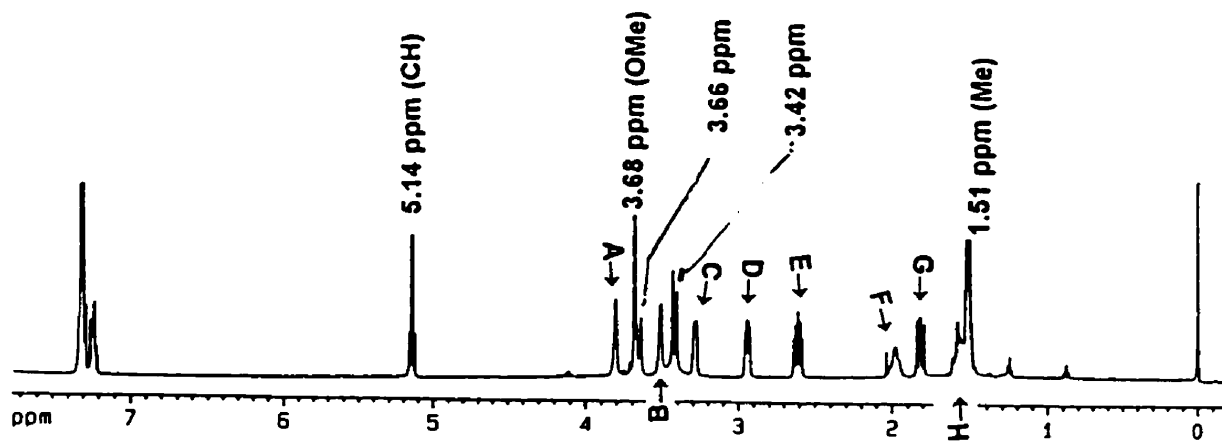
A horizontal line crossing the diagonal signal of H7x crossed through off-diagonal signals of H6, H7n and signal C (a doublet of doublets with $J = 7.2$ and 3.8 Hz). This doublet of doublets was assigned to the signal of the H1 proton.

On the basis of their chemical shifts, signals A and B must be due to H5 and H2. Since off-diagonal signals of both peak A and peak B both indicated coupling to the H1 proton, NOE experiments were required to determine which was H5 and which was H2. Irradiation of the H6 signal caused an enhancement in intensity of signal A and H7n, suggesting that signal A must be the H5 proton. Thus signal B was assigned to the H2 proton (Figure 22).

There were two off-diagonal signals linking F and H to the H5 proton, suggesting that signal F and one proton in signal H were the two H4 protons. By elimination, the two remaining protons in signal H must be the two H3 protons.

At this point, an NOE experiment was carried out to verify the stereochemistry of the 2-hydroxyl group. Irradiation of the H2 proton caused an enhancement in intensity of H7n and one of the H4 signals, signal F (Figure 22). The enhancement of H7n indicated that the 2-hydroxyl group was in the *exo* position. Therefore, compound **182C1** must be the 2-*exo* hydroxy compound **182A**. However, the absolute configuration of the bicyclic ring was still unknown.

Figure 21: ^1H - ^1H COSY spectrum of compound 182Cl.



Expansion of region 1.00 to 4.00 ppm

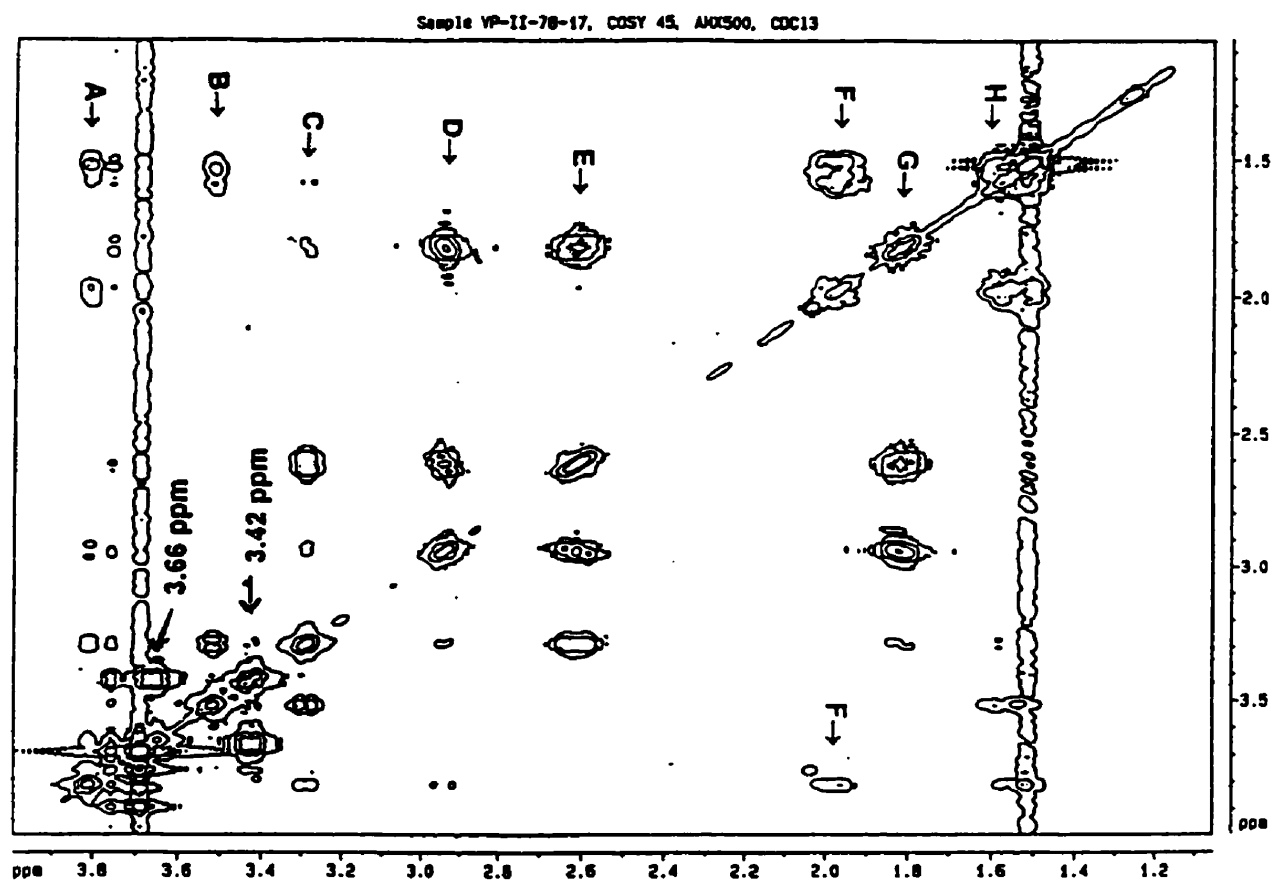
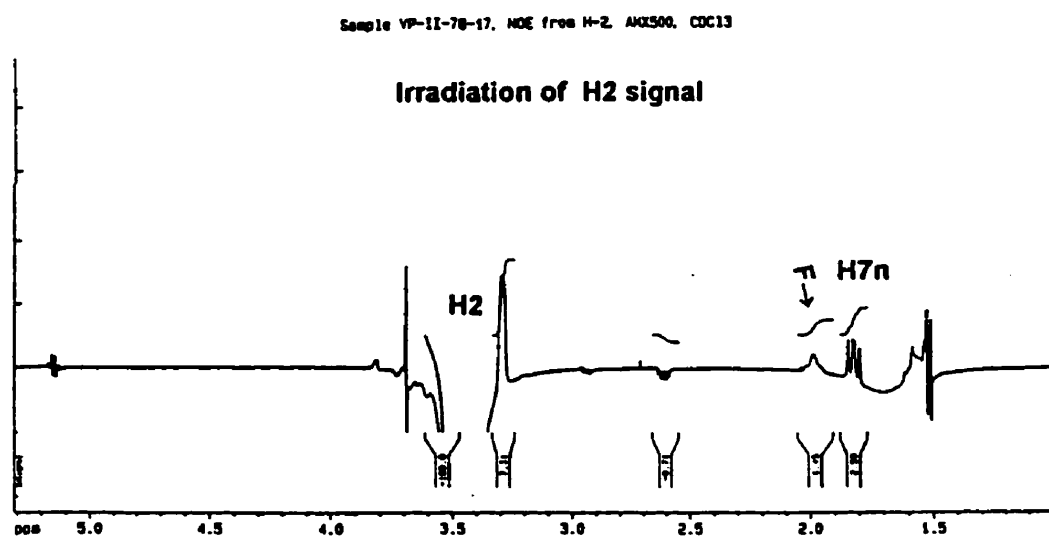
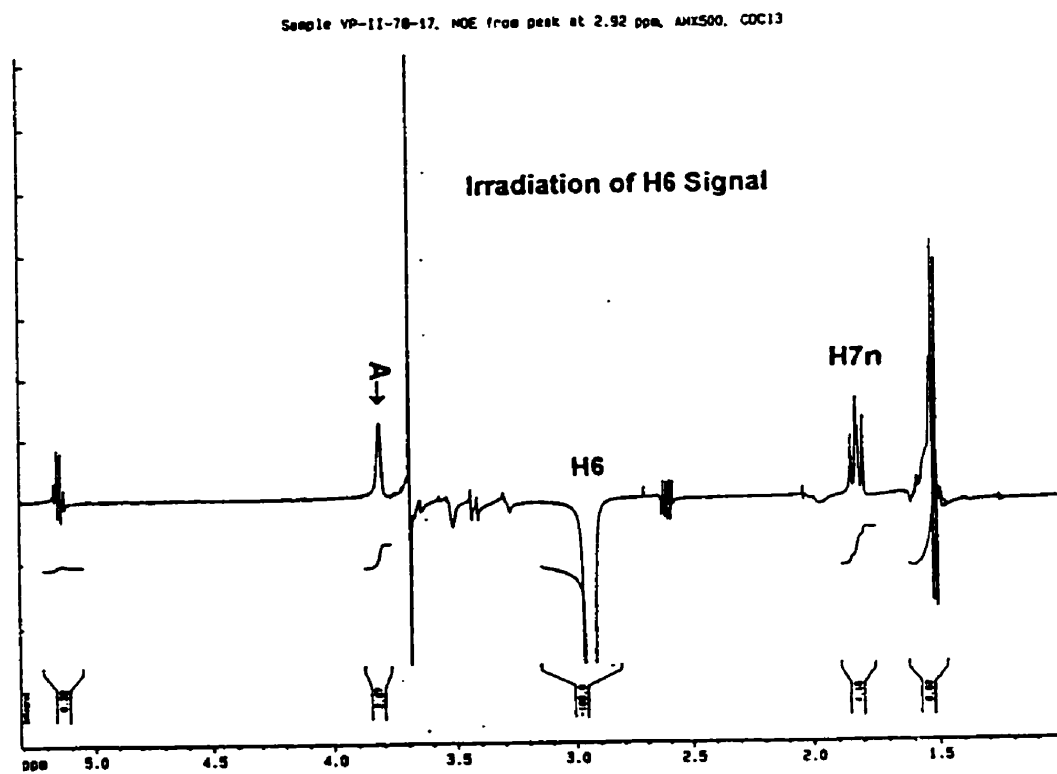


Figure 22: NOE experiments of compound 182C1.

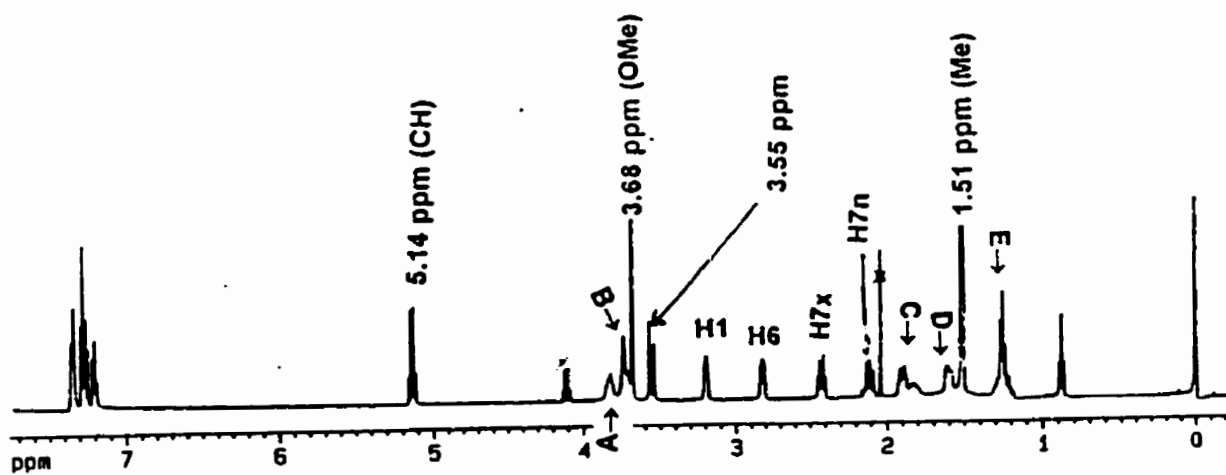
Since the H2 proton had been established as the H2n proton in **182A**, enhancement in signal F when irradiating the H2n proton suggested that signal F should belong to H4n since this proton was closer to H2n than the H4x proton.

It was previously shown by IR and COSY results that **182C1** was the *exo* alcohol compound, otherwise labeled as **182A**. It will now be shown that the COSY results indicate that compound **182C2** is the *endo* alcohol (**182B**) compound in agreement with the IR results. The method for the assignment of **182C2** which follows was very similar to that used for **182C1** or **182A** (as shown on page 128).

Signals belonging to the lactate part of the compound were easily identified from the proton spectrum. A methyl signal appeared as a doublet (1.51 ppm), a methoxy as a singlet (3.68 ppm) and the methine hydrogen as a quartet (5.14 ppm). A doublet at 3.55 ppm ($J = 13.4$ Hz) and another doublet, hidden under the methoxy signal and partially hidden in signal B, 3.75 ppm ($J = 13.4$ Hz), could be assigned to signals from the two benzylic H9 protons. The assignment of the H1, H6, H7x and H7n proton signals were made following the method used for the assignment of **182A**. The remaining signals were labeled in alphabetical order from A to E.

Irradiation of the H6 proton caused an enhancement in intensities of signals B, D, E and H7n (Figure 24). This result suggested that signal B was the H5 proton. Since the H4n and H3n are closer to H6 than the H4x and H3x protons, enhancement of signals D and E indicated that they were the H4n and H3n protons. By elimination, signal A must be the H2 proton.

Figure 23: ^1H - ^1H COSY spectrum of compound 182C2.



Expansion of region 0.70 to 4.30 ppm

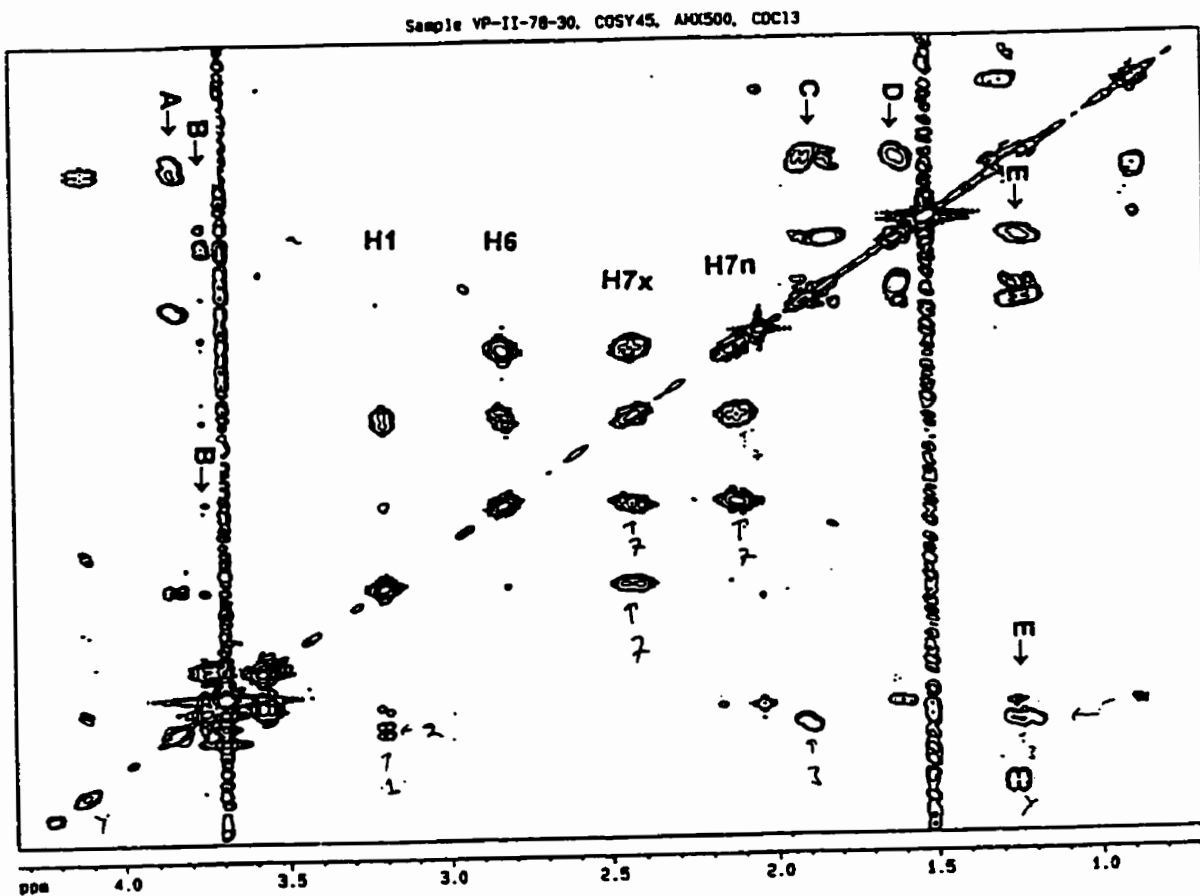
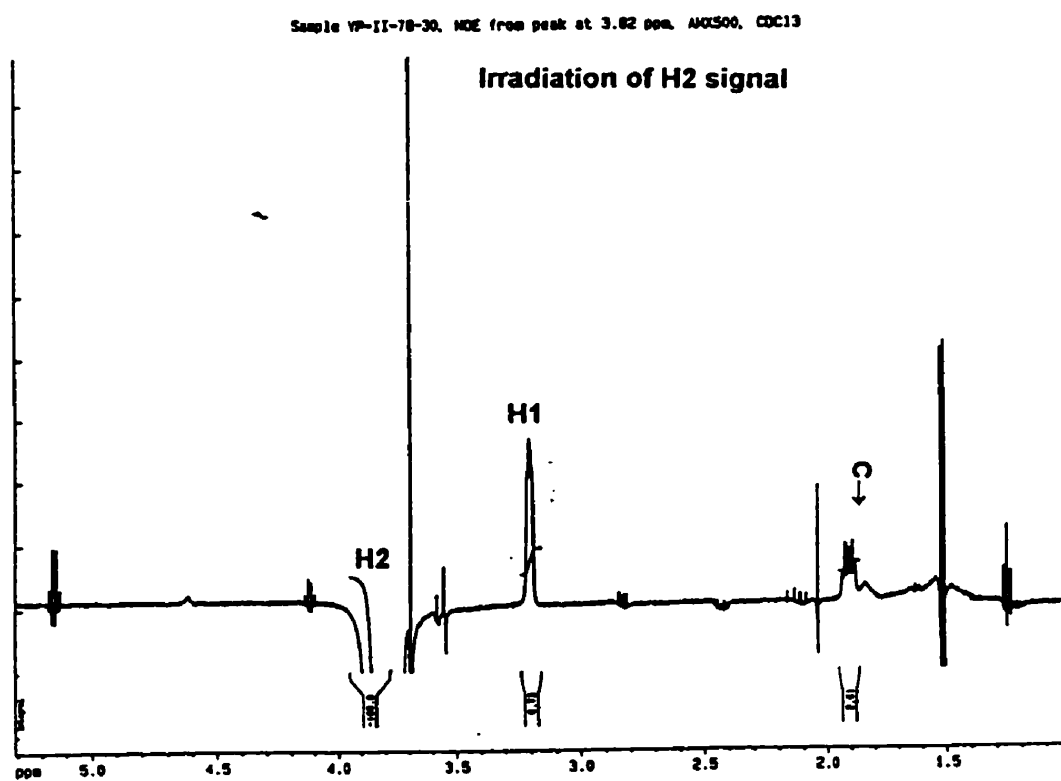
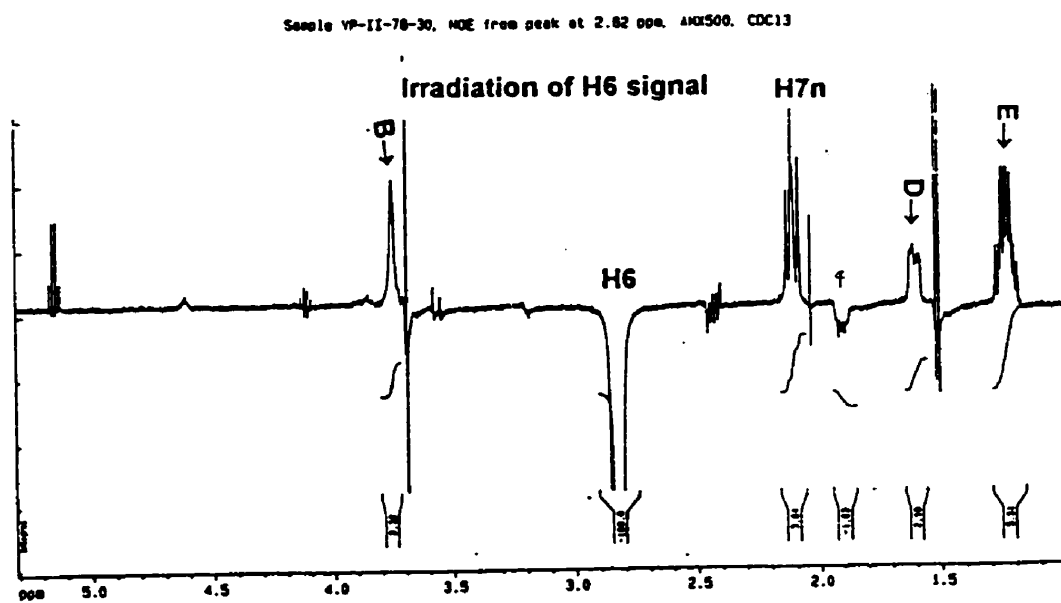


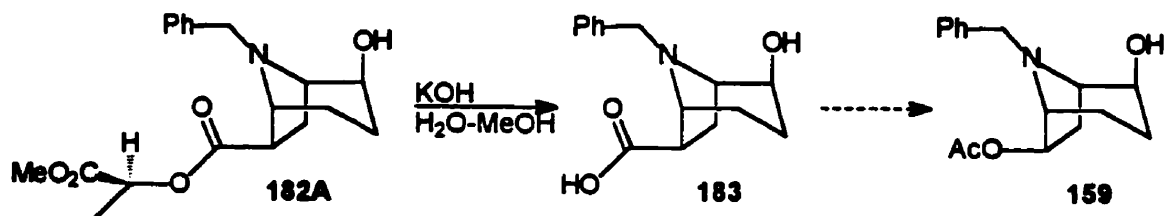
Figure 24: NOE experiment of compound 182C2.

In figure 23, a horizontal line through the diagonal signal of the H2 proton passed through cross peaks of signal C, E, and the H1 proton. This suggested that signal E and one proton of signal C were the two H3 protons. Combining this with the above NOE results, signal D and E could be assigned to signals from H4n and H3n, respectively. By elimination, signal C must originate from the overlapping signal arising from H4x and H3x protons.

Irradiation of the H2 signal did not cause an enhancement in intensity of the H7n signal, suggesting that the 2-hydroxyl group was in the *endo* position. Also, this irradiation caused an enhancement in intensities of H1, H3x and H4x signals, also indicating that the H2 proton was *exo* (hydroxyl group was *endo*, as shown in the figure for compound **182B**, see above).

The reduction of ketone **181** using sodium borohydride in THF described above had yielded the desired 2-*exo* alcohol **182A** as a minor product. In a search for more stereoselective reducing agents it was found that reduction using the bulkier lithium tri-*tert*-butoxyaluminum hydride at -4°C in THF gave predominately the desired alcohol **182A**.⁷⁹⁻⁸¹ After chromatography on silica gel, crystalline **182A**, and **182B** as a light yellow oil, were obtained in yields of 62 % and 21 %, respectively.

In order to obtain Bao Gong Teng A from alcohol **182A** the 6-*exo* ester functional group at C6 had to be converted to a 6-*exo* acetyl group (as in compound **159**) and then the benzyl group needed to be removed from the amine group (Scheme 51). The shortest way to convert the 6-ester group to a 6-acetyl group was to hydrolyze the ester to the corresponding carboxylic acid group as in **183**, and then oxidatively decarboxylate to directly produce the corresponding 6-acetyl compound **159** (Scheme 51).

Scheme 51:

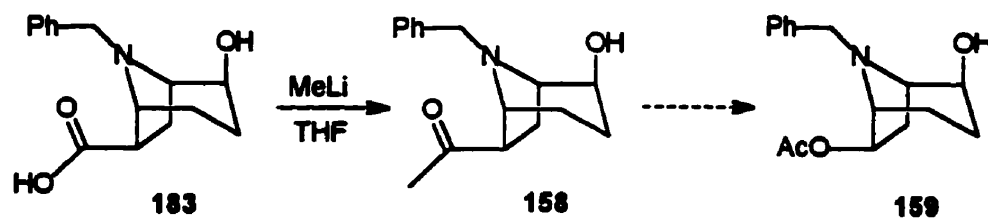
Potassium hydroxide in H₂O was added to a solution of ester **182A** in methanol and the resulting mixture was stirred at room temperature for 20 hours. Most of the methanol was then evaporated. Since it was not easy to extract the acid out of the aqueous solution, an ion exchange method was used. The resulting aqueous solution was adjusted to pH 2 by adding 3% HCl and then the solution was slowly poured onto a cation exchange column (Dowex 50W-X8, hydrogen form). The column was rinsed with aqueous HCl (pH 2) and then H₂O until no more chloride ion was eluted. This left compound **183** in its protonated form on the column. The neutral form of **183** was eluted from the column with aqueous ammonia (pH 11), and the solvent evaporated to give a colorless solid. The solid was dissolved in H₂O and then frozen and lyophilized under high vacuum overnight. The resulting amino acid appeared as a flaky, colorless solid. The ¹H-nmr spectrum of this product showed the presence of all the bicyclic ring proton signals, the signals of the benzylic H9 protons, and five aromatic ring protons. The ¹H-nmr spectrum also showed the absence of proton signals corresponding to the lactate group, suggesting that this compound was indeed compound **183**.

Attempts to decarboxylate amino acid **183** to directly produce the corresponding acetate **159** using lead tetraacetate⁸²⁻⁸⁶ were unsuccessful (Scheme 51). For this reason a longer route was chosen to complete the synthesis.

Another route to Bao Gong Teng from the acid **183** would be to first convert the 6-carboxylic acid group to the corresponding ketone (as in compound **158**, Scheme 52). The

ketone **158** could be transformed into the corresponding acetate using a Baeyer-Villiger oxidation, and then the N-benzyl group cleaved to give Bao Gong Teng A as in Jung's synthesis.⁶⁹

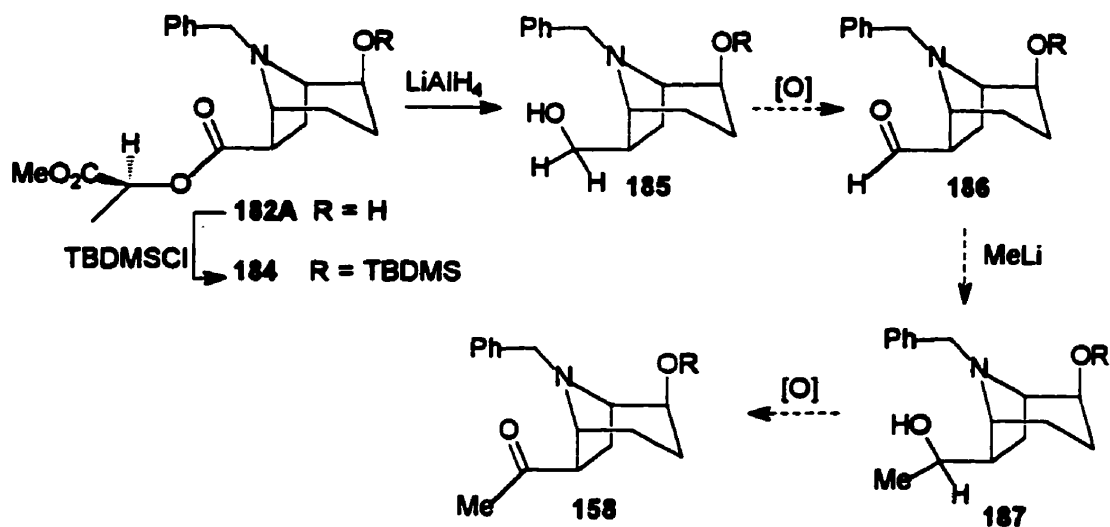
Scheme 52:



Methyl lithium (at least three equivalents) was added to a solution of acid **183** in dry THF under nitrogen atmosphere. The mixture was refluxed overnight, then cooled to ice temperature and the excess methyl lithium was rapidly quenched with methanol. Work up of the reaction produced a crude product which appeared to contain little of the desired ketone **158**. Changing the reaction temperature, solvent, amount of methyl lithium etc. did not improve the yield of ketone **158**.⁸⁷⁻⁸⁹ Adding cerium trichloride⁹⁰ or N, N, N, N-tetramethylethylenediamine to the reaction did not improve the situation either.

A longer method for the preparation of ketone **158** from **182A** was undertaken. This involved the reduction of ester **182A** to the corresponding alcohol **185**, then oxidizing this alcohol to aldehyde **186** (Scheme 53). Methyl lithium would then be used to convert the aldehyde to the corresponding secondary alcohol **187**, which could be oxidized again to yield the ketone **158**. Prior to this sequence, it was necessary to protect the alcohol at the 2-position.

Scheme 53:

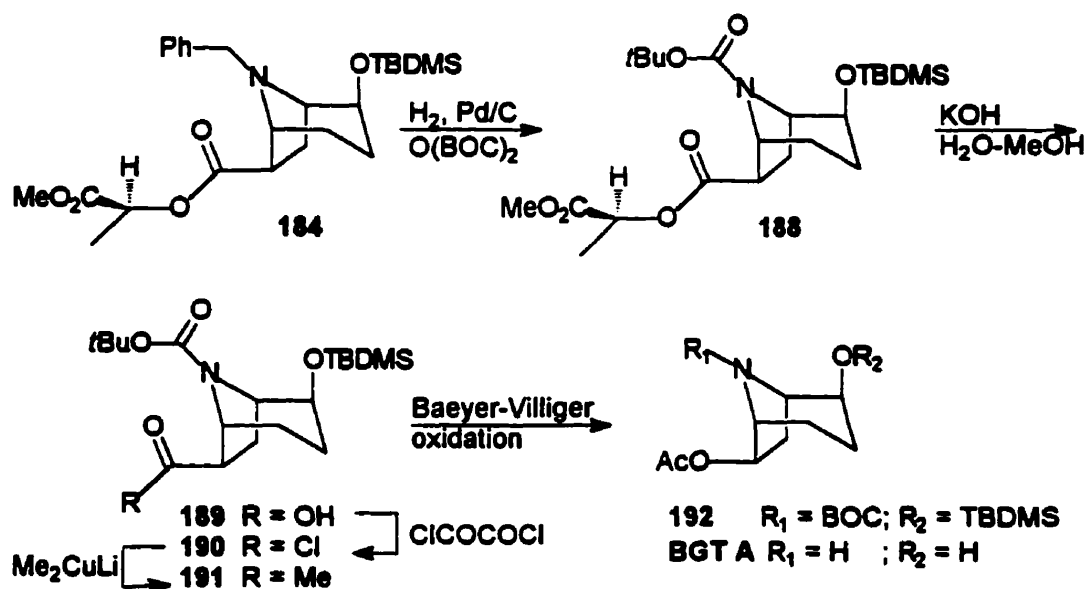


One and a half equivalents of *tert*-butyldimethylsilyl trifluoromethanesulfonate (TBDMSTf) was added to a mixture of triethylamine and 182A in dichloromethane under an argon atmosphere. Thin layer chromatography indicated that the reaction was complete within three minutes. The reaction was worked up to give a dark yellow oil, which was immediately filtered through a short column of silica gel with 30% ethyl acetate in hexane to provide 184 as a light yellow oil. The ¹H-nmr spectrum of 184 was very similar to the starting material, except that it had extra signals indicating the presence of the TBDMS group; three singlets at 0.92 ppm (9H, *t*Bu), 0.03 (3H, Me) and 0.00 ppm (3H, Me).

The TBDMS derivative 184 was reduced with lithium aluminium hydride (LiAlH₄) to give the 6-primary alcohol 185 in 34% yield. Oxidation of 185 using pyridinium dichromate (PDC)⁹¹ or Swern oxidation⁹² did not give an acceptable yield for aldehyde 186. Although there is no direct evidence, the failure of the oxidation step may be due to the nucleophilicity of the *tertiary* nitrogen, which might complex strongly to the dichromate or compete with alcohol for attack on the activated Me₂S⁺Cl species in the Swern oxidation.

Since it was not possible to synthesize Bao Gong Teng A using the strategy shown in Scheme 53, a new strategy for the synthesis was devised starting from ester **184** (Scheme 54). This strategy required blocking the nitrogen group with the *tert*-butoxycarbonyl group in order to reduce its nucleophilicity. The 6-*exo* ester group in **184** would then be converted to the corresponding 6-*exo* carboxylic acid group as in **189**. It should be then possible to convert this acid (**189**) to the 6-*exo* ketone **191** via the acid chloride, since the nitrogen should not interfere with the reaction. The ketone would be converted to the desired 6-acetate using the Baeyer-Villiger reaction. Removal of the protecting groups should yield Bao Gong Teng A.

Scheme 54:



Di-*tert*-butyl dicarbonate (1.5 eq) and 5% Pd/C were added to a solution of **184** in methyl alcohol. The solution mixture was hydrogenated (1 atm) for 15 hours and the Pd/C was filtered off. The filtrate was evaporated to leave a colorless oil with the unreacted di-*tert*-butyl dicarbonate as a contaminant. A small amount of the crude product was pumped under high vacuum for two weeks to obtain a sample of solid **188**. The bulk of the crude product was used in the next step without further purification. The ^1H -nmr spectrum of the product showed

no proton signals for the benzylic group, and there were new signals corresponding to the BOC group. Both the ^1H and the ^{13}C nmr spectra of the N-BOC compound **188** were complicated by doubling of peaks due to the presence of carbamate rotamers.⁹³⁻⁹⁵ The relative chemical shifts of the ring proton signals in the ^1H -nmr spectrum were very similar to those in the starting material.

Potassium hydroxide in H_2O was added to a solution of crude ester **188** in methanol, and the resulting mixture was stirred at room temperature for 15 hours. Most of the methanol was then evaporated (Scheme 54). The resulting aqueous solution was adjusted to pH 3 with 7M H_3PO_4 and then extracted with chloroform. The organic phase was dried and evaporated to give the acid **189** as a colorless solid in 94% yield from the N-benzyl ester **184**. A new ^1H -nmr signal at 11.3 ppm and the lack of all of the lactyl signals in the spectrum of the product indicated that acid **189** had formed. The spectrum was also complicated by doubling of peaks due to the presence of carbamate rotamers.

The acid **189** was treated with oxalyl chloride and a catalytic amount of dimethylformamide (DMF) in benzene to convert it to the corresponding acid chloride **190**. The resulting solution was evaporated to dryness. In order to convert the acid chloride to the corresponding ketone **191**, an excess amount of lithium dimethylcuprate (Me_2CuLi) in a mixture of diethyl ether and THF was added to the solution of crude acid chloride **190** in THF at -78°C under a nitrogen atmosphere.⁹⁵⁻⁹⁷ After 15 minutes of stirring, the reaction mixture was quenched with methanol and then slowly warmed to room temperature. Workup with 0.5 M potassium hydroxide solution and extraction gave a light yellow oil in 82% yield (assuming it to be the ketone **191**). The ^1H -nmr of the product had two new methyl ketone signals, 2.20 and 2.09 ppm (two rotamers). This and the disappearance of the carboxylic acid proton at 11.3

ppm indicated that ketone **191** had been formed. The ^1H and ^{13}C -nmr spectra did not show significant contaminants, thus there was no need to further purify this ketone.

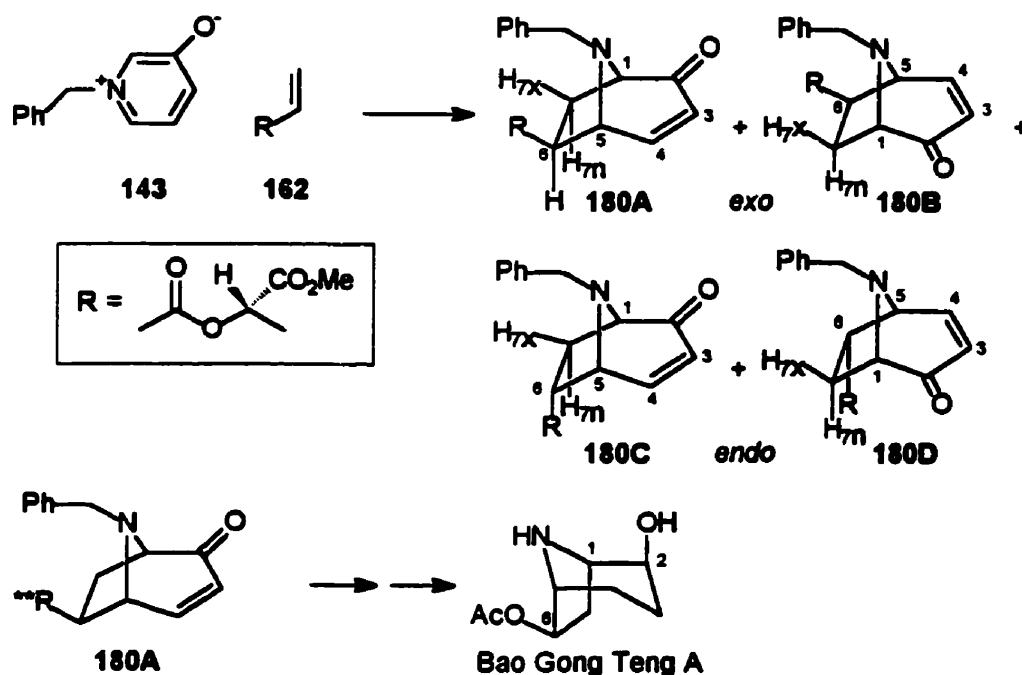
The protected Bao Gong Teng A **192** was obtained by the Baeyer-Villiger oxidation of ketone **191**. An excess of *meta*-chloroperbenzoic acid was added to a solution of **191** in a mixture of benzene and chloroform (1:2), and the mixture stirred for seven days. Work up gave an oil that was chromatographed to provide acetate **192** in 52% yield.

Finally, the removal of both the BOC and the TBDMS groups from **192** was achieved using 1% HCl in methanol. After stirring for two hours at room temperature, the methanol was evaporated by rotary evaporation at 70°C and water added. This solution was extracted with chloroform, washing with aqueous K_3PO_4 (2M). The organic phase was passed through a filter paper to remove H_2O (desiccants such as MgSO_4 appear to bind Bao Gong Teng irreversibly). Evaporation yielded Bao Gong Teng A in 61% yield. The overall yield from *N*-benzyl-3-oxidopyridinium betaine and the acrylate of methyl *S*-lactate was 9%.

The ^1H -nmr spectrum of synthetic Bao Gong Teng A was similar to that published by Jung *et al.* for the racemic compound⁶⁹ and was relatively free of contaminants. The acetate methyl appeared as a singlet at 2.04 ppm. The H6 proton appeared as a doublet of doublets ($J = 2.0$ and 6.90 Hz) at 5.13 ppm. In the ^1H - ^1H COSY spectrum, the off diagonal signals of a peak 2.16 ppm (a doublet of doublets with $J = 6.9$ and 14.76 Hz) and one of the protons in a multiplet signal at 1.70-1.94 ppm showed coupling to the H6 proton. These two signals were assigned to the H7x (*exo*) and H7n (*endo*), respectively. The H7x signal at 2.16 ppm was observed as a doublet of doublets. Jung's description of the ^1H -nmr spectrum of the racemic compound neglected to mention this signal.⁶⁹

The specific rotation of the synthetic Bao Gong Teng A was -7.5 in H_2O , in agreement with the literature value of -7.22 for the natural material.⁶⁹ This would indicate that the synthetic material had the same absolute configuration as that of the natural Bao Gong Teng A.

Scheme 55:



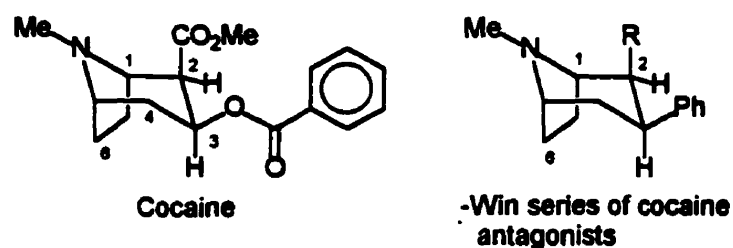
The fact that Bao Gong Teng A with the correct absolute configuration had been prepared indicated that betaine 143 had added to the *re* face of the acrylate of methyl (*S*)-lactate 162 with 6-*exo* regio- and stereoselectivity to give 180A as the major adduct as predicted (Scheme 55).

In conclusion, the acrylate of methyl (*S*)-lactate 162 appears to be a very suitable chiral dipolarophile for use in 1,3-dipolar cycloadditions to *N*-alkyl-3-oxidopyridinium betaines.

Section 6.4: Other possible applications

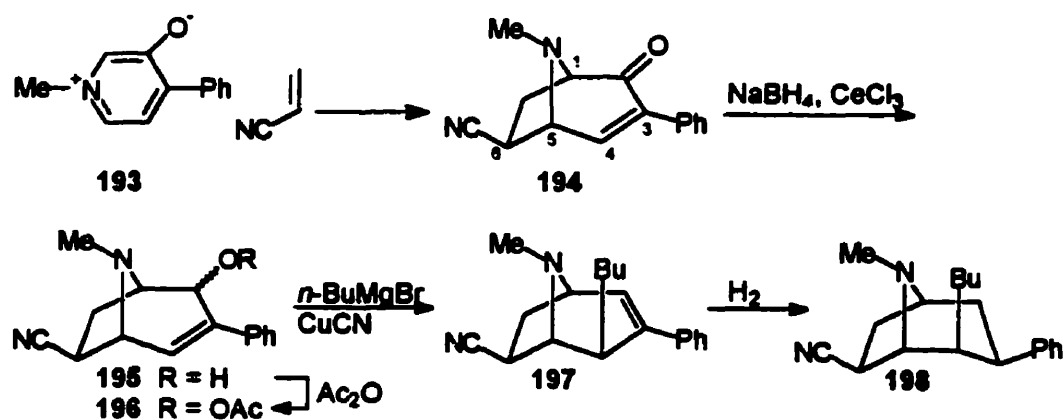
The 1,3-dipolar cycloaddition of the acrylate of methyl (*S*)-lactate to 3-oxidopyridinium betaines may also be useful for the synthesis of cocaine and its antagonists, drugs used for the treatment of individuals who have become dependent on cocaine.

Scheme 56:



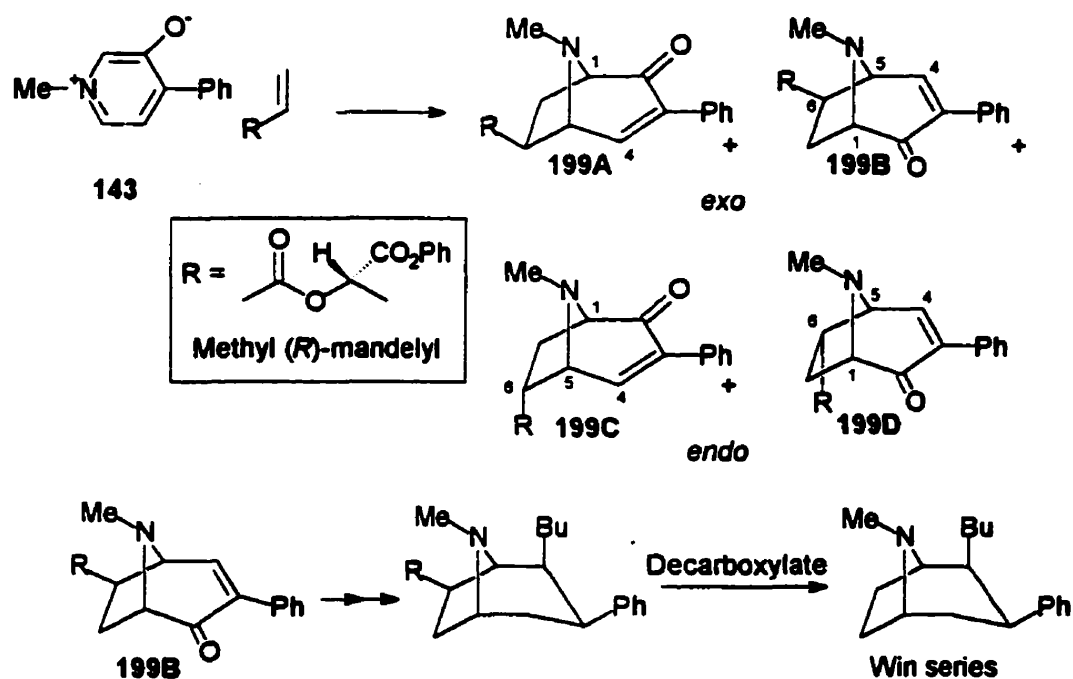
(*R*)-Cocaine is a well known tropane alkaloid, extracted from the leaves of *Erythroxylum coca*, and has long been recognized as a potent central nervous system stimulant (Scheme 56).

Cocaine antagonists having a phenyl group in place of the C-3 benzoate group, known as the Win series, have been prepared in racemic form via 1,3-dipolar cycloaddition of acrylonitrile to the betaine 193 (Scheme 57).⁹⁹ For example, the cycloadduct 194 was formed by such a reaction. It was subsequently reduced to the corresponding alcohol 195, the alcohol acetylated, and the resulting acetate alkylated at the C4 position to form alkene 197. The double bond was hydrogenated to obtain the Win analog 198.

Scheme 57:

On the basis of the above synthesis, an asymmetric synthesis of an optically pure Win compound (Scheme 56) might be possible if the cycloaddition could be performed asymmetrically. Using the strategy outlined for the asymmetric synthesis of Bao Gong Teng, one might prepare Win analogs as shown in Scheme 58. The cycloaddition of betaine 143 to the acrylate of methyl (*R*)-mandelate (opposite configuration to that of the acrylate of methyl (*S*)-lactate used in the Bao Gong Teng A synthesis) should result in the 6-*exo* cycloadduct 199B as shown in Scheme 58. Cycloadduct 199B has the correct absolute configuration for conversion to Win analogs, however, the 6-ester group would have to be removed in order to arrive at the structures shown in Scheme 56.

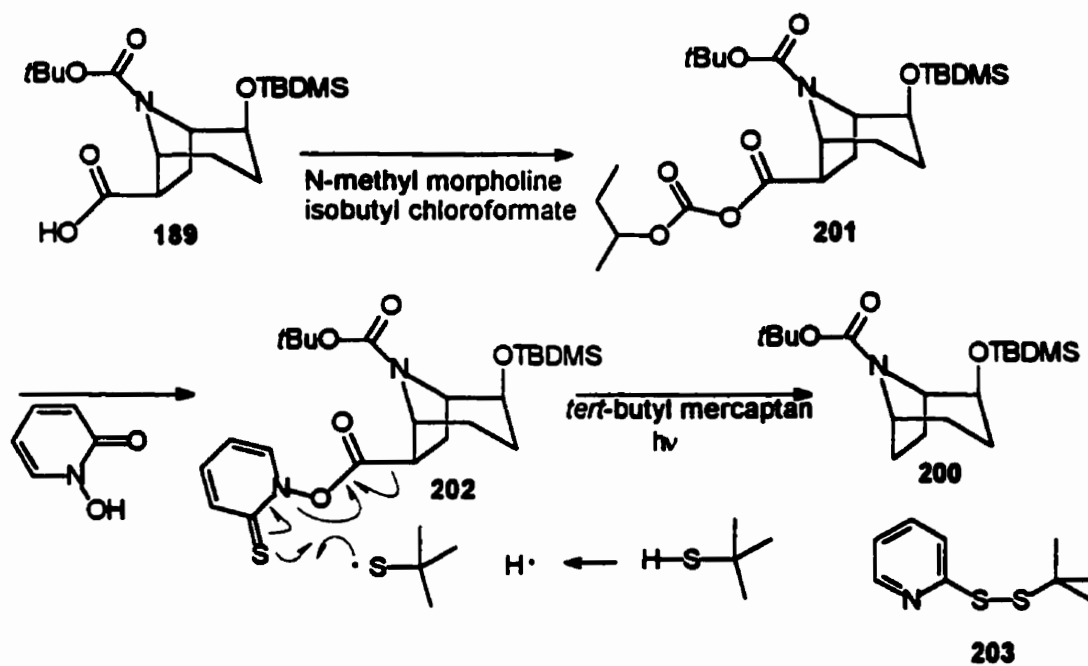
Scheme 58:



In an attempt to demonstrate the feasibility of the proposed synthesis, the 6-ester tropane **188** was decarboxylated to the corresponding 6-H product **200** (see Scheme 59) using a literature procedure that was used for decarboxylation of a tropane-2-carboxylic acid.¹⁰⁰

The ester **188** was hydrolyzed to the corresponding acid **189** as described previously (p. 138). The acid decarboxylation consisted of three steps.¹⁰⁰⁻¹⁰⁴ In the first step, acid **189** was converted to the corresponding *iso*-butyl carbamate **201** (Scheme 59) by adding it to a mixture of *N*-methyl morpholine and *isobutyl* chloroformate and stirring for 10 minutes. In the second step, the *iso*-butyl carbamate **201** was converted to the ester **202** by reacting the carbamate **201** with *N*-hydroxy-2-thiopyridone in the presence of triethylamine. In the third step, the ester **202** was converted to the 6-H derivative **200** by irradiating in the presence of *tert*-butyl mercaptan. Thin layer chromatography (TLC) of the final product indicated that there were two compounds present having very similar retention times. Based on their

visibility by means of TLC it was concluded that these could be byproduct **203** and the product **200**. In order to separate them, the mixture was oxidized with *meta*-chloroperbenzoic acid. The disulfide was oxidized quickly and a new spot appeared at lower R_f by means of TLC. Chromatography after oxidation gave the expected 6-decarboxylated tropane **200**. The ¹³C-nmr spectrum of the product indicated that the acid carbonyl had been removed. Other evidence for the loss of the carboxylic acid group was obtained from the C6 carbon signal. The DEPT spectrum (distortionless enhancement by polarization transfer), where the CH, CH₂ and CH₃ are distinguishable, indicated that the C6 carbon was attached to two protons. A comparison of the ¹H-nmr spectrum of the acid **189** and the product **200**, indicated that the H6 proton signal of the product had moved upfield and now overlapped the other methylene proton signals. From this evidence (and the mass spectral data) it was concluded that the product **200** had been successfully prepared.

Scheme 59:

In conclusion, it has been shown that asymmetric cycloaddition of chiral acrylates to 3-oxidopyridinium betaines, followed by removal of the 6 substituent is a reasonable route to cocaine antagonists. The same procedure may be applicable to synthesis of some compounds of the Win series (see Scheme 56).

Overall conclusion

In the first part of the thesis, asymmetric induction, imposed by the chiral auxiliary methyl (*S*)-lactate, on photodeconjugation reactions was studied. In this work, high asymmetric induction was obtained (de up to 70%). However, due to difficulty in separating diastereomeric products this was not considered good enough for synthetic applications. The search for more optimal conditions in this reaction was terminated after *Pete et al.* published some very impressive successful work in a similar system. The second objective of the first project was to examine trends in asymmetric induction and to attempt to determine the mechanism of asymmetric control. The trends in selectivity for the deconjugation of the chiral ester **84** can be summarized as follows: a) the diastereomer with an *S* configuration at the α center, **163S**, was the major product when ethanol, 2-propanol, *tert*-butyl alcohol or hexane was used as solvent. The isomer with an *R* configuration, **163R**, was the major product when the solvent was methanol, b) the presence of ammonium chloride enhanced the formation of **163S**, while the weakly basic salt KOAc increased the formation of the *R* isomer, **163R**, in methanol, 2-propanol, and in mixture of H₂O and 2-propanol, c) acids (H₂SO₄ and HCl) inverted the diastereoselectivity in both methanol (*R* to *S*) and in 2-propanol (*S* to *R*). Although an explanation for these observed trends was proposed, there was no definitive evidence to confirm the mechanism of asymmetric induction.

In the second part of the thesis work, chiral vinylsulfonates, (methyl (*S*)-lactyl) vinylsulfonate **101**, and (methyl (*R*)-lactyl) vinylsulfonate **102**, were successfully prepared and were reacted with cyclopentadiene. Bicyclo[2.2.1]heptane products (*endo*-**171** and

exo-171) prepared from the reaction of phenyl vinylsulfonate and cyclopentadiene, were fully analyzed using nmr methods including ¹H-nmr, COSY, NOE and computer simulation of the ¹H-nmr spectra. The nmr analyses were used as a basis for assigning relative stereochemistry to the cycloadducts formed from the chiral dienophiles. The Diels-Alder reactions provided excellent yields of cycloadducts, however no significant diastereoselectivity was observed for reaction of the chiral dienophiles, even in the presence of the Lewis acid CH₃AlCl₂. These results indicated that these chiral vinylsulfonates would not be useful in asymmetric Diels-Alder reactions. Thus, further experiments with these chiral vinylsulfonates were terminated.

In the last part of the thesis, diastereoselectivities for 1,3-dipolar cycloaddition reactions of (methyl (*S*)-lactyl) vinylsulfonate 101, and (methyl (*S*)-lactate) acrylate 162, with N-benzyl 3-oxidopyridinium betaine 143 were examined. As in Diels-Alder reactions, 1,3-dipolar cycloaddition of 101 to 143 resulted in no asymmetric induction. An explanation for the poor selectivity of 101, both in the 1,3 dipolar cycloaddition and in its Diels-Alder reaction, was suggested to be the lack of sufficient conformational rigidity of the dipolarophile or dienophile. As a consequence there may have been very little difference in the steric hindrance for approach to the *re* face and *si* faces of the dienophile.

The diastereoselectivity of the 1,3-dipolar cycloaddition of (methyl (*S*)-lactate) acrylate 162 to N-benzyl 3-oxidopyridinium betaine 143, was good (de of 65%), and the yield was excellent (ca. 90%). The asymmetric induction and yield of 162 in this reaction was satisfactory for synthetic applications. The major cycloadduct from this cycloaddition reaction was successfully converted to optically pure Bao Gong Teng A, a tropane alkaloid which might be useful for the treatment of glaucoma. The (methyl (*S*)-lactate)

acrylate of **162**, appears to be a very suitable chiral dipolarophile for use in 1,3-dipolar cycloadditions to N-alkyl 3-oxidopyridinium betaines. Future work in this area could include applying this reaction to the synthesis of other tropane compounds such as cocaine antagonists.

Experimental

Chapter 7

Gas chromatography-mass spectrometry (GC-MS) was carried out using a Varian 3400 chromatograph coupled to a Finnegan MAT 800 spectrometer. The column for the GC-MS was a 30m DB 5 capillary column. Helium was used as carrier gas. The ¹H-nmr spectra were recorded on a Bruker AM-300 instrument (unless otherwise specified) using tetramethylsilane and 3-(trimethylsilyl)-propanesulfonic acid sodium salt (TSP) as internal standards in CDCl₃ and D₂O respectively. ¹³C-nmr spectra were recorded at 75.47 MHz. Coupling constants for protons were measured directly from the spectra, or, when this was inappropriate, assigned using an ¹H-nmr simulation program.¹⁰⁶ The infrared (IR) spectra were recorded on a Perkin Elmer 881 spectrometer, using solution cells. Mass, and high resolution mass spectra were obtained on an Analytical VG 7070E-HF instrument. Melting points were measured on a hot stage instrument and are uncorrected. Optical rotations were recorded on a Rudolf Research Corporation Autopol III instrument. Tetrahydrofuran (THF) was distilled from sodium/benzophenone. Other solvents were reagent grade. *m*-Chloroperbenzoic acid (MCPBA) and CuI were purified by recrystallization before use.

(Methyl (*S*)-lactyl) (*S*)-2,4-dimethylpent-3-enoate (163S), and (Methyl (*S*)-lactyl) (*R*)-2,4-dimethylpent-3-enoate (163R). In a flame dried quartz tube (0.5 x 15 cm), a methanol solution of (methyl (*S*)-lactyl) 2,4-dimethylpent-2-enoate^{73,107} (**84**) (0.5 mL, 1 x 10⁻⁴ M, *E* and *Z* mixture), was deoxygenated by bubbling nitrogen gas through the

solution for one minute. The degassed solution was sealed and irradiated at 254 nm at 0°C for 10 min. The resulting solution was analyzed by GC-MS. The program for the gas chromatograph was a) initial column temperature 70°C, b) initial hold time 2 min., c) rate of heating 5°C per min., d) final column temperature 250°C, e) final hold time 10 min. When the mass spectrometer was configured to detect the total ion current from compounds eluted from the gas chromatograph, many small peaks were evident in the chromatogram. Setting the mass spectrometer to record only ion current from mass 83 gave two cleanly separated peaks at 727-729 and 740-742 sec. Mass 83 is the C₆H₁₁ radical cation formed from the loss of the carboxylalkyl group from the 2,4-dimethylpent-3-enoate esters. The ratio of the signal at 727-729 sec to that at 740-742 sec was 24:76. This ratio was very similar to the ratio (34:66) obtained from ¹H-nmr analysis of a similar reaction mixture. Charlton had previously characterized the two products and had determined the absolute configuration for each.⁷³ On the basis of his analysis the signal at 727-729 sec was assigned to diastereomer 163S and the signal at 740-742 sec to diastereomer 163R.

The procedure for irradiation of 84 in other solvent mixtures was the same as that described above. The procedures for GC-MS analysis of the products solution were the same as that used above when organic solvents were used, *i.e.* the irradiated solution was injected directly into the GC-MS, and the ratio of products was determined. When the irradiated solution contained added acids, bases, salts or water, the products were extracted into a small amount of hexane (0.5 mL). The hexane solution was then analyzed by GC-MS as described above.

(Methyl (*R*)-mandelyl) vinylsulfonate (102). Dry pyridine (0.7 mL, 8.6 mmol) was slowly added to a mixture of methyl (*R*)-mandelate (1.47 g, 8.8 mmol) and 2-chloroethanesulfonyl chloride (1.52 g, 9.3 mmol) in CH₂Cl₂ (10 mL) at -20°C with stirring. The reaction mixture was slowly warmed to 0°C over 2 h, then more 2-chloroethanesulfonyl chloride (3.18 g, 19.5 mmol) and pyridine (1.6 mL, 21 mmol) were added. After 3 h, more pyridine (2.3 mL, 30 mmol) was quickly added, the solution stirred for 15 min, then the solid filtered off and washed with benzene (2 X 40 mL). The organic layer was washed with saturated aqueous CuSO₄, H₂O, then dried (MgSO₄), filtered and evaporated to leave a clear oil. This oil was chromatographed on a silica gel column using 30% EtOAc hexane to provide 102 (0.85 g, 38%) as a crystalline solid: mp 54 - 57 °C; $[\alpha]_D^{23}$ -111.2 (c 1.2, CHCl₃); IR (CH₂Cl₂) 1764, 1375, 1175 cm⁻¹; ¹H-nmr (CDCl₃) δ 7.41 (5H, m), 6.54 (1H, dd, *J* = 9.7, 16.6 Hz), 6.37 (1H, d, *J* = 16.6 Hz), 6.04 (1H, d, *J* = 9.7 Hz), 5.81 (1H, s), 3.76 (3H, m); ¹³C-nmr (CDCl₃) δ 53.0, 79.2, 127.6, 128.9 (2C), 129.9 (3C), 132.6, 133.2, 167.8; mass spectrum *m/z* (rel %) 197 (M⁺ - CO₂Me, 9), 150 (29), 118 (21), 91 (100). *Exact Mass* calcd. for C₉H₉O₃S (M⁺ - CO₂Me) 197.0272, found 197.0266.

(Methyl (*S*)-lactyl) vinylsulfonate (101). 101 was prepared by a procedure identical to that used for preparation of 102 using methyl *S*-lactate (2.6 mL, 27.2 mmol), 2-chloroethanesulfonyl chloride (13.3 g, 81.3 mmol), and pyridine (13.2 mL, 162 mmol). 101 was obtained as a light yellow oil (41.1%): $[\alpha]_D^{23}$ -47.1 (c 1.2, CHCl₃); IR (CH₂Cl₂) 1762, 1374, 1177 cm⁻¹; ¹H-nmr (CDCl₃) δ 6.66 (1H, dd, *J* = 9.8, 16.6 Hz), 6.42 (1H, d, *J* = 16.6 Hz), 6.13 (1H, d, *J* = 9.8 Hz), 4.99 (1H, q, *J* = 7.0 Hz), 3.79 (3H, s), 1.61 (3H, d, *J* = 7.0 Hz); ¹³C-nmr (CDCl₃) δ 18.3, 52.7, 74.4, 129.8, 133.1, 169.4; mass spectrum *m/z*

(rel %) 163 (M^+ - OMe, 1), 135 (86), 91 (100), 59 (20). *Exact Mass* calcd. for $C_4H_7O_3S$ (M^+ - CO_2Me) 135.0116, found 135.0101.

Phenyl vinylsulfonate (120). Pyridine (0.55 mL, 6.8 mmol) was slowly added to a solution of 2-bromoethanesulfonyl chloride (1.52 g, 7.4 mmol) and phenol (0.64 g, 6.8 mmol) at 0°C. The resulting mixture was stirred for 1 h, then more 2-bromoethanesulfonyl chloride (0.63 g, 3.4 mmol) and pyridine (0.1 mL) were added and the solution stirred for another 12 h. Pyridine (0.55 mL) was added and the solution stirred for 2 h. The solid was removed by filtration, the filtrate diluted with CH_2Cl_2 (40 mL) and washed with HCl (3%, 3 x 20 mL). The organic layer was dried with $MgSO_4$, filtered and evaporated to leave a dark yellow oil (1.00 g). This oil was chromatographed on a silica gel column using 30% EtOAc in hexane to provide 120 (0.402 g, 32.1%) as a brown solid: mp 33.5 - 35.0 °C; IR (CH_2Cl_2) 1591, 1488 1378, 1146 cm^{-1} ; 1H -nmr ($CDCl_3$) δ 7.30 (5H, m), 6.66 (1H, dd, $J = 9.9, 16.6$ Hz), 6.35 (1H, d, $J = 16.6$ Hz), 6.14 (1H, d, $J = 9.9$ Hz); ^{13}C -nmr ($CDCl_3$) δ 122.2, 127.3 (2C), 129.8 (2C), 131.6, 132.0, 149.4; mass spectrum m/z (rel %) 184 (M^+ , 57), 120 (12), 95 (6.5), 94 (100), 65 (71). *Exact Mass* calcd. for $C_8H_8O_3S$ (M^+) 184.0194, found 184.0202.

Phenyl bicyclo[2.2.1]hept-5-ene-2-sulfonate (171). A mixture of freshly distilled cyclopentadiene (180.0 mg, 2.6 mmol) and phenyl vinylsulfonate (43.5 mg, 0.24 mmol) was refluxed in benzene (5 mL) for 2 h. The solvent was evaporated to give a clear oil. This oil was placed on a short silica gel column, the cyclopentadiene was eluted out with hexane (50 mL), and the mixture of cycloadducts (47.2 mg, 80.0%) was eluted out with 30% EtOAc in hexane as a clear oil. The cycloadduct mixture was separated on silica gel

with 1:1:8 CH₂Cl₂/ EtOAc/ hexane. The *exo*-171 (14 mg) was eluted first, followed by a mixed fraction (19 mg), followed by the *endo*-171 (14 mg), both were a colorless oil.

***Exo*-171:** IR (CH₂Cl₂) 1489, 1263 cm⁻¹; ¹H-nmr (CDCl₃) δ 7.2-7.5 (5H, m), 6.27 (1H, dd, *J* = 3.0, 5.6 Hz), 6.15 (1H, dd, *J* = 3.2, 5.6 Hz), 3.43 (1H, m), 3.10 (1H, ddd, *J* = 1.4, 4.9, 8.7 Hz), 3.07 (1H, m), 2.21 (1H, ddd, *J* = 3.4, 4.9, 12.5 Hz), 1.93 (1H, ddd, *J* = 1.4, 1.5, 9.1 Hz), 1.64 (1H, ddd, *J* = 2.6, 8.7, 12.5 Hz), 1.51 (1H, m, *J* = 1.4, 1.4, 1.5, 2.6, 9.1 Hz); ¹³C-nmr (CDCl₃) δ 29.3, 41.6, 45.4, 46.0, 59.9, 122.1, 127.0 (2C), 129.8 (2C), 134.9, 139.9, 149.3; mass spectrum *m/z* (rel %) 250 (M⁺, 2), 120 (100), 94 (12), 93 (78), 92 (11), 91 (60), 77 (52). *Exact Mass* calcd. for C₁₃H₁₄O₃S (M⁺) 250.0663, found 250.0647.

***Endo*-171:** IR (CH₂Cl₂) 1489, 1369, 1195 cm⁻¹; ¹H-nmr (CDCl₃) δ 7.2-7.5 (5H, m), 6.32 (1H, dd, *J* = 3.1, 5.6 Hz), 6.14 (1H, dd, *J* = 2.8, 5.6 Hz), 3.87 (1H, ddd, *J* = 3.3, 4.7, 9.2 Hz), 3.43 (1H, m), 3.05 (1H, m), 2.18 (1H, ddd, *J* = 3.7, 9.3, 12.8 Hz), 1.58 (2H, m), 1.33 (1H, m); ¹³C-nmr (CDCl₃) δ 29.9, 42.7, 45.6, 49.6, 60.4, 122.1, 126.9 (2C), 129.8 (2C), 131.4, 137.8, 149.3; mass spectrum *m/z* (rel %) 250 (M⁺, 8), 120 (100), 93 (81), 91 (68), 77 (57), 66 (40). *Exact Mass* calcd. for C₁₃H₁₄O₃S (M⁺) 250.0663, found 250.0664.

Methyl (*S*)-lactyl bicyclo[2.2.1]hept-5-ene-2-sulfonate (175). A mixture of freshly distilled cyclopentadiene (166.8 mg, 2.5 mmol) and (methyl (*S*)-lactyl) vinylsulfonate (121.5 mg, 0.63 mmol) was stirred in benzene (2 mL) for 5 h. The solvent was evaporated to give a clear oil. This oil was placed on a short silica gel column, the cyclopentadiene was eluted out with hexane (50 mL) and the mixture of *exo/endo* cycloadducts 175 (220.1 mg, 98.4%) was eluted out with 30% EtOAc in hexane. The

cycloadduct mixture was separated on a silica gel column with 1:1:8 CH₂Cl₂/ EtOAc/ hexane. The *exo*-175 (41 mg) was eluted first, followed by the *endo*-175 (156 mg), both were a colorless oil.

Exo-175 (mixture of two diastereomers with nearly identical chemical shifts and coupling constants. Both chemical shifts are given when the signals from the two diastereomers are resolved): IR (CH₂Cl₂) 1762, 1172 cm⁻¹; ¹H-nmr (CDCl₃) δ 6.27 (1H, dd, *J* = 2.6, 5.8 Hz), 6.16 and 6.15 (1H, dd, *J* = 3.1, 5.8 Hz), 5.15 and 5.14 (1H, q, *J* = 7.0 Hz), 3.80 and 3.79 (1H, s), 3.38 (1H, m), 3.09 and 3.08 (1H, ddd, *J* = 1.5, 4.8, 8.2 Hz), 3.03 (1H, m), 2.13 and 2.12 (1H, ddd, *J* = 3.4, 4.8, 12.9 Hz), 1.90 (1H, m), 1.63 (1H, m), 1.62 and 1.61 (3H, d, *J* = 7.0 Hz), 1.47 (1H, m); ¹³C-nmr (CDCl₃) δ 18.7, 29.2 and 28.9, 41.5 and 41.4, 45.3 and 45.1, 45.9 and 45.8, 52.7, 61.0 and 60.8, 73.1 and 73.0, 135.1, 139.7 and 139.6, 170.0; mass spectrum *m/z* (rel %) 201 (M⁺ - CO₂Me, 0.4), 195 (5), 93 (59), 92 (20), 91 (26), 77 (21), 66 (100). *Exact Mass* calcd. for C₉H₁₃O₃S (M⁺ - CO₂Me) 201.0585, found 201.0585.

Endo-175 (mixture of two diastereomers with nearly identical chemical shifts and coupling constants. Both chemical shifts are given when the signals from the two diastereomers are resolved): IR (CH₂Cl₂) 1762, 1360, 1224, 1175 cm⁻¹; ¹H-nmr (CDCl₃) δ 6.29 (1H, dd, *J* = 3.1, 5.5 Hz), 6.11 and 6.09 (1H, dd, *J* = 2.8, 5.5 Hz), 5.08 and 5.09 (1H, q, *J* = 7.0 Hz), 3.87 (1H, ddd, *J* = 3.4, 4.7, 9.4 Hz), 3.79 and 3.80 (3H, s), 3.42 and 3.38 (1H, m), 3.03 (1H, m), 2.17 and 2.21 (1H, ddd, *J* = 3.7, 9.4, 12.6 Hz), 1.60 and 1.58 (3H, d, *J* = 7.0 Hz), 1.56 (1H, m), 1.50 and 1.54 (1H, *J* = 2.8, 4.7, 12.6 Hz), 1.33 (1H, m); ¹³C-nmr (CDCl₃) δ 18.7 and 18.6, 29.6 and 29.7, 42.6, and 42.6, 45.5 and 45.4, 49.5 and 49.6, 52.7, 61.4 and 61.2, 72.8 and 72.7, 131.4, and 131.3, 137.7, 170.0; mass

spectrum m/z (rel %) 260 (M^+ , 0.5), 195 (5), 93 (45), 92 (16), 91 (23), 77(17), 66 (100).

Exact Mass calcd. for $C_9H_{13}O_3S$ (M^+ - CO_2Me) 201.0585, found 201.0580.

Methyl (*S*)-mandelyl bicyclo[2.2.1]hept-5-ene-2-sulfonate (176). A mixture of freshly distilled cyclopentadiene (0.8 mL, 15 mmol) and methyl (*R*)-mandelyl vinylsulfonate (229.5 mg, 0.90 mmol) was refluxed in benzene (5 mL) for 2 h. The solvent was evaporated to give a clear oil, which was then chromatographed on silica gel using 1:1:8 CH_2Cl_2 / EtOAc/ hexane to obtained the *exo*-176 (64 mg, 22%), followed by *endo*-176 (202 mg, 70%). Both were a colorless oil.

Exo-176 (mixture of two diastereomers with nearly identical chemical shifts and coupling constants. Both chemical shifts are given when the signals from the two diastereomers are resolved): IR (CH_2Cl_2) 1763, 1361, 1221, 1171 cm^{-1} ; 1H -nmr ($CDCl_3$) δ 7.35-7.5 (5H, m), 6.22 and 6.20 (1H, dd, $J = 3.0, 5.5$ Hz), 6.12 and 6.01 (1H, dd, $J = 3.2, 5.5$ Hz), 5.95 (1H, s), 3.77 (3H, s), 3.35 and 3.33 (1H, m), 3.00 (1H, m), 2.99 and 2.95 (1H, ddd, $J = 1.2, 5.0, 8.7$ Hz), 2.12 and 2.10 (1H, ddd, $J = 3.4, 5.0, 12.6$ Hz), 1.88 (1H, m), 1.57 and 1.51 (1H, ddd, $J = 2.6, 8.7, 12.6$ Hz), 1.44 (1H, m); ^{13}C -nmr ($CDCl_3$) δ 29.1 and 29.0, 41.5, 45.3 and 45.2, 45.8, 53.0, 61.4 and 61.3, 77.9, 127.7 and 127.6, 129.0 (2C), 129.8 (2C), 133.3 and 133.2, 135.1 and 135.0, 139.7 and 139.6, 168.3 and 168.2; mass spectrum m/z (rel %) 263 (M^+ - CO_2Me , 4), 199 (4), 150 (21), 149(25), 121 (13), 118 (8), 105 (9), 93 (100), 91 (74), 77 (31), 66 (46). *Exact Mass* calcd. for $C_{14}H_{15}O_3S$ (M^+ - CO_2Me) 263.0742, found 263.0729.

Endo-176 (mixture of two diastereomers with nearly identical chemical shifts and coupling constants. Both chemical shifts are given when the signals from the two diastereomers are resolved): IR (CH_2Cl_2) 1763, 1363, 1221, 1174 cm^{-1} ; 1H -nmr ($CDCl_3$)

δ 7.35-7.5 (5H, m), 6.26 and 6.25 (1H, dd, $J = 3.3, 5.6$ Hz), 6.09 and 6.06 (1H, dd, $J = 2.7, 5.6$ Hz), 5.89 (1H, s), 3.81 (1H, ddd, $J = 3.3, 4.8, 9.2$ Hz), 3.76 and 3.75 (3H, s), 3.36 (1H, m), 3.00 (1H, m), 2.09 (1H, ddd, $J = 3.6, 9.2, 12.5$ Hz), 1.52 (1H, m), 1.48 (1H, m), 1.27 (1H, m); ^{13}C -nmr (CDCl_3) δ 29.6, 42.6, 45.5 and 45.4, 49.5 and 49.4, 52.9, 61.7, 77.7 and 77.5, 127.6 (2C), 128.9 (2C), 129.7₃ and 129.7₀, 131.4, 133.2₉ and 133.2₇, 137.7, 168.3₁ and 168.2₇; mass spectrum m/z (rel %) 322 (M^+ , 0.5), 263 ($\text{M}^+ - \text{CO}_2\text{Me}$, 2), 150 (36), 149(79), 121 (32), 118 (20), 105 (9), 91 (99), 77 (24), 66 (100). *Exact Mass* calcd. for $\text{C}_{16}\text{H}_{18}\text{O}_5\text{S}$ (M^+) 322.0875 and $\text{C}_{14}\text{H}_{15}\text{O}_3\text{S}$ ($\text{M}^+ - \text{CO}_2\text{Me}$) 263.0742, found 322.0876 and 263.0744, respectively.

1-Benzyl-3-hydroxypyridinium chloride (143). A mixture of 3-hydroxypyridine (10.4 g, 109 mmol) and benzyl chloride (15.5 g, 122 mmol) in 1-propanol (90 mL) was refluxed overnight. The solvent was evaporated to leave a colorless solid which was recrystallized from acetonitrile to give crystalline 143 (18.2 g, 75.5%) : mp 158-159°C (Lit.⁵² mp 154-157°C).

Phenyl 8-benzyl-2-oxo-8-azabicyclo[3.2.1]oct-3-ene-6-*exo*-sulfonate (177). *N*-phenyl 3-hydroxy pyridinium hydrochloride (57 mg, 0.26 mmol) and triethylamine (80 μL , 5.7 mmol) were stirred in EtOAc (10 mL) for 2 h. The solid (Et_3NHCl) was filtered off, washed with EtOAc (3 mL) and the filtrate added to phenyl vinylsulfonate (120) (34.9 mg, 0.19 mmol). The mixture was refluxed under a nitrogen atmosphere for 12 h. Another equivalent of betaine (57 mg of the pyridinium hydrochloride) was added and the reflux continued for another 12 h. The solvent was evaporated and the crude product was chromatographed using 17:12:56 of CH_2Cl_2 :EtOAc: hexane. A mixture of cycloadducts (*endo* and *exo* 177) was obtained as a yellow oil (53 mg, 75.5%) in a ratio of 1:5.6.

All spectral data below were obtained from this mixture. Only the nmr signals for the major isomer (*exo*-177) are reported: IR (CH₂Cl₂) 1693, 1375, 1267, 1145 cm⁻¹; ¹H-nmr (CDCl₃) δ 7.2-7.4 (10H, m), 6.93 (1H, dd, *J* = 5.0, 9.8 Hz), 6.18 (1H, dd, *J* = 1.5, 9.8 Hz), 4.27 (1H, d, *J* = 5.0 Hz), 3.93 (1H, d, *J* = 13.4 Hz), 3.81 (1H, d, *J* = 13.4 Hz), 3.77 (1H, d, *J* = 7.7 Hz), 3.79 (1H, dd, *J* = 4.4, 9.0 Hz), 2.98 (1H, ddd, *J* = 4.4, 7.7, 14.3 Hz), 2.17 (1H, dd, *J* = 9.2, 14.3 Hz); ¹H-nmr (Benzene-d₆) δ 6.9-7.4 (10H, m), 5.76 (1H, dd, *J* = 4.8, 9.7 Hz), 5.69 (1H, dd, *J* = 1.3, 9.7 Hz), 4.02 (1H, d, *J* = 4.7 Hz), 3.60 (1H, d, *J* = 13.6 Hz), 3.47 (1H, d, *J* = 13.6 Hz), 3.48 (1H, d, *J* = 7.7 Hz), 3.24 (1H, dd, *J* = 4.4, 9.2 Hz), 2.65 (1H, ddd, *J* = 4.4, 7.7, 14.2 Hz), 1.54 (1H, dd, *J* = 9.2, 14.3 Hz); ¹³C-nmr (CDCl₃) δ 28.0, 51.5, 58.2, 62.7, 68.0, 122.0, 127.3 (2C), 127.6, 128.3 (2C), 128.5 (2C), 129.3, 130.0 (2C), 137.0, 144.8, 148.9, 197.3; mass spectrum *m/z* (rel %) 369 (M⁺, 5), 278 (28), 184 (20), 149 (64), 94 (33), 93 (17), 92 (31), 91 (100). *Exact Mass* calcd. for C₂₀H₁₉O₄SN (M⁺) 369.1035 found 369.1021.

(Methyl (*S*)-lactyl) 8-benzyl-2-oxo-8-azabicyclo[3.2.1]oct-3-ene-6-*exo*-sulfonate (179). A mixture of (methyl (*S*)-lactyl) vinylsulfonate 101 (191 mg, 0.98 mmol), N-phenyl-3-hydroxy pyridinium hydrochloride (55 mg, 0.25 mmol) and Et₃N (70 μL, 5.0 mmol) in EtOAc (5 mL) was stirred at rt for 1 week. The solution was diluted with EtOAc (40 mL), then washed with NaHCO₃ (5%, 3 x 20 mL). The organic layer was dried (MgSO₄), filtered and evaporated to leave an oil (68.3 mg). The crude product was chromatographed on silica gel using 30% EtOAc in hexane to obtain a mixture of cycloadducts (*exo*-179 as a mixture of diastereomers) (43.6 mg, 46.0%) as a light yellow oil: IR (CH₂Cl₂) 1758, 1691, 1370, 1226, 1177 cm⁻¹; (since this is a mixture of two diastereomers with nearly identical chemical shifts and coupling constants, both chemical

shifts are given when the signals from the two diastereomers are resolved) ^1H -nmr (CDCl_3) δ 7.2 - 7.4 (5H, m), 7.01 and 6.96 (1H, dd, $J = 5.0, 9.8$ Hz), 6.18 and 6.17₇ (1H, dd, $J = 1.1, 9.8$ Hz), 5.17 and 5.14 (1H, q, $J = 7.0$ Hz), 4.29 and 4.23 (1H, d, $J = 5.0$ Hz), 3.76 (1H, d, $J = 7.7$ Hz), 3.92 and 3.91 (1H, d, $J = 13.4$ Hz), 3.81 and 3.80 (1H, d, $J = 13.4$ Hz), 3.84 and 3.81 (1H, dd, $J = 4.4, 9.2$ Hz), 3.78 and 3.74 (3H, s), 2.91 and 2.96 (1H, ddd, $J = 4.4, 7.7, 14.3$ Hz), 2.14 and 2.20 (1H, dd, $J = 9.2, 14.3$ Hz), 1.60 (3H, d, $J = 7.0$ Hz); ^1H -nmr (Benzene- d_6) δ 7.0 - 7.4 (5H, m), 6.07 and 5.88 (1H, dd, $J = 5.0, 9.8$ Hz), 5.76 and 5.71 (1H, dd, $J = 1.4, 9.8$ Hz), 4.96 and 4.99 (1H, q, $J = 7.0$ Hz), 4.13 and 4.06 (1H, d, $J = 5.0$ Hz), 3.50 (1H, d, $J = 7.7$ Hz), 3.62 and 3.59 (1H, d, $J = 13.6$ Hz), 3.51 and 3.48 (1H, d, $J = 13.6$ Hz), 3.48 and 3.41 (1H, dd, $J = 4.5, 9.2$ Hz), 3.15 and 3.14 (3H, s), 2.71 and 2.73 (1H, ddd, $J = 4.5, 7.7, 14.3$ Hz), 1.64 and 1.70 (1H, dd, $J = 9.2, 14.3$ Hz), 1.18 and 1.17 (3H, d, $J = 7.0$ Hz); ^{13}C -nmr (CDCl_3) δ 18.6₃ and 18.5₇, 27.6 and 28.0, 51.6 and 51.5, 52.9 and 52.8, 58.6 and 58.2, 63.6 and 63.8, 68.1 and 68.0, 74.2 and 73.9, 127.5₁ and 127.4₈, 128.3 (2C), 128.5 (2C), 129.1 and 129.2, 137.2 and 137.1, 145.4 and 145.1, 169.9, 197.6. Anal. Calcd for $\text{C}_{18}\text{H}_{21}\text{NO}_6\text{S}$: C, 56.98; H, 5.58. Found: C, 57.43; H, 5.66.

(Methyl (S)-lactyl) 8-benzyl-2-oxo-8-azabicyclo[3.2.1]oct-3-ene-6-exo-carboxylate (180). A mixture of the pyridinium salt **143** (8.79 g, 39.6 mmol), the acrylate of methyl (*S*)-lactate (9.56 g, 60.4 mmol), triethylamine (15 mL) and a small amount of hydroquinone were stirred in EtOAc (200 mL) at room temperature under nitrogen atmosphere for 10 days. The solid precipitate was filtered and washed with EtOAc (2 x 30 mL). The combined EtOAc was washed with aqueous sodium bicarbonate (5%), and extracted with 3% HCl. The acid phase was made basic by adding solid sodium

bicarbonate and then extracted with CH_2Cl_2 . The organic phase was dried (MgSO_4), filtered and evaporated to give 13.0 g of crude product (mixture of **180A** and other isomers). A small amount of crude product was purified by HPLC (ODS-2, $\text{CH}_3\text{OH}/\text{H}_2\text{O}$ 70:30) to give **180A** as an oil: ^1H -nmr (CDCl_3) δ 7.20-7.34 (5H, m), 7.02 (1H, dd, $J = 9.8, 5.1$ Hz), 6.10 (1H, dd, $J = 9.8, 1.5$ Hz), 5.16 (1H, q, $J = 7.1$ Hz), 4.19 (1H, d, $J = 5.0$ Hz), 3.84 (1H, d, $J = 13.5$ Hz), 3.74 (1H, d, $J = 13.5$), 3.72 (3H, s), 3.65 (1H, d, $J = 7.8$ Hz), 3.03 (1H, dd, $J = 9.4, 3.8$ Hz), 2.86 (1H, ddd, $J = 13.8, 7.8, 3.8$ Hz), 1.94 (1H, dd, $J = 13.8, 9.5$ Hz), 1.52 (3H, d, $J = 7.1$ Hz); ^{13}C -nmr (CDCl_3) δ 16.94, 27.77, 47.04, 52.19, 52.33, 60.26, 68.58, 69.15, 127.19, 128.01, 128.34, 137.83, 147.74, 170.88, 172.02, 198.98. Analysis precluded due to thermal instability.

(Methyl (S)-lactyl) 8-benzyl-2-oxo-8-azabicyclo[3.2.1]octane-6-exo-carboxylate (181). A solution of **180** (13 g) in EtOAc and a catalytic amount of 5% Pd/C (110 mg) were stirred under hydrogen (1 atm) for 15 h at room temperature. The catalyst was filtered off and washed with EtOAc. The filtrate was evaporated to give a light yellow oil, which was crystallized from 20% EtOAc in hexane to give 8.41 g of **181** (61% for two steps) : mp 87-88.5°C; $[\alpha]_{\text{D}}^{23} -57.7$ (c 0.14, CHCl_3); IR (CH_2Cl_2): 1744 cm^{-1} ; ^1H -nmr (CDCl_3) δ 7.18 - 7.37 (5H, m), 5.16 (1H, q, $J = 7.1$ Hz), 3.89 (1H, br s), 3.83 (1H, d, $J = 13.8$ Hz), 3.72 (3H, s), 3.69 (1H, d, $J = 13.8$ Hz), 3.49 (1H, d, $J = 7.3$ Hz), 3.07 (1H, dd, $J = 9.6, 5.8$ Hz), 2.72 (1H, ddd, $J = 14.2, 7.3, 5.8$ Hz), 2.34-2.42 (2H, m), 2.29 (1H, m), 2.08 (1H, dd, $J = 14.2, 9.6$ Hz), 1.91 (1H, m), 1.52 (3H, d, $J = 7.1$ Hz); ^{13}C -nmr (CDCl_3) δ 16.89, 29.53, 30.44, 32.94, 46.33, 52.29, 53.98, 61.17, 68.93, 70.24, 127.03, 128.21, 128.33, 138.19, 170.96, 174.01, 208.58; mass spectrum m/z (rel %): 317

(M^+ - CO, 25), 242 (9.8), 186 (22), 159 (21), 158 (42), 91 (100). *Exact Mass* calcd. for $C_{18}H_{23}O_4N$ (M^+ - CO): 317.1627; found: 317.1612.

(Methyl (S)-lactyl) 8-benzyl-2-*exo*-hydroxy-8-azabicyclo[3.2.1]octane-6-*exo*-carboxylate (182A) and Methyl (S)-lactyl 8-benzyl-2-*endo*-hydroxy-8-azabicyclo[3.2.1]octane-6-*exo*-carboxylate (182B). $LiAl(OtBu)_3H$ (9.19 g, 35.8 mmol) in THF (60 mL) was added to a solution of ketone 181 (5.80 g, 16.8 mmol) in THF (40 mL) at $-4^\circ C$ under a nitrogen atmosphere, stirred for 3 hours and then quenched with 3% HCl (20 mL). Saturated sodium bicarbonate was added and the basic solution was extracted with CH_2Cl_2 . The organic phase was dried ($MgSO_4$), filtered and evaporated to leave a light yellow oil, which was chromatographed on silica gel, eluting with 3:7 EtOAc/hexane. Alcohol 182A (3.60 g, 61.8%) was obtained as colorless crystals followed by 182B as an oil (1.20 g, 20.6%).

Exo alcohol 182A: mp $73-74.5^\circ C$; $[\alpha]_D^{23}$ -106 (c 0.26, $CHCl_3$); IR (CH_2Cl_2): $3489, 1736\text{ cm}^{-1}$; 1H -nmr ($CDCl_3$) δ 7.18 - 7.35 (5H, m), 5.14 (1H, q, $J = 7.1$ Hz), 3.80 (1H, br s), 3.68 (3H, s), 3.66 (1H, d, $J = 13.4$ Hz), 3.50 (1H, br s), 3.42 (1H, d, $J = 13.4$ Hz), 3.28 (1H, dd, $J = 7.2, 3.8$ Hz), 2.94 (1H, dd, $J = 9.5, 5.9$ Hz), 2.61 (1H, ddd, $J = 14.1, 7.2, 5.9$ Hz), 1.98 (1H, m), 1.81 (1H, dd, $J = 14.1, 9.5$ Hz), 1.46-1.62 (3H, m), 1.51 (3H, d, $J = 7.1$ Hz); ^{13}C -nmr ($CDCl_3$) δ 16.92, 24.76, 28.19, 29.37, 45.24, 52.34, 57.69, 65.26, 66.43, 68.20, 68.83, 127.03, 128.30, 128.74, 139.43, 171.04, 175.29; mass spectrum m/z (rel %): 347 (M^+ , 7), 256 (23), 244 (13), 242 (17), 216 (28), 184 (20), 172 (16), 158 (17), 149 (24), 91 (100). *Exact Mass* calcd. for $C_{19}H_{25}O_5N$: 347.1733; found: 347.1721.

Endo alcohol **182B**: $[\alpha]_D^{23}$ -78.5 (c 0.37, CHCl₃); IR (CH₂Cl₂): 3606, 1739 cm⁻¹; ¹H-nmr (CDCl₃) δ 7.16 - 7.38 (5H, m), 5.14 (1H, q, J = 7.1 Hz), 3.82 (1H, m), 3.73 (1H, br s), 3.72 (1H, d, J = 13.9 Hz), 3.68 (3H, s), 3.55 (1H, d, J = 13.9 Hz), 3.19 (1H, dd, J = 6.5, 3.7 Hz), 2.82 (1H, dd, J = 9.6, 6.2 Hz), 2.42 (1H, ddd, J = 13.8, 6.5, 6.2 Hz), 2.10 (1H, dd, J = 13.8, 9.6 Hz), 1.75-1.96 (2H, m), 1.61 (1H, m), 1.51 (3H, d, J = 7.1 Hz), 1.25 (1H, m); ¹³C-nmr (CDCl₃) δ 16.94, 25.00, 26.34, 30.66, 46.82, 52.23, 56.84, 64.06, 65.57, 68.73, 69.31, 126.70, 128.07, 128.45, 139.84, 171.17, 175.38; mass spectrum m/z (rel %): 347 (M⁺, 5), 256 (10), 244 (6), 242 (6), 216 (13), 184 (9), 172 (9), 158 (10), 149 (20), 91 (65), 71 (100). *Exact Mass* calcd. for C₁₉H₂₅O₅N: 347.1733; found: 347.1738.

8-Benzyl-2-*exo*-hydroxy-8-azabicyclo[3.2.1]octane-6-*exo*-carboxylic acid (183). Potassium hydroxide (405 mg., 7.21 mmol) in H₂O (6 mL) was added to a solution of **182A** (336 mg, 96.8 mmol) in CH₃OH (12 mL), and the resulting mixture was stirred at room temperature for 20 hours. Most of the CH₃OH was then evaporated. The resulting aqueous solution was adjusted to pH 2 by adding 3% HCl then was slowly poured onto an acidic (pH 2) ion exchange column (Dowex 50W-X8, hydrogen form). The column was rinsed with aqueous HCl (pH 2, 100 mL), and then H₂O until no more chloride ion was eluted. The acid **183** was eluted with one litre of aqueous NH₃ (pH 11), and the solvent evaporated to give a colorless solid. The solid was dissolved in H₂O (20 mL), then frozen and lyophilized under high vacuum overnight. The resulting acid **183** (186 mg, 73.5%) appeared as flaky, colorless solid: $[\alpha]_D^{23}$ -9.6 (c 0.10, H₂O); ¹H-nmr (D₂O), δ 7.40-7.53 (5H, m), 4.39 (1H, d, J = 13.4 Hz), 4.36 (1H, s), 4.00 (1H, s), 3.92 (1H, d, J = 13.4), 3.66 (1H, m), 3.16 (1H, dd, J = 10.5, 5.6 Hz), 2.65 (1H, ddd, J = 15.2, 7.1, 5.6 Hz), 2.33 (1H, m), 2.23 (3H, dd, J = 10.5, 15.2 Hz), 1.78-2.00 (2H, m), 1.68 (1H, m); ¹³C-nmr (CDCl₃),

δ 22.73, 26.60, 26.76, 45.48, 55.99, 66.08, 67.79, 68.53, 129.92, 130.22, 130.85, 131.02, 179.94; mass spectrum m/z (rel %): 261 (7.1), 170 (30.6), 149 (18.8), 91 (100), 69 (51.6), 57 (47.5), 55 (42.1). *Exact Mass* calcd. for $C_{15}H_{19}O_3N$: 261.1365; found: 261.1364.

(Methyl (S)-lactyl) 8-benzyl-2-*exo*-[(*tert*-butyl-dimethylsilyl)oxy]-8-azabicyclo[3.2.1]octane-6-*exo*-carboxylate (184). To a mixture of **182A** (2.17 g, 6.24 mmol) and triethylamine (3.70 mL) was added TBDMSOTf (2.20 mL, 9.58 mmol) over 3 minutes under a nitrogen atmosphere. TLC indicated that the reaction was complete. The reaction mixture was poured into saturated NaCl solution (40 mL), then extracted with CH_2Cl_2 (4 x 20 mL). The combined organic phases were dried ($MgSO_4$), filtered and evaporated to leave a dark yellow oil. This yellow oil was filtered through a short silica gel column with 3:7 EtOAc/hexane to provide **184** as a light yellow oil (2.77 g, 96%): $[\alpha]_D^{23}$ -68.7 (c 0.60, $CHCl_3$); IR (CH_2Cl_2): 1741 cm^{-1} ; 1H -nmr ($CDCl_3$) δ 7.46 (2H, d, $J = 7.2$ Hz), 7.14-7.32 (3H, m), 5.15 (1H, q, $J = 7.1$ Hz), 3.87 (1H, d, 14.9 Hz), 3.76 (1H, d, $J = 14.9$ Hz), 3.74 (1H, br s), 3.69 (3H, s), 3.62 (1H, br s), 3.28 (1H, dd, 7.0, 3.0 Hz), 2.92 (1H, dd, $J = 9.4, 5.7$ Hz), 2.51 (1H, ddd, $J = 13.6, 7.0, 5.7$ Hz), 2.19 (1H, dddd, $J = 12.9, 12.9, 5.7, 2.7$ Hz), 1.71 (1H, m), 1.70 (1H, dd, $J = 13.6, 9.4$ Hz), 1.56 (1H, m), 1.52 (3H, d, $J = 7.1$ Hz); 1.40 (1H, m), 0.92 (9H, s), 0.03 (3H, s), 0.00 (3H, s); ^{13}C -nmr ($CDCl_3$) δ -4.96, -4.70, 16.92, 18.18, 25.75, 25.93, 26.62, 28.73, 45.42, 52.15, 55.89, 63.41, 65.37, 68.64, 70.23, 126.17, 127.83, 128.10, 140.50, 171.12, 175.46; mass spectrum m/z (rel %): 461 (M^+ , 2), 370 (5), 356 (8.4), 330 (6.4), 300 (9.5), 266 (9.2), 210 (15), 91 (100). *Exact Mass* calcd. for $C_{25}H_{39}O_5NSi$: 461.2598; found: 461.2563.

(Methyl (*S*-lactyl) 8-(*tert*-butoxycarbonyl)-2-*exo*-[(*tert*-butyl-dimethylsilyl)oxy]-8-azabicyclo[3.2.1]octane-6-*exo*-carboxylate (188). Di-*tert*-butyl dicarbonate (1.15 g, 5.26 mmol) was added to a solution of **184** (1.33 g, 2.89 mmol) in CH₃OH (70 mL) followed by 5% Pd/C (150 mg). The resulting suspension was hydrogenated (H₂, 1 atm) for 15 hours and then filtered. The catalyst was thoroughly washed with CH₃OH and the combined filtrates evaporated to leave a colorless oil with di-*tert*-butyl dicarbonate as a contaminant. A small amount of the crude product was pumped under high vacuum for 2 weeks to obtain a sample of solid **188** for characterization purposes (the bulk of the crude product was used in the next step without further purification): mp 53-55°C; [α]_D²³ -14.0 (c 0.47, CHCl₃); IR (CH₂Cl₂): 1744, 1691 cm⁻¹; ¹H-nmr (CDCl₃), mixture of two rotamers, δ 5.06 (1H, q, J = 7.1 Hz), 4.52 and 4.63 (1H, br s), 4.22 and 4.27 (1H, m), 3.71 and 3.72 (3H, s), 3.62 and 3.65 (1H, br s), 2.82 (1H, m), 2.26 (1H, m), 2.04 (1H, m), 1.57-1.84 (2H, m), 1.45 (3H, d, J = 7.1 Hz), 1.41 (9H, s), 1.30-1.57 (2H, m), 0.86 and 0.87 (9H, s), 0.05 (3H, s), 0.02 (3H, s); ¹³C-nmr (CDCl₃), mixture of two rotamers, δ -5.12 and -5.00, -4.90 and -4.73, 16.83, 18.05 and 18.10, 25.48, 25.77 and 25.86, 26.70 and 26.90, 28.38, 29.78 and 30.36, 44.71 and 45.20, 52.18 and 52.28, 56.26 and 57.00, 57.96 and 59.29, 68.51 and 68.78, 68.88 and 68.96, 78.47 and 78.80, 152.63 and 153.17, 170.95 and 171.08, 173.89 and 173.96; mass spectrum m/z (rel %): 398 (M⁺ - OtBu, 3.1), 370 (6.6), 358 (31), 314 (85), 83 (49), 73 (49), 57 (100). *Exact Mass* calcd. for C₁₉H₃₂O₆NSi (M⁺ - OtBu): 398.1999; found: 398.2018.

8-(*tert*-Butoxycarbonyl)-2-*exo*-[(*tert*-butyl-dimethylsilyl)oxy]-8-azabicyclo[3.2.1]octane-6-*exo*-carboxylic acid (189). Potassium hydroxide (2.43 g, 43.3 mmol) in H₂O (30 mL) was added to a solution of crude **188** from the previous procedure in

CH₃OH (60 mL), and the resulting mixture was stirred at room temperature for 15 hours. Most of the CH₃OH was then evaporated. The resulting aqueous solution was adjusted to pH 3 by adding 7M H₃PO₄ then extracted with CHCl₃. The organic phase was dried (MgSO₄), filtered and evaporated to give the acid **189** as a colorless solid (1.05 g, 94.3% for the two steps): mp 131.5-133.5°C; [α]_D²³ +1.4 (c 1.0, CHCl₃); IR (CH₂Cl₂): 1713, 1695, 1643 cm⁻¹; ¹H-nmr (CDCl₃), mixture of two rotamers, δ 11.29 (1H, br s), 4.44 and 4.63 (1H, br s), 4.18 and 4.26 (1H, m), 3.60 (1H, s), 2.74 (1H, m), 2.23 (1H, m), 2.01 (1H, m), 1.55-1.68 (2H, m), 1.37 (9H, s), 1.32-1.60 (2H, m), 0.84 (9H, s), 0.02 (3H, s), -0.01 (3H, s); ¹³C-nmr (CDCl₃), mixture of two rotamers, δ -5.08 and -4.94, -4.86 and -4.78, 18.08, 25.35, 25.85, 26.62 and 26.90, 28.40, 29.94 and 30.04, 44.77 and 45.35, 56.94 and 57.18, 58.10 and 59.55, 68.77 and 68.91, 78.84 and 79.84, 153.06 and 154.37, 177.94 and 179.85; mass spectrum m/z (rel %): 312 (M⁺ - OtBu, 2.6), 272 (28), 228 (100), 210 (48), 114 (48), 108 (46), 82 (45), 75 (69), 73 (64), 69 (49), 57 (80). *Exact Mass* calcd. for C₁₅H₂₆O₄NSi (M⁺ - OtBu): 312.1631; found: 312.1642. Anal. Calcd for C₉H₃₅O₅NSi: C, 59.19; H, 9.15; N, 3.63. Found: C, 59.1; H, 9.31; N, 3.60.

6-*exo*-Aceto-8-(*tert*-butoxycarbonyl)-2-*exo*-[(*tert*-butyl-dimethylsilyl)oxy]-8-azabicyclo[3.2.1]octane (191). Oxalyl chloride (0.71 mL, 8 mmol) was added to a solution of acid **13** (1.05 g, 2.72 mmol) and a catalytic amount of DMF (5 drops) in benzene (40 mL), and the resulting solution was stirred for 2 h, and then evaporated to dryness. A solution of Me₂CuLi (11.6 mmol) in Et₂O/THF (1:4.9, 48.3 mL) was cannulated into the solution of the crude acid chloride in THF (30 mL) at -78°C under nitrogen. After stirring at -78°C for 15 min, the reaction mixture was quenched by addition of methanol (15 mL) and allowed to warm to room temperature. The reaction

mixture was poured into 0.5 M KOH (40 mL) and extracted with CHCl₃. The organic phase was dried (MgSO₄), filtered and evaporated to leave the ketone **191** as a light yellow oil (0.851 g, 81.5%): [α]_D²³ +16.2 (c 0.79, CHCl₃); IR (CH₂Cl₂): 1713, 1691 cm⁻¹; ¹H-nmr (CDCl₃), mixture of two rotamers, δ 4.36 and 4.52 (1H, s), 4.21 and 4.30 (1H, m), 3.65 and 3.68 (1H, s), 2.84 (1H, m), 2.32 and 2.17 (1H, m), 2.15 and 2.20 (3H, s), 2.13 (1H, m), 1.64-1.82 (2H, m), 1.50-1.64 (2H, m), 1.43 (9H, s), 0.88 and 0.89 (9H, s), 0.07 (3H, s), 0.05 (3H, s); ¹³C-nmr (CDCl₃), mixture of two rotamers, δ -5.08 and -4.95, -4.85 and -4.73, 18.12, 25.47, 25.79 and 25.87, 26.88 and 27.11, 27.30 and 27.87, 28.12, 28.37 and 28.52, 52.94 and 53.70, 55.50 and 55.90, 58.14 and 59.57, 68.77 and 68.95, 78.72 and 79.16, 152.61 and 153.78, 207.45 and 207.60; mass spectrum m/z (rel %): 310 (M⁺ - OtBu, 0.4), 270 (21), 226 (69), 73 (66), 57 (100). *Exact Mass* calcd. for C₁₆H₂₃O₃NSi (M⁺ - OtBu): 310.1838; found: 310.1846.

6-*exo*-Acetyl-8-(*tert*-butoxycarbonyl)-2-*exo*-[(*tert*-butyl-dimethylsilyl)oxy]-8-azabicyclo[3.2.1]octane (192). To a solution of ketone **191** (0.658 g, 1.71 mmol) was added *m*-chloroperbenzoic acid (1.044 g, 6.05 mmol) in 1:2 benzene/chloroform (60 mL). After stirring for 7 days the solution was washed with 5% sodium bicarbonate (2 x 20 mL) to remove *m*-chlorobenzoic acid, back extracting with CHCl₃. The organic phase was dried (MgSO₄), filtered, and further *m*-chloroperbenzoic acid (0.406 g, 2.36 mmol) added. Stirring was continued for another two days. The reaction mixture was washed with aqueous NaHCO₃ (5%), then with aqueous Na₂SO₃ (10%) to destroy the excess peracid, and again with aqueous NaHCO₃ (5%). The organic phase was dried (MgSO₄), filtered and evaporated to give the crude acetate **192** as a light yellow oil (0.672 g, 98.0%). Column chromatography using 15% EtOAc in hexane gave a colorless oil (0.35 g,

52.0%): $[\alpha]_D^{23}$ -14.9 (c 0.74, CHCl_3); IR (CH_2Cl_2): 1734, 1692 cm^{-1} ; ^1H -nmr (CDCl_3), mixture of two rotamers, δ 5.03 (1H, m), 4.25 and 4.33 (1H, m), 4.07 and 4.29 (1H, s), 3.61 and 3.64 (1H, m), 1.95-2.12 (2H, m), 2.02 and 2.03 (3H, s), 1.85 (1H, m), 1.59 (1H, m), 1.38-1.56 (2H, m), 1.45 and 1.47 (9H, s), 0.88 and 0.89 (9H, s), 0.07 and 0.08 (3H, s), 0.04 (3H, s); ^{13}C -nmr (CDCl_3), mixture of two rotamers, δ -5.08 and -4.96, -4.87 and -4.64, 18.11 and 18.18, 21.14 and 21.18, 23.89 and 23.91, 25.54 and 25.59, 25.80 and 25.93, 28.46 and 28.54, 34.90 and 35.76, 57.98 and 58.47, 59.18 and 59.79, 68.65 and 68.80, 76.31 and 77.22, 78.68 and 79.11, 153.45 and 154.05, 170.91 and 170.93; mass spectrum m/z (rel %): 326 (M^+ - OtBu, 3.1), 286 (40), 242 (95), 182 (63), 75 (77), 73 (78), 57 (100). *Exact Mass* calcd. for $\text{C}_{16}\text{H}_{28}\text{O}_4\text{NSi}$ (M^+ - OtBu): 326.1788; found: 326.1797.

BAO GONG TENG A [(-)1]. The pure acetate **192** (35.7 mg, 0.089 mmol) was stirred in a solution of 1% HCl in EtOH (5 mL) for 2 h. The EtOH was evaporated by rotary evaporation at 70°C, dissolved in CHCl_3 and washed with aqueous K_3PO_4 (2M). The organic phase was filtered through a filter paper to remove H_2O and evaporated to yield Bao Gong Teng A (10.1 mg, 61.3%): $[\alpha]_D^{23}$ -7.5 (c 0.34, H_2O) [Lit.¹⁵ -7.2° (c 0.97, H_2O)]; IR (CH_2Cl_2): 1732, 1623 cm^{-1} ; ^1H -nmr (CDCl_3) δ 5.12 (1H, dd, $J = 6.9, 2.1$ Hz), 3.54 (1H, br s), 3.52 (1H, s br), 3.28 (1H, br s), 2.16 (1H, dd, $J = 14.7, 6.9$ Hz), 2.05-2.14 (2H, exchangeable, br s), 2.04 (3H, s), 1.70-1.94 (2H, m), 1.44-1.63 (3H, m) (Lit¹); ^{13}C -nmr (CDCl_3), δ 21.26, 24.78, 25.02, 37.24, 60.57, 61.10, 67.47, 78.10, 170.73; mass spectrum m/z (rel %): 185 (M^+ , 7.0), 149 (52), 142 (18), 126 (48), 99 (76), 82 (68), 81 (45), 80 (100), 68 (47). *Exact Mass* calcd. for $\text{C}_9\text{H}_{15}\text{O}_3\text{N}$: 185.1052; found: 185.1037.

8-(*tert*-butoxycarbonyl)-2-*exo*-[(*tert*-butyl-dimethylsilyl)oxy]-8-azabicyclo[3.2.1]octane (189). N-methyl morpholine (0.12 mL, 1.1 mmol) and isobutyl chloroformate (0.14 mL, 1.1 mmol) were added to a solution of acid **189** (405 mg, 1.0 mmol) in THF (10 mL) with stirring, under nitrogen atmosphere at -20°C. After stirring for 20 min, a solution of N-hydroxy-2-thiopyridone (224 mg, 1.77 mmol) and Et₃N (0.18 mL, 1.3 mmol) was added. The resulting mixture was stirred for 1 h and then the solid filtered off. *t*-Butyl mercaptan (0.12 mL, 1.1 mmol) was added to the filtrate, the mixture was degassed with nitrogen and irradiated with a 450 watt Hanovia medium pressure quartz UV lamp (Pyrex filter) for 20 min. The THF solution was diluted with Et₂O (100 mL) and washed with aqueous KOH (1 M), H₂O, and dilute HCl (5%). The organic layer was separated, dried (MgSO₄) and evaporated to leave a yellow oil (286 mg). This yellow oil (55.6 mg) and *m*-CPBA (100 mg, 0.5 mmol) were stirred in CHCl₃ (3 mL) for 3 min. The solution was diluted with EtOAc and washed with aqueous KOH (1 M). The organic layer was dried (MgSO₄), filtered and evaporated to give an oil. The oil was chromatographed on silica gel using 10% EtOAc in hexane to provide **200** (44 mg, 63% from the acid **183**) as a clear oil: $[\alpha]_D^{23} +0.8$ (c 2.0, CHCl₃); IR (CH₂Cl₂) 1686 cm⁻¹; ¹H-nmr (CDCl₃), mixture of two rotamers, δ 4.35 and 4.12 (1H, br s), 4.15 and 4.12 (1H, br s), 3.61 (1H, br s), 2.05 (1H, m), 1.84 (3H, m), 1.53 (3H, m), 1.44 (9H, s), 1.25 (1H, m), 0.89 (9H, s), 0.07 (3H, s), 0.04 (3H, s); ¹³C-nmr (CDCl₃), mixture of two rotamers, δ -5.0 and -4.5, -4.6 and -4.9, 18.1, 25.5 and 25.4, 25.9₄ and 25.8₆, 26.3, 27.1 and 26.9, 27.1, 28.5, 53.1 and 52.0, 58.9 and 57.7, 69.9 and 69.5, 78.6 and 78.1, 153.8 and 152.9; mass spectrum *m/z* (relative intensity) 268 (M⁺ - OtBu, 4), 240 (10), 229 (14), 228 (82), 57 (100). *Exact Mass* calcd. for C₁₄H₂₆O₂SiN (M⁺ - OtBu) 268.1733 found 268.1722.

REFERENCES

1. a) B. Testa, "Drug Metabolism" in *Burger's Medicinal Chemistry and Drug Discovery*, 1995, Vol 1, p 129-180, Ed 5th. John Wiley & Sons, Inc. and references therein.
b) S. C. Stinson, *Chemical & Engineering News*, 1992, September 28, 46.
2. J. L. Charlton, G. L. Plourde, K. Koh, and A. S. Secco, *Can. J. Chem.*, 1989, 67, 574 and references therein.
3. a) M. J. Jorgenson, *J. C. S., Chem. Comm.*, 1965, 137.
b) N. C. Yang and M. J. Jorgenson, *Tetrahedron Lett.*, 1964, 1203.
4. R. R. Rando and W. von E. Doering, *J. Org. Chem.*, 1968, 33, 1671.
5. M. Tada and K. Miura, *Bull. Chem. Soc. Jpn.*, 1976, 49, 713.
6. R. Ricard, P. Sauvage, C. S. K. Wan, A. C. Weedon, and D. F. Wong, *J. Org. Chem.*, 1986, 51, 62 and references therein.
7. M. Marjerrison and A. C. Weedon, *J. Photochem.*, 1986, 33, 113.
8. R. M. Duhaime and A. C. Weedon, *Can. J. Chem.*, 1987, 65, 1867.
9. C. S.K. Wan, A. C. Weedon, D. F. Wong, *J. Org. Chem.*, 1986, 51, 3335.
10. A. Weedon and D. F. Wong, *J. Photochem.*, 1987, 38, 289.
11. F. Henin, R. Mortezaei, J. Muzart and J. P. Pete, *Tetrahedron Lett.*, 1985, 26, 4945.
12. R. Mortezaei, F. Henin, J. Muzart and J. P. Pete, *Tetrahedron Lett.*, 1985, 26, 6079.

13. R. Mortezaei, O. Piva, F. Henin, J. Muzart and J. P. Pete, *Tetrahedron Lett.*, **1986**, *27*, 2997.
14. O. Piva, F. Henin, J. Muzart and J. P. Pete, *Tetrahedron Lett.*, **1986**, *27*, 3001.
15. J. P. Pete, F. Henin, R. Mortezaei, J. Muzart and O. Piva, *Pure & Appl. Chem.*, **1986**, *58*, 1257.
16. R. M. Duhaime and A. C. Weedon, *J. Am. Chem. Soc.*, **1985**, *107*, 6723.
17. T. Gramstad, *Acta Chemica Scandinavica*, **1962**, *16*, 807.
18. O. Piva, F. Henin, J. Muzart and J. P. Pete, *Tetrahedron Lett.*, **1987**, *28*, 4825.
19. O. Piva and J. P. Pete, *Tetrahedron Lett.*, **1990**, *31*, 5157.
20. R. Mortezaei, D. Awandi, F. Henin, J. Muzart and J. P. Pete, *J. Am. Chem. Soc.*, **1988**, *110*, 4824.
21. D. Awandi, F. Henin, J. Muzart and J. P. Pete, *Tetrahedron Asymmetry*, **1991**, *2*, 1101.
22. O. Piva and J. P. Pete, *Tetrahedron Asymmetry*, **1992**, *3*, 759.
23. O. Piva, *J. Org. Chem.*, **1995**, *60*, 7879 and references therein.
24. O. Diels and K. Alder, *Liebigs. Ann. Chem.*, **1928**, *460*, 98.
25. a) J. March, *Advanced Organic Chemistry*, **1992**, p 839-847, Ed 4th. Wiley-Interscience.
b) F. A. Carey and R. J. Sunberg. *Advanced Organic Chemistry.*, **1990**. Ed 4th. Part B: Reaction and Synthesis. Plenum Press, New York.
c) F. Fringuelli and Taticchi. *Dienes in the Diels-Alder reaction.*, **1990**. Wiley-Interscience, New York.

26. T. Poll, G. Helmchen and B. Bauer, *Tetrahedron Lett.*, **1984**, *25*, 2191.
27. H. Hartmann, A. Fattah, A. Hady, K. Sartor, J. Weetman and G. Helmchen, *Angew. Chem. Int. Ed. Engl.*, **1987**, *26*, 1143 and references therein.
28. Y. Arai and T. Koizumi, *Sulfur Reports.*, **1993**, *15*, 41 and references therein.
29. I. Alonso, J. Carretero and J. L. G. Ruano, *J. Org. Chem.*, **1994**, *59*, 1499 and references therein.
30. W. F. Whitmore and E. F. Landau, *J. Am. Chem. Soc.*, **1946**, *68*, 1797.
31. H. Distler, *Angew. Chem. Int. Ed. Engl.*, **1965**, *4*, 300.
32. J. Morris and D. Whishka, *J. Org. Chem.*, **1991**, *56*, 3549.
33. C. S. Marvel and M. S. Sparberg, *Organic Syntheses*, Coll. Vol. II, p 558, John Wiley and Sons, Inc., New York, N. Y.
34. C. S. Marvel, C. F. Bailey and M. S. Sparberg, *Am. Chem. J.*, **1927**, *49*, 1833.
35. A. A. Goldberg, *J. Chem. Soc.*, **1945**, 464.
36. C. S. Rondestvedt, Jr., *J. Am. Chem. Soc.*, **1954**, *76*, 1926.
37. A. A. Lambert and J. D. Rose, *J. Chem. Soc.*, **1949**, 46.
38. C. S. Rondestvedt and J. Wygant, *J. Am. Chem. Soc.*, **1951**, *73*, 5785.
39. H. Kotsiki, K. Asao and H. Ohnishi, *Bull. Chem. Soc. Jpn.*, **1984**, *57*, 3339.
40. T. M. Balthazor, B. Gaede, D. E. Korte and H. S. Shieh, *J. Org. Chem.*, **1984**, *49*, 4547.
41. W. G. Dauben and H. O. Krabbenhoft, *J. Am. Chem. Soc.*, **1976**, *98*, 1992.
42. L. L. Klein and T. M. Deeb, *Tetrahedron Lett.*, **1985**, *26*, 3935.
43. E. Bovenschulte, P. Metz and G. Henkel, *Angew. Chem. Int. Ed. Engl.*, **1989**, *28*, 202.

44. P. Metz, M. Fleischer and R. Frohlich, *Tetrahedron*, **1995**, *51*, 711.
45. P. Metz and E. Cramer, *Tetrahedron Lett.*, **1993**, *34*, 6371.
46. P. Metz and B. Plietker, *Tetrahedron Lett.*, **1996**, *37*, 3841.
47. R. Huisgen, "10 Jahre Fonds der Chemischen Industrie," Dusseldorf, **1960**, p. 73; reprinted in *Naturwiss. Rundschau*, **1961**, *14*, 63.
48. R. Huisgen, Centenary Lecture, London, December 8, 1960; *Proc. Chem. Soc.*, **1961**, 357.
49. A. Padwa, "1,3-Dipolar Cycloaddition Chemistry", **1983**, p. 1-176 and 653-732, Wiley-Interscience Publication.
50. a) D. P. Curran, B. H. Kim, H. P. Piyasena, R. J. Loncharich, and K. N. Houk, *J. Org. Chem.*, **1987**, *52*, 2137.
b) D. P. Curran, B. H. Kim, J. Daugherty and T. A. Heffner, *Tetrahedron Lett.*, **1988**, *29*, 3555.
c) T. Olsson, K. Stern and S. Sundell, *J. Org. Chem.*, **1988**, *53*, 2468.
d) D. P. Curran and S. A. Gothe, *Tetrahedron*, **1988**, *44*, 3945.
e) A. Brandi and P. Cannavo, *J. Org. Chem.*, **1989**, *54*, 3073.
f) S. Kanemasa, K. Onimura, E. Wada and J. Tanaka, *Tetrahedron Asymmetry*, **1991**, *2*, 1185.
g) W. Oppolzer, A. J. Kingma and S. K. Pillai, *Tetrahedron Lett.*, **1991**, *32*, 4893.
h) T. Akiyama, K. Okada and S. Ozaki, *Tetrahedron Lett.*, **1992**, *33*, 5763.
i) G. Negron, G. Roussi and J. Zhang, *Heterocycles*, **1992**, *34*, 293.

- j) J. A. Stack, T. A. Heffner, S. J. Geib and D. P. Curran, *Tetrahedron*, **1993**, *49*, 995.
51. A. R. Katritzky and N. Dennis, *Chem. Rev.*, **1989**, *88*, 827.
52. S. L. Shapiro, K. Weinberg and L. Freedman, *J. Am. Chem. Soc.*, **1959**, *81*, 5140.
53. N. Dennis, A. R. Katritzky and H. Wilde, *J. C. S. Perkin I*, **1976**, 2338.
54. A. R. Katritzky, S. I. Bayyuk, N. Dennis and G. Musumarra, *J. C. S. Perkin I*, **1979**, 2535.
55. N. Dennis, B. Ibrahim and A. R. Katritzky, *J. C. S. Chem. Comm.*, **1974**, 500.
56. N. Dennis, B. Ibrahim and A. R. Katritzky, *J. C. S. Perkin I*, **1976**, 2307.
57. A. R. Katritzky, N. Dennis, M. Chaillet, C. Larrieu and M. E. Mouhtadi, *J. C. S. Perkin I*, **1979**, 408
58. A. R. Katritzky, A. T. Cutler, N. Dennis, G. J. Sabongi, S. Rahimi-Rastgoo, G. W. Fisher and I. J. Fletcher, *J. C. S. Perkin I*, **1980**, 1176.
59. C. Y. Ishag, K. J. Fisher, B. Ibrahim, G. M. Iskander and A. R. Katritzky, *J. Chem. Soc. Perkin Trans. I*, **1988**, 917.
60. A. R. Katritzky, Y. Takeuchi, *J. C. S. Perkin I*, **1971**, 874.
61. N. Dennis, A. R. Katritzky, T. Matsuo and S. K. Parton, *J. C. S. Perkin I*, **1974**, 746.
62. N. Dennis, A. R. Katritzky and S. K. Parton, *J. C. S. Perkin I*, **1976**, 2285.
63. N. Dennis, A. R. Katritzky, S. K. Parton, Y. Nomura, Y. Takahashi and Y. Takeuchi, *J. C. S. Perkin I*, **1974**, 746.
64. J. Banerji, N. Dennis, J. Frank, A. R. Katritzky and T. Matsuo, *J. C. S. Perkin I*, **1976**, 2334.

65. N. Dennis, A. R. Katritzky and Y. Takeuchi, *Angew. Chem. Int. Ed. Engl.*, **1976**, *15*, 1.
66. a) R. Susrman, *Tetrahedron Lett.*, **1971**, 2717.
b) K. N. Houk, *Acc. Chem. Res.*, **1975**, *8*, 361.
c) K. N. Houk, J. Sims, R. E. Duke, R. W. Strozier and J. K. George, *J. Am. Chem. Soc.*, **1973**, *95*, 7287.
d) K. N. Houk, J. Sims, C. R. Watts and L. J. Luskus, *J. Am. Chem. Soc.*, **1973**, *95*, 7301.
67. M. Lounasmaa, "*The alkaloids: Chemistry and Physiology*", **1988**, *33*, p 1-81, Academic Press, Inc.
68. A. Yu, C. Sun, *Zhonggao Yaoli Xuebao*, **1990**, *11*, 394; *Chem. Abstr.* **1990**, *113*, 224464u.
69. M. E. Jung, Z. Longmei, P. Tangsheng, Z. Huiyan, L. Yan and S. Jingyu, *J. Org. Chem.*, **1992**, *57*, 3528.
70. P. Wang, T. Yao, Z. Chen, *Huaxue Xuebao*, **1989**, *47*, 1002; *Chem. Abstr.* **1990**, *113*, 78746u.
71. Bao Gong Teng cooperative research group, *Zhongcaoyao*, **1982**, *13*, 20.
72. T. Takahashi, A. Fujii, J. Sugita, T. Hagi, K. Kitano, Y. Arai and T. Koizumi, *Tetrahedron Asymmetry*, **1991**, *2*, 1379.
73. a) J. L. Charlton, V. C. Pham and J. P. Pete, *Tetrahedron Lett.*, **1992**, *33*, 6073.
b) J. L. Charlton, unpublished results.

74. L. Chee, Ph. D. Thesis, University of Manitoba, 1997.
75. E. F. Landau, *J. Am. Chem. Soc.*, 1947, 69, 1219.
76. E. Lippmaa, T. Pehk, J. Paasivirta, N. Belikova and A. Plate, *Org. Mag. Reson.*, 1970, 2, 581 and references therein.
77. J. C. Davis and T. V. Van Auken, *J. Am. Chem. Soc.*, 1965, 87, 3900.
78. J. Fisher and M.J. Gradwell, *Mag. Reson. Chem.*, 1991, 29, 1068.
79. H. C. Brown and R. F. McFarlin, *J. Am. Chem. Soc.*, 1956, 78, 252.
80. H. C. Brown and R. F. McFarlin, *J. Am. Chem. Soc.*, 1958, 80, 5372.
81. H. C. Brown and H. M. Hess, *J. Org. Chem.*, 1969, 34, 2206.
82. A. P. Gledhill, C. J. McCall and M. M. Threadgill, *J. Org. Chem.*, 1986, 51, 3196.
83. H. Ishibashi, C. Kameola, H. Iriyama, K. Kodama, T. Sato and M. Ikeda, *J. Org. Chem.*, 1995, 60, 1276.
84. E. J. Corey and J. Casanova, Jr., *J. Am. Chem. Soc.*, 1963, 85, 165.
85. E. J. Corey, J. Casanova, Jr., P. A. Vatakencherry and R. Winter, *J. Am. Chem. Soc.*, 1963, 85, 169.
86. R. C. Corcoran and J. M. Green, *Tetrahedron Lett.*, 1990, 31, 6827.
87. J. D. Albright and L. Goldman, *J. Am. Chem. Soc.*, 1967, 2023.
88. R. Levine and M. Karten, *J. Org. Chem.*, 1976, 41, 1176.
89. C. Tegner, *Acta Chemica Scandinavica*, 1952, 6, 782.
90. Y. Ahn and T. Cohen, *Tetrahedron Lett.*, 1994, 35, 203.
91. E. J. Corey and G. Schmidt, *Tetrahedron Lett.*, 1979, 5, 399.
92. M. Marx and T. T. Tidwell, *J. Org. Chem.*, 1984, 49, 788.

93. F. J. Sardina, M. H. Howard, M. Morningstar and H. Rapoport, *J. Org. Chem.*, **1990**, *55*, 5025.
94. J. S. Petersen, G. Fels and H. Rapoport, *J. Am. Chem. Soc.*, **1984**, *106*, 4539.
95. F. J. Sardina, M. H. Howard, A. M. P. Koskinen and H. Rapoport, *J. Org. Chem.*, **1989**, *54*, 4654.
96. G. H. Posner and C. E. Whitten, *Tetrahedron Lett.*, **1970**, *53*, 4647.
97. D. D. Perrin and W. L. F. Armarego, *Purification of Laboratory Chemicals*, **1988**, p 322, Ed 3rd. Pergamon Press, New York.
98. R. K. Dieter, L. A. III.; Silks, J. R. Fishpauch, M. E. Kasner, *J. Am. Chem. Soc.*, **1985**, *107*, 4679.
99. A. P. Kozikowki, G. L. Araldi and R. G. Ball, *J. Org. Chem.*, **1997**, *62*, 503.
100. A. S. Hernandez, A. Thaler, J. Castells and H. Rapoport, *J. Org. Chem.*, **1996**, *61*, 314.
101. J. H. Rigby and F. C. Pigge, *J. Org. Chem.*, **1995**, *60*, 7392.
102. H. M. Davies, E. Saikali and W. B. Young, *J. Org. Chem.*, **1991**, *56*, 5696.
103. D. H. R. Barton, Y. Herve, P. Potier and J. Thierry, *Tetrahedron*, **1988**, *44*, 5479.
104. D. H. R. Barton, D. Crich and W. B. Motherwell, *Tetrahedron*, **1985**, *41*, 3901.
105. D. H. R. Barton, D. Crich and W. B. Motherwell, *J. C. S., Chem. Commun.*, **1983**, 939.
106. K. Marat, Xsim, **1995**. Using numeric algorithm from J. S. Martin and A. J. Quirt, *J. Mag. Reson.*, **1971**, 318. Modified by R. Sabastian, **1993**.
107. (Methyl (*S*-lactyl) (*S*)-2,4-dimethylpent-2-enoate was prepared by J. Charlton, Chemistry Department, University of Manitoba, Winnipeg, Canada.



VP371817.001
AU PROG:
IFZ6.AU
DATE 6-12-95

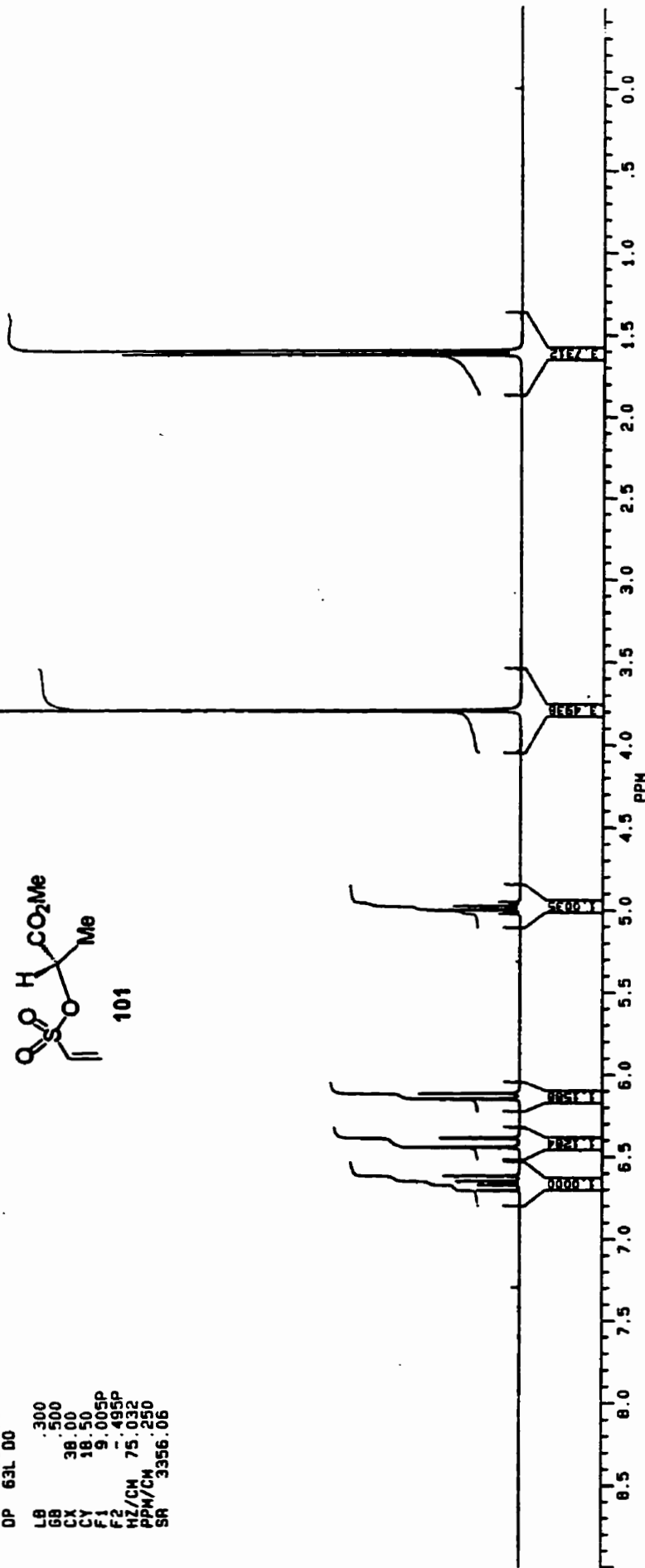
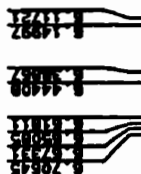
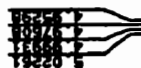
SF 300.133
SY 100.0
O1 5500.000
SI 32768
TD 32768
SM 5494.505
HZ/PT .335

PH 8.0
RD 4.000
AQ 2.982
RG 4
NS 32
TE 300

FW 6900
O2 20000.000
DP 63L D0

LB .300
GB .500
CX 38.00
CY 18.50
F1 9.005P
F2 -495P
HZ/CM 75.032
PPM/CM 250
SR 3356.06

SAMPLE VP3-71-817 1-H AT 300 MHZ IN CDCL3





VP3817C.004
AU PROG:
AUTOC13.AU
DATE 6-12-95

SF 75.469
SY 112.0500000
O1 47000.000
SI 32768
TO 32768
SH 17857.143
HZ/PT 1.090

PW 5.0
RD 0.0
AQ 918
RG 200
MS 320
TE 300

FM 22400
O2 5000.000
DP 18H CPD

LB 1.000
GB 1.700
CX 38.00
CY 18.00
F1 223.355P
F2 2.640P
HZ/CM 452.802
PPM/CM 6.000
SR 38601.46

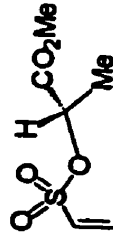
SAMPLE VP3-71-817 13-C AT 75.47 MHZ IN CDCL3

133.028
129.848

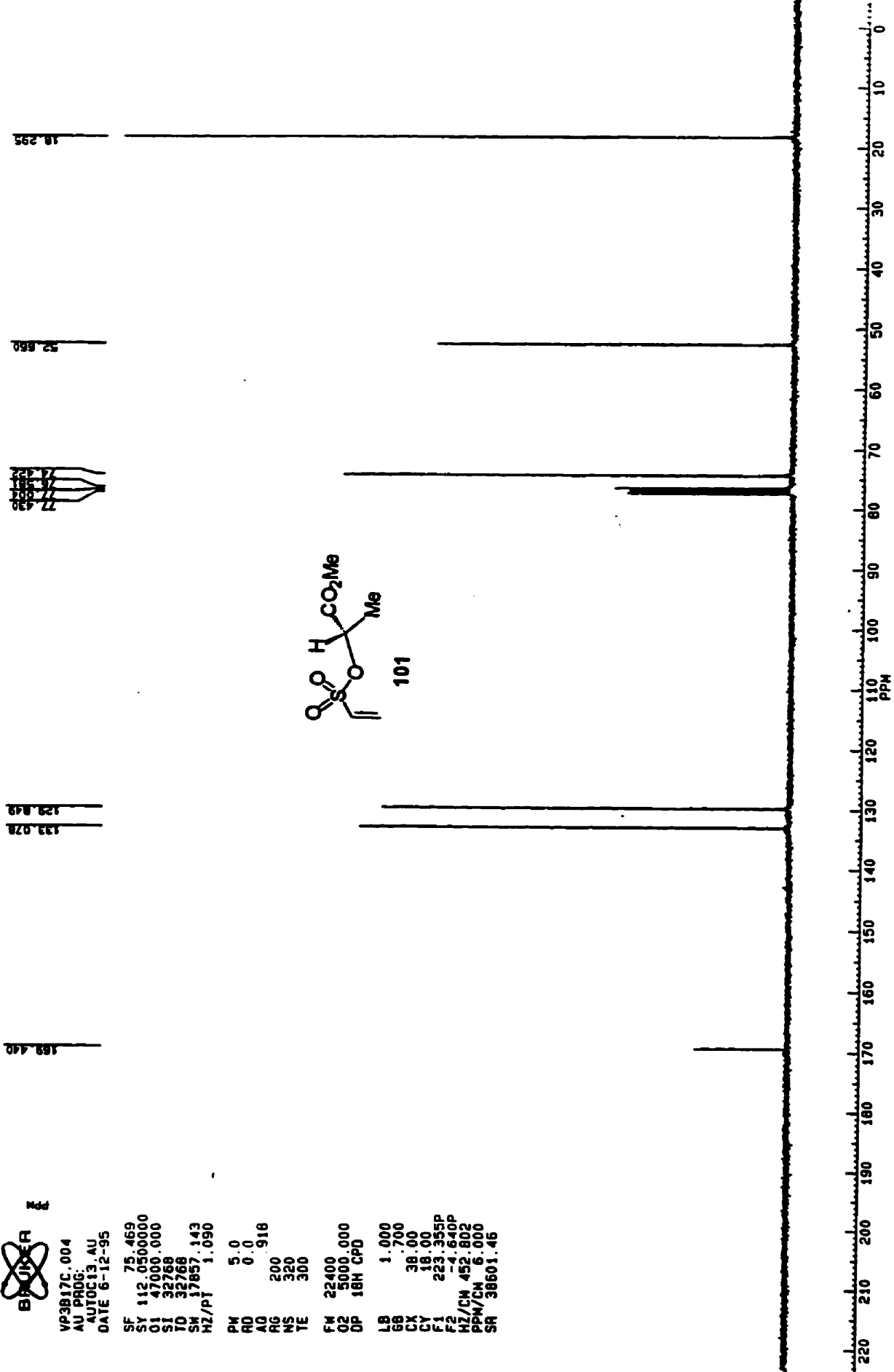
77.429
77.000
76.571

52.860

18.295



101



SAMPLE VP3-101C11 1-H AT 300 MHZ IN CDCL3

VP3C11.001
AU PROG.
TFZG.AU
DATE 2-2-96

SF 300.133
SY 100.0
Q1 5500.000
S1 32768
TD 32768
SM 5494.505
HZ/PT .335

PW 8.0
RD 4.000
AO 2.982
RG 8
NS 32
TE 300

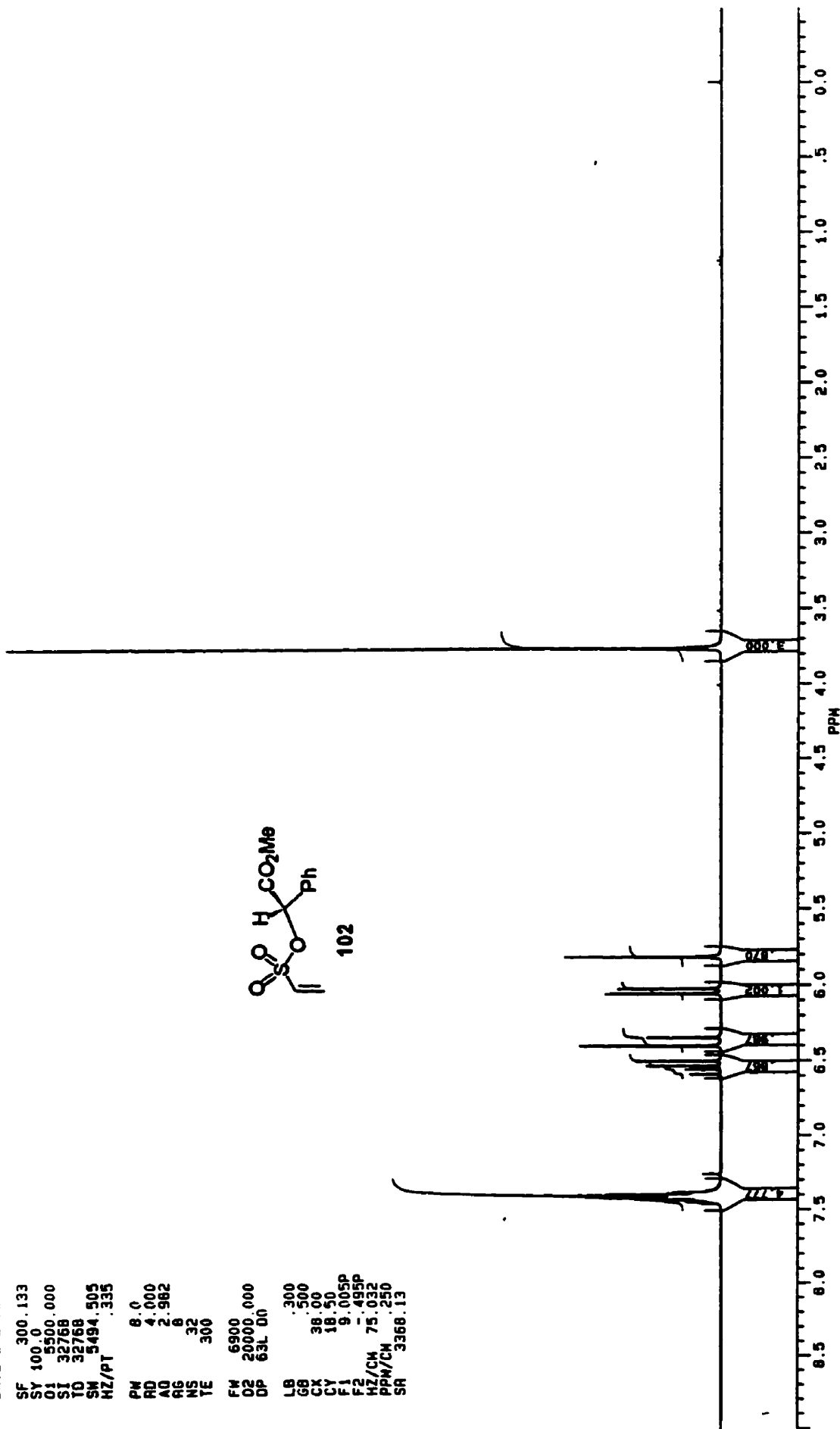
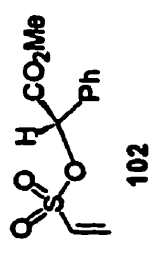
FW 6900
D2 20000.000
DP 63L 00

LB .300
GB .500
CA 38.00
CY 18.50
F1 9.005P
F2 - .495P
HZ/CM 75.032
PPM/CM 250
SR 3368.13

4.77
6.52
6.58
6.64
6.70
6.76
6.82
6.88
6.94
6.99

5.0288
5.40001
5.85457
5.88216
5.91349

3.76025





Model

VP3C11C.004
AU PROG.
AUTOC13 AU
DATE 5-2-96

SF 75.469
SY 112.0500000
O1 47000.000
SI 32768
TD 32768
SM 17857.143
HZ/PT 1.090

PW 5.0
RD 0.0
AU 200.918
RB 200
NS 320
TE 300

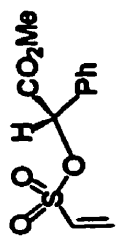
FW 22400
O2 5000.000
DP 18H CPD

LB 1.000
GB 1.700
CX 38.00
CY 18.00
F1 223.369P
F2 -4.626P
HZ/CN 452.802
PRM/CN 6.000
SR 38600.37

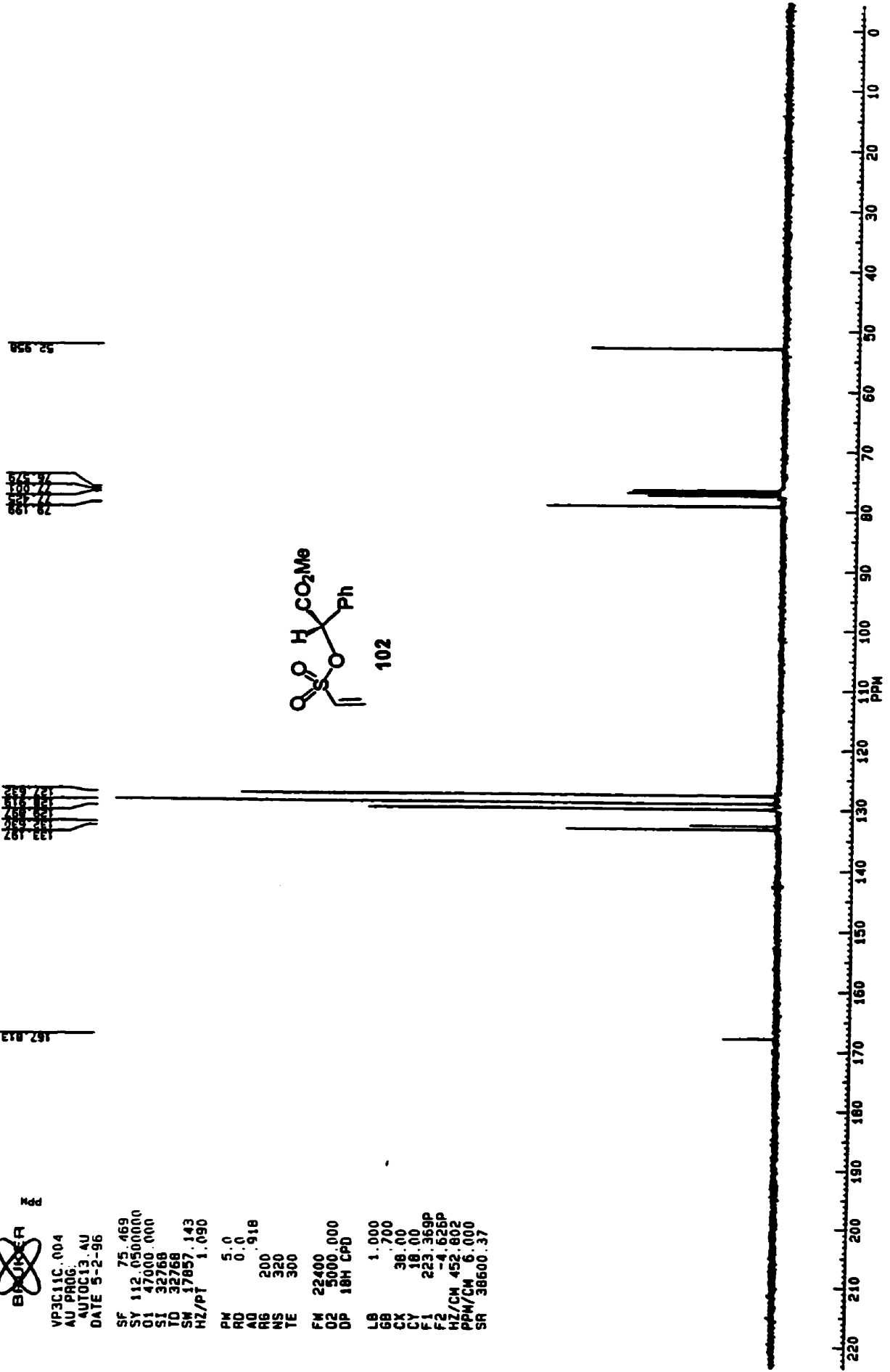
SAMPLE VP3-101C11 13-C AT 75.47 MHZ IN CDCL3

167.813

52.958



102



SAMPLE VP3-93A1 1-H AT 300 MHZ IN CDCL3



VP393A1.001
AU PROG:
TFZ6.AU
DATE 29-1-96

SF 300.133
SY 100.0
O1 5500.000
SI 32768
TD 32768
SW 3494.505
HZ/PT .335

PH 8.0
PD 4.000
AQ 2.982
RG 10
MS 32
TE 300

FW 6900
DZ 20000.000
OP 63L 00

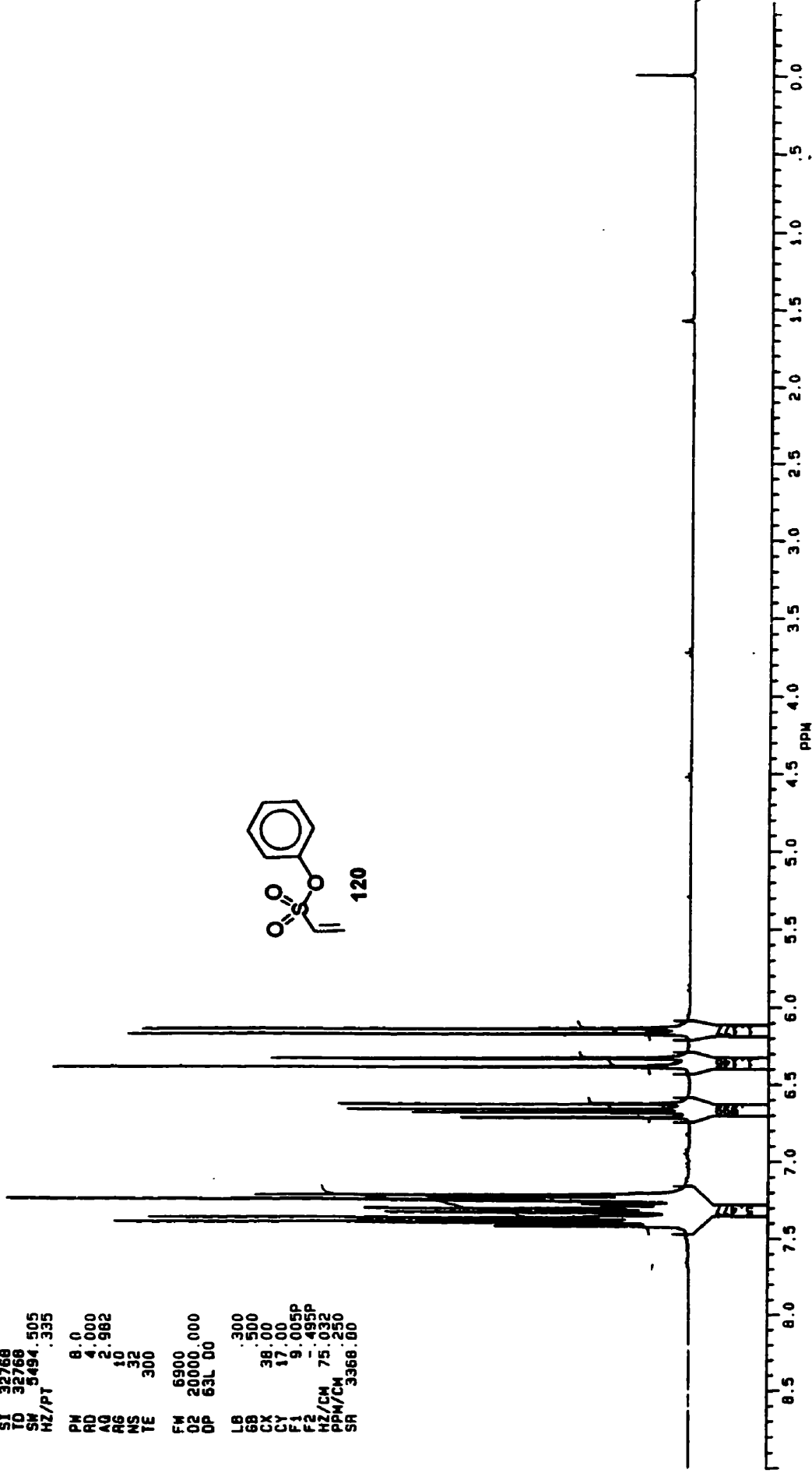
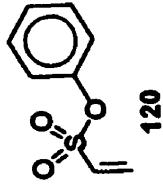
LB .300
GB .500
CX 36.00
CY 17.00
F1 9.005P
F2 .485P
HZ/CM 75.032
PRM/CM .250
SR 3366.00

7.494
7.494
7.494
7.494
7.494
7.494
7.494
7.494
7.494
7.494

6.62235

6.38908
6.32497

6.16634
6.16634



SAMPLE VP3-93A1 13-C AT 75.47 MHZ IN CDCL3

122.192
127.272
128.758
129.122
131.222

149.354



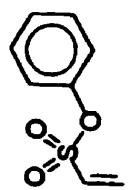
VP393A1C.004
AU PROG
AUTOC13 AU
DATE 29-1-96

SF 75.469
SY 112.0500000
O1 47000.000
SI 32768
TD 32768
SM 17857.143
HZ/PT 1.090

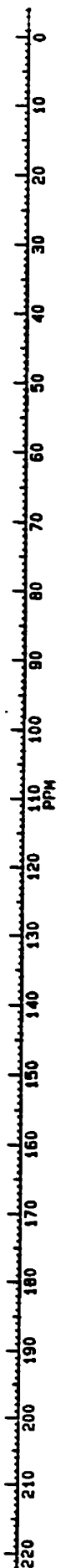
PM 5.0
RD 0.0
AQ 0.918
RG 200
NS 1280
TE 300

FM 22400
O2 5000.000
DP 18H CPD

LB 1.000
GB 0.700
CX 38.00
CY 18.00
F1 223.384P
F2 -4.611P
HZ/CH 452.802
PPM/CH 6.000
SR 38599.28



120



SAMPLE VP3-104-C6 1-H AT 300 MHZ IN CDCL3



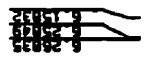
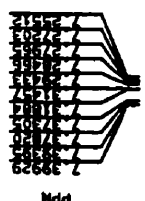
VP34C6.001
AU PRO6.
TFZG AU
DATE 13-2-96

SF 300.133
SY 100.0
O1 5500.000
SI 32768
TD 32768
SM 5494.505
HZ/PT .335

PM 8.0
RD 4.000
AD 2.982
RG 32
NS 32
TE 300

FM 6900
D2 20000.000
DP 63L D0

LB .300
GB .500
CX 38.00
CY 18.50
F1 9.005P
F2 - 495P
HZ/CM 75.032
PPM/CM .250
SR 3368.00

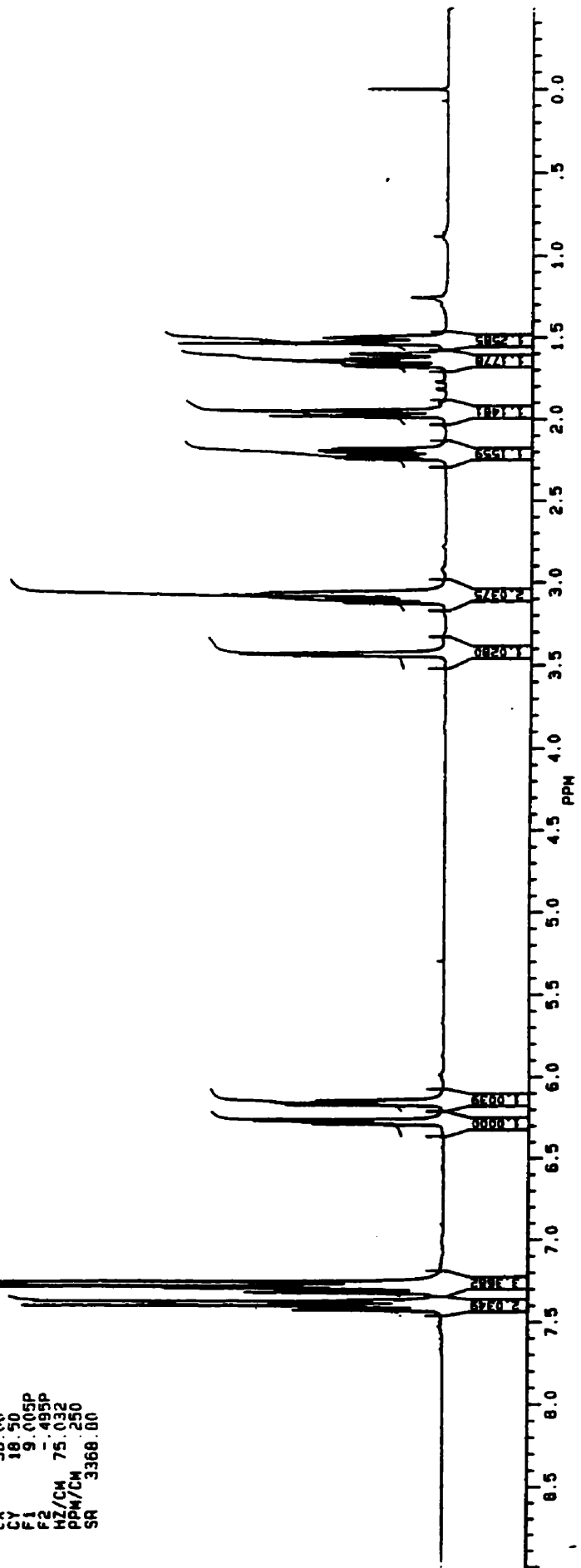
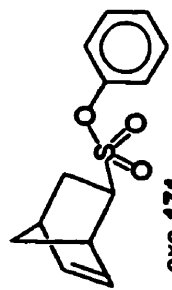


3.43037

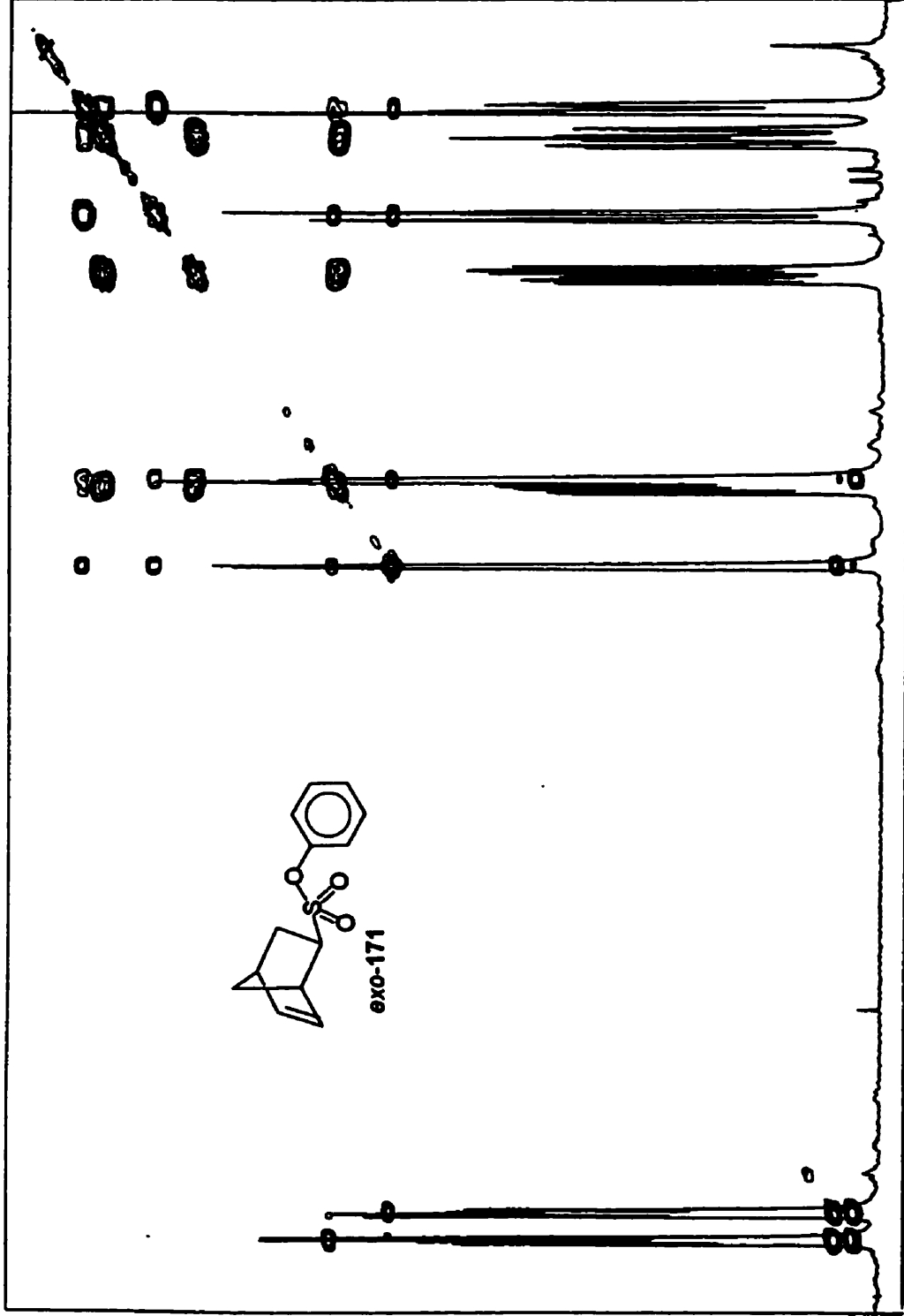
3.02650

1.92803
1.91755

1.59515



SAMPLE VP3-10406 COSY-45 300 MHZ IN CDCL3



~~BRUKER~~

VP3406H.SMX
AU 0906
COSY .AU
DATE 23-2-96

SI2 1024
SI1 512
SM2 2212.389
SM1 1106.195
ND0 1

WDW2 S
WDW1 S
SSB2 0
SSB1 0
MC2 M
PL1M ROW
F1 6.577P
F2 1.063P
AND COLUMN
F1 6.577P
F2 1.063P

D1 3.0000000
P1 10.50
D0 .0000030
P2 5.30
RD 0.0 0.0
RW 285.00
DE 24
NS 2
DS 256
NE .0004520
IN

6.50 6.00 5.50 5.00 4.50 4.00 3.50 3.00 2.50 2.00 1.50
PPM



VP34C6C.004
AU PROG.
AUTOC13.AU
DATE 22-2-96

SF 75.469
SY 112.0500000
O1 47000.000
SI 32768
TD 32768
SM 17857.143
HZ/PT 1.090

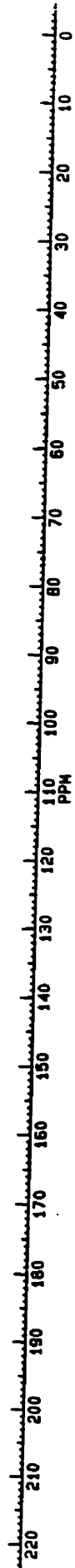
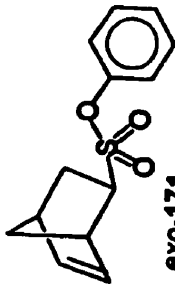
PW 5.0
RD 0.0
AQ 918
RG 200
NS 1408
TE 300

FW 22400
O2 5000.000
DP 18H CPD

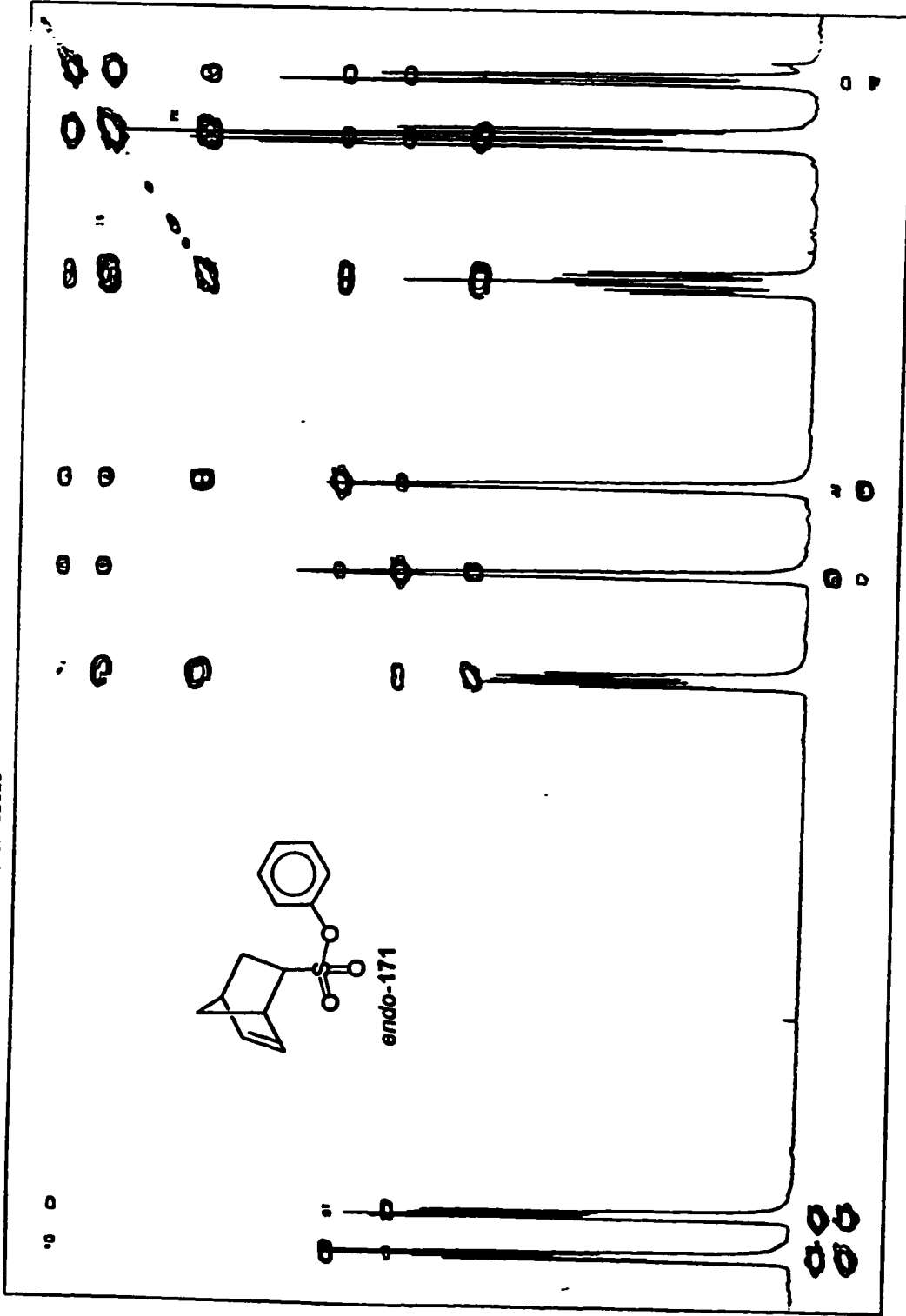
LB 1.000
GB 1.700
CX 38.00
CY 18.00
F1 223.427P
F2 -4.568P
HZ/CM 452.602
PPM/CM 6.000
SR 38596.01

SAMPLE VP3-10406 13-C AT 75.47 MHZ IN CDCL3

149.323
139.870
134.940
129.856
127.014
122.085
77.469
77.000
76.532
59.919
48.987
48.157
41.647
29.329



SAMPLE VP3-104C12 COSY-45 AT 300 MHZ IN CDCL3



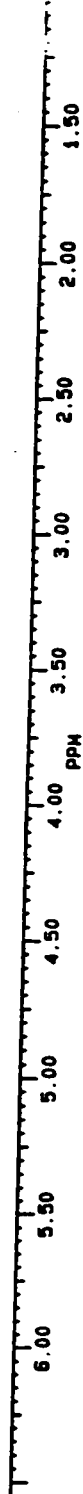
BPXJER

VP34C12H.SMX
AU PROG.
COSY.AU
DATE 23-2-96

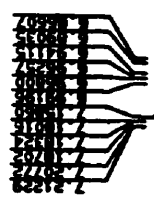
SI2 1024
SI1 512
SM2 2000.000
SM1 1000.000
NDO 1

MDH2 S
MDH1 S
SSB2 0
SSB1 0
MC2 0
MC1 M
PLTM ROW
F1 6.542P
F2 1.050P
AND COLUMN:
F1 6.542P
F2 1.050P

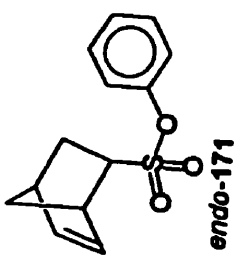
D1 3.000000
P1 10.50
D0 .0000030
P2 5.30
RD 0.0
PH 0.0
DE 215.00
NS 16
DS 2
ME 256
IN .0005000



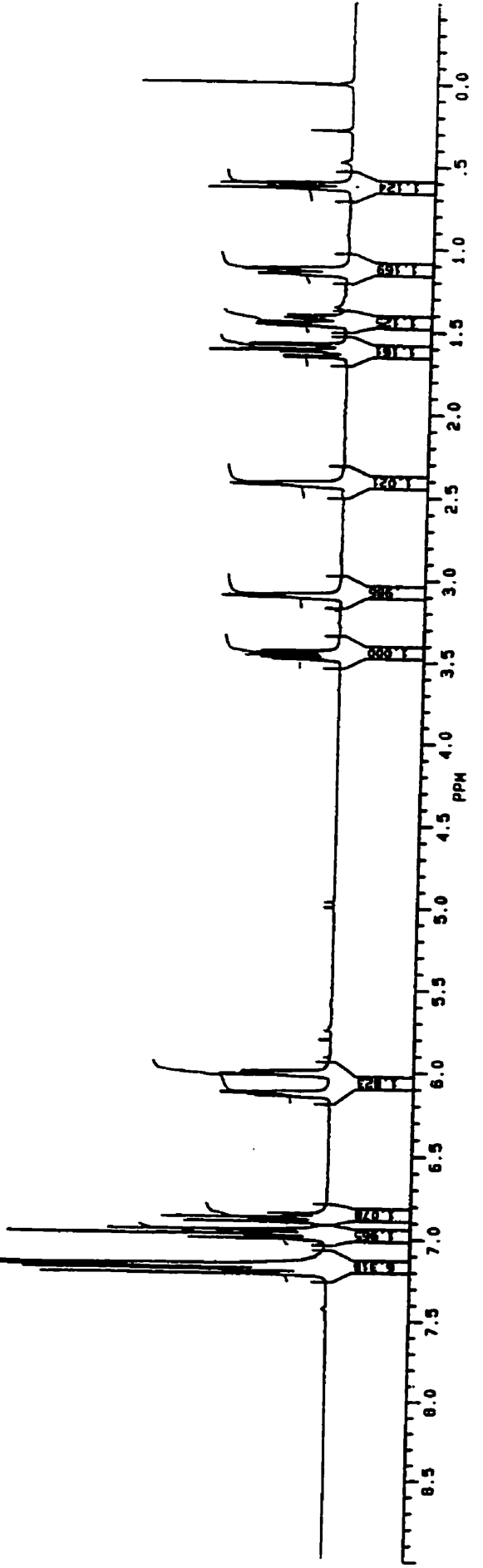
SAMPLE VP3-104C120 1-H AT 300 MHZ IN BENZENE-D6



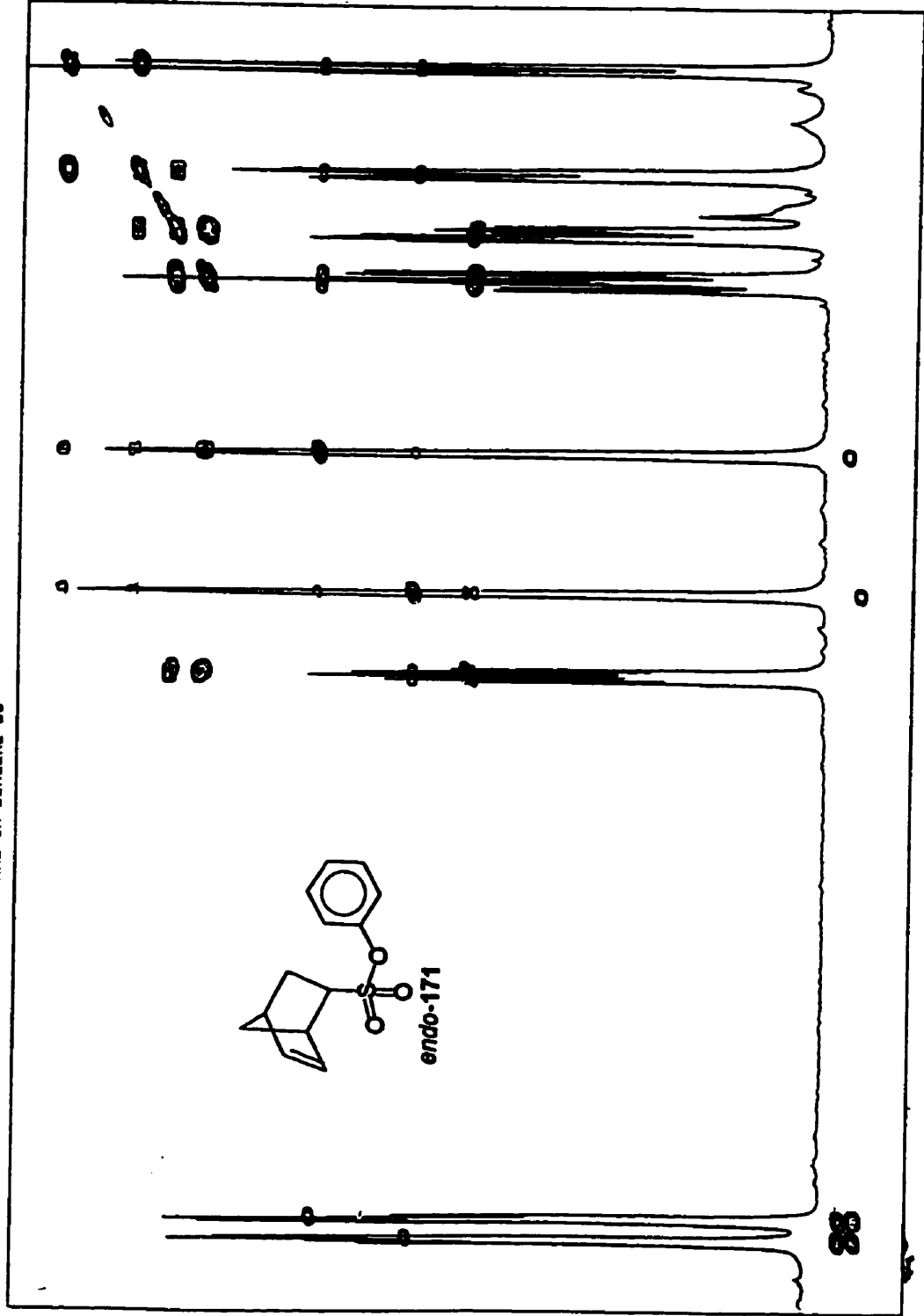
BRUKER
 VP104120.001
 AU PROG.
 IFZG.4U
 DATE 1-5-96
 SF 300.133
 SY 100.0
 O1 5500.000
 S1 35768
 T0 35768
 SW 5494.505
 HZ/PT .335
 PH 8.0
 RD 4.000
 AD 2.982
 RG 20
 NS 32
 TE 300
 FH 6900
 O2 20000.000
 OP 63L 00
 LB .300
 GB .500
 CX 38.00
 CY 18.50
 F1 9.000P
 F2 .499P
 HZ/CM 75.032
 PPM/CM 250
 SR 3362.21



3.09317
 1.61505
 0.0010
 0.0010
 0.0010



SAMPLE VP3-104C12BZ COSY-45 AT 300 MHZ IN BENZENE-D6



~~BUKER~~

VP12BZHH.SMX
AU PROG:
COSY AU
DATE 23-10-96
SI2 1024
SI1 512
SM2 2369.668
SM1 1184.034
ND0 1

NOH2 S
NOH1 S
SSB2 0
SSB1 0
MCR M
PLIM ROM 6.461P
F1 6.461P
F2 .386P
AND COLUMN:
F1 6.461P
F2 .386P
D1 3.000000
P1 10.50
D0 .0000030
P2 5.30
RD 0.0
PW 0.0
DE 266.30
NS 16
DS 2
NF 256
IN .0004220

6.0 5.5 5.0 4.5 4.0 3.5 3.0 2.5 2.0 1.5 1.0 .5
PPM

SAMPLE VPJ-104012 13-C AT 75.47 MHZ IN CDCL3

 **BRUKER**

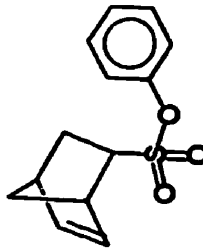
VP3412C.004
AU PROB.
AUTOC13.AU
DATE 21-2-96

SF 75.469
SY 112.0500000
O1 47000.000
SI 32768
TD 32768
SM 17857.143
HZ/PT 1.090

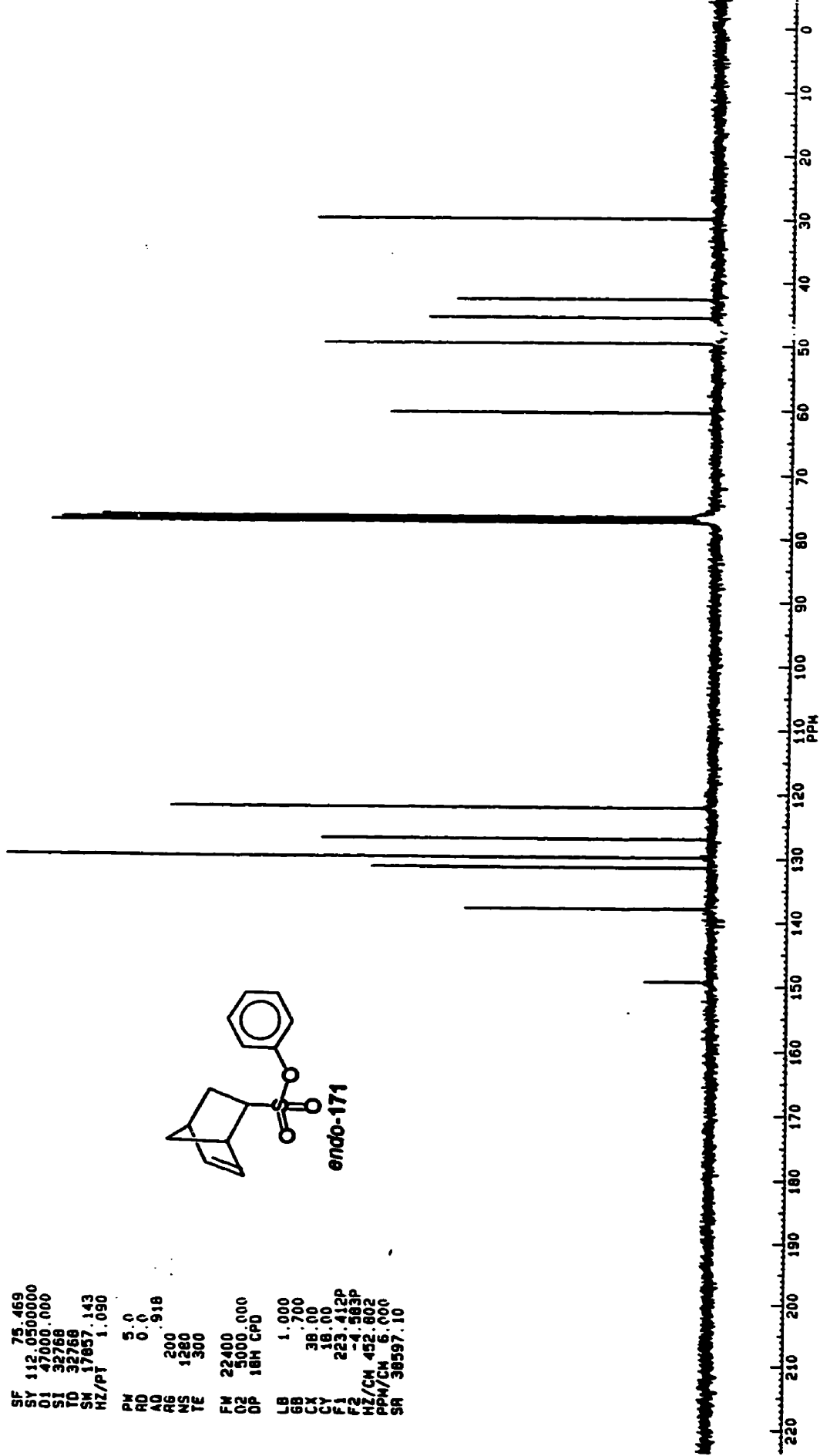
PH 5.0
RD 0.0
AD 0.918
RS 200
NS 1280
TE 300

FM 22400
O2 5000.000
DP 18M CPD

LB 1.000
GB 0.700
CX 38.00
CY 18.00
F1 223.412P
F2 -4.583P
HZ/CH 452.802
PPM/CH 6.000
SR 38597.10



149.238
137.823
131.360
128.912
122.052
77.418
77.371
77.324
50.362
49.602
45.615
42.705
29.904





VP15P.001
 AU PR06:
 IFZ6.AU
 DATE 12-4-96

SF 300.133
 SY 100.0
 O1 5500.000
 SI 32768
 TO 32768
 SM 5494.505
 HZ/PT .335

PW 8.0
 RD 4.000
 AQ 2.982
 RG 10
 NS 32
 TE 300

FW 6900
 O2 20000.000
 DP 63L 00

LB .300
 GB .500
 CX 38.00
 CY 18.50
 F1 9.000P
 F2 -.499P
 PPM/CH 75.032
 SR 3366.45

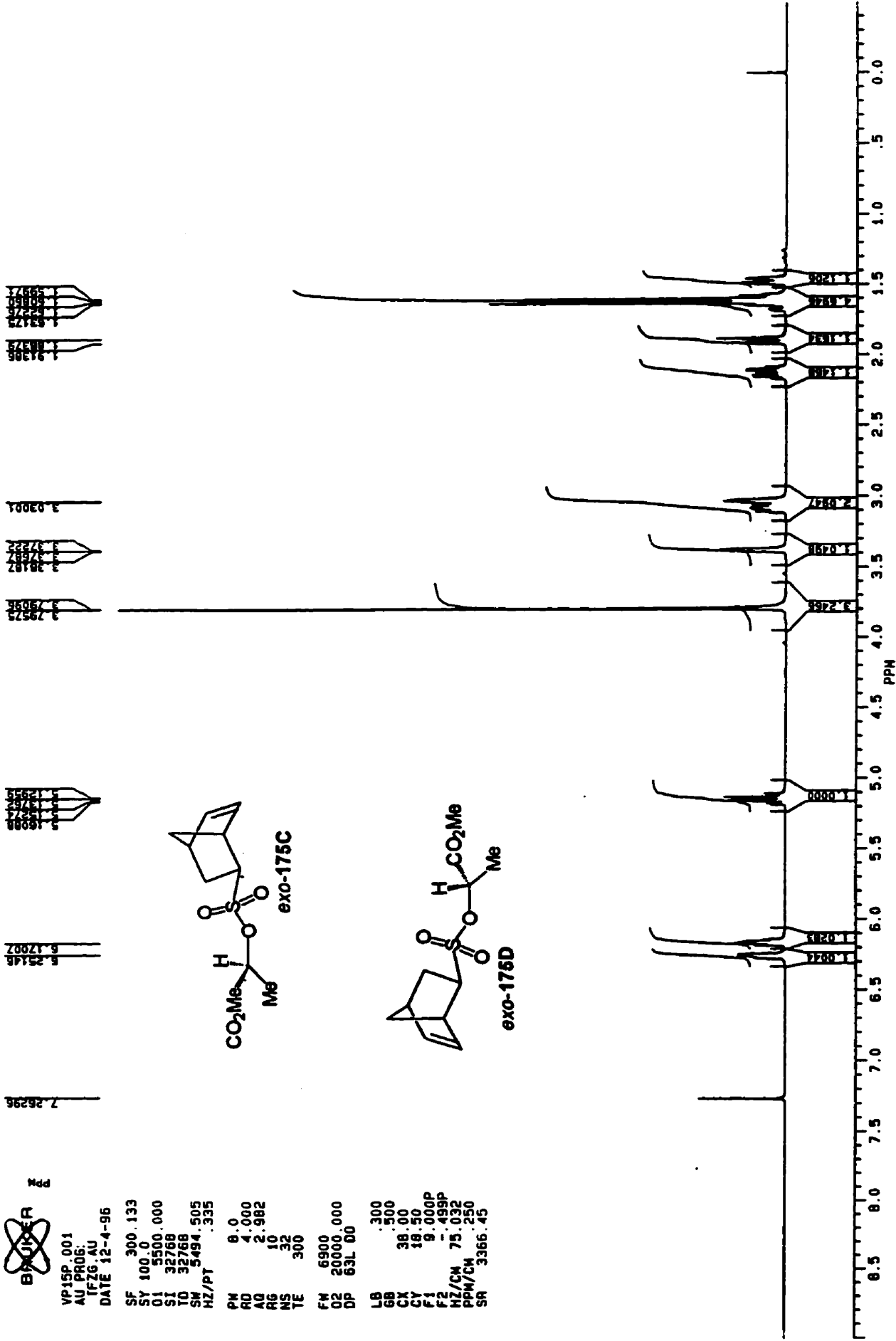
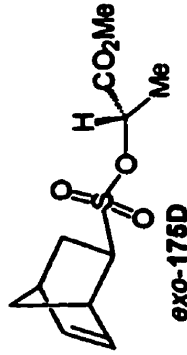
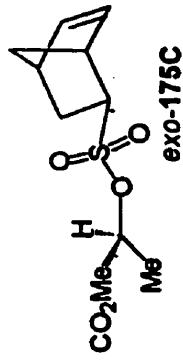
SAMPLE VP3-123C15P 1-H AT 300 MHZ IN CDCL3

7.26296
 6.25148
 6.17007
 5.90098
 5.82000
 5.74000
 5.66000
 5.58000
 5.50000
 5.42000
 5.34000
 5.26000
 5.18000
 5.10000
 5.02000
 4.94000
 4.86000
 4.78000
 4.70000
 4.62000
 4.54000
 4.46000
 4.38000
 4.30000
 4.22000
 4.14000
 4.06000
 3.98000
 3.90000
 3.82000
 3.74000
 3.66000
 3.58000
 3.50000
 3.42000
 3.34000
 3.26000
 3.18000
 3.10000
 3.02000
 2.94000
 2.86000
 2.78000
 2.70000
 2.62000
 2.54000
 2.46000
 2.38000
 2.30000
 2.22000
 2.14000
 2.06000
 1.98000
 1.90000
 1.82000
 1.74000
 1.66000
 1.58000
 1.50000
 1.42000
 1.34000
 1.26000
 1.18000
 1.10000
 1.02000
 0.94000
 0.86000
 0.78000
 0.70000
 0.62000
 0.54000
 0.46000
 0.38000
 0.30000
 0.22000
 0.14000
 0.06000
 0.00000

3.2488
 3.2288
 3.2088
 3.1888
 3.1688
 3.1488
 3.1288
 3.1088
 3.0888
 3.0688
 3.0488
 3.0288
 3.0088
 2.9888
 2.9688
 2.9488
 2.9288
 2.9088
 2.8888
 2.8688
 2.8488
 2.8288
 2.8088
 2.7888
 2.7688
 2.7488
 2.7288
 2.7088
 2.6888
 2.6688
 2.6488
 2.6288
 2.6088
 2.5888
 2.5688
 2.5488
 2.5288
 2.5088
 2.4888
 2.4688
 2.4488
 2.4288
 2.4088
 2.3888
 2.3688
 2.3488
 2.3288
 2.3088
 2.2888
 2.2688
 2.2488
 2.2288
 2.2088
 2.1888
 2.1688
 2.1488
 2.1288
 2.1088
 2.0888
 2.0688
 2.0488
 2.0288
 2.0088
 1.9888
 1.9688
 1.9488
 1.9288
 1.9088
 1.8888
 1.8688
 1.8488
 1.8288
 1.8088
 1.7888
 1.7688
 1.7488
 1.7288
 1.7088
 1.6888
 1.6688
 1.6488
 1.6288
 1.6088
 1.5888
 1.5688
 1.5488
 1.5288
 1.5088
 1.4888
 1.4688
 1.4488
 1.4288
 1.4088
 1.3888
 1.3688
 1.3488
 1.3288
 1.3088
 1.2888
 1.2688
 1.2488
 1.2288
 1.2088
 1.1888
 1.1688
 1.1488
 1.1288
 1.1088
 1.0888
 1.0688
 1.0488
 1.0288
 1.0088
 0.9888
 0.9688
 0.9488
 0.9288
 0.9088
 0.8888
 0.8688
 0.8488
 0.8288
 0.8088
 0.7888
 0.7688
 0.7488
 0.7288
 0.7088
 0.6888
 0.6688
 0.6488
 0.6288
 0.6088
 0.5888
 0.5688
 0.5488
 0.5288
 0.5088
 0.4888
 0.4688
 0.4488
 0.4288
 0.4088
 0.3888
 0.3688
 0.3488
 0.3288
 0.3088
 0.2888
 0.2688
 0.2488
 0.2288
 0.2088
 0.1888
 0.1688
 0.1488
 0.1288
 0.1088
 0.0888
 0.0688
 0.0488
 0.0288
 0.0088
 0.00000

3.2488
 3.2288
 3.2088
 3.1888
 3.1688
 3.1488
 3.1288
 3.1088
 3.0888
 3.0688
 3.0488
 3.0288
 3.0088
 2.9888
 2.9688
 2.9488
 2.9288
 2.9088
 2.8888
 2.8688
 2.8488
 2.8288
 2.8088
 2.7888
 2.7688
 2.7488
 2.7288
 2.7088
 2.6888
 2.6688
 2.6488
 2.6288
 2.6088
 2.5888
 2.5688
 2.5488
 2.5288
 2.5088
 2.4888
 2.4688
 2.4488
 2.4288
 2.4088
 2.3888
 2.3688
 2.3488
 2.3288
 2.3088
 2.2888
 2.2688
 2.2488
 2.2288
 2.2088
 2.1888
 2.1688
 2.1488
 2.1288
 2.1088
 2.0888
 2.0688
 2.0488
 2.0288
 2.0088
 1.9888
 1.9688
 1.9488
 1.9288
 1.9088
 1.8888
 1.8688
 1.8488
 1.8288
 1.8088
 1.7888
 1.7688
 1.7488
 1.7288
 1.7088
 1.6888
 1.6688
 1.6488
 1.6288
 1.6088
 1.5888
 1.5688
 1.5488
 1.5288
 1.5088
 1.4888
 1.4688
 1.4488
 1.4288
 1.4088
 1.3888
 1.3688
 1.3488
 1.3288
 1.3088
 1.2888
 1.2688
 1.2488
 1.2288
 1.2088
 1.1888
 1.1688
 1.1488
 1.1288
 1.1088
 1.0888
 1.0688
 1.0488
 1.0288
 1.0088
 0.9888
 0.9688
 0.9488
 0.9288
 0.9088
 0.8888
 0.8688
 0.8488
 0.8288
 0.8088
 0.7888
 0.7688
 0.7488
 0.7288
 0.7088
 0.6888
 0.6688
 0.6488
 0.6288
 0.6088
 0.5888
 0.5688
 0.5488
 0.5288
 0.5088
 0.4888
 0.4688
 0.4488
 0.4288
 0.4088
 0.3888
 0.3688
 0.3488
 0.3288
 0.3088
 0.2888
 0.2688
 0.2488
 0.2288
 0.2088
 0.1888
 0.1688
 0.1488
 0.1288
 0.1088
 0.0888
 0.0688
 0.0488
 0.0288
 0.0088
 0.00000

3.2488
 3.2288
 3.2088
 3.1888
 3.1688
 3.1488
 3.1288
 3.1088
 3.0888
 3.0688
 3.0488
 3.0288
 3.0088
 2.9888
 2.9688
 2.9488
 2.9288
 2.9088
 2.8888
 2.8688
 2.8488
 2.8288
 2.8088
 2.7888
 2.7688
 2.7488
 2.7288
 2.7088
 2.6888
 2.6688
 2.6488
 2.6288
 2.6088
 2.5888
 2.5688
 2.5488
 2.5288
 2.5088
 2.4888
 2.4688
 2.4488
 2.4288
 2.4088
 2.3888
 2.3688
 2.3488
 2.3288
 2.3088
 2.2888
 2.2688
 2.2488
 2.2288
 2.2088
 2.1888
 2.1688
 2.1488
 2.1288
 2.1088
 2.0888
 2.0688
 2.0488
 2.0288
 2.0088
 1.9888
 1.9688
 1.9488
 1.9288
 1.9088
 1.8888
 1.8688
 1.8488
 1.8288
 1.8088
 1.7888
 1.7688
 1.7488
 1.7288
 1.7088
 1.6888
 1.6688
 1.6488
 1.6288
 1.6088
 1.5888
 1.5688
 1.5488
 1.5288
 1.5088
 1.4888
 1.4688
 1.4488
 1.4288
 1.4088
 1.3888
 1.3688
 1.3488
 1.3288
 1.3088
 1.2888
 1.2688
 1.2488
 1.2288
 1.2088
 1.1888
 1.1688
 1.1488
 1.1288
 1.1088
 1.0888
 1.0688
 1.0488
 1.0288
 1.0088
 0.9888
 0.9688
 0.9488
 0.9288
 0.9088
 0.8888
 0.8688
 0.8488
 0.8288
 0.8088
 0.7888
 0.7688
 0.7488
 0.7288
 0.7088
 0.6888
 0.6688
 0.6488
 0.6288
 0.6088
 0.5888
 0.5688
 0.5488
 0.5288
 0.5088
 0.4888
 0.4688
 0.4488
 0.4288
 0.4088
 0.3888
 0.3688
 0.3488
 0.3288
 0.3088
 0.2888
 0.2688
 0.2488
 0.2288
 0.2088
 0.1888
 0.1688
 0.1488
 0.1288
 0.1088
 0.0888
 0.0688
 0.0488
 0.0288
 0.0088
 0.00000



SAMPLE VP3-123C1919 13-C AT 75.47 MHZ IN CDCL3

BOEYER
NMR

VP1919C.004
AU PROG:
AUTOC13.AU
DATE 13-4-96

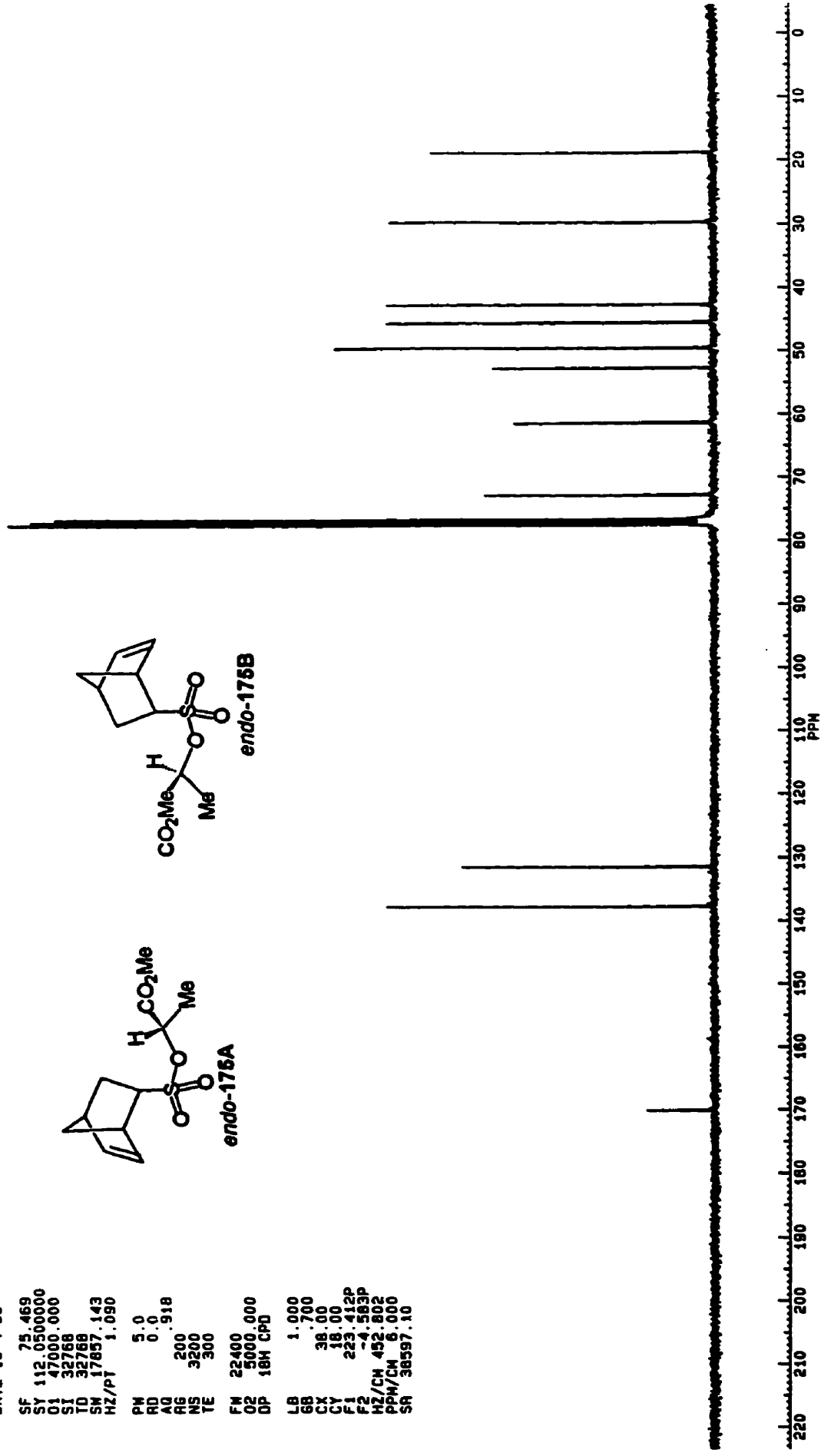
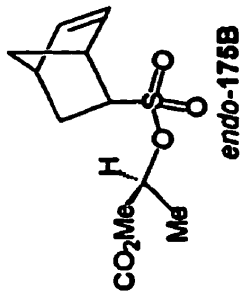
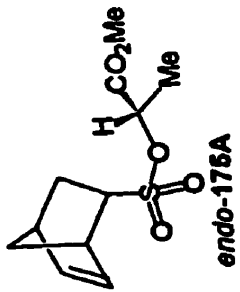
SF 75.469
SY 112.0500000
O1 47000.000
SI 32768
TD 32768
SM 17857.143
HZ/PT 1.090

PW 5.0
RD 0.0
AQ 0.918
RG 200
NS 3200
TE 300

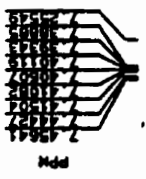
FW 22400
O2 5000.000
DP 18M CPD

LB 1.000
GB 0.700
CX 36.00
CY 16.00
F1 223.412P
F2 -4.583P
HZ/CH 452.802
PPM/LM 6.000
SR 38597.10

137.625
131.429
131.371
77.46
77.00
76.54
61.38
58.55
57.92
51.9
51.5
51.1
49.5
47.5
42.8
28.9
28.1



SAMPLE VP3-103C43 1-H AT 300 MHZ IN CDCL3



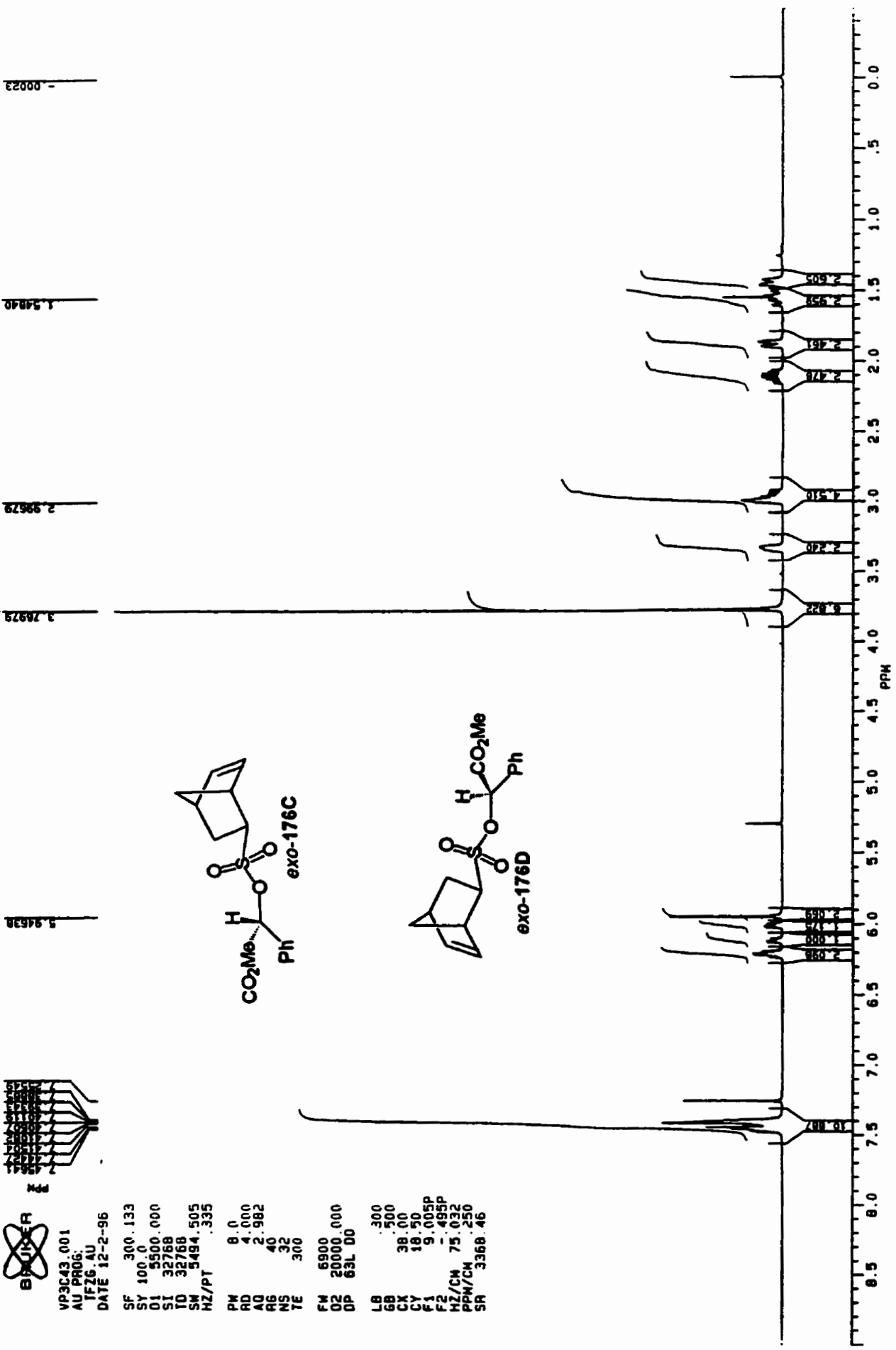
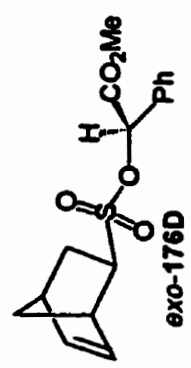
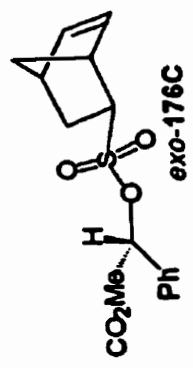
BRUKER

VP3C43.001
 AU PR06:
 TFZ6 AU
 DATE 12-2-96
 SF 300.133
 SY 100.0
 O1 9500.000
 SI 32768
 TD 32768
 SM 5484.505
 HZ/PT .335

PM 8.0
 RD 4.000
 AQ 2.982
 RG 40
 NS 32
 TE 300

FM 6900
 O2 20000.000
 OP 63L 00

LB .300
 GB .500
 CK 38.00
 CY 18.50
 F1 9.005P
 F2 -495P
 HZ/CH 75.032
 PPM/CH .250
 SR 3368.46



SAMPLE VP3-103C43 13-C AT 75.47 MHZ IN CDCL3

BURK
Ndd

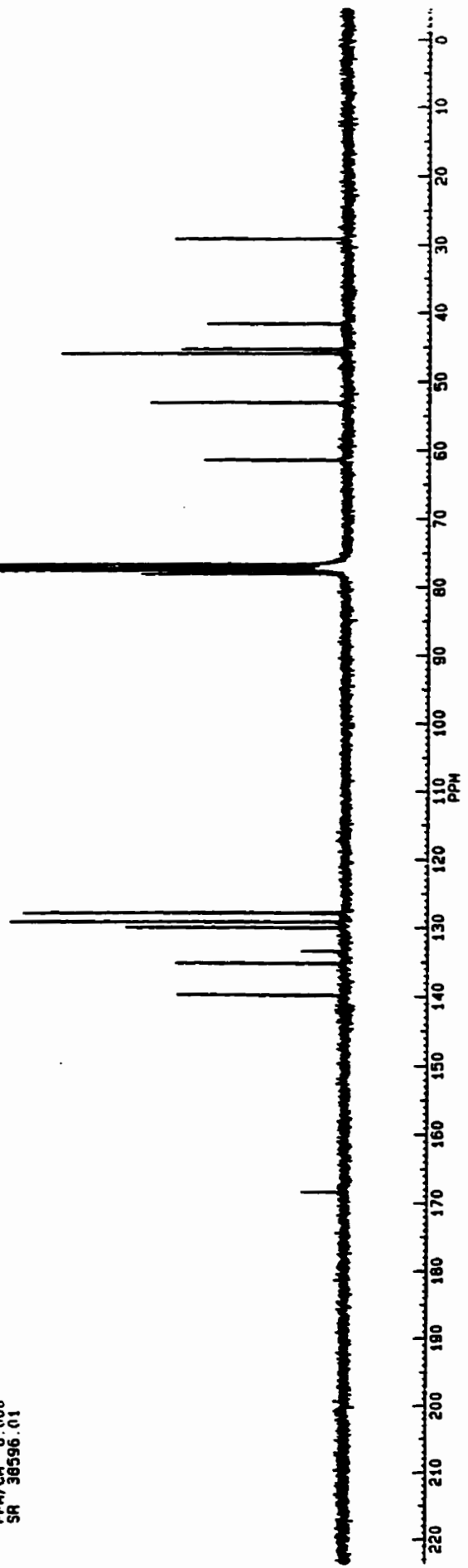
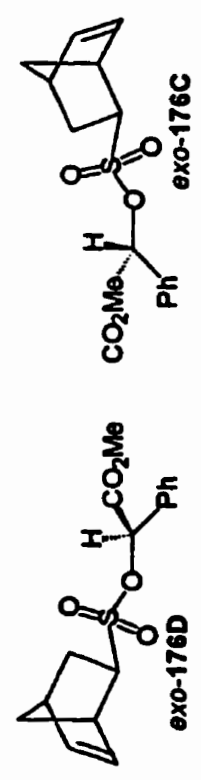
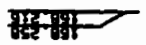
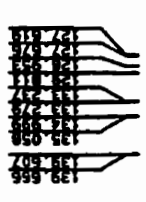
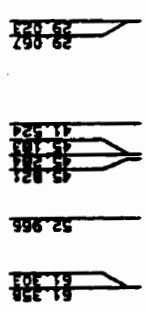
VP3C43C.004
AU PR06.4U
DATE 13-2-96

SF 75.469
SY 112.0500000
O1 47000.000
SI 32788
F0 32788
SM 17857.143
HZ/PT 1.090

PW 5.0
RD 0.0
AQ .918
RG 200
NS 3200
TE 300

FW 22400
O2 5000.000
DP 18H CPD

LB 1.000
GB .700
CX 38.00
CY 8.00
F1 223.427P
F2 -4.558P
HZ/CM 452.802
PPM/CM 6.000
SR 36596.01





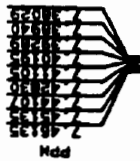
VP3C60.001
AU PROG: IF26.AU
DATE 12-2-96

SF 300.133
BY 100.0
Q1 3500.000
SI 32768
TD 32768
SM 5494.505
HZ/PT .335

PH 8.0
RD 4.000
AG 2.982
NS 8
TE 300

FM 6900
DZ 20000.000
DP 63L DO

LB .300
GB .500
CX 38.00
CY 18.50
F1 9.005P
F2 .495P
HZ/CM 75.032
PPM/CM .250
SR 3367.79



5.89479

SAMPLE T1.3 400000 1.11 M1 000 M12 AIR 000003

3.76230

3.35911

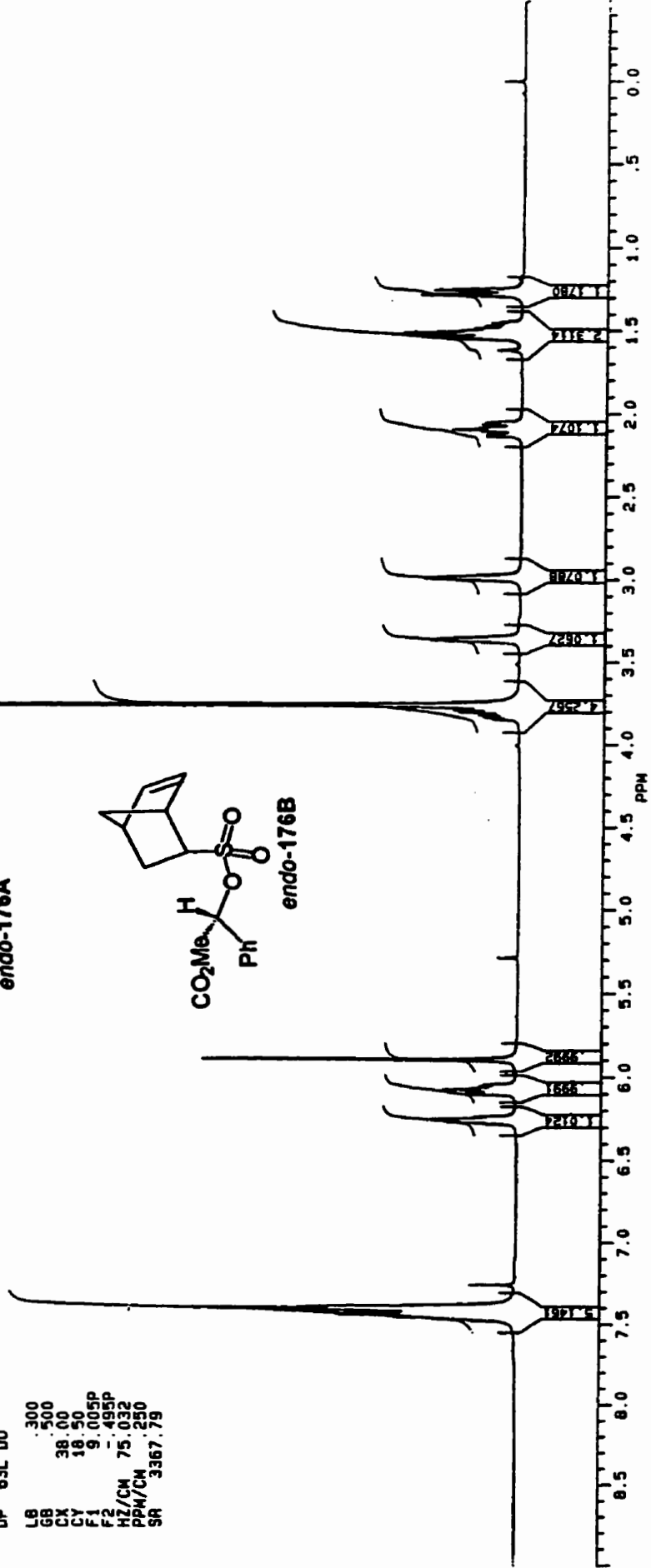
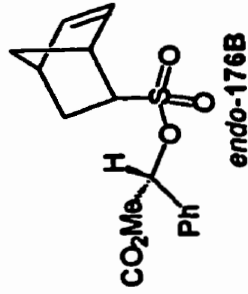
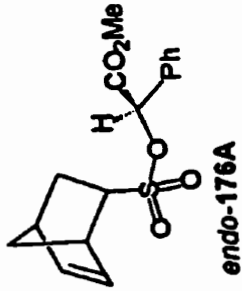
2.98811

1.78150

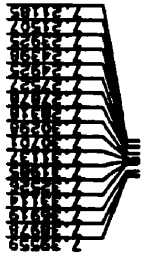
1.54922

1.51181

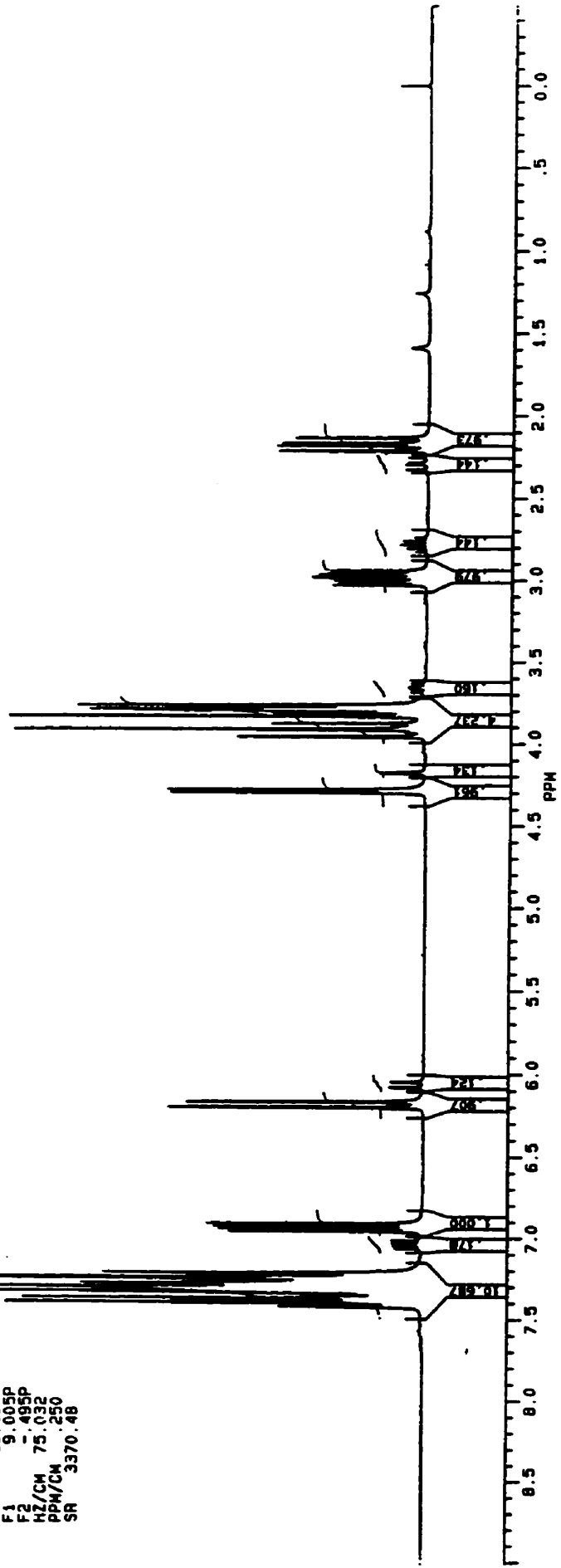
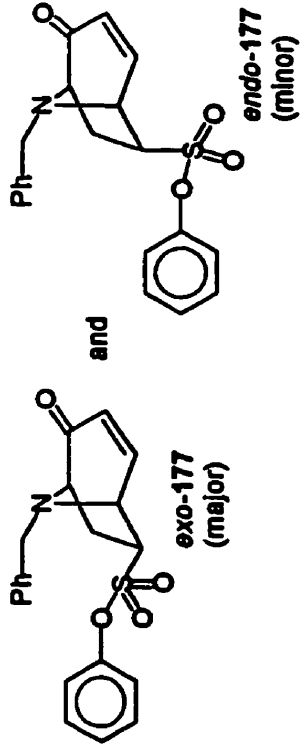
1.49222



SAMPLE VP3-100C20 1-H AT 300 MHZ IN CDCL3



VP30C20.001
AU PROG.
IPZ6.AU
DATE 13-2-96
SF 300.133
SY 100.0
O1 5500.000
S1 32768
I1 32768
SM 5494.505
HZ/PT .335
PM 8.0
RD 4.000
AD 2.982
RG 8
NS 32
TE 300
FW 6900
O2 20000.000
DP 63L D0
LB .300
GB .500
CX 38.00
CY 18.50
F1 9.005P
F2 .495P
HZ/CM 75.032
PPM/CM .250
SR 3370.48



SAMPLE VP3-100C200 1-H AT 300 MHZ IN BENZENE-D6

BP

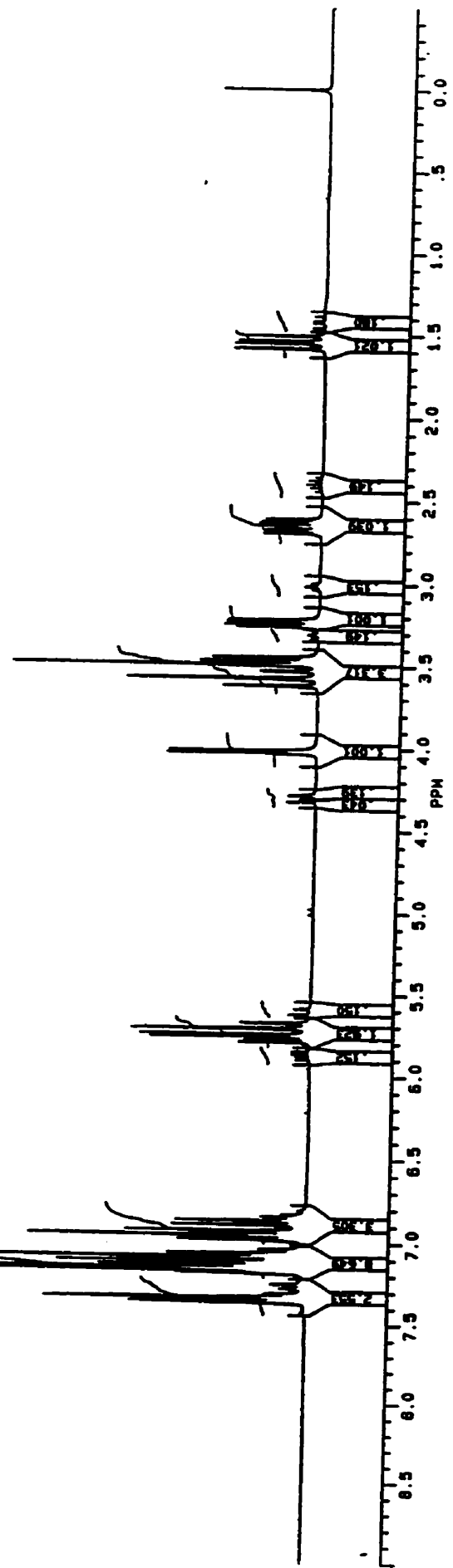
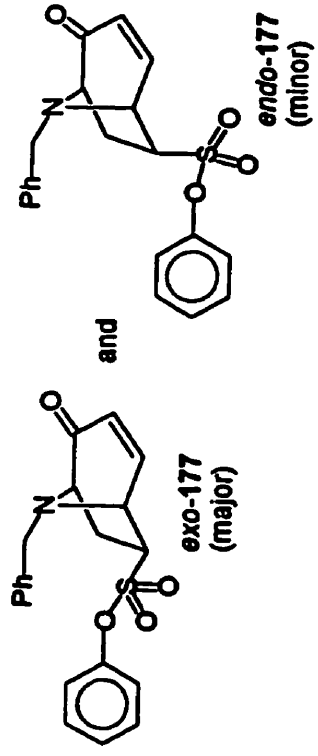
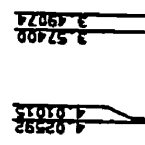
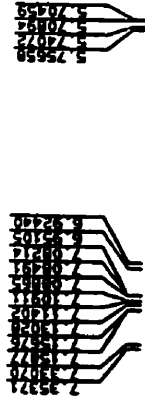

VP100200.001
 AU PROG: IFZG.AU
 DATE 1-5-96

SF 300.133
 SY 100.0
 O1 3500.000
 SI 32768
 TD 32768
 SH 5494.505
 HZ/PT .335

PW 6.0
 AQ 4.000
 RG 2.982
 NS 32
 TE 300

FW 6900
 O2 20000.000
 DP 83L.D0

LB .300
 GB .500
 CX 38.00
 CY 18.50
 F1 9.000P
 F2 -498P
 HZ/CM 75.032
 PPM/CM 3381.86



SAMPLE VP3-72CC26 1-H AT 300 MHZ IN BENZENE-D6

BRUKER

VP72CC26.001
 AU PR06.
 TF26.AU
 DATE 7-5-96

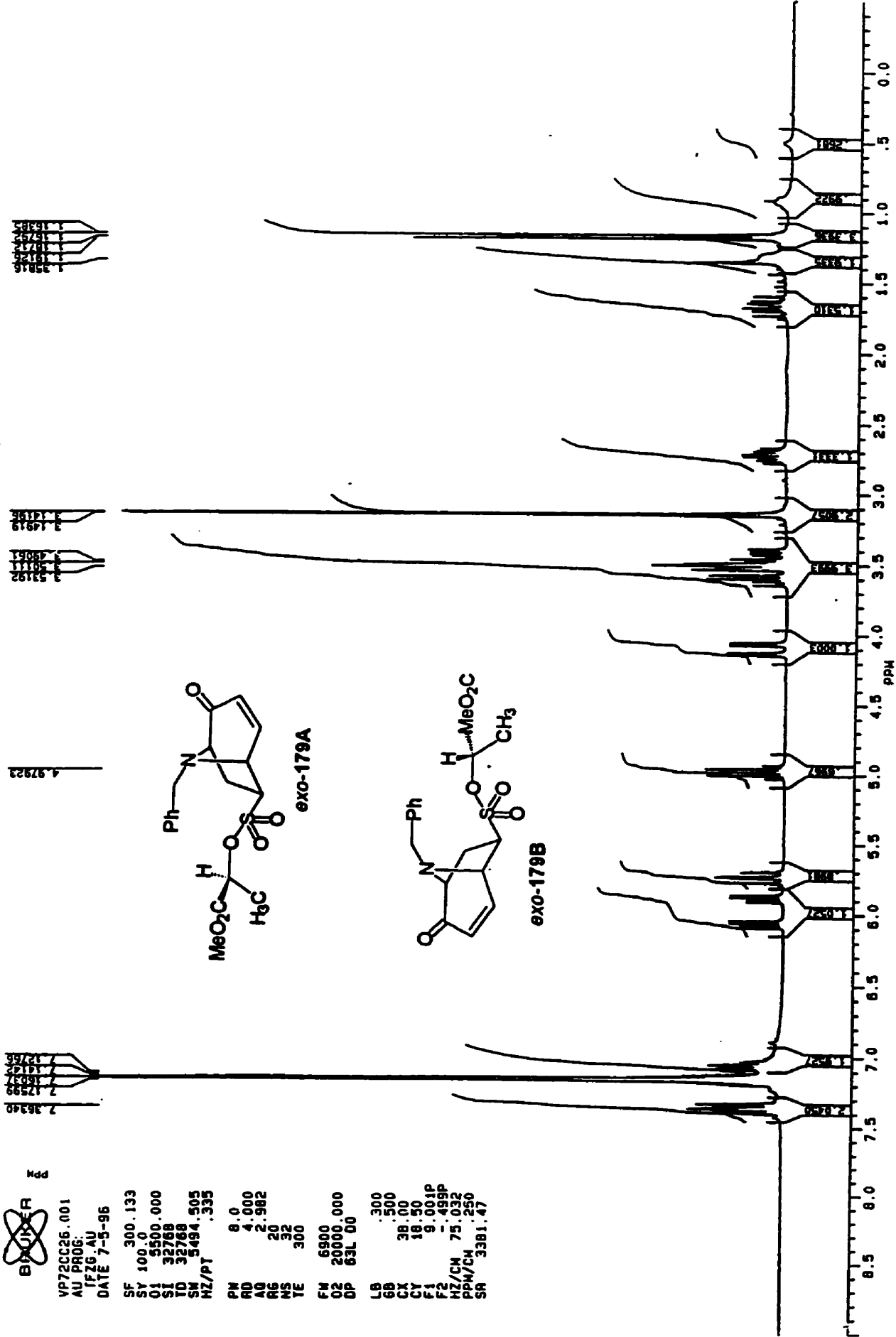
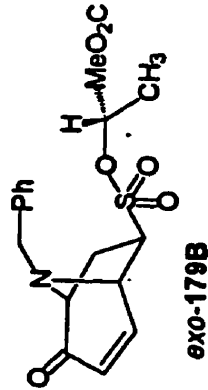
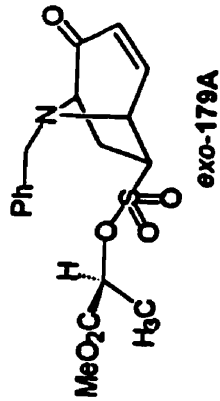
SF 300.133
 SY 100.0
 O1 5500.000
 SI 32788
 ID 32788
 SM 5494.505
 HZ/PT .335

PH 8.0
 RD 4.800
 AD 2.982
 RG 20
 NS 32
 TE 300


FW 6900
 O2 20000.000
 DP 63L 00

LB .300
 GB .500
 CX 38.00
 CY 18.50
 F1 9.001P
 F2 .495P
 HZ/CH 75.032
 PPM/CM .250
 SR 3381.47

7.36340
 7.17599
 6.95127
 6.71171
 6.47215
 6.23259
 6.01303
 5.77347
 5.53391
 5.29435
 5.05479
 4.81523
 4.57567
 4.33611
 4.09655
 3.85699
 3.61743
 3.37787
 3.13831
 2.89875
 2.65919
 2.41963
 2.18007
 1.94051
 1.70095
 1.46139
 1.22183
 0.98227
 0.74271
 0.50315
 0.26359
 0.02403



SAMPLE VP3-72-C33 13-C AT 75.47 MHZ IN CDCL3



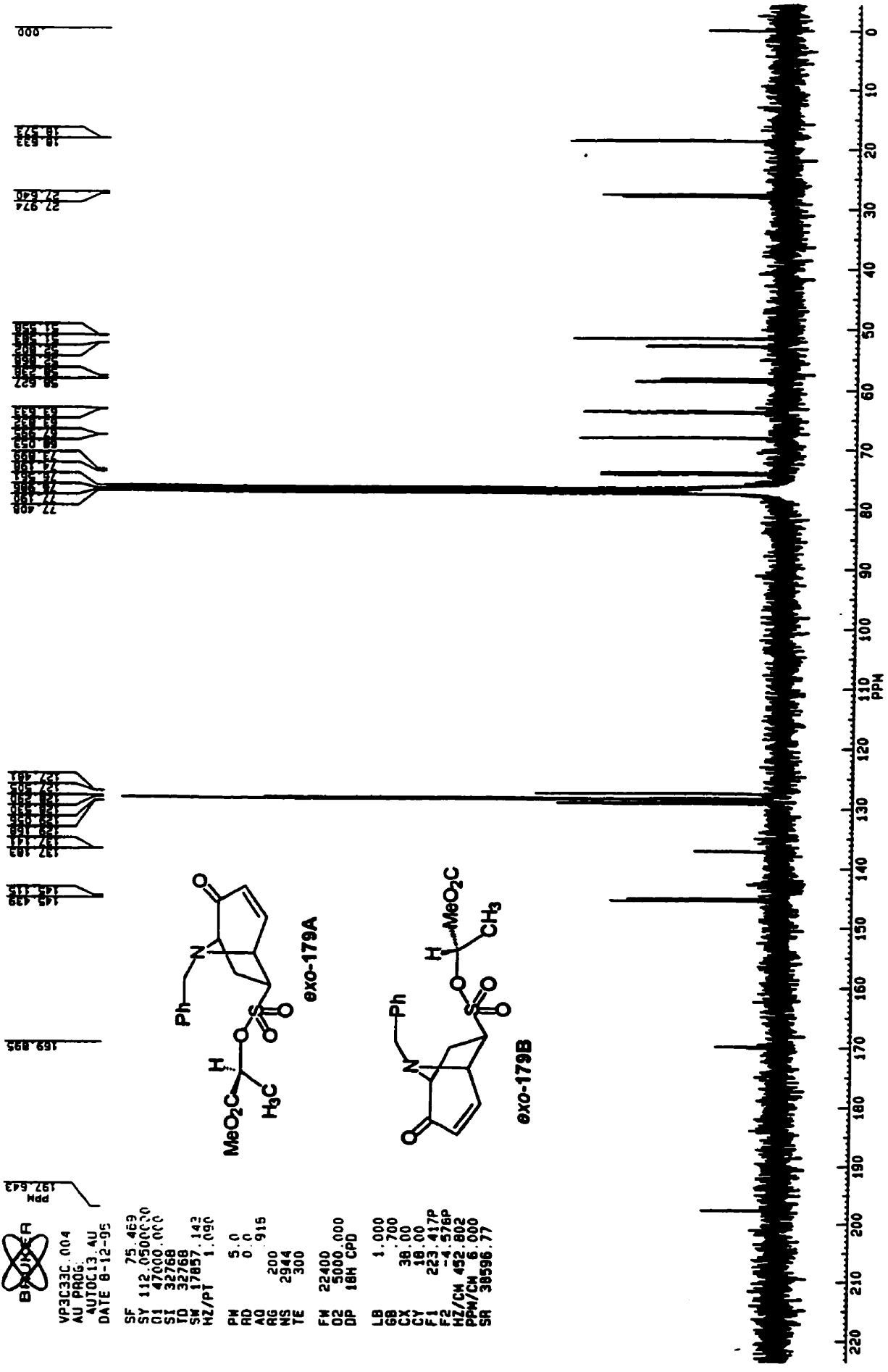
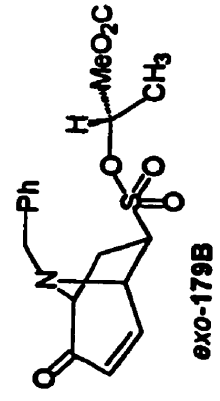
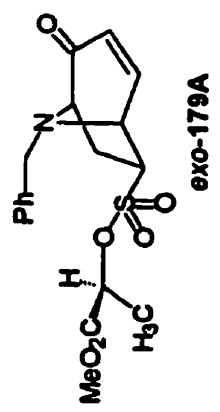
 VP3C33C.004
 AU PROG.
 AUTOC13.4U
 DATE 8-12-95

SF 75.469
 SY 112.0500000
 O1 47000.000
 S1 32768
 I0 32768
 SM 17857.142
 HZ/PT 1.090

PH 5.0
 PD 0.0
 AQ 915
 RG 200
 NS 2944
 TE 300

FW 22400
 O2 5000.000
 DP 18H CPD

LB 1.000
 GB 700
 CX 36.00
 CY 16.00
 F1 223.417P
 F2 -1.576P
 HZ/CH 452.802
 PPM/CH 6.000
 SR 38596.77





VPII28PI.001
DATE 17-3-93

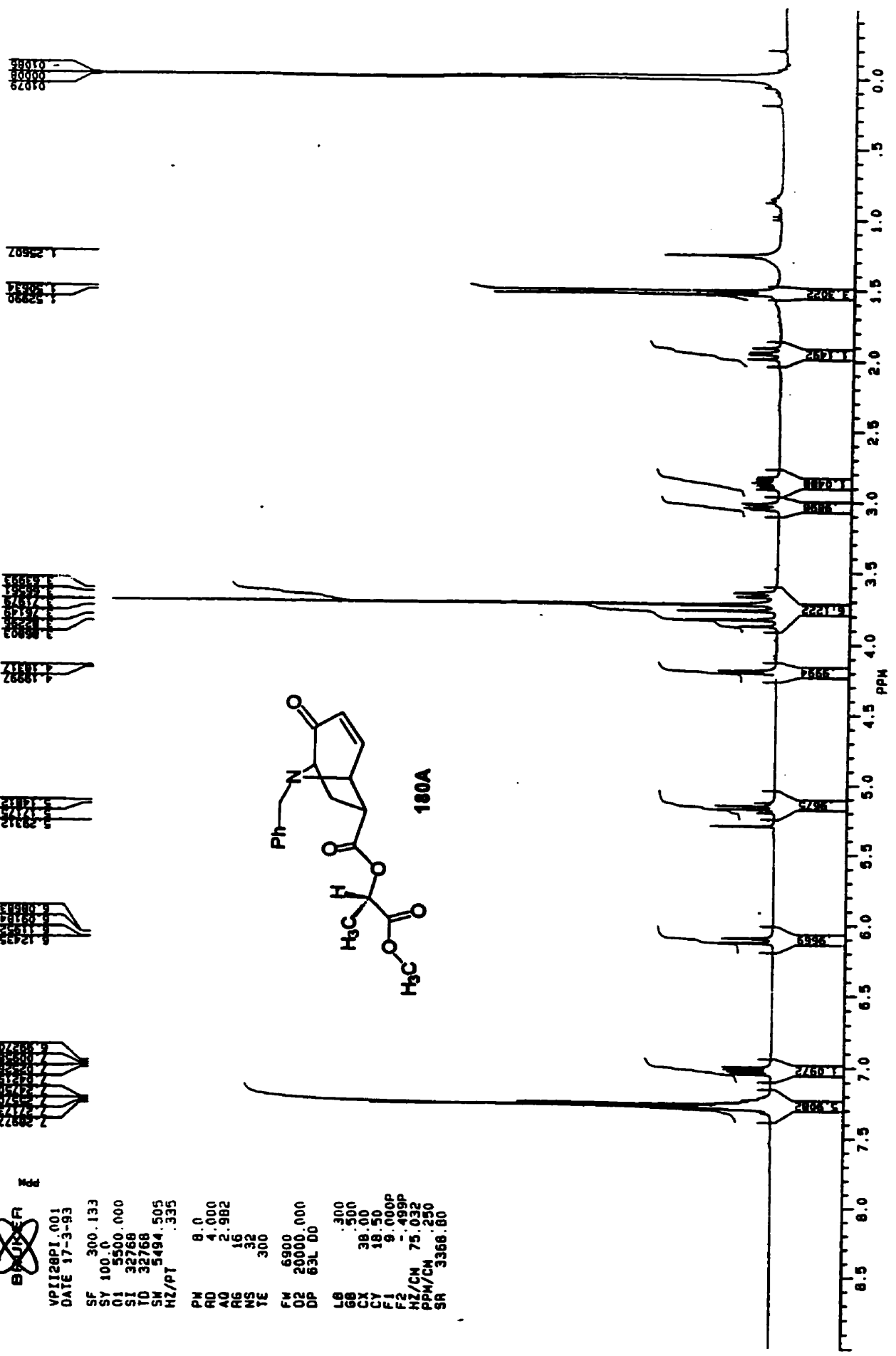
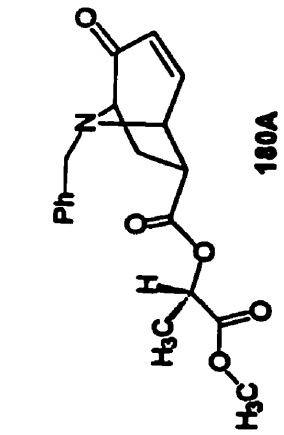
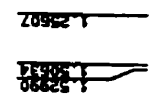
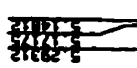
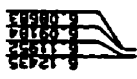
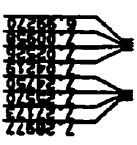
SF 300.133
SI 100.0
SI 5500.000
SI 32768
TD 32768
SM 5494.505
HZ/PT .335

PH 8.0
RD 4.000
AQ 2.982
RG 16
NS 32
TE 300

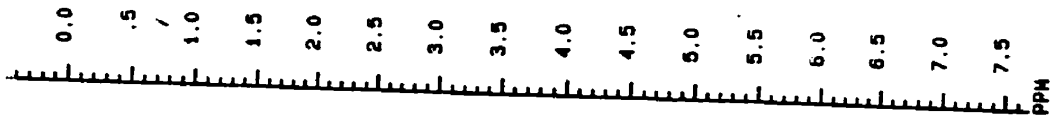
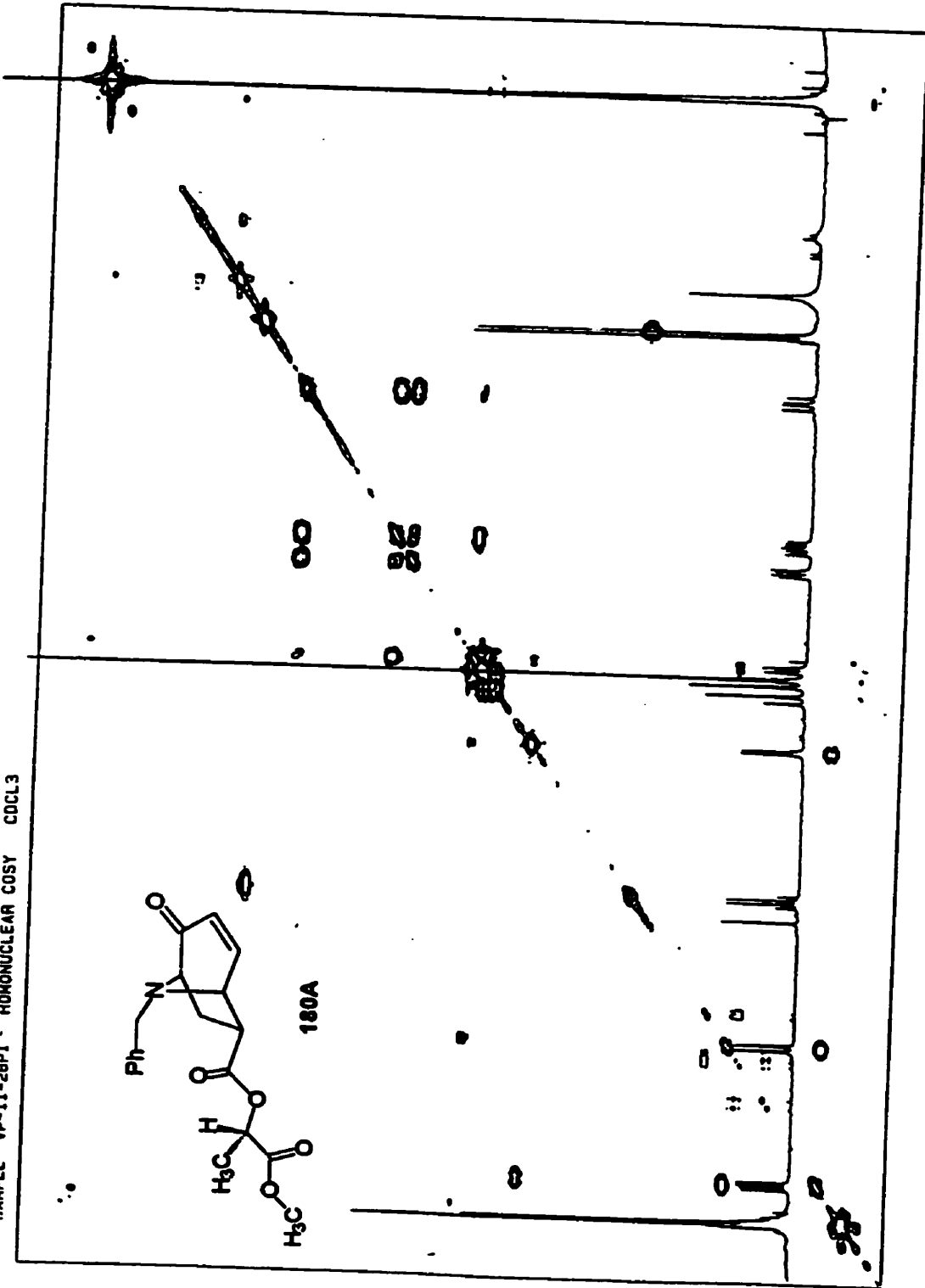
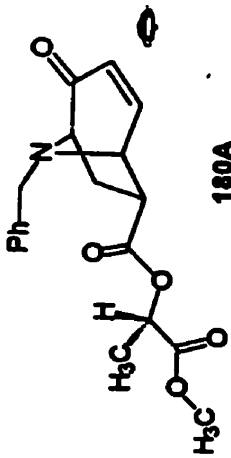
FM 6800
O2 20000.000
DP 63L 00

LB .300
GB .500
CX 38.00
CY 18.50
F1 9.000P
F2 .499P
HZ/CM 75.032
PPM/CM .250
SR 3368.80

SAMPLE VP-II-28PI 1-H 300 MHZ CDCL3



SAMPLE VP-II-28PI - HOMO NUCLEAR COSY CDCL3

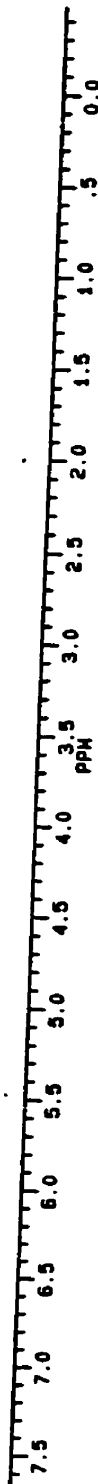


VPICOSY.SMX
AU PROG.
COSY.AU
DATE 18-3-93

SI2 1024
SI1 512
SM2 2450.940
SM1 1225.450
NDO 1

MDM2 S
MDM1 S
SSB2 0
SSB1 0
MC2 M
PLIM ROM 7.672P
F1 -.478P
F2 -.478P
AND COLUMN:
F1 7.672P
F2 -.478P

D1 3.0000000
P1 11.50
D0 .0000030
F2 5.00
PD 0.0
PW 0.0
OE 257.50
NS 16
DS 2
NE 256
IN .0004080



SAMPLE VP-II-28PI 13-C 75.47 MHZ CDCL3



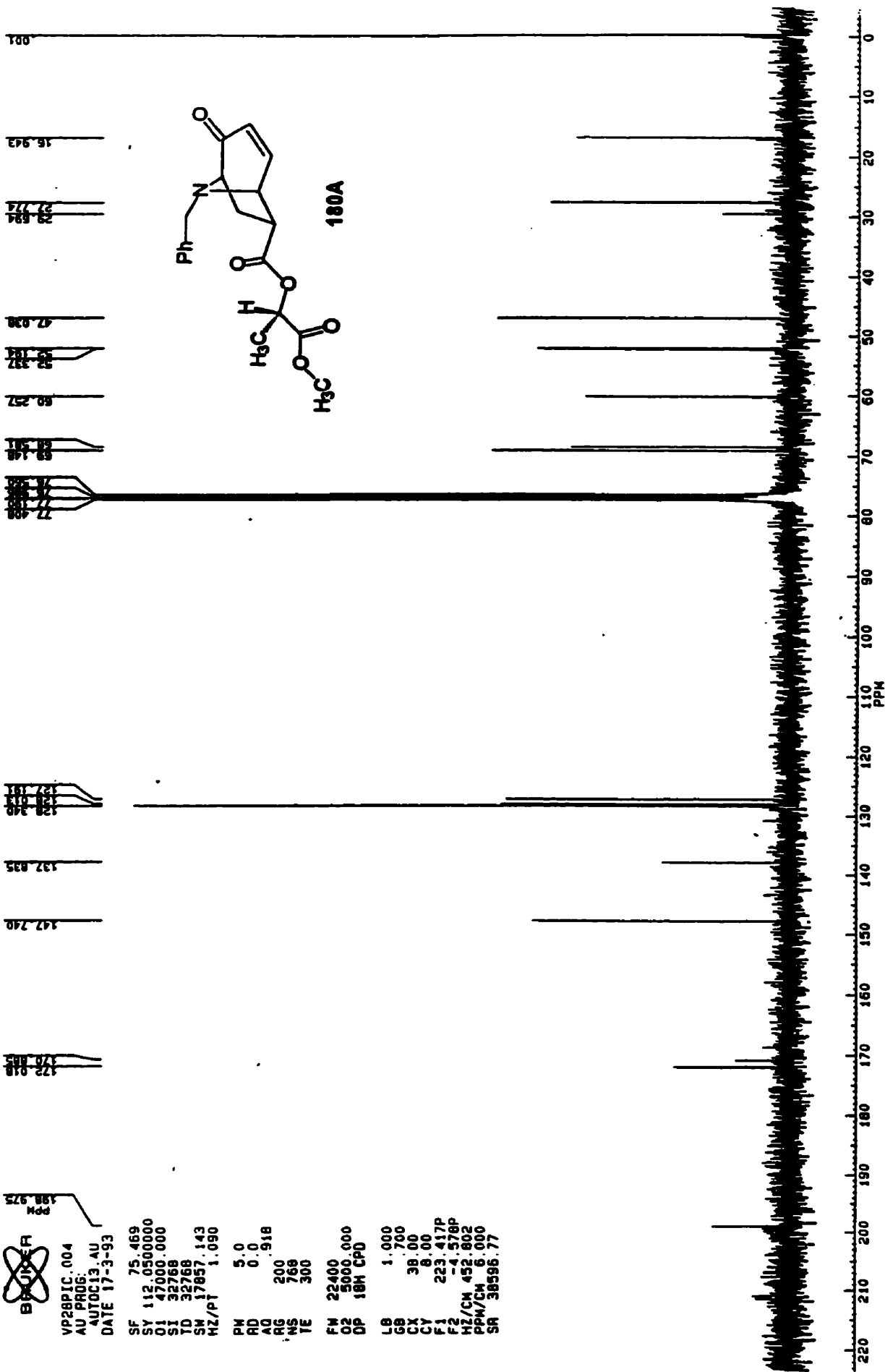
VR28PIC.004
AU PROG.
AUTOC13.AU
DATE 17-3-93

SF 75.469
SY 112.0500000
O1 47000.000
SI 32768
TD 35768
SM 17857.143
HZ/PT 1.090

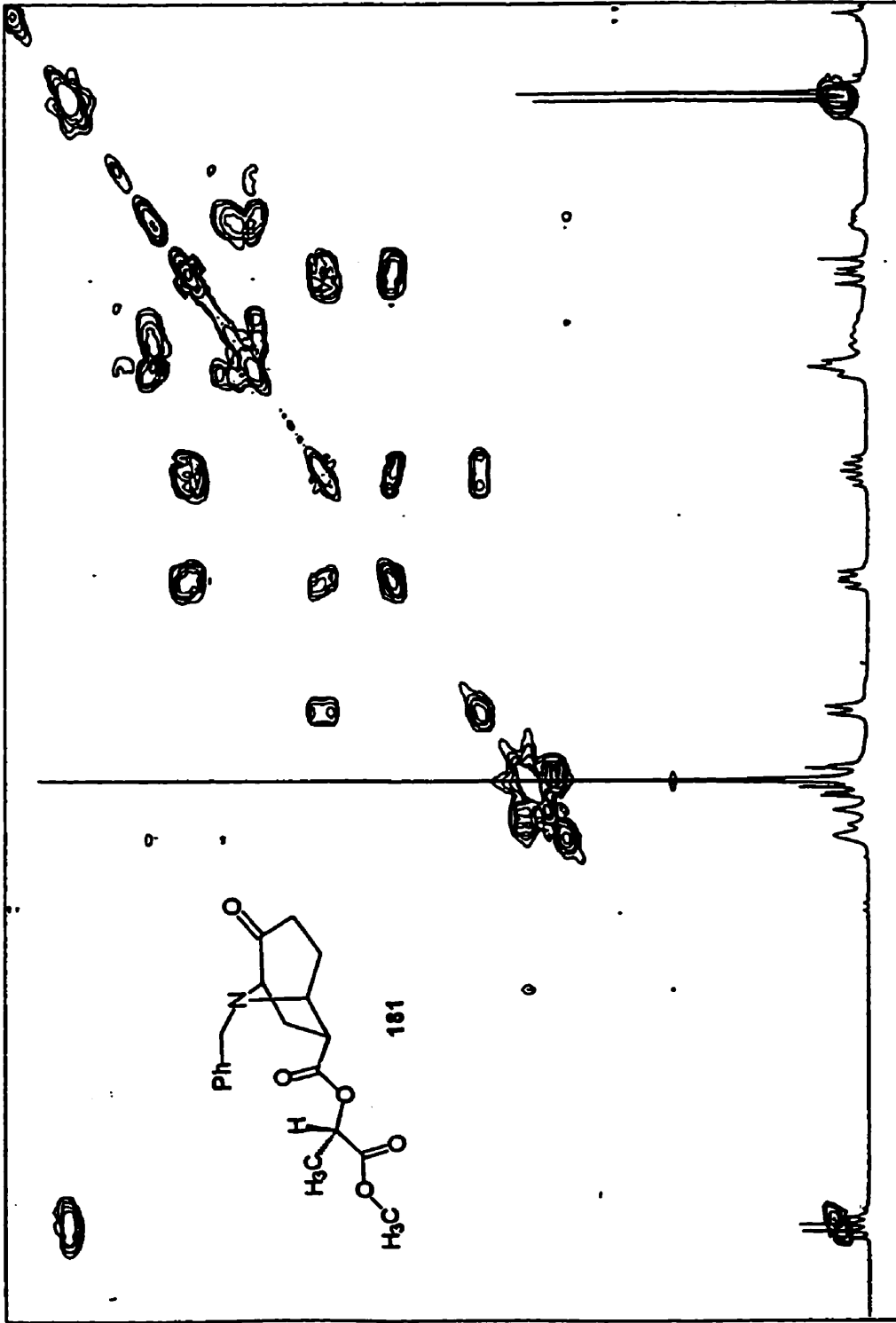
PH 5.0
RD 0.0
AQ 0.918
RG 200
NS 768
TE 300

FM 22400
O2 5000.000
DP 18K CPD

LB 1.000
GB 700
CX 38.00
CY 8.00
F1 223.417P
F2 -4.578P
HZ/CM 452.602
PPM/CM 6.000
SR 38596.77



SAMPLE VP-11-36-RC COSY AT 300 MHZ IN COCL3



BRUKER

VP36RCHH 5MX
AU PR06
LOS Y AU

DATE 26-5-92

SI2 1024
SI1 512
SM2 2890.173
SM1 1445.087
NDC 1

WDW2 S
WDW1 S
SSB2 0
SSB1 0
ML2 H
ML1M ROW
F1 5.473P
F2 1.223P
AND. COLUMN
F1 5.473P
F2 1.223P
D1 3.000000
D0 11.50
D2 5.00
P4 0.0
P5 0.0
DE 218.00
NS 16
OS 2
ME 256
IN .0003460

5.4 5.2 5.0 4.8 4.6 4.4 4.2 4.0 3.8 3.6 3.4 3.2 3.0 2.8 2.6 2.4 2.2 2.0 1.8 1.6 1.4
PPM

SAMPLE VP-II-38 13-C AT 75.47 MHZ IN CDCL3



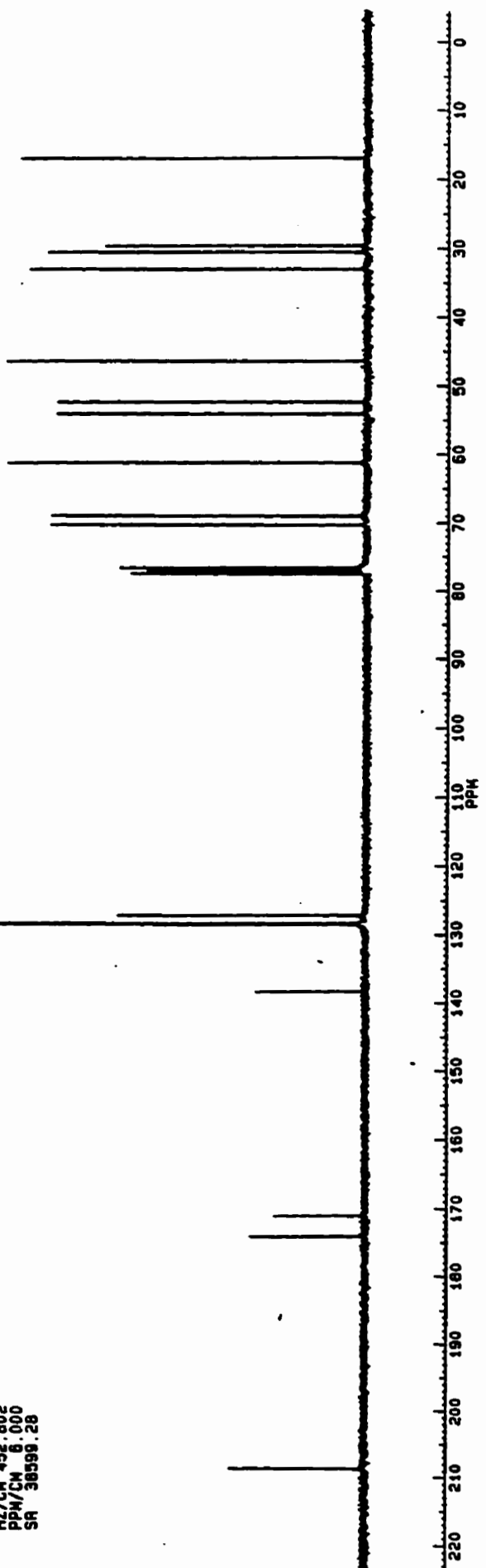
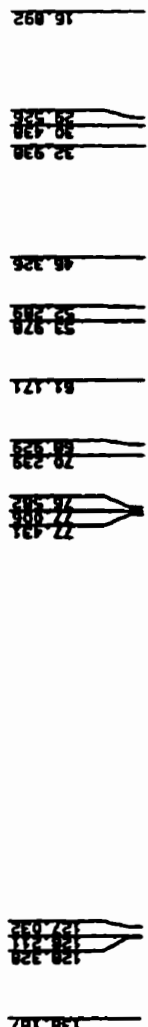
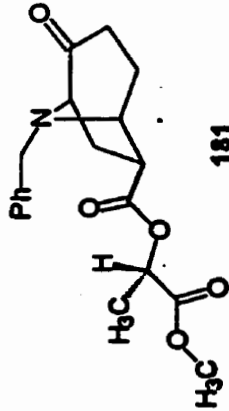
VPI138C.004
 AU PR06:
 AUTOCPS.AU
 DATE 10-7-95

SF 75.469
 SY 112.050000
 O1 47000.000
 SI 32768
 ID 32768
 SM 17857.143
 HZ/PT 1.090

PH 5.0
 RD 0.0
 AG 200
 NS 640
 TE 300

FM 22400
 O2 50000.000
 OP 18H CPD

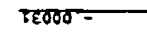
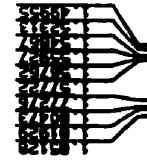
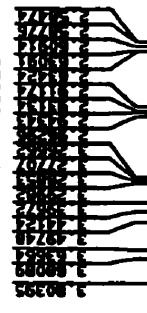
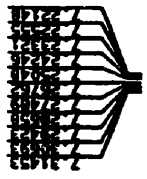
LB 1.000
 GB 38.00
 CX 18.00
 F1 223.384P
 F2 -4.611P
 HZ/CM 452.802
 PPM/CM 6.000
 SR 38598.28



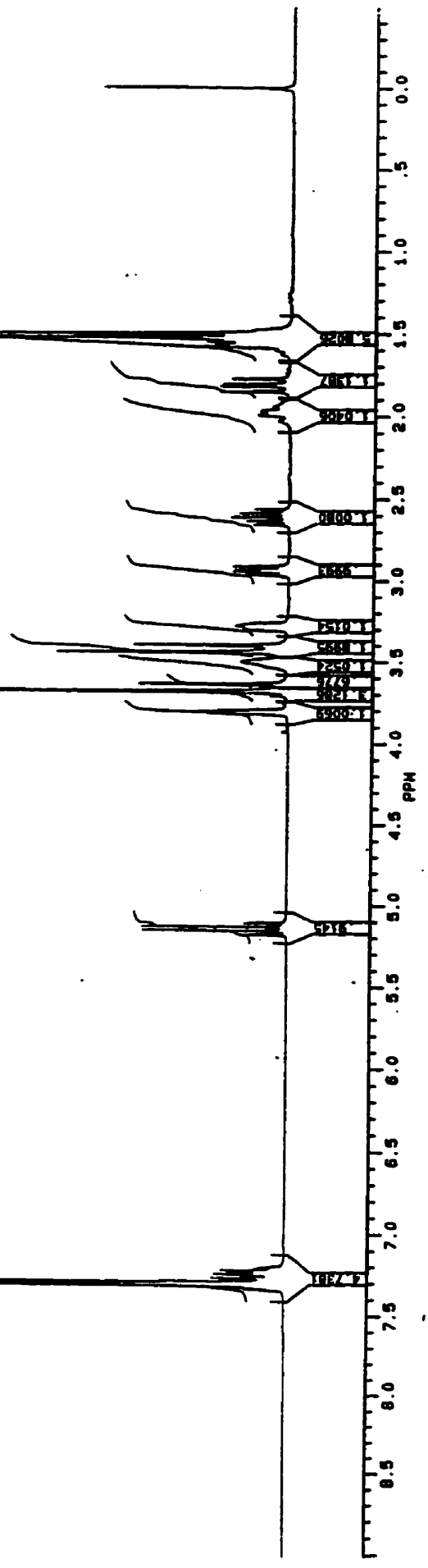
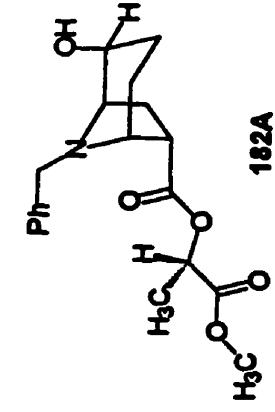
220 210 200 190 180 170 160 150 140 130 120 110 100 90 80 70 60 50 40 30 20 10 0

PPM

SAMPLE VP-II-78-17 1-H AT 300 MHZ IN CDCL3



VP117817.001
 AU PAR6.
 FZ6.AU
 DATE 26-11-93
 SF 300.133
 SY 100.0
 O1 5500.000
 SI 32768
 ID 32768
 SM 5494.505
 HZ/PT .335
 PH 8.0
 PD 4.000
 AU 2.982
 RB 4
 NS 32
 TE 300
 FM 6900
 O2 20000.000
 DP 63L D0
 LB .300
 GB 500
 CX 38.00
 CY 18.50
 F1 9.006P
 F2 .494P
 HZ/CM 75.032
 PPM/CM .250
 SR 3367.12





Mdd

VP7817C.004
AU PROG:
AUTOC13 AU
DATE 30-11-93

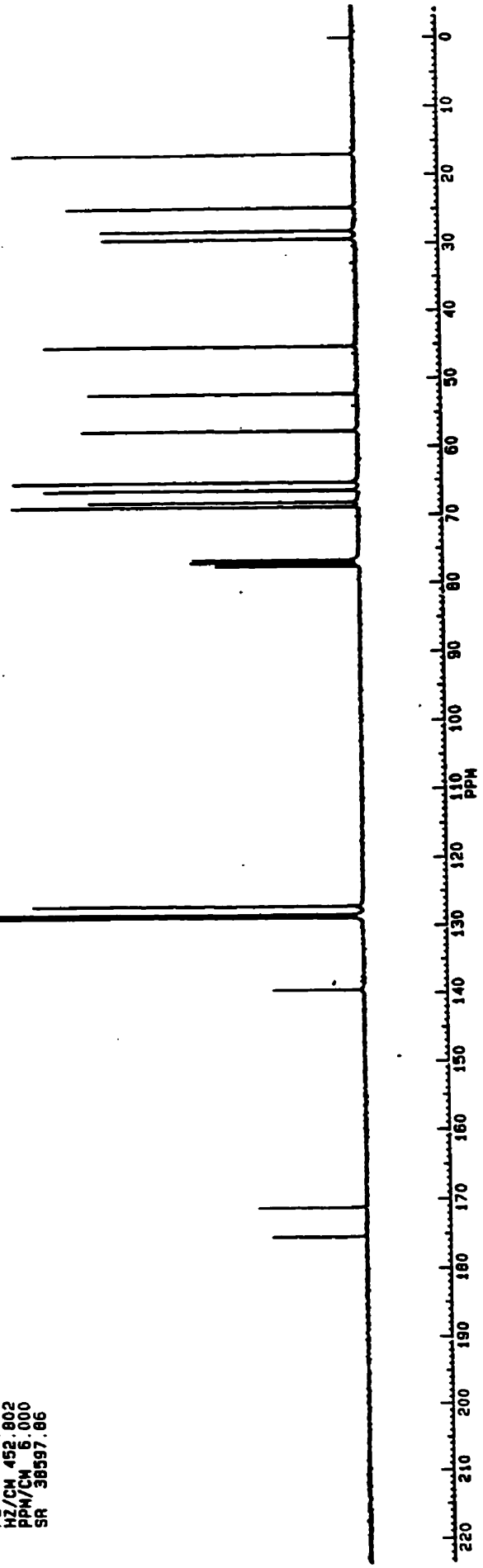
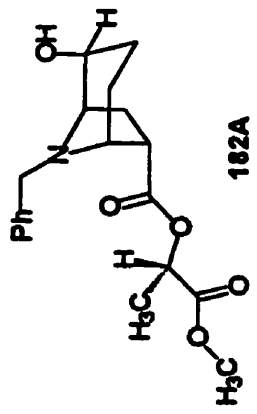
SF 75.469
SY 112.0500000
O1 47000.000
S1 32768
I0 32768
SN 17857.143
HZ/PT 1.090

PH 5.0
RD 0.0
AD 0.910
RS 200
NS 560
TE 300

FM 22400
O2 5000.000
DP 18H CPD

LB 1.000
GB 700
CX 38.00
CY 18.00
F1 223.402P
F2 -4.593P
HZ/CH 452.802
PPH/CH 6.000
SR 38597.86

SAMPLE VP-II-78-17 13-C AT 75.47 MHZ IN CDCL3





VPII7830.001
 AU PROG:
 TE7G AU
 DATE 26-11-93

SF 300.133
 SY 100.0
 OI 5500.000
 SI 32768
 TO 32768
 SW 5494.505
 HZ/PT .335

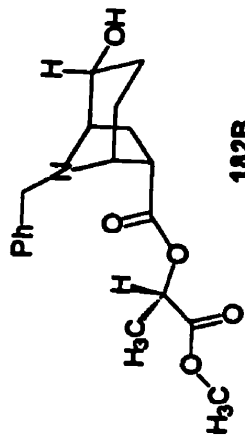
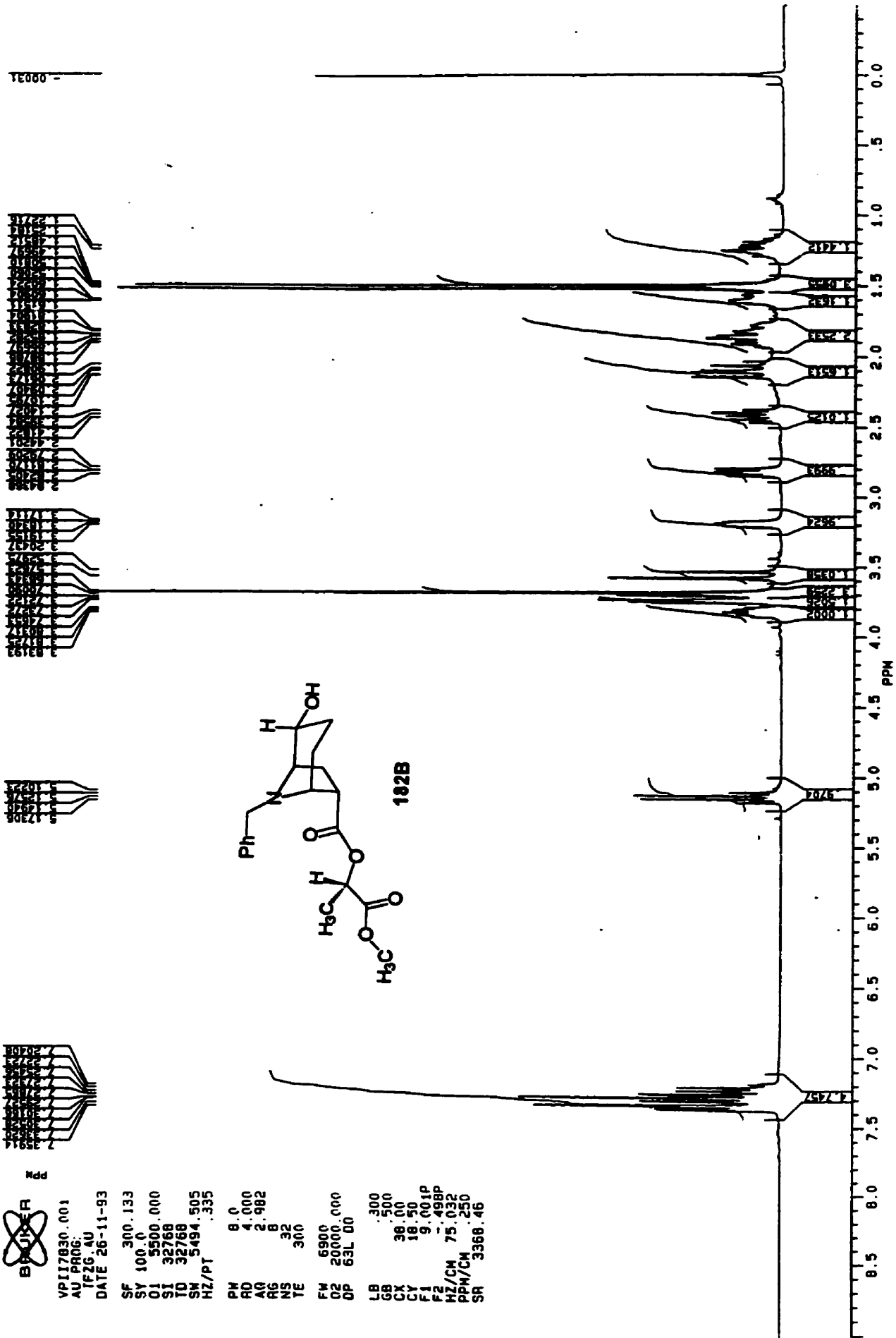
PH 8.0
 RD 4.000
 AQ 2.982
 RG 8
 NS 32
 YE 300

FW 6900
 OZ 20000.000
 OP 63L 00

LB .300
 GB .500
 CX 38.00
 CY 18.50
 F1 19.001P
 F2 .498P
 HZ/CM 75.032
 PPA/CM .250
 SR 3368.46

Mdd

SAMPLE VP-II-78-30 1-H AT 300 MHZ IN CDCL3



SAMPLE VP-II-78-30 13-C AT 75.47 MHZ IN CDCL3

BRUKER
 VP7830C.004
 AU PRO6:
 AUTOC13.AU
 DATE 1-12-93

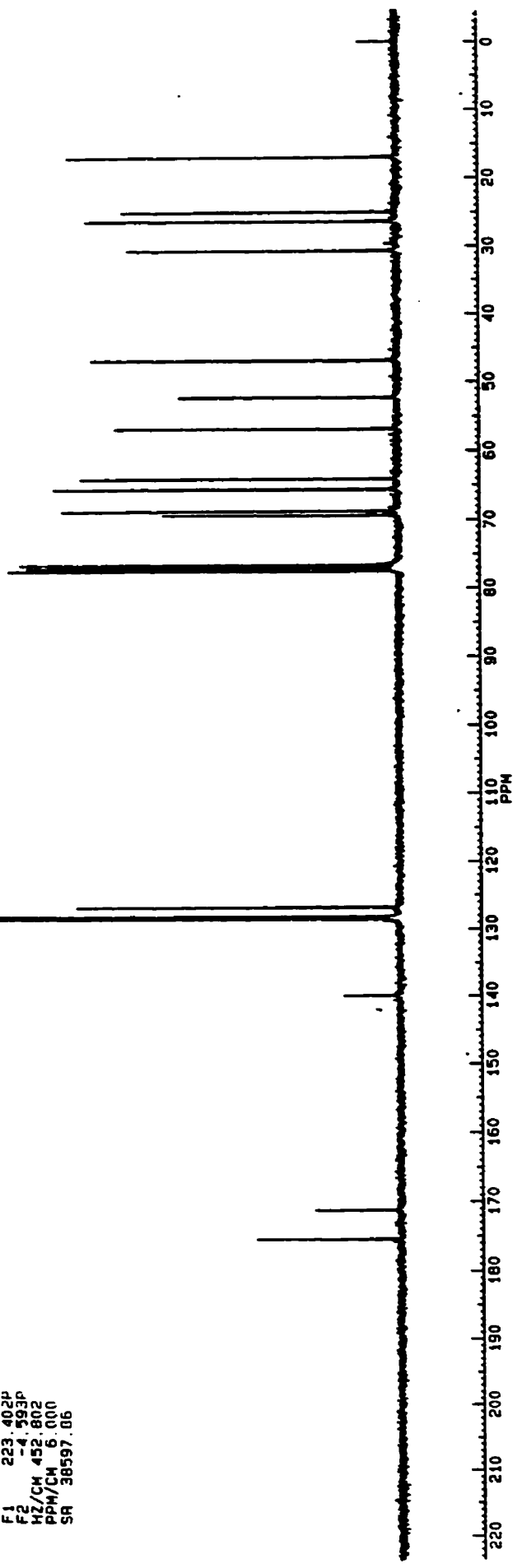
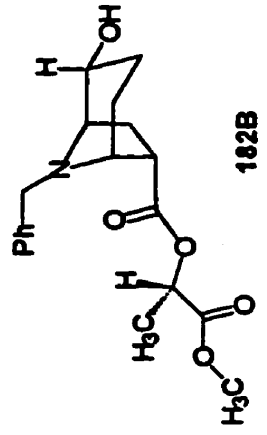
SF 75.469
 SY 112.0500000
 O1 47000.000
 S1 32768
 T0 32768
 SM 17857.143
 HZ/PT 1.090

PW 5.0
 RD 0.0
 AD .918
 RG 200
 NS 1024
 TE 300

FM 22400
 O2 5000.000
 OP 18H CPD

LB 1.000
 GB .700
 CX 38.00
 CY 18.00
 F1 223.402P
 F2 -4.993P
 HZ/CH 452.802
 PPM/CM 6.000
 SR 38597.06

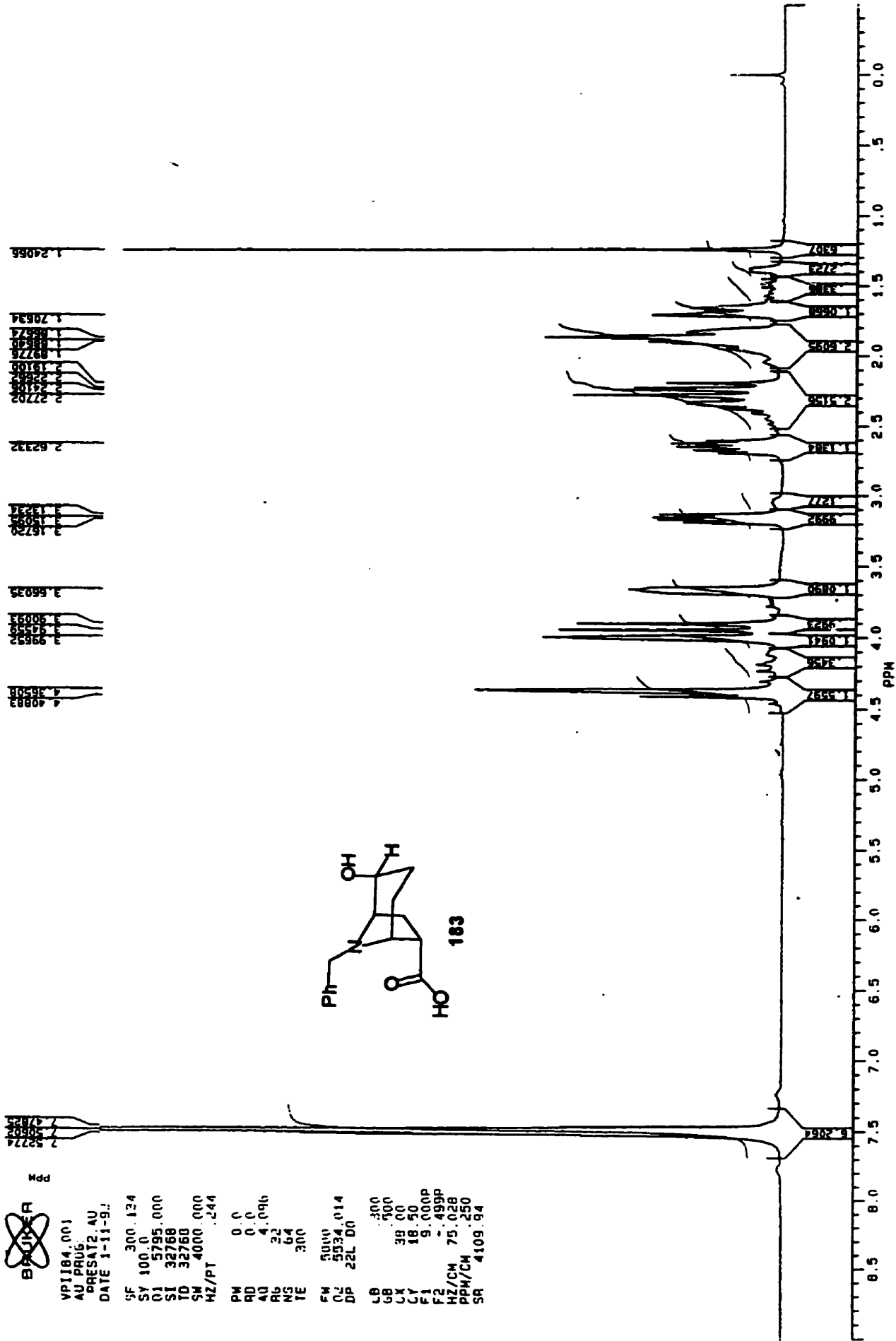
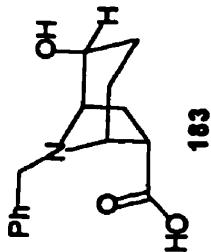
175.384
 171.159
 139.842
 128.415
 128.415
 128.788
 77.432
 76.841
 69.313
 68.711
 65.586
 64.083
 56.841
 52.230
 46.822
 30.668
 25.342
 24.997
 16.939



SAMPLE VP-11-84 1-H AT 300 MHZ IN D2O TSP ADDED SOLVENT SUPPRESSED



VP1184.001
 AU PRUG
 PRESAT2.AU
 DATE 1-11-91
 SF 300.134
 SY 100.0
 O1 5795.000
 SI 32768
 TD 32768
 SM 4000.000
 NZ/PT .244
 PW 0.0
 RD 0.0
 AU 4.096
 RB 22
 NC 64
 TE 300
 CW 5000
 CZ 5534.014
 DP 22L 00
 LB 300
 GB 500
 LX 38 00
 CY 18 50
 F1 9.000P
 F2 -499P
 HZ/CH 75.028
 PPM/CH .250
 SR 4109.94



SAMPLE VP-11-84 13-C AT 75.47 MHZ IN D2O



62

VP1184C.004
AU PROG:
AUTOC13.AU
DATE 16-11-93

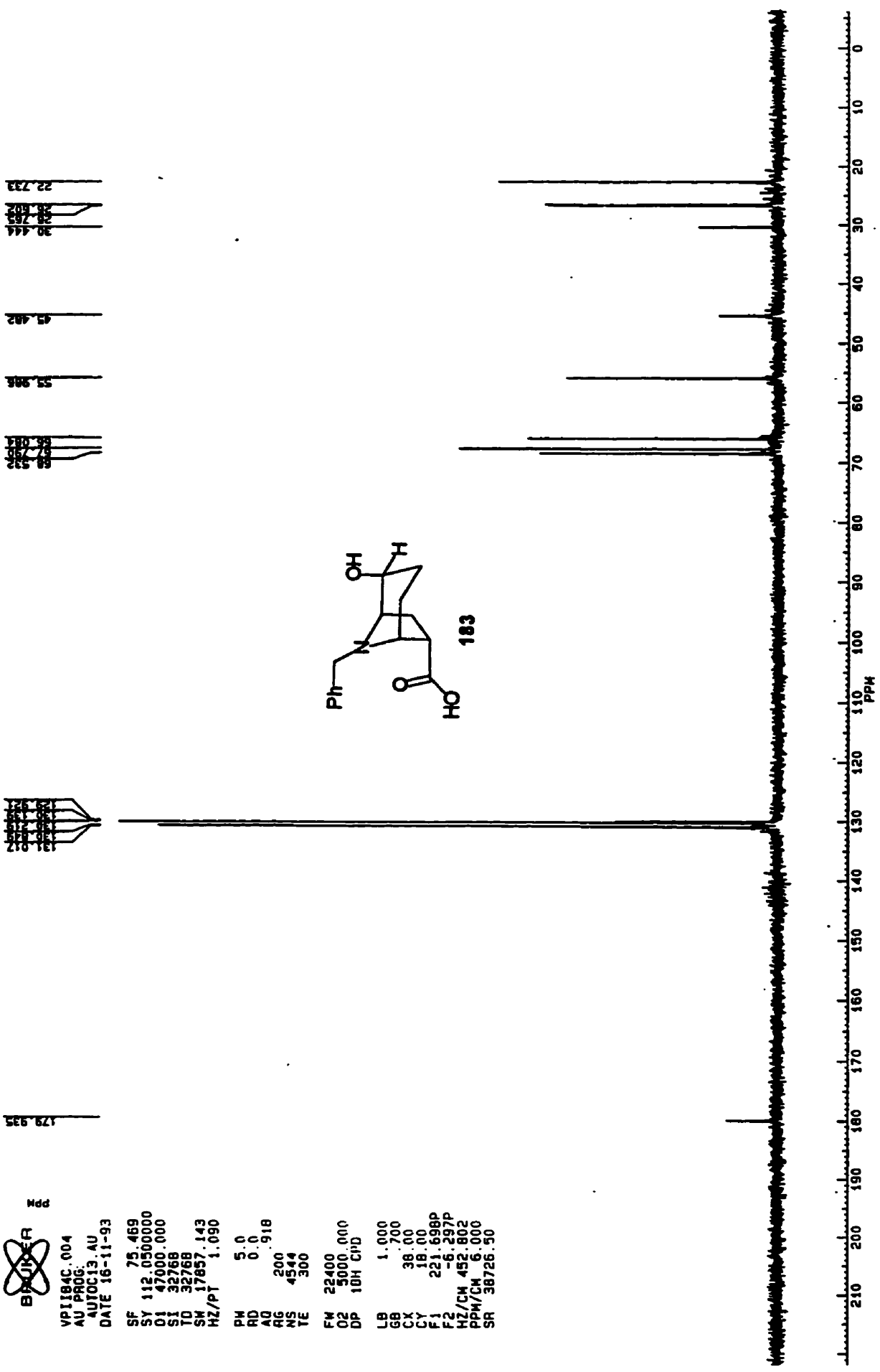
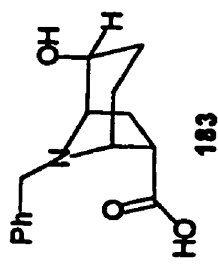
SF 75.469
SY 112.0500000
O1 47000.000
SI 32768
TD 32768
SM 17857.143
HZ/PT 1.090

PH 5.0
RD 0.0
AQ 0.918
RG 200
NS 4544
TE 300

FM 22400
O2 5000.000
DP 10H CPD

LB 1.000
GB 0.700
CX 38.00
CY 18.00
F1 221.698P
F2 -6.297P
HZ/CM 452.802
PPM/CM 6.000
SR 38726.50

129.935
130.000
130.065
130.130
130.195
130.260
130.325
130.390
130.455
130.520
130.585
130.650
130.715
130.780
130.845
130.910
130.975
131.040
131.105
131.170
131.235
131.300
131.365
131.430
131.495
131.560
131.625
131.690
131.755
131.820
131.885
131.950
132.015
132.080
132.145
132.210
132.275
132.340
132.405
132.470
132.535
132.600
132.665
132.730
132.795
132.860
132.925
132.990
133.055
133.120
133.185
133.250
133.315
133.380
133.445
133.510
133.575
133.640
133.705
133.770
133.835
133.900
133.965
134.030
134.095
134.160
134.225
134.290
134.355
134.420
134.485
134.550
134.615
134.680
134.745
134.810
134.875
134.940
135.005
135.070
135.135
135.200
135.265
135.330
135.395
135.460
135.525
135.590
135.655
135.720
135.785
135.850
135.915
135.980
136.045
136.110
136.175
136.240
136.305
136.370
136.435
136.500
136.565
136.630
136.695
136.760
136.825
136.890
136.955
137.020
137.085
137.150
137.215
137.280
137.345
137.410
137.475
137.540
137.605
137.670
137.735
137.800
137.865
137.930
138.000



SAMPLE VP-III-4A 1-H AT 300 MHZ IN CDCL3

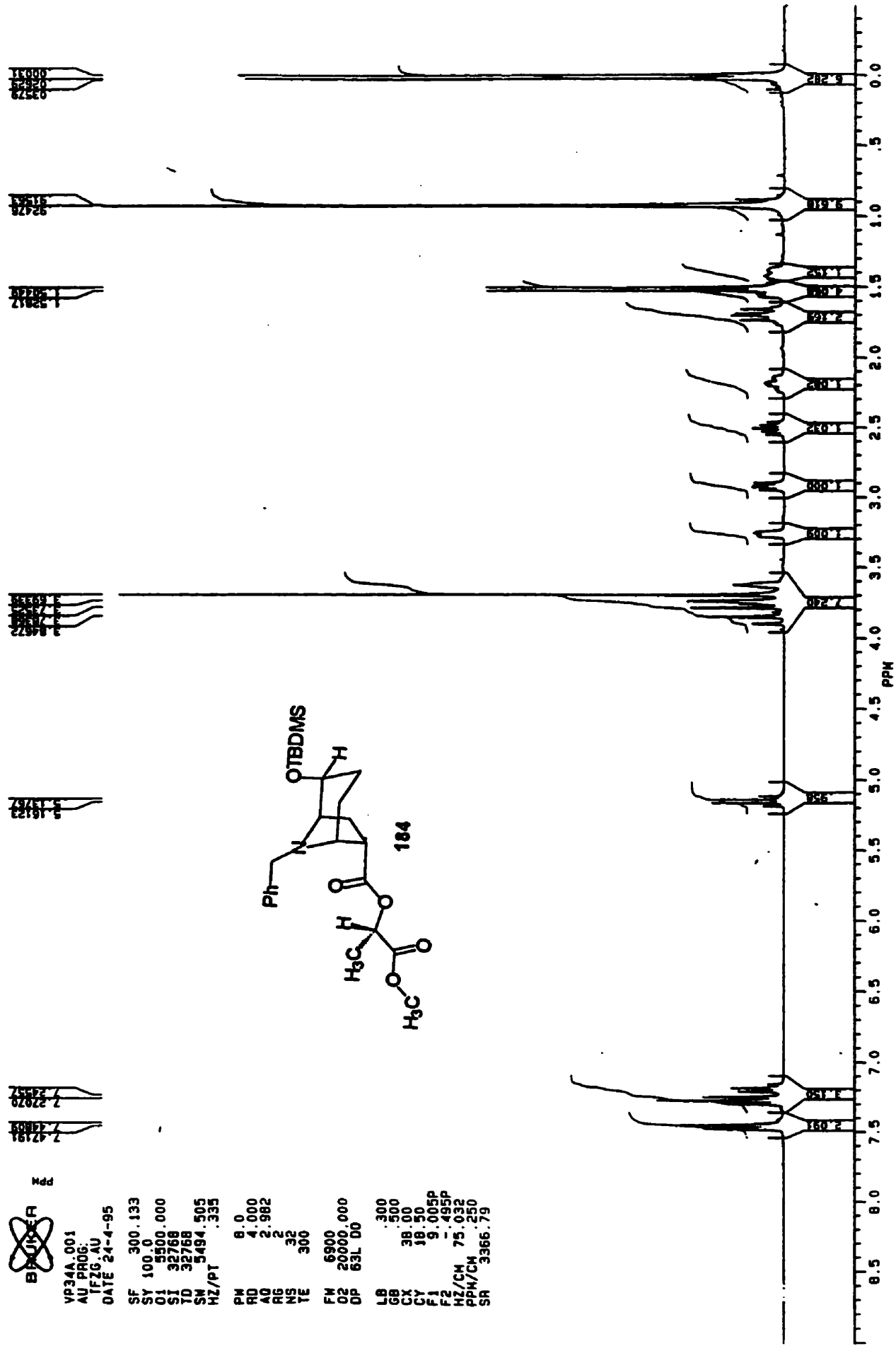
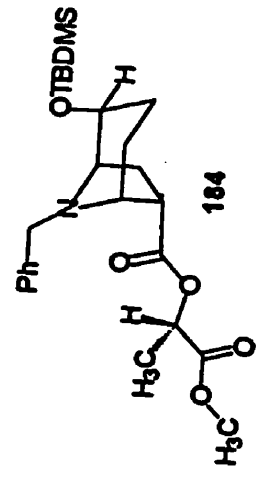
BUKER
 VP34A.001
 AU PROG.
 IFZG.AU
 DATE 24-4-95

SF 300.133
 SY 100.0
 O1 3500.000
 SI 32768
 TD 32768
 SN 5494.505
 HZ/PT .335

PW 8.0
 RD 4.000
 AQ 2.982
 RG 2
 NS 32
 TE 300

FW 6900
 OZ 20000.000
 DP 63L 00

LB .300
 GB .500
 CY 38.00
 CY 18.50
 F1 9.005P
 F2 -.495P
 HZ/CM 75.032
 PPM/CM .250
 SR 3366.79



SAMPLE VP-III-4A 13-C AT 75.47 MHZ IN CDCL3



VP34C.004
 AU PROG:
 AUTOC13.AU
 DATE 24-4-95

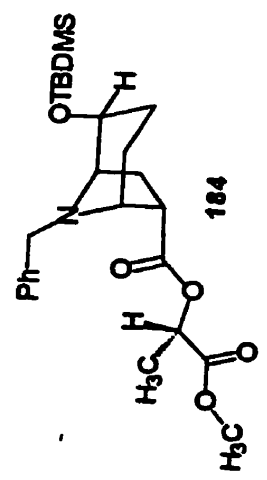
SF 75.469
 SY 112.050000
 O1 47000.000
 ST 32768
 TD 32768
 SW 17857.143
 HZ/PT 1.090

PW 5.0
 RD 0.0
 AU 0.918
 RG 200
 NS 640
 TE 300

FM 23400
 O2 5000.000
 DP 18H CPD

LB 1.000
 GB 700
 CX 38.00
 CY 38.00
 F1 221.001P
 F2 -6.954P
 HZ/CM 452.802
 PPM/CM 6.000
 SR 38600.37

172.485
 171.118
 140.591
 128.029
 127.221
 126.171
 77.467
 77.000
 76.842
 76.684
 76.526
 76.368
 76.210
 59.898
 52.148
 49.418
 38.234
 37.777
 37.320
 36.863
 36.406
 18.427
 18.269
 18.111
 -4.202
 -4.360



SAMPLE VP-II-259-D 1-H AT 300 MHZ IN CDCL3



VP2590.001
 AU PR06
 IFZ6.AU
 DATE 12-12-94
 SF 300.133
 SY 100.0
 O1 5500.000
 SI 32768
 TO 32768
 SW 5494.505
 HZ/PT .335
 PM 8.0
 RD 4.000
 AQ 2.982
 RG 2
 NS 32
 TE 300
 FM 6900
 O2 20000.000
 DP 63L 00
 LB .300
 GB .500
 CX 38.00
 CY 18.50
 F1 9.005P
 F2 .495P
 HZ/CM 75.032
 PPM/CM .250
 SR 3367.42

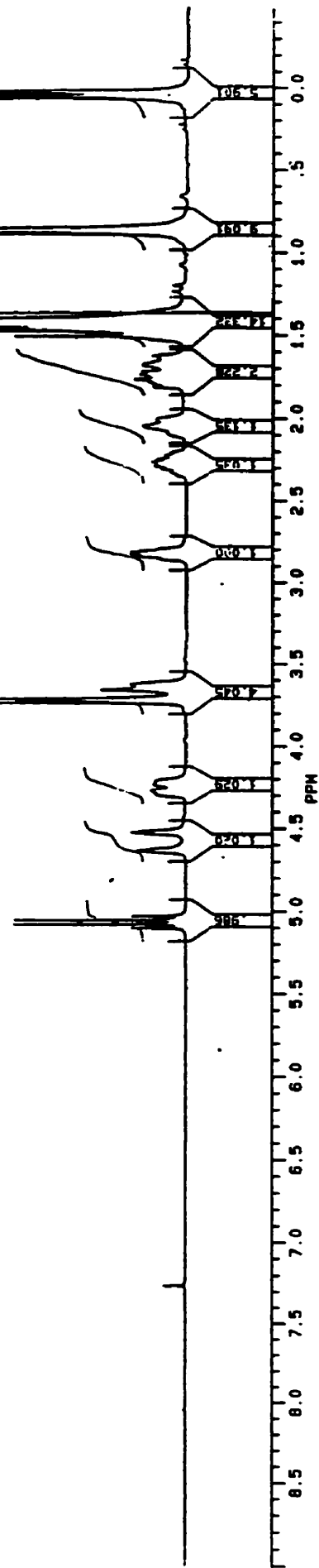
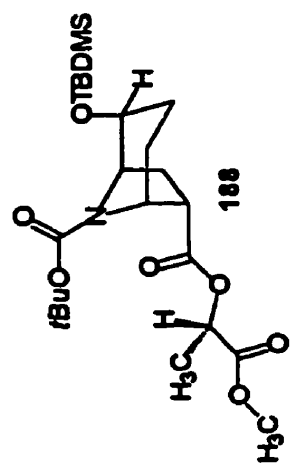
9342
 9276
 9277
 9278
 9279
 9280

4.52880
 4.51751

72387
 71157
 69249

9386
 9387
 9388
 9389
 9390

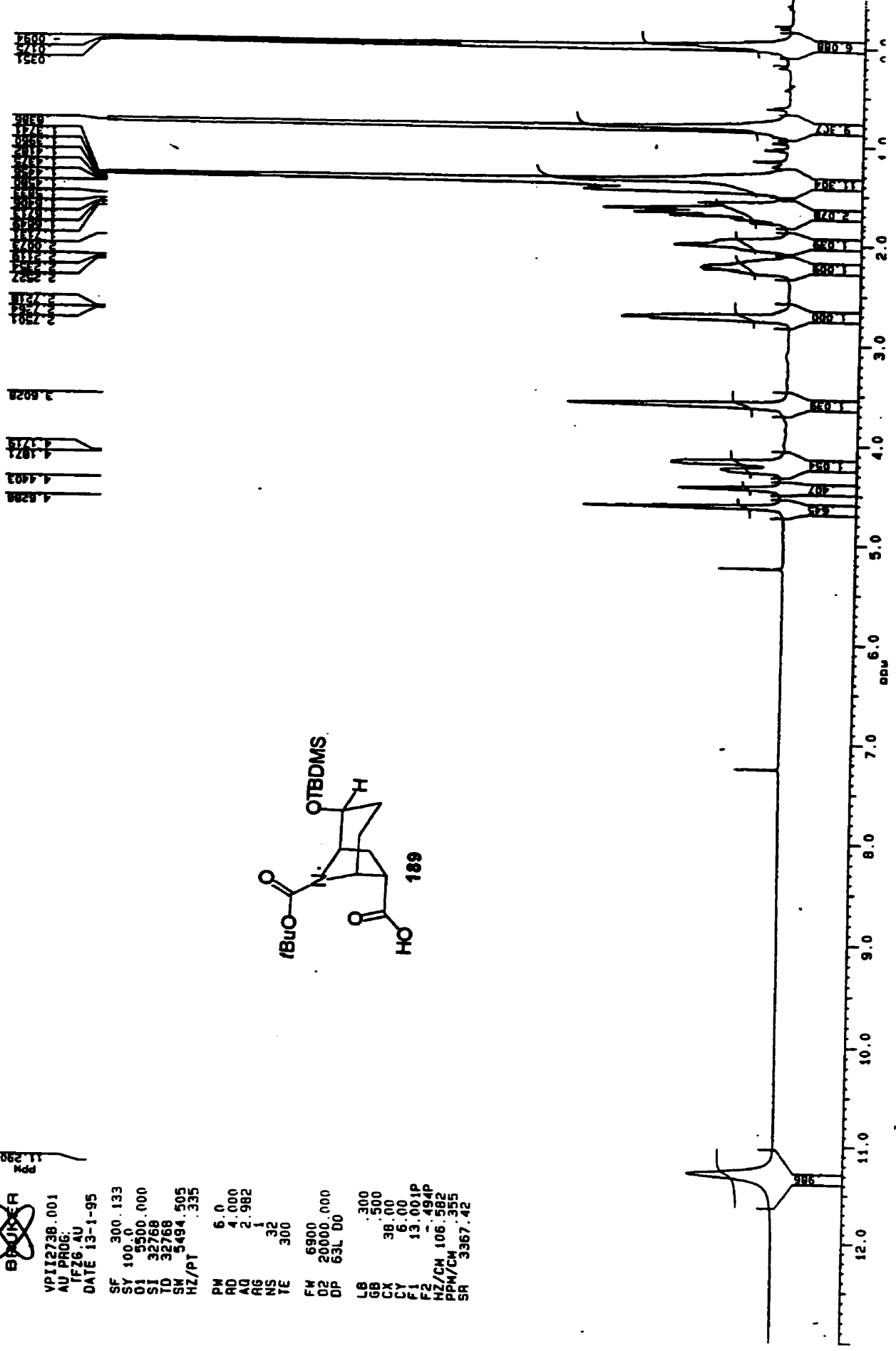
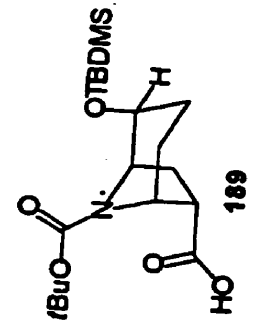
1.76303
 9344
 9345
 9346
 9347
 9348
 9349
 9350
 9351
 9352
 9353
 9354
 9355
 9356
 9357
 9358
 9359
 9360
 9361
 9362
 9363
 9364
 9365
 9366
 9367
 9368
 9369
 9370
 9371
 9372
 9373
 9374
 9375
 9376
 9377
 9378
 9379
 9380
 9381
 9382
 9383
 9384
 9385



SAMPLE VP-II-273-B 1-H AT 300 MHZ IN COCL3

BUKER
11.2901
Mod

VPI1273B.001
AU PROG.
F76 AU
DATE 13-1-95
SF 300.133
SY 100.0
O1 5500.000
SI 32768
TD 32768
SM 5494.505
HZ/PT .335
PW 6.0
RD 4.000
AQ 2.982
RG 1
NS 32
TE 300
FM 6900
O2 20000.000
DP 63L 00
LB .300
GB .500
CA 38.00
CY 6.00
F1 13.001P
F2
HZ/CH 106.582
PPM/CH .355
SR 3367.42



SAMPLE VP-II-273-B 13-C AT 75.47 MHZ IN CDCL3

BLUKEA
Mdd

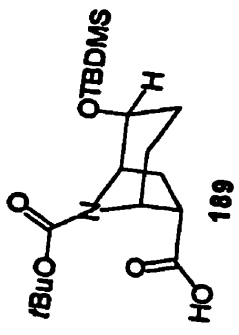
VP273BC.004
AU PROG.
AUTOC13.4U
DATE 23-2-95

SF 75.469
SY 112.0500000
OI 47000.000
SI 32768
TD 32768
SM 17857.143
HZ/PT 1.090

PM 5.0
RD 0.0
AQ .918
RG 200
NS 632
TE 300

FW 22400
D2 3000.000
DP 18H CPD

LB 1.000
GB 1.700
CX 38.00
CY 18.00
F1 221.065P
F2 -6.990P
HZ/CM 452.802
PPM/CM 6.000
SR 38594.59



179.834
177.939

121.171
120.151

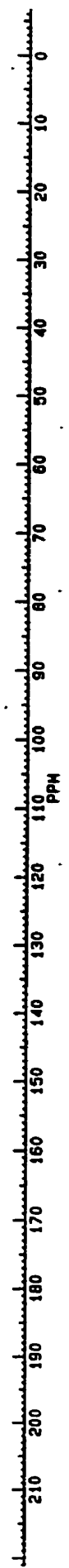
77.709
77.000
76.809

51.101
50.801
50.501

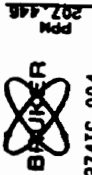
29.729
29.267

28.801
28.501
28.201
27.901
27.601
27.301
27.001

9.700
9.400
9.100
8.800
8.500
8.200



SAMPLE VP-II-274-I 13-C AT 75.47 MHZ IN CDCL3



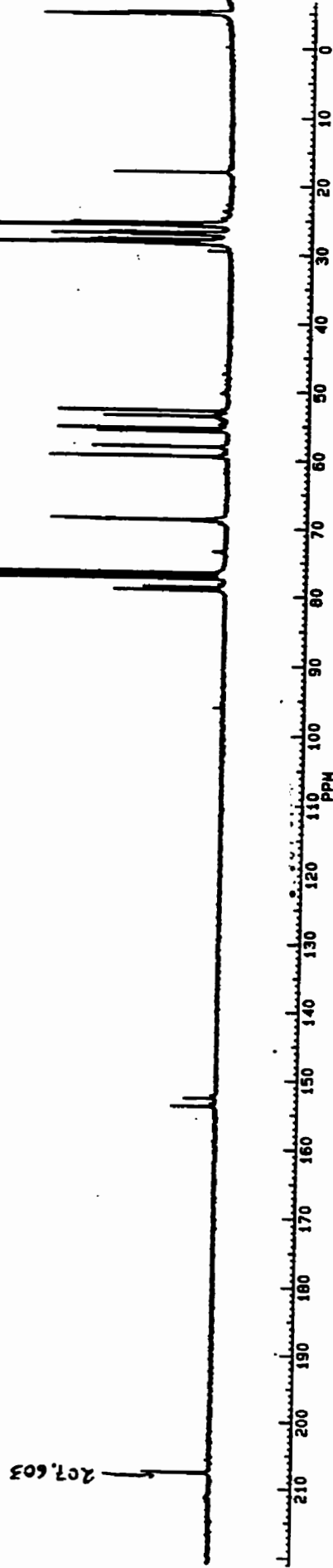
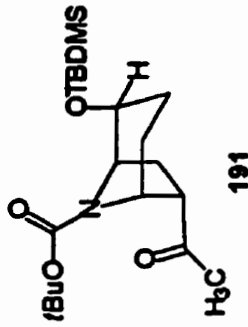
VP274IC.004
AU PROG. AU
AUTOF13.AU
DATE 23-2-95

SF 75.469
SI 112.0500000
O1 47000.000
SI 32768
TD 32768
SN 17857.143
HZ/PT 1.090

PH 5.0
RD 0.0
AQ 0.918
RG 200
NS 2560
TE 300

FW 22400
DZ 5000.000
DP 18H CPD

LB 1.000
GB 700
CX 38.00
CY 18.00
F1 221.005P
F2 -6.950P
HZ/CN 452.802
PPM/CM 6.000
SR 38594.59

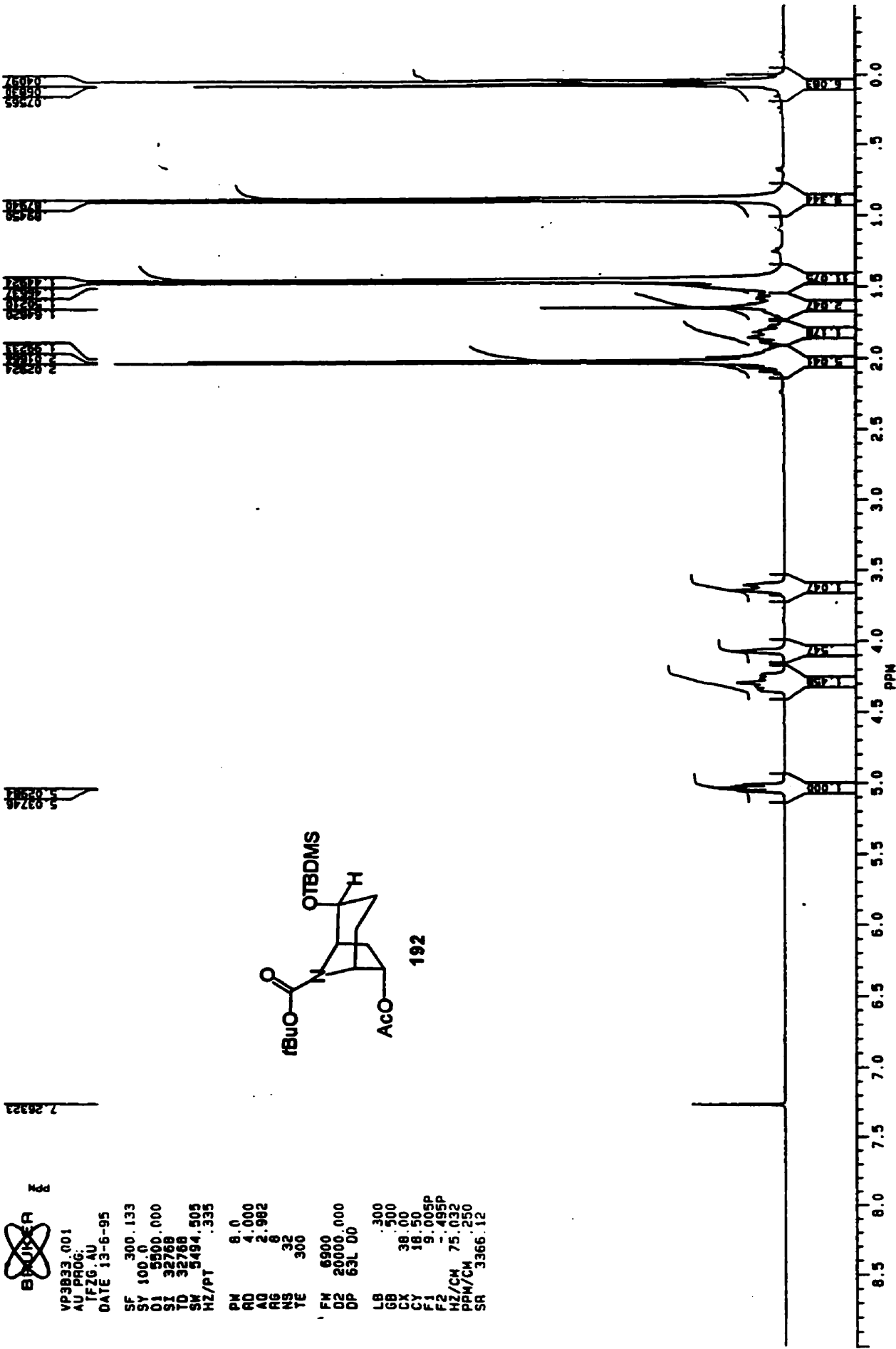
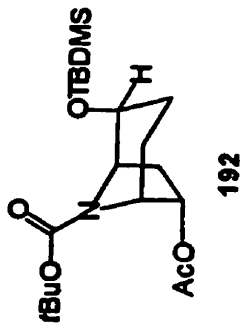


SAMPLE VP-III-20-833 1-H AT 300 MHZ IN CDCL3



VP3833.001
AU PROG:
TFZG AU
DATE 13-6-95
SF 300.133
SY 100.0
O1 5500.000
SI 32768
TD 32768
SW 5494.505
HZ/PT .335

PN 8.0
RD 4.000
AQ 2.982
RG 6
RS 32
TE 300
FM 6900
D2 20000.000
DP 63L 00
LB .300
GB .500
CX 38.00
CY 18.50
F1 9.005P
F2 -.495P
HZ/CH 75.032
PRM/CM
SR 3366.12



SAMPLE VP-III-20-C8 13-C AT 75.47 MHZ IN CDCL3

 Bruker
Kdd

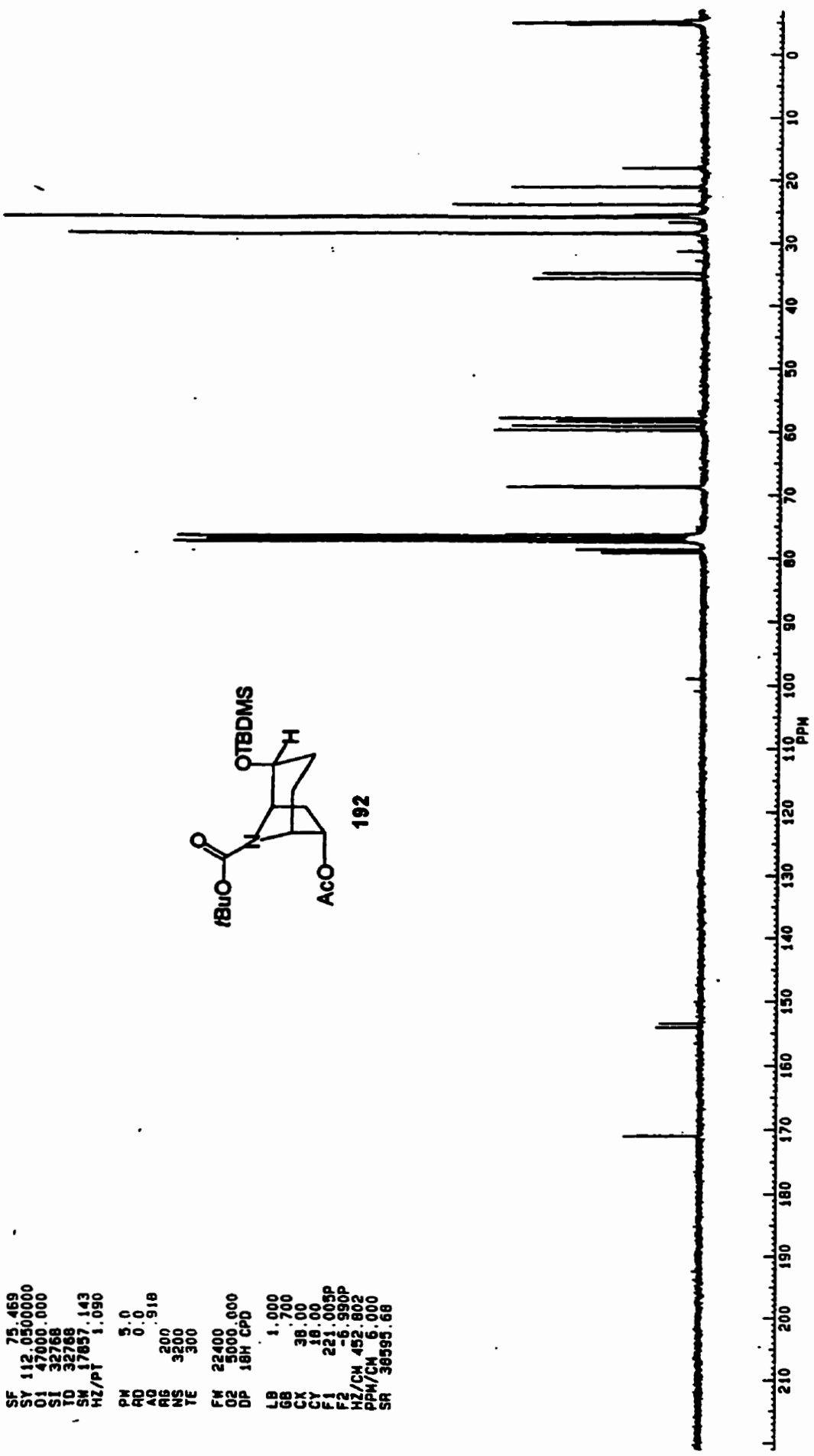
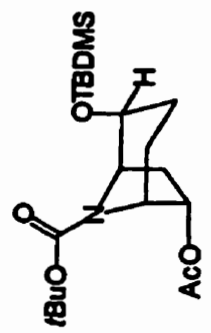
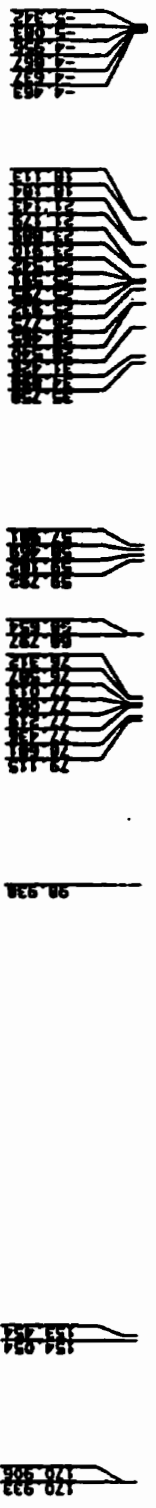
VP3C8C.004
AU PR06:
AUTOC13.AU
DATE 6-6-95

SF 75.469
SY 112.0500000
O1 47000.000
SI 32768
TD 32768
SM 17857.143
HZ/PT 1.090

PM 5.0
RD 0.0
AQ 9.18
RG 200
NS 3200
TE 300

FM 22400
DZ 5000.000
DP 18H CPD

LB 1.000
GB 1.700
CX 38.00
CY 18.00
F1 221.005P
F2 -8.990P
HZ/CH 452.802
PPM/CH 6.000
SR 38595.68



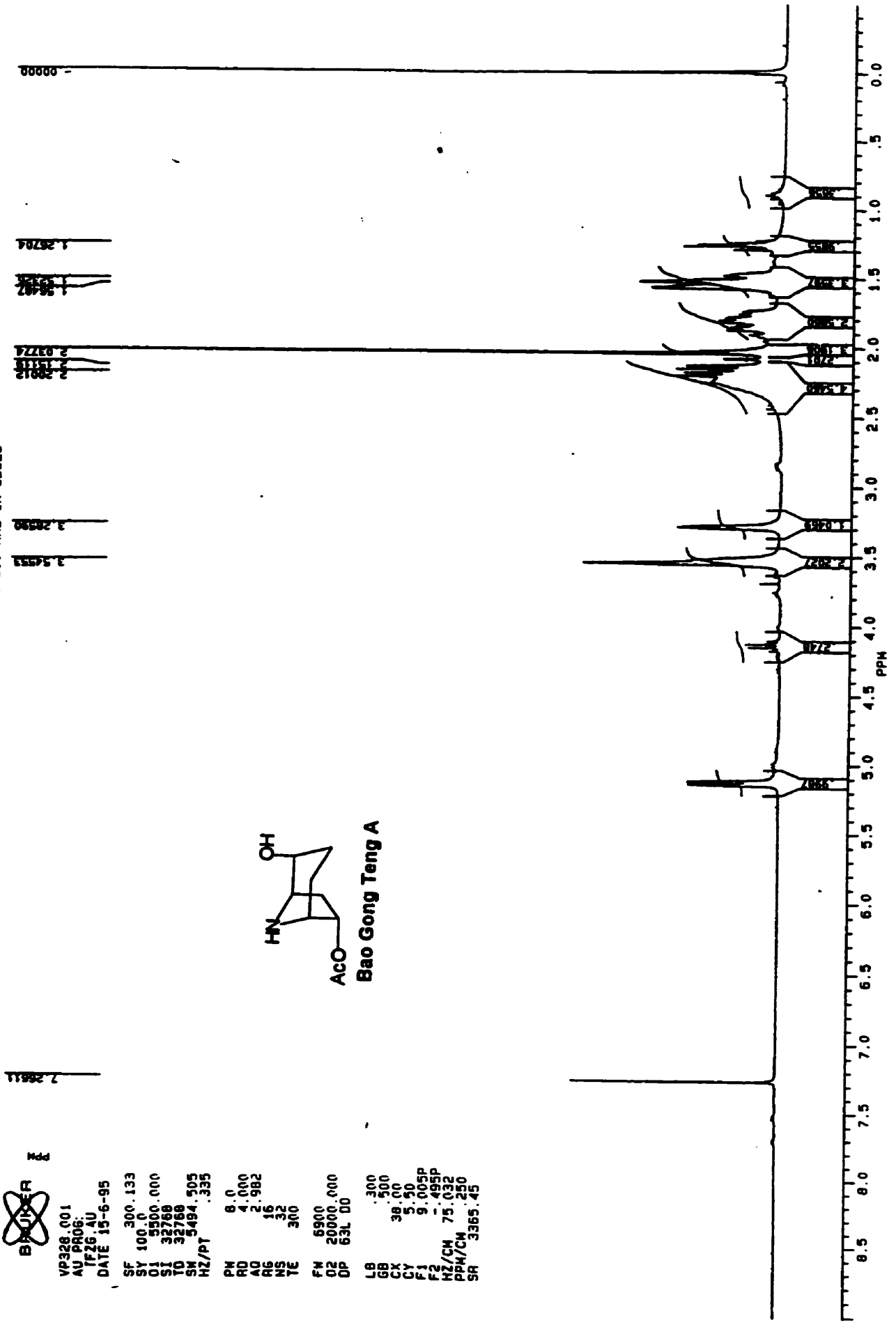
SAMPLE VP-III-28 1-H AT 300 MHZ IN CDCL3

BROKER
PPM

VP328.001
 AU PROG: TF26 AU
 DATE 15-6-95
 SF 300.133
 SY 100.0
 O1 5500.000
 SI 32768
 TO 32768
 SM 5494.505
 HZ/PT .335
 PM 8.0
 RD 4.000
 AO 2.982
 RS 15
 NS 32
 TE 300
 FM 6900
 O2 20000.000
 OP 63L 00
 LB .300
 GB .500
 CX 38.00
 CY 5.50
 F1 9.005P
 F2 .455P
 NZ/CH 75.032
 PPM/CH .250
 SR 3365.45



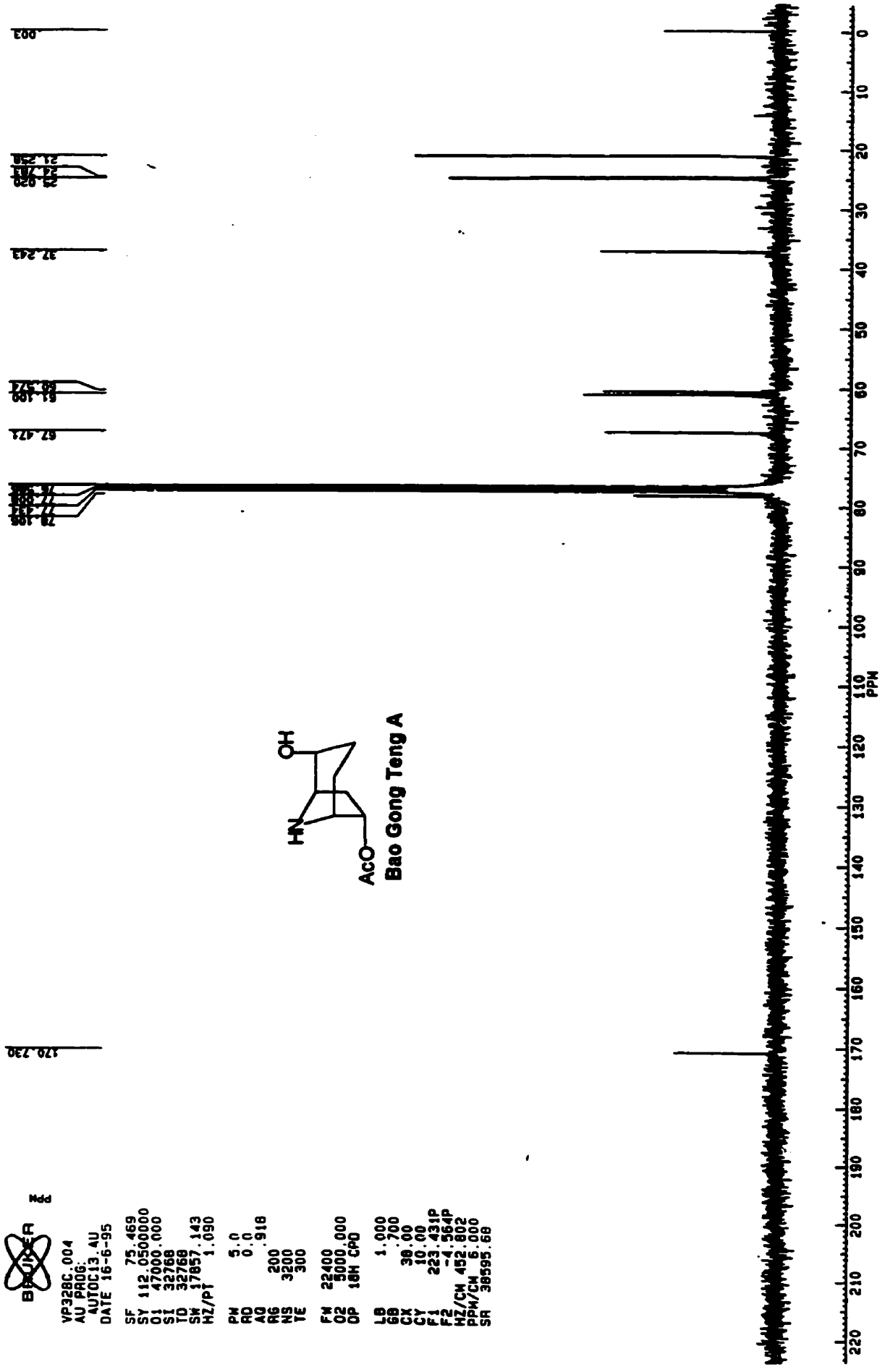
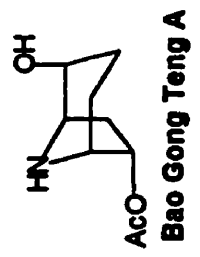
Bao Gong Teng A



SAMPLE VP-III-28 13-C AT 75.47 MHZ IN CDCL3



VP32BC.004
AU PROG.
AUTOC13.AU
DATE 16-6-95
SF 75.469
SI 112.0500000
O1 47000.000
SI 32768
TD 32768
SW 17857.143
HZ/PT 1.090
PW 5.0
RD 0.0
AQ 0.918
RG 200
NS 3200
TE 300
FW 22400
O2 5000.000
OP 18H CPD
LB 1.000
GB 1.700
CX 38.00
CY 10.00
F1 223.431P
F2 -4.564P
HZ/CM 452.802
PPM/CM 5.000
SR 38595.68



RAMPLE VP3-124P 1-H AT 300 MHZ IN CDCL3



PM

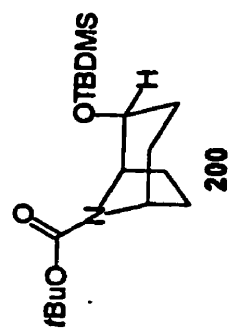
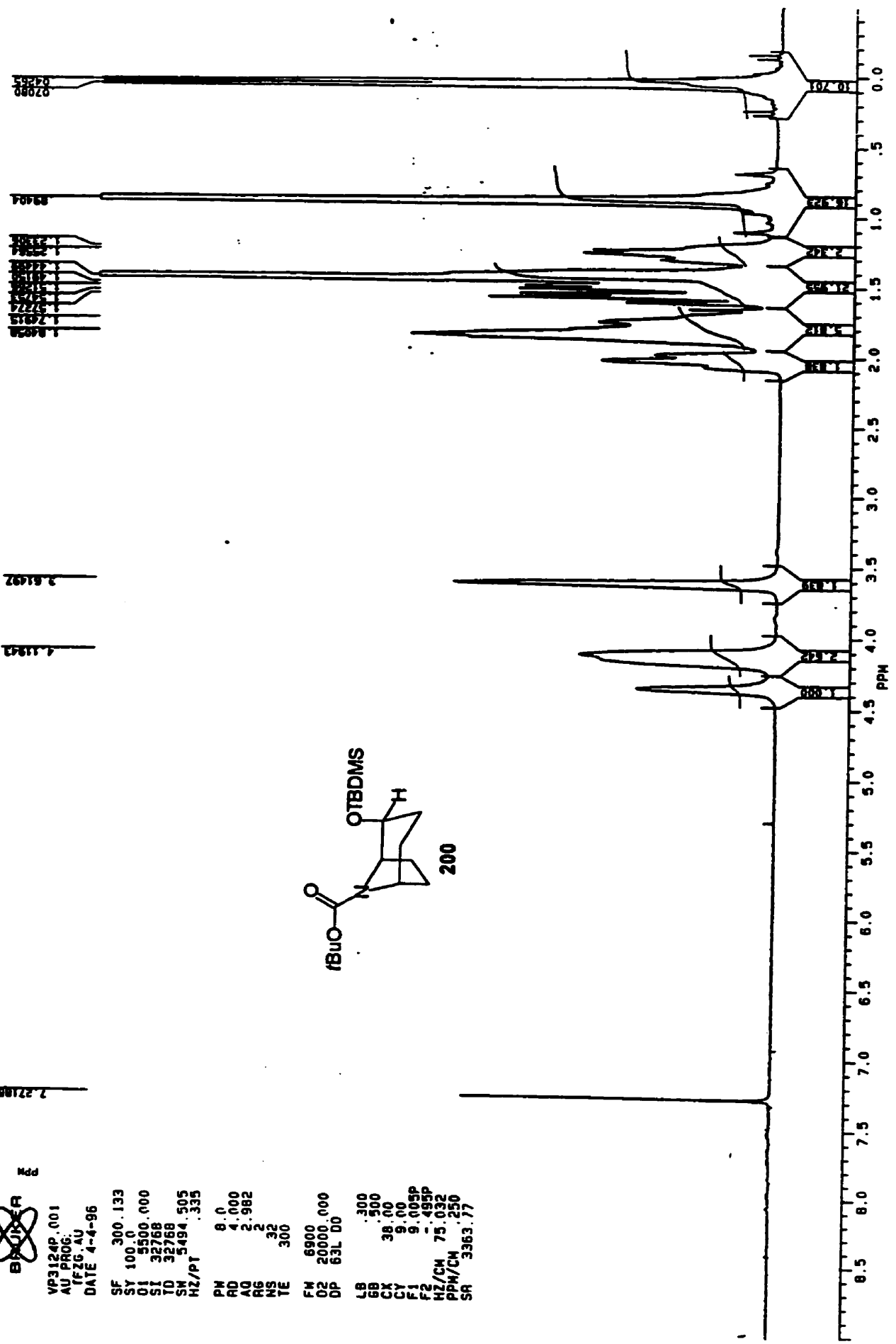
VP3124P.001
AU 8806.
TEG.AU
DATE 4-4-96

SF 300.133
SY 100.0
O1 5500.000
SI 32768
TD 32768
SW 3494.505
HZ/PT .335

PM 8.0
RD 4.000
AQ 2.982
RG 2
NS 32
TE 300

FM 6900
D2 20000.000
DP 63L D0

LB .300
GB .500
CX 38.00
CY 9.00
F1 9.005P
F2 .495P
HZ/CH 75.032
PPH/CH .250
SR 3363.77





VP3124PC.004
AU PROG:
AUTOC13 AU
DATE 6-4-96

SF 75.469
SY 112.0500000
O1 47000.000
SI 32768
TD 32768
SM 17657.143
HZ/PT 1.090

PW 5.0
RD 0.0
AO .918
RG 200
NS 3200
TE 300

FW 22400
O2 5000.000
OP 18H CPD

LB 1.000
GB .700
CX 38.00
CY 6.50
F1 220.004P
F2 -7.891P
M7/CM 452.802
PPM/CM 6.000
SR 38597.10

SAMPLE VP3-124P 13-C AT 75.47 MHZ IN CDCL3

